DISS. ETH Nr. 23612

SECRETORY IgA ENFORCES "CAGED GROWTH" OF SALMONELLA TYPHIMURIUM

- A STORY OF BEING TRAPPED

A thesis submitted to attain the degree of

DOCTOR OF SCIENCE of ETH ZURICH

(Dr. sc. ETH Zurich)

presented by

KATHRIN MOOR

MSc ETH in Biology, ETH Zurich

born on May 14th 1985

citizen of Zofingen (AG)

accepted on the recommendation of

Prof. Dr. Wolf-Dietrich Hardt

Dr. Emma Slack

Prof. Dr. Annelies Zinkernagel

Prof. Dr. Manfred Kopf

2016

To my beloved ones

The important thing is not to stop questioning. Curiosity has its own reason for existing.
Albert Einstein

TABLE OF CONTENTS

THESIS SUMMARY

Mucosal surfaces are prominent sites for non-vector borne pathogen-entry. In the intestine, the situation is especially challenging, since the dense microbiota and potential enteropathogens are separated by only a few layers from the sterile lamina propria. It is broadly accepted that immunoglobulin A (IgA) plays an important role in coordinating the establishment and the maintenance of the intestinal microbiota, however very little is understood about the protective mechanisms attributed to this antibody isotype. Only very few mucosal vaccines that aimed at inducing intestinal IgA are in regular clinical use, predominantly as trials have ended with excess adverse effects or poor protection. This can most likely be attributed to our poor understanding of how exactly protective immunity at mucosal surfaces functions. The presented work aims towards a better mechanistic understanding of IgA-mediated protection during blooms of *Salmonella* Typhimurium (*S.* Typhimurium) after antibiotic-induced dysbiosis.

In order to study the mechanism of IgA-mediated protection in the intestine, we first had to develop tools to reliably induce intestinal high-avidity IgA and to measure and characterize the nature of this antibody response. The mucosal immune system is compartmentalized away from systemic sites. Therefore, induction of intestinal IgA responses requires oral delivery of the antigen. However, since the gastrointestinal tract is colonized with a dense microbiota and constantly flooded by a variety of antigens, the induction of adaptive immunity in the intestine is tightly regulated, and the threshold for inducing immune responses is extremely high. To reliably inactivate high numbers of bacteria, while maintaining their antigenic properties, our strategy was to incubate them with the strongly oxidizing reagent peracetic acid. We could demonstrate that this treatment is much more efficient to inactivate high numbers of a broad range of bacteria as compared to traditional methods such as pasteurization, and maintains antigenicity better than autoclaving. The oral administration of peracetic acid killed bacteria leads to the robust induction of high-avidity, T cell dependent intestinal IgA responses specific for the bacterial strain used for vaccine production. This occurs in the absence of intestinal inflammation or colonization of the host by the vaccination strain. Therefore, this vaccination strategy allows the study of high-avidity IgA-mediated protection in an otherwise unperturbed host. Due to its sterile nature, this vaccine is safe even in the context of severe immunodeficiency. In combination with a newly developed method for the analysis of bacterial surface-specific antibodies by flow cytometry, we could demonstrate that vaccination with peracetic acid-inactivated *S.* Typhimurium (PA.STm) protects from systemic pathogen spread and pathology in the murine model of non-typhoidal Salmonellosis in an O-antigen- and IgA-dependent manner.

In order to further study the mechanism of IgA-mediated protection, we applied a variety of microscopy techniques, combined with mathematical models that aim to describe the within-host population dynamics of *S.* Typhimurium. Thereby we found that in the presence of high-avidity IgA and an open niche for colonization, *S.* Typhimurium undergo caged growth. This growth pattern is caused by the unsuccessful physical segregation of two cells after division, resulting in the formation of clonal microcolonies that fuse into more complex oligoclonal aggregates as the bacterial population in the intestine reaches higher densities. We could demonstrate that caged growth is far more efficient than density-dependent classical agglutination when realistic infectious inocula sizes are ingested. Since in PA.STm-vaccinated mice most intestinal bacteria reside in aggregates, the actual infectious bacterial population (that is the non-aggregated bacteria) is reduced by roughly hundredfold. As the bacterial tissue invasion and further systemic spread in PA.STm-vaccinated mice are reduced by the same order of magnitude, this phenomenon is in fact sufficient to explain all vaccine-mediated protection in our model.

Interestingly, caged growth also has several consequences for *S.* Typhimurium population genetics. We found that clonal growth delays the density-dependent exchange of genetic material. As IgA-mediated caged growth leads to the confinement of potential plasmid donor and recipient clones in physically separated microcolonies, we observed a delay in the rate of plasmid transfer. Interestingly, we could also demonstrate a secondary effect of high-avidity IgA on the induction of inflammation-mediated phage transfer between *Salmonella* spp.. Additionally, the non-segregation of clones results in more extensive clonal extinction in the gut lumen. Therefore, we report for the first time that vaccine induced high-avidity IgA has the potential to decrease horizontal gene transfer which can be observed during blooms of enteropathogens.

Taken together, this work presents new tools to induce intestinal high-avidity IgA and mechanistically study its protective properties. We have found unexpected effects of high-avidity IgA on pathogen within-host evolution and horizontal gene transfer. This new insight in how IgA can protect against fast-growing bacteria could help to improve the current difficulties in the development of efficient vaccines against enteric bacterial pathogens.

ZUSAMMENFASSUNG

Schleimhäute sind prominente Eintrittspforten für Pathogene, die nicht durch Vektoren übertragen werden. Im Darm ist die Situation besonders kritisch, da die dichte Mikrobiota und potentielle Darmpathogene nur durch wenige Schichten von der sterilen darunterliegenden Lamina Propria getrennt sind. Die Meinung, dass Immunglobulin A (IgA) eine wichtige Rolle dabei spielt, die Etablierung und den Erhalt der Mikrobiota zu koordinieren, ist weit verbreitet. Über die genauen Schutzmechanismen, die diesem Antikörper-Isotyp zugeschrieben werden, ist jedoch wenig bekannt. Es sind nur sehr wenige mukosale Impfungen zur Induktion intestinaler IgA-Antworten in regelmässigem klinischem Gebrauch, da die bisherigen Studien starke Nebenwirkungen oder schlechten Impfschutz zeigten. Dies kann höchstwahrscheinlich darauf zurückgeführt werden, dass unser Verständnis, wie genau protektive Immunität an Schleimhäuten erreicht werden kann, nach wie vor sehr unzureichend ist. Das Ziel der präsentierten Arbeit ist, ein besseres mechanistisches Verständnis des Schutzes durch IgA während dem extremen Wachstum von *Salmonella* Typhimurium (*S.* Typhimurium) nach Antibiotikabehandlungen zu erreichen.

Um die Schutzmechanismen von IgA im Darm zu untersuchen, mussten wir zuerst Methoden entwickeln, die es uns auf der einen Seite ermöglichten, verlässlich intestinale IgA-Antworten zu induzieren, die sich durch eine hohe Antikörperavidität auszeichnen. Auf der anderen Seite sollten diese Methoden es zusätzlich ermöglichen die Antikörperantwort charakterisieren. Das mukosale Immunsystem ist von systemischen immuninduktiven Stellen getrennt. Deshalb ist es für die Induktion von intestinalen IgA-Antworten unerlässlich, das Antigen oral zu verabreichen. Infolge der dichten Besiedlung des Darms durch die Mikrobiota und den konstanten Durchfluss einer Vielfalt von Antigenen ist die Induktion von adaptiven Immunantworten im Darm streng reguliert und der Grenzwert des Stimulus, der überschritten werden muss, um erfolgreich eine Immunantwort zu induzieren, extrem hoch. Um verlässlich grosse Mengen an Bakterien zu inaktivieren und gleichzeitig ihre Antigencharakterisiken zu erhalten, verwendeten wir Peressigsäure, welches stark oxidierende Eigenschaften aufweist. Wir konnten zeigen, dass diese Behandlung, verglichen mit traditionellen Methoden wie Pasteurisierung, viel effizienter ist, um grosse Mengen einer breiten Reihe von Bakterien zu inaktivieren und gleichzeitig deren antigenes Potential besser zu erhalten als durch Autoklavierung. Die orale Verabreichung solcher durch Peressigsäure inaktivierter Bakterien induziert eine robuste, T-Zellen abhängige IgA-Antwort mit starker Avidität für den Bakterienstamm, der für die Produktion der Impfung verwendet wurde. Dies geschieht ohne die Induktion intestinaler Entzündungsreaktionen sowie Kolonisierung des Wirts durch den Impfstamm. Deshalb ermöglicht diese Impfstrategie Studien über den mechanistischen Schutz von hoch spezifischem IgA in einem sonst unveränderten Organismus. Durch die sterile Verabreichungsform ist die Anwendung dieser Impfung sogar im Kontext schwerer

angeborener Immundefekte sicher. In Kombination mit einer neu entwickelten Methode zur Analyse von bakterienoberflächenspezifischen Antikörpern konnten wir zeigen, dass Impfung mit Peressigsäure-inaktivierten *Salmonella* Typhimurium (PA.STm) vor einer systemischen Ausbreitung des Pathogens und vor intestinaler Pathogenese im Mausmodel der nicht-typhoidalen Salmonellose schützt und dies in einer O-Antigen- und IgA-abhängigen Weise geschieht.

Um die Mechanismen dieses IgA-abhängigen Schutzes genauer zu untersuchen, verwendeten wir verschiedene Mikroskopie-Techniken und kombinierten diese mit mathematischen Modellen, die darauf abzielen, Populationsdynamiken von *S.* Typhimurium im Wirt zu beschreiben. Dadurch fanden wir heraus, dass Salmonellen in der Gegenwart von hochavidem IgA und einer offenen Nische kettenartig wachsen. Dieses Wachstumsmuster hat seine Ursache in der nicht erfolgreichen physikalischen Trennung zweier Bakterien nach deren Teilung und resultiert in der Bildung von klonalen Mikrokolonien, die zu komplexeren oligoklonalen Aggregaten fusionieren, wenn die Bakterienpopulation im Darm eine höhere Dichte erreicht. Wir konnten zeigen, dass diese wachstumsbedingte Agglutination effizienter ist als klassische dichteabhängige Agglutination, wenn realistische Mengen an Bakterien eingenommen werden. Da sich die meisten Bakterien im Darm von PA.STm-geimpften Mäusen in Aggregaten befinden, verringert dies die effektive infektiöse Population (die freien Bakterien) etwa um den Faktor hundert. Weil die Invasion der Bakterien ins Gewebe und deren weitere systemische Verbreitung in PA.STm-geimpften Mäusen um denselben Faktor verringert ist, reicht dieses Phänomen aus, um den kompletten Impfschutz in unserem Model zu erklären.

Dieses Wachstumsmuster hat auch Konsequenzen für die Populationsgenetik von *S.* Typhimurium. Wir fanden heraus, dass der dichteabhängige Austausch von genetischem Material verlangsamt wird. Weil das kettenartige Wachstum potentielle Plasmid-Spender- und Empfängerklone räumlich trennt, konnte eine Verlangsamung des Plasmidtransfers beobachtet werden. Interessanterweise konnten wir einen sekundären Effekt von hochavidem IgA nachweisen und zeigen, dass der entzündungsinduzierte Transfer von Phagen zwischen *Salmonella* spp. unterbunden wird. Zusätzlich resultiert die klonale Struktur der intestinalen Bakterienpopulation in einem erheblichen Verlust von Klonen aus dem Darm. Somit konnten wir zum ersten Mal zeigen, dass hochavides IgA das Potential hat, den horizontalen Gentranfer zwischen schnellwachsenden bakteriellen Darmpathogenen zu verringern.

Zusammenfassend präsentiert diese Arbeit neue Methoden, um hochavides intestinales IgA zu induzieren und seine protektiven Funktionen zu untersuchen. Unerwarteterweise konnten wir dadurch auch sehr interessante Effekte von hochavidem IgA auf die Evolution von Bakterien und den horizontalen Gentransfer im Darm nachweisen. Dieses neugewonnene

Wissen, wie hochavides IgA gegenüber schnellwachsenden Bakterien wirkt, könnte helfen, die aktuellen Schwierigkeiten bei der Entwicklung effizienter Impfungen gegen bakterielle Darmpathogene zu überwinden.

CHAPTER 1

-

GENERAL INTRODUCTION

The intestinal mucosa - survailling and keeping the barrier

The intestinal mucosa is the largest mucosal surface in our body. It is constantly exposed to a variety of antigen, either derived from food or from the dense consortium of microbes that co-exist with their host. In the lower intestine, these microbes (bacteria, viruses and fungi) reach a density of 10^{12} colony-forming units (CFU) per gram content (Gill *et al.*, 2006). Under homeostatic conditions, the host and its microbiota not only live in peaceful coexistence, but rather in a mutualistic relationship. The resident microbes are essential for the development and function of the intestinal immune system and also play an important metabolic role by fermenting non-digestible carbohydrates and contributing to the synthesis of certain vitamins (Hooper *et al.*, 2012). Furthermore, the microbiota confers its host "colonization resistance" by protecting against invasion and infection by ingested enteropathogens (Stecher *et al.*, 2013a; Stecher *et al.*, 2011). The mechanisms underlying colonization resistance are thought to include competition for nutrients and niches as well as direct inhibition by secretion of compounds that negatively influence the growth of other species (Stecher *et al.*, 2011).

However, it is crucial that the microbiota stays confined to the intestinal lumen. The intestinal mucosal barrier system therefore constantly faces the enormous challenge to separate the microbiota by only a few layers from the sterile lamina propria. The majority of immunological processes required for the peaceful co-existence of the host and the microbiota, take place in the intestinal mucosa, which comprises the intestinal epithelium, the underlying lamina propria and the muscularis mucosa, a thin muscle layer below the lamina propria (Figure 1) (Mowat *et al.*, 2014).

A first barrier is the intestinal epithelium itself. It consists of a single layer of absorptive enterocytes joined by tight junctions to their neighbouring cells to form a semi-permeable physical barrier (Matter *et al.*, 2014). The luminal side of the intestinal epithelium is covered with a thick layer of mucus, primarily composed of mucins. Mucins are high-molecular weight glycoproteins, produced and secreted by goblet cells that are interspersed within the enterocytes. After secretion they aggregate and form a gel-like barrier (Kim, J. J. *et al.*, 2013). Close to the epithelial cells, the densely aggregated mucins act as size exclusion filter to keep bacteria away from the epithelial cell surface (Johansson *et al.*, 2008). Besides forming a physical barrier, mucins also serve as an energy source for both the resident microbiota as well as enteric pathogens that are capable of adhering to the mucus (Marcobal *et al.*, 2013). Paneth cells, located at the base of the epithelial crypts, produce and secrete a variety of antimicrobial peptides into the mucus layer. Examples of antimicrobial peptides are defensins, cathelicidins, lactoferrins and histatins (Wiesner *et al.*, 2010). Due to their positive charge, defensins interact with the negatively charged membrane of pathogenic bacteria, consequently causing membrane destabilization and pore formation (Chu *et al.*, 2012; Salzman *et al.*, 2003). Cathelicidins are also positively charged and were shown to neutralize

bacterial lipopolysaccharide (LPS) (Rosenberger *et al.*, 2004; Turner *et al.*, 1998). Other antimicrobial peptides such as lactoferrins or histatins can sequester iron and thereby inhibit microbial respiration or generate reactive oxygen species (ROS) (Wiesner *et al.*, 2010). In addition to antimicrobial peptides, the mucus layer also contains secretory immunoglobulin A (hereafter referred to as "IgA") which is produced by plasma cells in the lamina propria underlying the intestinal epithelium, transported across the epithelium and secreted into the intestinal lumen via receptor-mediated transcytosis. The main function attributed to IgA is keeping antigen distant from the epithelium, a mechanism also referred to as "immune exclusion" (Brandtzaeg, 2013). The exact mechanisms of how IgA protects against a specific bacterial pathogen is the central topic of the presented thesis. Therefore, the induction of IgA and its proposed modes of action will be discussed in detail below.

The epithelium and the lamina propria as effector sites of the intestinal immune system

The epithelium and the underlying lamina propria are the effector sites of the intestinal immune system. Besides providing a physical barrier, intestinal epithelial cells are equipped with a variety of different pattern-recognition receptors (PRRs) that enable them to sense microbes in their environment and pathogens that breach the barrier (Fukata *et al.*, 2013). The PRRs include Toll-like receptors (TLRs) and C-type lectin receptors on the cell surface membrane (i.e. TLR5 for the recognition of bacterial flagellin, or Dectins for the recognition of β-glycans) as well as a variety of intracellular PRRs. NOD-like receptors (NLRs) are located in the cytoplasm and are specialized for the recognition of parts of the bacterial cell wall such as muramyldipeptid or flagellin, and bacterial DNA (Kim, Y. K. *et al.*, 2016). The activation of these receptors result in the formation of the inflammasome complex with subsequent release of the pro-inflammatory cytokines interleukin (IL)-1β and IL-18 (Lamkanfi *et al.*, 2014). Besides of being located on the cell surface, several TLRs are found in endosomes (i.e. TLR3, TLR7 and TLR8 for the recognition of double- and single-stranded RNA) or on the basolateral membrane of the intestinal epithelial cells (i.e. TLR4 or TLR5 for recognition of LPS and flagellin), where they recognize pathogen associated molecular patterns (PAMPs) after pathogen invasion into cells or into the lamina propria. Activation of TLRs generally induces a signalling cascade, leading via the adaptor molecules MyD88 and/or TRIF to the activation of MAP kinase or NFκB. This results in the subsequent transcription of a variety of pro-inflammatory genes, causing changes in the cytokine milieu and shifting the intestinal mucosa towards an inflammatory state (Fukata *et al.*, 2013).

At a frequency of 10-15 per 100 absorptive enterocytes, the intestinal epithelium contains a heterologous population of intraepithelial lymphocytes (IELs). These comprise "innate type"

IELs, but mainly antigen-experienced T cells belonging both to the T cell receptor-γδ (TCRγδ)+ and TCRαβ+ lineages (Cheroutre *et al.*, 2011; Ferguson, 1977; Sheridan *et al.*, 2010). IELs generally serve as sentinels along the intestinal epithelium and constantly monitor its state of damage and/or infection. Due to their heterogeneity, they have a wide range of functions. Upon infection, IELs rapidly react via direct cytotoxic functions or via the production of cytokines, thereby initiating inflammatory responses and clearance of pathogens.
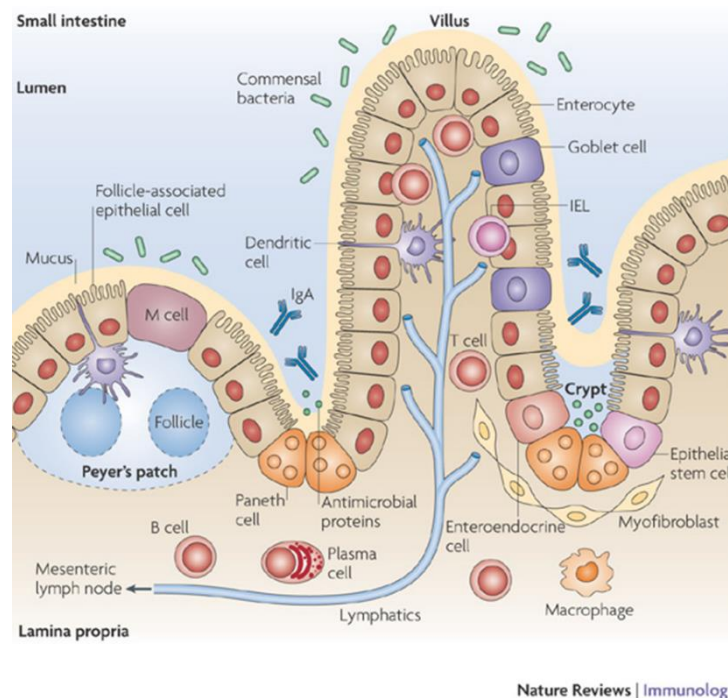
Figure 1 The intestinal mucosal barrier system. The intestinal lumen is separated from the lamina propria by a single layer of intestinal epithelial cells, organized in crypts and villi. At the bottom of the crypt, epithelial stem cells constantly divide and differentiate into intestinal epithelial cells and more specialized cell types. Interspersed between the intestinal epithelial cells are mucus secreting goblet cells and Paneth cells specialized for the production and secretion of antimicrobial peptides. The intestinal epithelium also contains intraepithelial lymphocytes (not shown), which constantly survey the environment. Microfold (M) cells overlay organized lymphoid structures such as Peyer's patches and facilitate transport of luminal antigen into these immune-inductive sites. Lamina propria migratory dendritic cells and resident macrophages take up and process antigen and eventually migrate to immuninductive sites to induce adaptive immune responses. Picture modified from Nature Reviews Immunology 10, 131-144 ((Abreu, 2010).

The lamina propria, a loose connective tissue underlying the intestinal epithelium, contains blood and lymph vessels and the nervous system of the mucosa. Interspersed within this network reside and traffic T cells, B cells and a variety of innate immune cells such as macrophages, dendritic cells (DCs), eosinophils and mast cells as wells as several innate lymphoid subsets (Mowat *et al.*, 2014; Tomasello *et al.*, 2013).

The intestinal lamina propria contains a heterologous group of CD11c+ mononuclear phagocytes that constantly monitor their environment for the presence of antigen. These mononuclear phagocytes can be classified into CD11c^{hi}CD103+CD11b+CX3CR1− cells (DCs) and CD11c^{int}CD103−CD11b+CX3CR1+ cells (macrophages). Under homeostatic conditions, CD103+CD11b+ DCs are important mediators to maintain tolerance against commensal bacteria and food antigen. These tolerogenic DCs reside close to the intestinal epithelium where they are involved in production of retinoic acid, antigen uptake and migration to secondary lymphoid structures. They favour the induction of IgA-producing B cells and regulatory T cell responses, thereby enhancing tolerance and tissue homeostasis (Aliberti, 2016; Molenaar *et al.*, 2011; Mora *et al.*, 2006). Tissue resident CD11b+CX3CR1+ macrophages can extend their long dendrites across the intestinal epithelium and sample particulate luminal antigen and bacteria (Chieppa *et al.*, 2006; Müller *et al.*, 2012; Niess *et al.*, 2005). These macrophages are directly involved in bacterial clearance, the production of IL-10 and the induction of regulatory T cell responses. Thereby they contribute to maintain the homeostatic state in the lamina propria.

The lamina propria also contains a variety of innate lymphoid cells (ILCs), characterized by their lack of antigen receptors and immunological memory. Nevertheless, they are activated during early phases of immune responses and secrete cytokines. These ILCs can be classified according to their cytokine profile like adaptive Th1-, Th2- and Th17-T lymphocytes into three main subsets: ILC1 produce Th1-cytokines like IFN-γ, ILC2s are a source of the Th2 cytokines IL-5 and IL-13, whereas ILC3s secrete IL-17A and IL-22 like their adaptive Th17 counterparts (Spits *et al.*, 2013). These ILCs are important effectors of innate immunity and have a central role in tissue remodelling and induction of lymphoid tissues (Spits *et al.*, 2013).

In addition to the IELs and the loosely distributed phagocytes and innate effector cells, the lamina propria contains organized gut-associated lymphoid tissues (GALT) throughout the intestine. These tissues are the inductive sites of the intestinal immune system, where adaptive immune responses get initiated (Figure 1).

Organized lymphoid structures in the intestine

The organized lymphoid structures of the GALT and the draining lymph nodes are the sites for priming antibody and T cell responses in the intestine. The development of these organized tissues starts prenatal and is dependent on the interaction of lymphotoxin-α1β2-expressing lymphoid-tissue inducer cells and lymphotoxin-β receptor-expressing stromal organizer cells (Mebius, 2003). The full development and function of the GALT after birth is dependent on the presence of intestinal microbes, demonstrated by the underdeveloped Peyer's patches

and low levels of IgA in neonates and in animals raised under germ-free conditions (Hanson *et al.*, 2002; Shroff *et al.*, 1995).

The best characterized tissues of the GALT are the Peyer's patches. Mature Peyer's patches contain germinal centres with B cell follicles that are surrounded by T cell areas. In contrast to the draining lymph nodes, the Peyer's patches are not encapsulated. They are the main inductive sites for the priming of intestinal IgA and T cell responses (Macpherson *et al.*, 2008). Besides the prominent Peyer's patches, the GALT also contains smaller lymphoid aggregates, ranging from small cryptopatches to mature isolated lymphoid follicles. These solitary lymphoid tissues also contain B cell areas and germinal centres, but in contrast to the Peyer's patches no T cell zones (Figure 2A) (Mowat *et al.*, 2014). Generally, these organized subepithelial lymphoid aggregates are overlaid by a follicle-associated epithelium containing microfold cells (M cells). M cells lack microvilli on their surface and are not covered with the normal thick mucus layer. They are specialized for phagocytosis and transcytosis of luminal bacteria (Owen *et al.*, 1986; Sansonetti *et al.*, 1996; Walker *et al.*, 1988), viruses (Amerongen *et al.*, 1991; Karapetian *et al.*, 1994; Sicinski *et al.*, 1990) and other particulate antigens (Ermak *et al.*, 1995). Antigens are released into the underlying supepithelial dome which contains phagocytes and DCs. After antigen uptake, the cells move towards the T cell and B cells follicles and present the processed antigen to naïve lymphocytes.

As mentioned, Peyer's patches are the major priming sites for the induction of IgA responses. In the germinal centres of the Peyer's patches, naïve B cells interact with antigen-presenting T cells or dendritic cells. Supported by the local cytokine milieu in the germinal centres, B cells undergo immunoglobulin class from IgM to IgA and can develop into IgA secreting plasma cells (discussed in detail in below).

Since antigen-loaded DCs continuously migrate from the lamina propria to the Peyer's patches and to the mesenteric lymph nodes (mLN), T cells can be activated at both of these inductive sites. During priming in the GALT, lymphocytes selectively upregulate α4β7 integrin and chemokine receptors CCR9, allowing them respond to the intestinal epithelial cell derived chemokine CCL25 and to home back to mucosal surfaces that express mucosal addressin cell-adhesion molecule 1 (Berlin *et al.*, 1993; Butcher *et al.*, 1999). The expression of this "gut-homing" pattern of adhesion-molecules and chemokine-receptors is induced through the action of retinoic acid (Hammerschmidt *et al.*, 2011; Iwata *et al.*, 2004; Mora *et al.*, 2006) and is distinct from the pattern of T cells that are primed in peripheral lymphoid organs (Campbell *et al.*, 2002). The distinct expression of homing receptors is the molecular explanation behind the compartmentalization of the intestinal immune system, meaning that priming of immune responses at systemic sites (i.e. after parenteral vaccination) does not induce a strong antibody and T cell responses at mucosal sites and vice versa (Lycke, 2012; Macpherson *et al.*, 2013; Macpherson *et al.*, 2004a; Martinoli *et al.*, 2007; Mowat *et al.*, 2014)

Induction and secretion of Immunoglobulin A

Immunoglobulin A is secreted in massive amounts into the intestinal lumen, whereas it constitutes only about 10-15% of the total immunoglobulins in the serum. Besides being secreted into the intestinal lumen, IgA is also found in other external secretions such as breast milk, saliva, tears and in the mucus of the bronchial and genitourinary tract. In its secretory form, IgA exhibits unique molecular properties. Whereas in the serum, IgA primarily exists as monomer, in external secretions IgA is found in polymeric form (mainly dimers), joined by a J-chain polypeptide and covalently associated with an 80-kDa epithelial glycoprotein, the secretory component (Pabst, 2012; Strugnell *et al.*, 2010).

The development of intestinal IgA is largely dependent on the presence of intestinal microbes, demonstrated by the much lower levels of intestinal IgA in germ free mice (Hapfelmeier *et al.*, 2010; Moreau *et al.*, 1978). As mentioned, the sites of intestinal IgA induction are the Peyer's patches, the isolated lymphoid follicles, cryptopatches and the gut-draining lymph nodes. In order to generate IgA that binds with high avidity to an antigen, two types of genetic alterations of the immunoglobulin gene are required. IgD-positive B cells that experience sufficient surface antibody cross-linking are selected into germinal centers where they receive T cell help. In the IgA-inductive sites, B cells are stimulated to replace the existing immunoglobulin heavy chain with the α heavy chain. This is accomplished by class switch recombination, which joins the heavy chain variable region to the constant Cα gene. This process takes place in the germinal centres in the Peyer's patches and is dependent on AID (activation-induced cytidine deaminase), a RNA-editing deaminase that is expressed in germinal centre B cells (Muramatsu *et al.*, 2000; Muramatsu *et al.*, 1999). Generation of IgA that binds with high-avidity to microbes (mainly pathogens) further requires somatic hypermutation, which is also dependent on AID and mediated via the help of CD4+ T cells during the germinal centre reactions (Muramatsu *et al.*, 2000; Muramatsu *et al.*, 1999).

For the T cell-dependent generation of high-avidity IgA, antigen gets sampled by M cells or DCs, which then process the antigen, migrate from the subepithelial dome into the T cell zone of the Peyer's patches (Figure 2B, left). There, antigen gets presented to naïve CD4+ T cells, which differentiate into effector T cells and upregulate the CXC-chemokine receptor 5 (CXCR5) and CD40 ligand (CD40L). The expression of CXCR5 enables the effector T cells to migrate to the B cell zone of the germinal centre, where they stimulate B cells via TCR-MHCII interactions, cytokine and co-stimulatory molecule production and CD40. This stimulation induces the expression of AID and initiates class switch recombination. The Peyer's patches contain tumour growth factor-β (TGF-β) IL-4, IL-6, and IL-10 and retinoic acid, which facilitate the expansion of IgA-expressing B cells and their differentiation to IgA-secreting plasma cells (Cazac *et al.*, 2000; Defrance *et al.*, 1992; Okahashi *et al.*, 1996; Sato *et al.*, 2003). Retinoic acid and IL-6 are thought to stimulate the differentiation of IgA-expressing cells into plasma cells

and to upregulate the expression of the gut-homing receptors CCR9 and α4β7 integrin on IgA-expressing B cells (Mora *et al.*, 2006). Local production of nitric oxide (NO) via the inducible nitric oxide synthase has been shown to be a critical mediator of class switch recombination to IgA in the intestinal lamina propria (Lee *et al.*, 2011; Tezuka *et al.*, 2007). Although the exact cellular source of NO is still under debate, NO was shown to upregulate the expression of the TGF-β receptor on B cells and has also been suggested to induce the production of BAFF (B cell activating factor) and APRIL (a proliferation inducing ligand) (Fritz *et al.*, 2012; Tezuka *et al.*, 2007). BAFF and APRIL are TNF family ligands that stimulate B cells, promote their survival and differentiation into antibody secreting plasma cells (Castigli *et al.*, 2004; Castigli *et al.*, 2005; Schneider, 2005).

Nevertheless, also T cell deficient mice can produce so-called "primitive" IgA that was shown to bind to commensals (Macpherson *et al.*, 2000; Macpherson *et al.*, 2001). B cells can become activated through multiple innate signalling pathways without the help of T cells (Figure 2B, right). The induction of T cell independent IgA is regulated by a similar set of cytokines, including IL-4, IL-10 and TGF-β. In isolated lymphoid follicles, DCs and intestinal epithelial cells can directly induce IgA class switch through the production of BAFF and APRIL (Cerutti *et al.*, 2011). Following TLR stimulation and the activation of NFκB, DCs in the lamina propria can secrete BAFF and APRIL and also express iNOS (Tezuka *et al.*, 2007). TLR stimulation in intestinal epithelial cells also contributes to the T cell independent activation of B cells. Upon recognition of bacteria through TLRs, intestinal epithelial cells themselves produce BAFF and APRIL as well as thymic stromal lymphopoietin (TSLP) and stimulate DCs in the lamina propria (He *et al.*, 2007). The presence of the CD40L-related cytokines BAFF and APRIL can lead to the expression of AID in B cells and thereby induce class switching to IgA in the absence of T cell help. Although being able to bind to commensals, the T cell independently induced "primitive" IgA binds to antigens with a much lower avidity than "classical" IgA (Macpherson *et al.*, 2000).

In addition to "primitive" and "classical" IgA, the presence of so called "natural" or "innate" IgA was described. "Natural" IgA-responses are pre-existing antibody-responses that are produced without any overt antigenic stimulation (i.e. in germ-free mice) (Slack *et al.*, 2012). However, recent next-generation sequencing indicates that the "natural" IgA repertoire originates from a pool of plasma cells that is comparable to the plasma cell pool of mice raised with a normal SPF microbiota (Lindner *et al.*, 2012). It remains possible that self- or food-antigens are responsible for expanding these clones, and it should be noted that "natural" IgA may include both T-dependent and T-independent specificities.
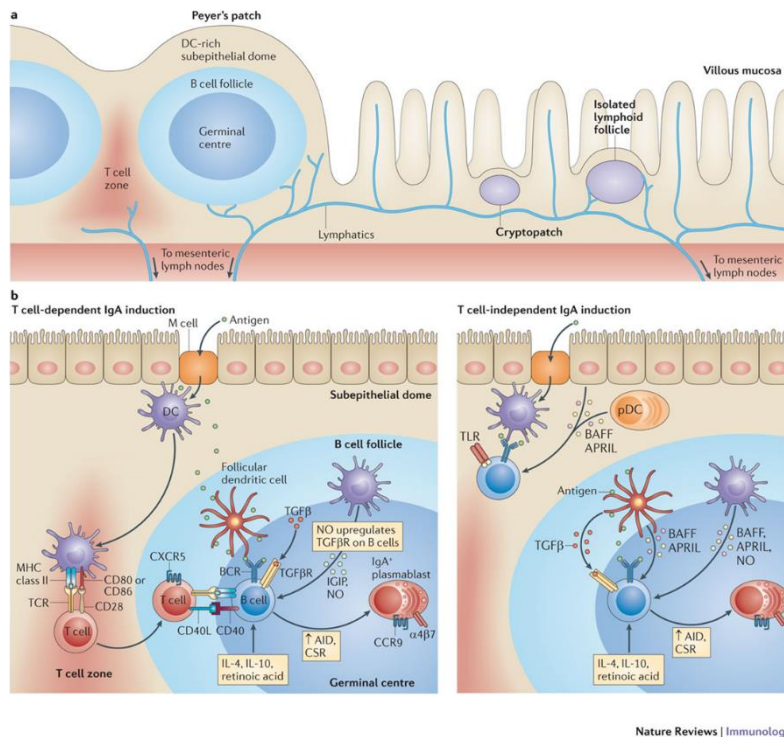
Figure 2 Induction of IgA in the gut-associated lymphoid tissues. A) Main IgA-inductive sites in the lamina propria. B) The generation of IgA-producing B cells in the germinal centres of the Peyer's patches is mainly T cell dependent. The contact of antigen-experienced T cells with naïve B cells occurs through the interaction of T cell and B cell receptor and CD40-CD40L. This induces expression of AID in B cells with subsequent class-switch recombination (CSR). C) During T cell independent IgA induction, the expression of AID is induced through innate mechanisms, including Toll-like receptor (TLR) signalling and CD40L-related cytokines B cell-activating factor (BAFF) and a proliferation-inducing ligand (APRIL), which are produced by several subsets of activated dendritic cells. Both pathways are promoted through the local micromilieu, characterized by the presence of IL-4, IL-10 and retinoic acid. Figure originally published in *Nature Reviews Immunology* 12, 821-832 (Pabst, 2012).

B cells that have undergone class switch recombination in the lamina propria (with or without the help of T cells), further differentiate into memory B cells and plasmablasts (Macpherson *et al.*, 2008). After upregulation of the gut-homing receptors α4β7, CCR9 and/or CCR10, the differentiated cells home to the intestinal lamina propria, where the plasmablasts terminally differentiate into IgA-secreting plasma cells (Brandtzaeg *et al.*, 1999). The IgA-secreting plasma cells also synthesize the J-chain, which allows the formation of stable IgA dimers or multimers. The J chain has an important role in the transport of dimeric IgA into the intestinal lumen. This transport occurs via receptor-mediated transcytosis via the polymeric-immunoglobulin receptor (pIgR) (Johansen *et al.*, 1999) (Figure 3). The pIgR is expressed at the basolateral membrane of intestinal epithelial cells and specifically binds the J chain as well as other regions of the immunoglobulin. Upon binding, the pIgR-IgA dimer complex gets internalized into a vesicle, transported to the apical membrane, where the complex is exocytosed. Upon exocytosis, the pIgR is proteolytically cleaved and the extracellular proportion of the pIgR, the secretory component, stays associated with the IgA dimer, forming

secretory IgA. The secretory component is an essential part of IgA. It ensures stability by protecting IgA from stomach acid and intestinal proteases (Lindh, 1975; Underdown *et al.*, 1974) and confers hydrophilic properties that are important for the interaction of IgA with the mucus (Phalipon *et al.*, 2002). The secretory component can also be found in a free form in the mucosal lumen as a result of transcytosis and cleavage of unbound pIgR (Strugnell *et al.*, 2010).
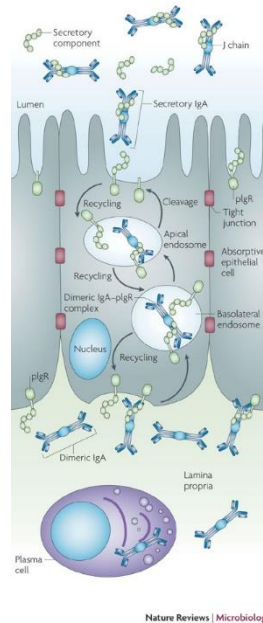
Figure 3 Secretion of IgA via receptor-mediated transcytosis across the intestinal epithelium. The polymeric-immunoglobulin receptor (pIgR) is expressed on the basolateral side of epithelial cells and specifically binds the J-chain of the immunoglobulin. The pIgR-J-chain-complex gets internalized into a vesicle, which is directed to the apical membrane for exocytosis. Following exocytosis at the apical membrane, the extracellular portion of the pIgR is proteolytically cleaved released and dimeric IgA, associated with the secretory component gets released into the intestinal lumen. Figure originally published in *Nature Reviews Microbiology* 8, 656-667 (Strugnell *et al.*, 2010).

Proposed mechanisms for IgA-mediated protection in the intestine

In humans, selective IgA deficiency is the most common primary immunodeficiency (Hammarstrom *et al.*, 2000). Although most cases are asymptomatic (Yel, 2010), in some individuals IgA-deficiency is linked to a tendency to develop recurrent respiratory and gastrointestinal infections, other disorders of the gastrointestinal tract and autoimmunity (Jorgensen *et al.*, 2013). The mild consequences of IgA deficiency could raise the question about the relevance of IgA. However, with better understanding of the complex interactions between the host and its microbiota, the role of IgA has become clearer. In the context of IgA deficiency the gut epithelium was shown to increase its antimicrobial functions by upregulating interferon-inducible immune response pathways (Shulzhenko *et al.*, 2011).

Furthermore, in many IgA-deficient patients the production and secretion of IgM is increased and therefore, a compensatory mechanism of IgM was suggested (Brandtzaeg *et al.*, 1987; Klemola, 1988). It was demonstrated that in the absence of IgA, a greater proportion of the intestinal bacteria is coated with IgM (Bunker *et al.*, 2015). However, this compensatory increase of IgM is not uniformly observed in IgA-deficient patients (Mellander *et al.*, 1986).

Mostly, the function of secretory IgA (and also IgM) has been studied in mice that lack the pIgR and therefore cannot transport these immunoglobulins across the mucosa. Compared with littermate controls, these mice show significant differences in the composition of the microbiota and increased translocation of bacteria into the gut-draining lymph nodes and to systemic sites (Reikvam *et al.*, 2012; Rogier *et al.*, 2014). The role of IgA in influencing the microbiota composition was further demonstrated in AID-deficient mice, which harbour 100-fold more anaerobic bacteria in the small intestine compared to littermate controls (Fagarasan *et al.*, 2002). Later, it was also found that these mice have increased numbers of segmented filamentous bacteria and *Clostridium* species in the small intestine (Suzuki *et al.*, 2004).

Under normal circumstances, many of the bacteria residing the intestinal tract, oral cavity, and respiratory and genital tracts are coated with IgA. It has been proposed that this limits the epithelial adherence and penetration of bacteria, thus confining bacteria to the mucosal surfaces (Macpherson *et al.*, 2005). "Primitive" IgA, produced without the help of T cells, has a rather low antigen-avidity and does not necessarily bind sufficiently strongly to intestinal microbes to exert a measurable effect. While the mode of induction and (if any) protective mechanisms of "natural" IgA and low-avidity "primitive" IgA are not well understood, high-avidity "classical" IgA can play an important role in maintaining host-microbiota mutualism and protecting the host from infections by enteropathogens (Slack *et al.*, 2012). It is generally accepted, that IgA plays an important role in the protection and homeostatic regulation of mucosal surfaces as well as for protection against enteric pathogens, however, the exact mechanisms by which IgA protects mucosal surfaces is not yet fully understood.

The primary protective mechanism attributed to IgA is immune exclusion (Figure 4A). This can be achieved by several IgA-mediated mechanisms preventing the attachment of microorganisms or toxins to the epithelial target cell. Thereby, epithelial cell surface colonization, damage and subsequent invasion are massively reduced. The main mechanism leading to immune exclusion is the ability of IgA to cross-link various antigens in the intestinal lumen. Due to its dimeric (or polymeric) form, IgA has at least four antigen binding sites. This facilitates extensive crosslinking of intestinal bacteria, viruses and proteins into macroscopic aggregates. Through steric hindrance, the densely packed mucus layer prevents too close proximity of these aggregates to the intestinal epithelium. Consequently, microorganisms, when confined within these aggregates, are thought have a massively decreased potential of reaching, adhering and potentially penetrating epithelial cells. Furthermore, due to their size,

the aggregates are thought to be more efficiently cleared from the gut via peristalsis (Lievin-Le Moal *et al.*, 2006; Mantis *et al.*, 2010; Stokes *et al.*, 1975).
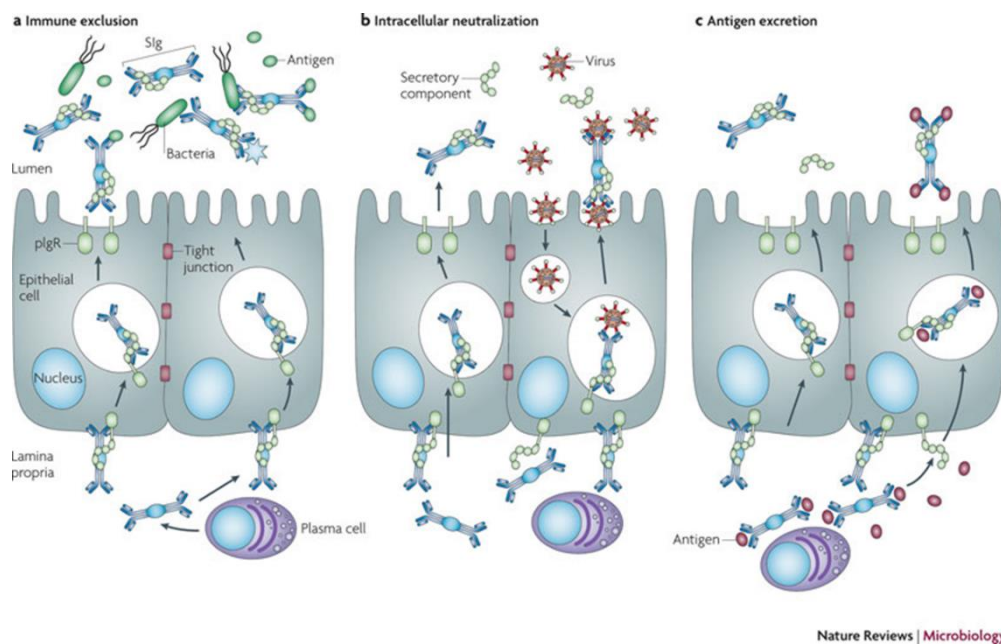
Figure 4 Proposed mechanisms for IgA-mediated protection at mucosal surfaces. A) Immune exclusion. Secretory immunoglobulins bind to luminal antigens and prevent or inhibit their attachment to and/or invasion of epithelial cells. B) Intracellular neutralization. The IgA–'joining' (J) chain–polymeric-immunoglobulin receptor (pIgR) complex mediates intracellular neutralization of pathogens that have invaded the epithelial cells. C) Antigen excretion. Excretion of antigen from the lamina propria via receptor-mediated transcytosis. Figure originally published in *Nature Reviews Microbiology* 8, 656-667 (September 2010) (Strugnell *et al.*, 2010).

Several animal models and *in vitro* studies support the theory of IgA-mediated formation of bacterial aggregates. Passive delivery of specific antibodies against *Salmonella* Typhimurium (*S.* Typhimurium) (Forbes *et al.*, 2008; Forbes *et al.*, 2012; Michetti *et al.*, 1992), *Vibrio cholerae* (Apter *et al.*, 1993; Sun *et al.*, 1990), *Shigella flexneri* (Mathias *et al.*, 2013; Phalipon *et al.*, 1995) and *Helicobacter pylori* (Blanchard *et al.*, 1995) were demonstrated to be protective against these intestinal bacterial pathogens. A recent immunization study also showed that IgA-mediated agglutination prevents *Streptococcus pneumoniae* from colonizing the upper respiratory tract of mice (Roche *et al.*, 2015). Besides passive delivery, the function of IgA was also studies in "backpack-models", where IgA-secreting hybridoma clones with a certain antigen-specificity were implanted in the back of mice (Apter *et al.*, 1993; Winner *et al.*, 1991).

Besides leading to the formation of macroscopic aggregates, IgA was also shown to directly interfere with the fitness of infectious bacteria. One of the most studied monoclonal IgA

antibodies is Sal4, which is specific for *S.* Typhimurium O antigen. When used at sub-agglutinating concentrations, Sal4 was shown to completely paralyze bacteria. The same effect was observed when Fab-fragments derived from this antibody were used (Forbes *et al.*, 2008). One of the consequences of the Sal4-mediated loss of motility was the subsequent inability of *S.* Typhimurium to invade polarized epithelial cell monolayers. Whereas the bacterial growth rates were not affected by the antibody, treatment with Sal4 was also shown to lead to an impaired translocation of effector proteins via the bacterial type-III secretion system (Forbes *et al.*, 2012) and to induce antibody-mediated distortion of the bacterial membrane. Similar effects were demonstrated for IgAC5, a murine monoclonal antibody against *S. flexneri* (Forbes *et al.*, 2011; Mathias *et al.*, 2013) and for 2D6 IgA against *V. cholerae* (Levinson *et al.*, 2015).

For *Vibrio cholerae*, the mechanism by which IgA protects goes beyond agglutination of the bacteria. In contrast to the mechanisms described above, IgA-mediated protection against *V. cholerae* is mainly mediated by blocking the attachment of cholera toxin to the GM_1 ganglioside expressed on epithelial cells. Cholera toxin consists of a B-subunit pentamer (CTB) and a single A subunit (CTA). Via CTB, the toxin binds to GM_1, followed by CTA-mediated elevation of intracellular cAMP levels, which alters the intracellular transport of sodium and calcium, and thereby causes watery diarrhoea (Ganguly *et al.*, 1996). In some studies with *V. cholerae*, IgA was shown to be protective not by crosslinking the bacteria, but by blocking the GM_1 receptor and thereby preventing the attachment of the CTB subunit (Apter *et al.*, 1993). IgA-mediated blocking of toxin binding to intestinal epithelial cells, thereby preventing damage and intoxication of the exposed cells, was also shown for *Clostridium difficile* toxin A (Stubbe *et al.*, 2000) and ricin (Mantis *et al.*, 2006). However, several other studies demonstrate that O-antigen-specific IgA is essential for protection (Kabir, 2014), presumably via aggregation, and it seems likely that both mechanisms work in parallel.

IgA-mediated blocking of adhesion to epithelial cells was also shown for viruses. By binding to surface-epitopes that are involved in the attachment to epithelial cell receptors, IgA can prevent the entry of reovirus type 1 Lang into Peyer's patches (Helander *et al.*, 2004; Hutchings *et al.*, 2004). The monoclonal antibody used in these studies was demonstrated to bind to a viral adhesion fibre, involved in the attachment of the virus to M cells (Helander *et al.*, 2003).

In addition to agglutinating bacteria, directly interfering with their fitness or preventing the binding to receptors on the intestinal epithelium, polymeric IgA was also suggested to neutralize viruses or bacterial toxins that already reside within epithelial cells (Figure 4B). Several monoclonal IgAs were shown to neutralize the replication of viruses (Burns *et al.*, 1996; Mazanec *et al.*, 1992; Ruggeri *et al.*, 1998). This neutralization is thought to occur during transcytosis of IgA across the epithelial membrane. In endosomes, specific IgA can interact with viral proteins and inhibit key processes in the replication of the virus. Furthermore, the

trafficking of bacterial toxins to their intracellular receptors can be impaired through IgA located inside the intestinal epithelial cells (Strugnell *et al.*, 2010).

A further mechanism attributed to IgA is the removal of antigen from the lamina propria back into the intestinal lumen and thereby decreasing the antigen load in the systemic compartment (Figure 4C). The export of antigen is facilitated via binding of dimeric IgA and subsequent pIgR-mediated transport across intestinal epithelial cells. IgA-pIgR-mediated transport of antigen from the basolateral membrane and apical release has so far been shown *in vitro* for soluble immune complexes (Kaetzel *et al.*, 1991) and measles- and HIV-virions (Kaetzel *et al.*, 1994; Wright *et al.*, 2008; Yan *et al.*, 2002). Further, IgA-mediated export of the antigen was demonstrated in immunized mice after intravenous challenge (Robinson *et al.*, 2001).

Although there is no clear evidence for an IgA-specific receptor on M cells, these cells were shown to selectively bind and take up IgA and IgA-immune-complexes by a still unknown mechanism (Mantis *et al.*, 2002; Rochereau *et al.*, 2013). After transcytosis, IgA-antigen complexes get phagocytosed by dendritic cells in the subepithelial dome. Therefore, beside excluding antigen from the intestinal epithelium or even excreting antigen from the lamina propria back into the intestinal lumen, IgA was also suggested to have a more "pro-inflammatory" role by promoting antigen uptake by M cells.

Most of the studies discussed above were performed either *in vitro* with polarized cell layers, *in vivo* by passive transfer of monoclonal antibodies, or in mice carrying IgA-secreting backpack tumours. Although these studies contributed significantly to a better understanding of how IgA can protect at mucosal surfaces, one needs to keep in mind that a) under natural conditions, mucosal immune responses are polyclonal and probably more efficient, and b) the therapeutic applications of monoclonal antibacterial antibodies are extremely limited, if not impossible (Gisbert *et al.*, 2009). In order to induce polyclonal intestinal IgA responses, a variety of oral vaccination approaches have been tested (discussed below).

Strategies to induce anti-bacterial IgA responses by oral vaccines

The mucosal immune system is compartmentalized away from systemic sites (Macpherson *et al.*, 2004a; Martinoli *et al.*, 2007). Therefore, induction of intestinal IgA responses requires oral delivery of the antigen. However, since the gastrointestinal tract is colonized with a dense microbiota and repeatedly flooded with food antigens, the induction of adaptive immunity in the intestine is tightly regulated. We have recently reviewed the current understanding of the requirements for the successful induction of an anti-bacterial IgA response by an oral vaccine

(Moor *et al.*, 2015). These requirements are summarized in this section and further discussed in Chapter 6 of the presented thesis.

For the successful induction of an intestinal IgA response it is crucial that enough antigen is delivered to the GALT. Studies with reversible colonizing avirulent bacteria in germ-free mice have revealed a high threshold for induction of high-avidity IgA (Hapfelmeier *et al.*, 2010). In order to deliver high amounts of antigen via the oral route live-attenuated bacterial strains were extensively studied. When using live attenuated vaccine strains, a challenging balance needs to be completed. Live vaccine strains need to be sufficiently attenuated in order to avoid persistent colonization and induction of clinical symptoms; on the other hand, over-attenuation can lead to the loss of immunogenicity (recently reviewed in (Moor *et al.*, 2015)). In *Salmonella*, attenuation is achieved by deletion of a variety of genes encoding for proteins required for either key steps in bacterial metabolism, or signalling and regulation of virulence factors. All strategies result in impaired survival of the vaccine strain after oral administration. The targeted genes encode for proteins involved in aromatic amino acid biosynthesis (*aroA*, *aroC*, *aroD*) (Eisenstein *et al.*, 1984; Harrison *et al.*, 1997; Hoiseth *et al.*, 1981; Hormaeche *et al.*, 1996; Killar *et al.*, 1985), galactose biosynthesis (*galE*), heat shock protein (*htrA*) (Chatfield *et al.*, 1992; Lowe *et al.*, 1999; Tacket *et al.*, 1997), guanine or purine nucleotide biosynthesis (*guaA*, *guaB purA*, *purB*, *purE*, *purH*) (Simon *et al.*, 2011), adenylate cyclase signalling (*cya*, *crp*) (Coe *et al.*, 1992; Curtiss *et al.*, 1987; Hassan *et al.*, 1990, 1996), two-component regulatory systems (*phoP*, *phoQ*) (Galan *et al.*, 1989; Hohmann *et al.*, 1996; Matsui *et al.*, 2015), regulators of protein metabolism (*clpP*, *clpX*) (Matsui *et al.*, 2003), outer membrane proteins (*ompC*, *ompF*, *ompR*) (Simon *et al.*, 2011), and DNA recombination and repair pathways (*recA*, *recB*, *recC*) (Simon *et al.*, 2011). Although many of these studies demonstrated successful vaccination protection in mouse models (Simon *et al.*, 2011), most of them failed in human clinical trials, often due to unfavourable side effects in healthy volunteers (Dilts *et al.*, 2000; Hone *et al.*, 1992; Tacket *et al.*, 1992). A risk with any live-attenuated oral vaccine is, that they are likely to cause severe infection in patients with inherited or acquired immuodeficiencies (Casanova *et al.*, 1995; Felmy *et al.*, 2013; Hesseling *et al.*, 2006). In order to improve safety in immunocompromised mice, recent studies with superattenuated *S.* Typhimurium strains have been performed. These strains harbour additional mutations on top of the defect in the structural protein type III secretion system 2 (*ssaV*) (Pati *et al.*, 2013; Periaswamy *et al.*, 2012; Vishwakarma *et al.*, 2012; Vishwakarma *et al.*, 2014). Nevertheless, even though these strains were safer than less attenuated vaccine strains, they were still able to colonize tissues and safety was only reported at early time points after application in immunodeficient animals. Further strategies have employed so called "delayed-attenuated" strains, which are only virulent under *in vitro* culture conditions but lose their virulence in the gastrointestinal tract

(Curtiss *et al.*, 2009) or vaccine strains that spontaneously lyse after a short period *in vivo* (Kong *et al.*, 2008).

An alternative strategy is the repeated oral delivery of high amounts of sterile antigen. Both currently available Cholera vaccines Shanchol[TM] and Dukoral[TM] consist of inactivated whole cells. Shanchol[TM] contains three strains of *V. cholerae* O1 and one of *V. cholerae* O129 and is orally administered in two doses of 1.75×10^{11} cells in a 14-day schedule. Dukoral[TM] consists of whole cell *V. cholerae* O1 plus recombinant cholera toxin B subunit (rCTB) and is administered on a similar schedule. Both vaccines are inactivated by either formalin treatment or heat. The major difference between Shanchol[TM] and Dukoral[TM] is the presence of rCTB. These vaccines were always assumed to work due to the presence of cholera toxin, either at very low concentrations in the inactivated whole cells or additionally added in recombinant form. Cholera toxin is one of very few known mucosal adjuvants that can promote immunity (Langridge *et al.*, 2010; Svennerholm *et al.*, 1976). However, in controlled clinical trials such synergistic effect could not be demonstrated (Black *et al.*, 1987). The dose of killed bacteria given with these vaccines may actually be sufficient to induce mucosal immunity, without any additional adjuvant. In agreement with this, the oral administration of high doses of peracetic acid killed *Salmonella* without any added adjuvant induced protective intestinal IgA-responses in mice (Moor *et al.*, 2016).

In the blood, spleen and peripheral lymph nodes it has long been noted that generation of effective memory responses requires not just antigen, but also adjuvant (Janeway, 1989). This is not an absolute requirement for the generation of intestinal high-avidity IgA. Nevertheless, cholera toxin (and the closely related heat-labile toxin from *E. coli*) and retinoic acid, a product of Vitamin A metabolism, have demonstrated strong adjuvantivity for the induction of high-avidity IgA. Cholera toxin B subunit, the toxin portion responsible for translocating the catalytic A subunit across the plasma membrane, appears to function by disrupting homeostatic signalling in epithelial cells after binding to surface GM1 receptor (Glenn *et al.*, 2009). This seems to generate a "danger signal" that translates well into local germinal centre formation. Retinoic acid induces the expression of gut-homing addressins (Iwata *et al.*, 2004) and can directly modulate T cell responses (Benson *et al.*, 2007). In addition, retinoic acid induces isotype switching to IgA (Chen *et al.*, 2013; Mora *et al.*, 2006) and retinoic acid signalling in B cells has been shown to be essential for induction of antigen-specific high-avidity IgA responses after oral immunization (Pantazi *et al.*, 2015). Several studies have demonstrated a positive effect of retinoic acid as an adjuvant for vaccination against mucosal infections (Hammerschmidt *et al.*, 2011; Pantazi *et al.*, 2015; Tan *et al.*, 2011).

A further requirement for the induction of high-avidity IgA responses seems to be that antigen is delivered in particulate form. This enables antigen uptake via M cells (Mabbott *et al.*, 2013) or intestinal phagocytes that sample luminal antigen via their long dendrites (Chieppa *et al.*,

2006; Müller *et al.*, 2012; Niess *et al.*, 2005). In contrast, the oral administration of ultraheat-killed bacteria that have lost structural integrity is much less efficient in inducing high-avidity IgA responses (Hapfelmeier *et al.*, 2010; Macpherson *et al.*, 2004b). Rather than inducing high-avidity IgA responses, the oral administration of soluble antigen leads to the induction of oral tolerance. Oral tolerance has been defined as unresponsiveness to systemic challenge with antigens previously administered orally, e.g., lack of delayed type hypersensitivity reactions and failure to boost systemic IgG responses (Weiner *et al.*, 2011). This process is thought to play a crucial role in preventing hypersensitivity reactions towards food antigens. In agreement with the need for particulate antigen, it was shown that oral administration of nanoparticles coated with OVA can induce high-avidity IgA responses (Howe *et al.*, 2015). It has further been suggested that antigen encapsulation in beta-glucan micro- or nanoparticles enhances the mucosal immune response induced after oral application (De Smet *et al.*, 2013). This effect may be due to the interaction of beta glucans with the pattern recognition receptor Dectin-1, which has also been suggested to play a role in transcytosis by M cells (Rochereau *et al.*, 2013). Inclusion of other M-cell-targeting moieties such as IgA-specific lectins or DEC205-binding proteins into nanoparticles may also enhance M cell transcytosis from the gut lumen into the Peyer's patches (Vyas *et al.*, 2007), thus further improving antigen delivery.

Besides the antigen-delivery form, there is increasing evidence that the state of the host affects the success of high-avidity IgA induction by oral vaccines. Several clinical trials have demonstrated diminished immune responses and/or lower vaccine efficacy of oral vaccines in developing countries (Levine, 2010). Several factors are thought to lead to this phenomena. The lack of micronutrients such as vitamin A (Kaufman *et al.*, 2011; Mora *et al.*, 2008) and zinc (Ibs *et al.*, 2003) as well as pre-existing intestinal inflammation (chronic environmental enteropathy) are suspected to causes of the failure of oral vaccines (Keusch *et al.*, 2014; Korpe *et al.*, 2012). In endemic regions, it has also been hypothesized that transfer of maternal antibodies (via placenta or breast milk) could negatively influence the potential of oral vaccines to induce immune responses in young children (Levine, 2010). In addition, differences in host genetics were correlated to variation in seroconversion to an oral cholera vaccine (Majumder *et al.*, 2013). Besides pathogenic infection and genetic factors, there is strong evidence that also the host microbiota influences the responsiveness to oral vaccines (Moor *et al.*, 2016; Stecher *et al.*, 2010). Certain species of the intestinal microbiota can degrade the secretory component of IgA and thereby reduce the levels of total intestinal IgA (Moon *et al.*, 2015). Further, there are numerous studies suggesting that antibiotic treatment either enhances or inhibits the response to oral vaccines (Endt *et al.*, 2012; Moor *et al.*, 2016; Praharaj *et al.*, 2015; Uchiyama *et al.*, 2014).

Quantification of vaccine-induced antibodies at mucosal surfaces.

The role of antibodies in host-bacterial interactions is clearly critical in both protection from pathogenic infection (Maclennan, 2014) and in influencing mutualistic interactions with the microbiota (Slack *et al.*, 2014). The correlation between high avidity IgA-titres and resistance to infection was described in several studies, mainly dealing with immunity to *V. cholerae* in humans (Johnson *et al.*, 2012; Uddin *et al.*, 2014; Uddin *et al.*, 2011) and protection against influenza virus in mice (Eliasson *et al.*, 2011).

In order to quantify the amount of antibodies specific for bacteria or viruses, several techniques have been used. The presence of high-avidity antibodies (i.e. IgA against cholera-LPS in the faeces) can be quantified by plate-based assays like ELISA or ELISPOT. Therefore, plastic plates are loaded with purified surface carbohydrates, toxins or whole bacteria (Johnson *et al.*, 2012; Lécuyer *et al.*, 2014; Saletti *et al.*, 2013; Uddin *et al.*, 2014; Uddin *et al.*, 2011). In addition, semi-quantitative gel/membrane based techniques such as dot-blotting and western blotting can be used, where the target material is loaded on membranes (Endt *et al.*, 2010; Macpherson *et al.*, 2004b). Although these techniques have a long tradition and yielded useful data, they have several disadvantages. The use of cell lysates as target material can lead to an overestimation of the result, since bacterial cytosolic proteins are highly conserved and result in cross-reactivity (Yutin *et al.*, 2012). In order to avoid high cross-reactivity, bacterial compounds need to be purified to homogeneity. Further, there can be high variation in the binding efficiency of the target material to plastic or membrane scaffolds.

Quantification of antibodies isolated from mucosal surfaces is extremely challenging. In contrast to the systemic immune system, which is compartmentalized away from bacterial exposure on mucosal surfaces (Macpherson *et al.*, 2013), the mucosal immune system will always produce a immunoglobulins against the present microbiota. Therefore antibody fluids isolated from mucosal surfaces (i.e. from the intestine) will always contain antibodies against the microbiota (Macpherson *et al.*, 2004b). Here, the issue of high level cross-reactivity can make it extremely challenging to quantify the immune response of interest using techniques based on bulk lysed bacteria.

In order to quantify IgA induced by oral delivery of antigen a flow cytometry based technique can be used (Endt *et al.*, 2010; Hapfelmeier *et al.*, 2010; Moor *et al.*, 2016; Slack *et al.*, 2009). The so called bacterial FACS method is based on the incubation of a low number of bacterial cells from a pure culture with an antibody-containing bodily fluid (serum, plasma, intestinal/bronchial/vaginal lavage, purified antibodies from saliva, breast milk etc.). After washing, bound antibody is visualized with appropriate secondary reagents and the median fluorescence is detected by single cell flow cytometry. The ability to gate on whole bacterial cells exclusively quantifies antibodies bound to bacterial surface-exposed epitopes. Median

fluorescence intensities, relative to the dilution factor or antibody concentrations can then be analysed to calculate titres.

Bacterial FACS is an extremely sensitive technique and has several advantages over other techniques as it requires only minute quantities of immunoglobulins and very low densities of bacterial targets, thereby allowing analysis of responses against fastidious species. Since the technique quantifies bacterial surface binding antibodies, it can be used to track the success of oral vaccination. When combined with cross-adsorption (i.e. removal of specific antibodies by saturating out-titration with the same bacterial strain or related strains of interest), it permits the identification of immunologically relevant exposure to defined bacterial species with much greater certainty than other techniques (Balmer *et al.*, 2014; Endt *et al.*, 2010; Haas *et al.*, 2011; Hapfelmeier *et al.*, 2010; Seleznik *et al.*, 2012; Slack *et al.*, 2009). It is therefore particularly useful in quantifying antibody titres in situations where other techniques yield high background (Balmer *et al.*, 2014; Endt *et al.*, 2010; Haas *et al.*, 2011).

The detailed protocol for antibody analysis by bacterial FACS the applications and limitations are described in Chapter 3 of the present thesis.

The streptomycin mouse model- a broadly used tool to study pathogen-host interactions

Gastro-intestinal infections due to the consumption of contaminated food or water are still a leading cause of morbidity and mortality, especially in the developing world. A substantial proportion of food-borne infection is caused by gram-negative, facultative intracellular *Salmonella* species. Most clinical relevant serovars belong to *S. enterica* subspecies enterica and they cause various symptoms in the infected host. After ingestion, the typhoid serovars *S.* Typhi and *S.* Paratyphi A cause typhoid fever, a systemic infection (Wain *et al.*, 2015). These serovars are strictly adapted to humans and higher primates, therefore there exists no suitable mouse-infection model that would allow studies of pathogen-host interaction with these serovars. In contrast, the non-typhoidal serovars *S.* Enteritidis and *S.* Typhimurium can infect a broad range of hosts, causing diseases from self-limiting gastroenteritis to systemic typhoid fever-like infections (Gal-Mor *et al.*, 2014).

The only licensed oral vaccine against *Salmonella* is Vivotif^{TM}, based on the live attenuated *S.* Typhi strain Thy21a (Levine *et al.*, 1999; Tennant *et al.*, 2015; Wahid *et al.*, 2012). However, like with other oral vaccines, the efficacy of Thy21a is rather poor, especially in developing countries (Levine, 2010). There are no licensed human vaccines against non-typhoidal *Salmonella* strains. In order to study how and to what extend oral vaccines can protect against *Salmonella* species, we have developed an inactivated oral vaccine and demonstrated its

ability to induce high levels of intestinal high-avidity IgA responses in the complete absence of intestinal pathology. Further, we tested the safety of the killed vaccine in immunocompromised mice (Moor *et al.*, 2016). In order to investigate the mechanism of how vaccine-induced IgA can protect against *S.* Typhimurium, we made use of the well-established streptomycin mouse model (Barthel *et al.*, 2003).

If SPF mice are infected orally with *S.* Typhimurium only about 5% of the animals develop enteropathy (Stecher *et al.*, 2010; Stecher *et al.*, 2011). To overcome this colonization resistance, mice can be treated orally with a single dose of streptomycin one day prior to infection (Barthel *et al.*, 2003). The transient suppression of the microbiota enables *S.* Typhimurium to rapidly and efficiently colonize the murine cecum and colon, reaching numbers of up to 10^{10} CFU per gram content, independent of the infection dose (Barthel *et al.*, 2003; Stecher *et al.*, 2007). The pathogen then uses its flagella and follows chemotactic gradients to swim towards the epithelium. To adhere to the intestinal epithelium, *S.* Typhimurium employs adhesins and fimbriae. *S.* Typhimurium uses several mechanisms to cross the epithelium and elicit this acute mucosal inflammatory response by several pathways (Hapfelmeier *et al.*, 2004; Hapfelmeier *et al.*, 2008). The two main virulence factors of *S.* Typhimurium are the two type-III secretion systems TTSS-1 and TTSS-2, which are encoded in the *Salmonella* pathogenicity island 1 (SPI1) and SPI2. Upon adhesion to intestinal epithelial cells, *S.* Typhimurium injects a cocktail of effector proteins (SipA, SopB, SopE and SopE2) into the host cell via the TTSS-1 (Galan, 2001; Hapfelmeier *et al.*, 2004). These effectors were shown to actively destroy M cells overlaying the Peyer's patches (Clark *et al.*, 1996; Jones *et al.*, 1994) and thereby disrupting the epithelial cell barrier. Further, after injection into intestinal epithelial cells, these effectors lead to rearrangement of the actin cytoskeleton and facilitate the invasion of the bacterium (Galan, 2001; Hapfelmeier *et al.*, 2004). The pathogen was also shown to degrade tight junctions between intestinal epithelial cells (Boyle *et al.*, 2006; Jepson *et al.*, 1995) also leading to disruption of the epithelial cell barrier. After entering the intestinal epithelial cell, *S.* Typhimurium employs the TTSS-2 to reside within a *Salmonella* containing vacuole, in which the bacterium traffics to the basolateral side of the cell, where its gets released into the interstitial space (Müller *et al.*, 2012). The extracellular pathogens can also be internalized by lamina propria mononuclear phagocytes, including CX_3CR1^{high} macrophages which extend their dendrites across the epithelium to take up luminal antigen (Niess *et al.*, 2005). These phagocytes on one hand eradicate the pathogen by phagocytosis, on the other hand signalling via their pathogen recognition receptors stimulates the production of various pro-inflammatory cytokines, switching the intestinal mucosa to a defense state. However again by employing the TTSS-2, the pathogen can not only survive, but also replicate in these phagocytes, which then serve as replicative niche (Hapfelmeier *et al.*, 2008; Müller *et al.*, 2012).

As a consequence of the high pathogen load in the intestinal mucosa, all infected mice develop robust intestinal inflammation, characterized by mucosal oedema, infiltration of polymorphonuclear granulocytes and monocytic phagocytes, epithelial damage and reduced numbers of goblet cells (Barthel *et al.*, 2003). At later stages of the infection, S. Typhimurium spreads to systemic sites, like the mLN, liver and spleen. This well-established and robust infection protocol makes the streptomycin mouse model a powerful tool to study defense mechanisms in the intestine.

The break of colonization resistance by antibiotic perturbation and the rapid overgrowth of *Salmonella* shifts the intestinal ecosystem to a state of massive dysbiosis (Stecher *et al.*, 2007). Such "blooms" can also occur as a consequence of the introduction of new nutrients into an ecosystem or as a result of host immunodeficiency or disease (Stecher *et al.*, 2011). The overgrowth of bacteria that under homeostatic conditions are absent or underrepresented was shown to be associated with an increased rate of horizontal gene transfer between bacteria (Stecher *et al.*, 2013b). Due to the enormous density of bacteria in the intestine, the frequency of horizontal gene transfer is per se higher than in other ecosystems (Kelly *et al.*, 2009). Horizontal gene transfer can occur via the uptake of naked DNA by natural transformation, phage-mediated transduction and the exchange of plasmids by conjugation (Soucy *et al.*, 2015). The genetic elements that are transmitted often encode for virulence or fitness factors (Brussow *et al.*, 2004; Elwell *et al.*, 1980). It was recently shown that during *Salmonella* colitis, the conjugative colicin plasmid p2 is transferred at high frequency from S. Typhimurium to the resident *E. coli* by conjugation, whereas under normal condition this process is blocked by the commensal microbiota (Stecher *et al.*, 2012). Therefore, blooms of *Salmonella* not only damage the host, but they are also a hotspot for horizontal gene transfer and can contribute to pathogen evolution.

Besides of investigating molecular mechanisms characterizing this bacterial infection, recent work using the streptomycin mouse model has focused on population biological aspects of how *S*. Typhimurium colonizes its host. Infections with bacteria harbouring neutral barcodes in their genome (Grant *et al.*, 2008) and/or bacteria carrying plasmids that get lost upon replication in the host (Gil *et al.*, 1991), have enabled us to dissect the infection process in distinct steps. During the first twelve hours post infection, *S*. Typhimurium rapidly replicates and colonizes the cecum at a density of 10^{10} CFU per gram content. The next step towards a systemic infection is the migration to and colonization of the mLN. Using a stochastic birth-death model, the bacterial population size in the mLN nodes can be predicted as a function of the bacterial immigration rate into the mLN, the replication within the mLN and the rate of clearance from the mLN (Figure 5) (Kaiser *et al.*, 2013). Further, it was shown that upon antibiotic treatment of the mouse, the *Salmonella* can exist in two different states: as a fast-growing population that spreads in the host's tissues and as a slow-growing "persister"

subpopulation that hides inside dendritic cells and therefore cannot be killed by the antibiotic (Kaiser *et al.*, 2014). Another study focussing on the *Salmonella* population in the intestinal lumen could show that at day 2 post infection, this population drastically drops. Granulocytes infiltrating the intestinal lumen reduce the size of the luminal *Salmonella* population by as much as 10^5-fold. This drastic reduction is again followed by a growth phase, allowing *S.* Typhimurium to re-colonize the intestinal lumen at high numbers (Maier *et al.*, 2014).
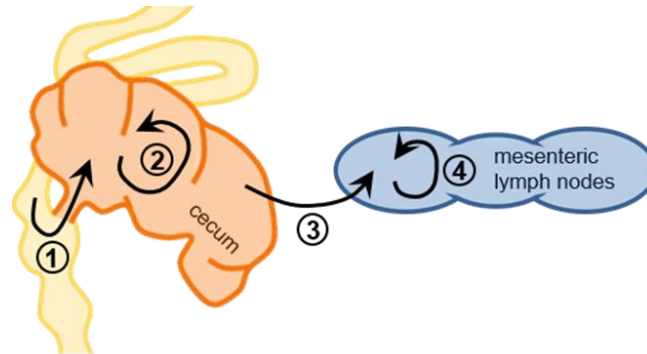

Figure 5 Modelling within-host population dynamics during *Salmonella* infection. After oral infection, S*. Typhimurium* colonizes the cecum (1), replicates in the cecum (2) and reaches densities of 10^{10} CFU per gram content. At later stages of the infection, the bacteria migrate to the mesenteric lymph nodes (mLN) (3). Inside the mLN, the bacteria replicate but also get killed, resulting in a net replication rate. At later stages, S*. Typhimurium* spreads to other systemic sites such as the spleen and liver (not shown). Picture adapted from PLoS Pathogen. 2013 Sep; 9(9) (Kaiser *et al.*, 2013).

The understanding of where exactly the pathogen enters, which compartments it colonizes, where it replicates and eventually gets cleared or hides has profited a lot from these within-host population dynamic models. This knowledge is absolutely required in order to understand, how and to what extent the mucosal immune system can counteract these processes.

Therefore, besides serving as a reliable model to study the molecular basis of *S.* Typhimurium infection, the streptomycin mouse model, in combination with a variety of genetic tools (on the bacterial as well as on the host side) and within-host population dynamical models, is an optimal system to study and decipher the mechanism of IgA-mediated protection against *S.* Typhimurium and will be used throughout the presented thesis.

Aims of the presented thesis

IgA is an enigmatic antibody secreted in massive amounts across mucosal surfaces. Although it is broadly accepted that IgA plays an important role in coordinating the establishment and the maintenance of the intestinal microbiota (Pabst *et al.*, 2016), very little is understood about the protective mechanisms attributed to this antibody isotype. Only very few mucosal vaccines that aim at inducing intestinal IgA are in regular clinical use, predominantly as trials have ended with excess adverse effects or poor protection (Lycke, 2012). This can most likely be attributed to our poor understanding of how exactly protective immunity at mucosal surfaces functions. The presented work aims towards a better understanding of IgA-mediated protection during blooms of *S.* Typhimurium after antibiotic-induced dysbiosis.

In Chapter 2 we aimed to develop a robust non-inflammatory protocol for the induction of high-avidity intestinal IgA. As oral high-doses of live non-virulent bacteria had previously been shown to induce high-avidity IgA (Hapfelmeier *et al.* 2010), we investigated the immunogenic potential of inactivated oral vaccines. A variety of inactivation methods were tested for sufficiently efficient bacterial inactivation. The only procedure that could reliably inactivated concentrations of more than 10^{11} *Salmonella* CFU whilst maintaining antigenicity was 1% peracetic acid treatment. We therefore tested the ability of this protocol to generate oral vaccines from a broad range of bacterial species, and to mediate protection from non-typhoidal Salmonellosis in mice with severe innate immune deficiencies.

In Chapter 3 we aimed to develop a protocol to reliably quantify only high-avidity bacterial surface-specific antibodies: i.e. the responses most likely to be relevant to protection. This technique is was extensively tested in a broad range of systems. Further, a cross-adsorption technique was developed to investigate the specificity of antibody responses. This protocol has several advantages over ELISA and Western blotting-based techniques and was used to measure vaccine induced antibody-titres throughout the presented thesis.

In Chapter 4 we aimed to investigate the effect of the host on phage transfer *in vivo*. We were testing the role of inflammation, and hence the ability of vaccination, which inhibits inflammation, to prevent phage transfer.

In Chapter 5 we aimed to determine mechanistically how high avidity IgA protects during non-typhoidal Salmonellosis. Therefore we applied mathematical modelling techniques to reveal complex behaviours of the system and investigated the presence of predicted population genetics effects of IgA-mediated enchained growth.

Chapter 6 contains the overall conclusion of the presented work and discusses limitations and further perspectives.

References

Abreu, M. T. (2010). Toll-like receptor signalling in the intestinal epithelium: how bacterial recognition shapes intestinal function. *Nat Rev Immunol, 10*(2), 131-144.

Aliberti, J. (2016). Immunity and Tolerance Induced by Intestinal Mucosal Dendritic Cells. *Mediators Inflamm, 2016*, 3104727.

Amerongen, H. M., Weltzin, R., Farnet, C. M., Michetti, P., Haseltine, W. A., & Neutra, M. R. (1991). Transepithelial transport of HIV-1 by intestinal M cells: a mechanism for transmission of AIDS. *J Acquir Immune Defic Syndr, 4*(8), 760-765.

Apter, F. M., Michetti, P., Winner, L. S., 3rd, Mack, J. A., Mekalanos, J. J., & Neutra, M. R. (1993). Analysis of the roles of antilipopolysaccharide and anti-cholera toxin immunoglobulin A (IgA) antibodies in protection against Vibrio cholerae and cholera toxin by use of monoclonal IgA antibodies in vivo. *Infect Immun, 61*(12), 5279-5285.

Balmer, M. L., Slack, E., de Gottardi, A., Lawson, M. A., Hapfelmeier, S., Miele, L., Grieco, A., Van Vlierberghe, H., Fahrner, R., Patuto, N., Bernsmeier, C., Ronchi, F., Wyss, M., Stroka, D., Dickgreber, N., Heim, M. H., McCoy, K. D., & Macpherson, A. J. (2014). The liver may act as a firewall mediating mutualism between the host and its gut commensal microbiota. *Sci Transl Med, 6*(237), 237ra266.

Barthel, M., Hapfelmeier, S., Quintanilla-Martinez, L., Kremer, M., Rohde, M., Hogardt, M., Pfeffer, K., Russmann, H., & Hardt, W. D. (2003). Pretreatment of mice with streptomycin provides a Salmonella enterica serovar Typhimurium colitis model that allows analysis of both pathogen and host. *Infect Immun, 71*(5), 2839-2858.

Benson, M. J., Pino-Lagos, K., Rosemblatt, M., & Noelle, R. J. (2007). All-trans retinoic acid mediates enhanced T reg cell growth, differentiation, and gut homing in the face of high levels of co-stimulation. *J Exp Med, 204*(8), 1765-1774.

Berlin, C., Berg, E. L., Briskin, M. J., Andrew, D. P., Kilshaw, P. J., Holzmann, B., Weissman, I. L., Hamann, A., & Butcher, E. C. (1993). Alpha 4 beta 7 integrin mediates lymphocyte binding to the mucosal vascular addressin MAdCAM-1. *Cell, 74*(1), 185-195.

Black, R. E., Levine, M. M., Clements, M. L., Young, C. R., Svennerholm, A. M., & Holmgren, J. (1987). Protective efficacy in humans of killed whole-vibrio oral cholera vaccine with and without the B subunit of cholera toxin. *Infect Immun, 55*(5), 1116-1120.

Blanchard, T. G., Czinn, S. J., Maurer, R., Thomas, W. D., Soman, G., & Nedrud, J. G. (1995). Urease-specific monoclonal antibodies prevent Helicobacter felis infection in mice. *Infect Immun, 63*(4), 1394-1399.

Boyle, E. C., Brown, N. F., & Finlay, B. B. (2006). Salmonella enterica serovar Typhimurium effectors SopB, SopE, SopE2 and SipA disrupt tight junction structure and function. *Cell Microbiol, 8*(12), 1946-1957.

Brandtzaeg, P. (2013). Secretory IgA: Designed for Anti-Microbial Defense. *Front Immunol, 4*, 222.

Brandtzaeg, P., Farstad, I. N., Johansen, F. E., Morton, H. C., Norderhaug, I. N., & Yamanaka, T. (1999). The B-cell system of human mucosae and exocrine glands. *Immunol Rev, 171*, 45-87.

Brandtzaeg, P., Karlsson, G., Hansson, G., Petruson, B., Bjorkander, J., & Hanson, L. A. (1987). The clinical condition of IgA-deficient patients is related to the proportion of IgD- and IgM-producing cells in their nasal mucosa. *Clin Exp Immunol, 67*(3), 626-636.

Brussow, H., Canchaya, C., & Hardt, W. D. (2004). Phages and the evolution of bacterial pathogens: from genomic rearrangements to lysogenic conversion. *Microbiol Mol Biol Rev, 68*(3), 560-602, table of contents.

Bunker, J. J., Flynn, T. M., Koval, J. C., Shaw, D. G., Meisel, M., McDonald, B. D., Ishizuka, I. E., Dent, A. L., Wilson, P. C., Jabri, B., Antonopoulos, D. A., & Bendelac, A. (2015). Innate and Adaptive Humoral Responses Coat Distinct Commensal Bacteria with Immunoglobulin A. *Immunity, 43*(3), 541-553.

Burns, J. W., Siadat-Pajouh, M., Krishnaney, A. A., & Greenberg, H. B. (1996). Protective effect of rotavirus VP6-specific IgA monoclonal antibodies that lack neutralizing activity. *Science, 272*(5258), 104-107.

Butcher, E. C., Williams, M., Youngman, K., Rott, L., & Briskin, M. (1999). Lymphocyte trafficking and regional immunity. *Adv Immunol, 72*, 209-253.

Campbell, D. J., & Butcher, E. C. (2002). Rapid acquisition of tissue-specific homing phenotypes by CD4(+) T cells activated in cutaneous or mucosal lymphoid tissues. *J Exp Med, 195*(1), 135-141.

Casanova, J. L., Jouanguy, E., Lamhamedi, S., Blanche, S., & Fischer, A. (1995). Immunological conditions of children with BCG disseminated infection. *Lancet, 346*(8974), 581.

Castigli, E., Scott, S., Dedeoglu, F., Bryce, P., Jabara, H., Bhan, A. K., Mizoguchi, E., & Geha, R. S. (2004). Impaired IgA class switching in APRIL-deficient mice. *Proc Natl Acad Sci U S A, 101*(11), 3903-3908.

Castigli, E., Wilson, S. A., Scott, S., Dedeoglu, F., Xu, S., Lam, K. P., Bram, R. J., Jabara, H., & Geha, R. S. (2005). TACI and BAFF-R mediate isotype switching in B cells. *J Exp Med, 201*(1), 35-39.

Cazac, B. B., & Roes, J. (2000). TGF-beta receptor controls B cell responsiveness and induction of IgA in vivo. *Immunity, 13*(4), 443-451.

Cerutti, A., Chen, K., & Chorny, A. (2011). Immunoglobulin responses at the mucosal interface. *Annu Rev Immunol, 29*, 273-293.

Chatfield, S. N., Strahan, K., Pickard, D., Charles, I. G., Hormaeche, C. E., & Dougan, G. (1992). Evaluation of Salmonella typhimurium strains harbouring defined mutations in htrA and aroA in the murine salmonellosis model. *Microb Pathog, 12*(2), 145-151.

Chen, Q., Mosovsky, K. L., & Ross, A. C. (2013). Retinoic acid and alpha-galactosylceramide regulate the expression of costimulatory receptors and transcription factors responsible for B cell activation and differentiation. *Immunobiology, 218*(12), 1477-1487.

Cheroutre, H., Lambolez, F., & Mucida, D. (2011). The light and dark sides of intestinal intraepithelial lymphocytes. *Nat Rev Immunol, 11*(7), 445-456.

Chieppa, M., Rescigno, M., Huang, A. Y., & Germain, R. N. (2006). Dynamic imaging of dendritic cell extension into the small bowel lumen in response to epithelial cell TLR engagement. *J Exp Med, 203*(13), 2841-2852.

Chu, H., Pazgier, M., Jung, G., Nuccio, S. P., Castillo, P. A., de Jong, M. F., Winter, M. G., Winter, S. E., Wehkamp, J., Shen, B., Salzman, N. H., Underwood, M. A., Tsolis, R. M., Young, G. M., Lu, W., Lehrer, R. I., Baumler, A. J., & Bevins, C. L. (2012). Human alpha-defensin 6 promotes mucosal innate immunity through self-assembled peptide nanonets. *Science, 337*(6093), 477-481.

Clark, M. A., Reed, K. A., Lodge, J., Stephen, J., Hirst, B. H., & Jepson, M. A. (1996). Invasion of murine intestinal M cells by Salmonella typhimurium inv mutants severely deficient for invasion of cultured cells. *Infect Immun, 64*(10), 4363-4368.

Coe, N. E., & Wood, R. L. (1992). The effect of exposure to a delta cya/delta crp mutant of Salmonella typhimurium on the subsequent colonization of swine by the wild-type parent strain. *Vet Microbiol, 31*(2-3), 207-220.

Curtiss, R., 3rd, & Kelly, S. M. (1987). Salmonella typhimurium deletion mutants lacking adenylate cyclase and cyclic AMP receptor protein are avirulent and immunogenic. *Infect Immun, 55*(12), 3035-3043.

Curtiss, R., 3rd, Wanda, S. Y., Gunn, B. M., Zhang, X., Tinge, S. A., Ananthnarayan, V., Mo, H., Wang, S., & Kong, W. (2009). Salmonella enterica serovar typhimurium strains with regulated delayed attenuation in vivo. *Infect Immun, 77*(3), 1071-1082.

De Smet, R., Demoor, T., Verschuere, S., Dullaers, M., Ostroff, G. R., Leclercq, G., Allais, L., Pilette, C., Dierendonck, M., De Geest, B. G., & Cuvelier, C. A. (2013). beta-Glucan microparticles are good candidates for mucosal antigen delivery in oral vaccination. *J Control Release, 172*(3), 671-678.

Defrance, T., Vanbervliet, B., Briere, F., Durand, I., Rousset, F., & Banchereau, J. (1992). Interleukin 10 and transforming growth factor beta cooperate to induce anti-CD40-activated naive human B cells to secrete immunoglobulin A. *J Exp Med, 175*(3), 671-682.

Dilts, D. A., Riesenfeld-Orn, I., Fulginiti, J. P., Ekwall, E., Granert, C., Nonenmacher, J., Brey, R. N., Cryz, S. J., Karlsson, K., Bergman, K., Thompson, T., Hu, B., Bruckner, A. H., & Lindberg, A. A. (2000). Phase I clinical trials of aroA aroD and aroA aroD htrA attenuated S. typhi vaccines; effect of formulation on safety and immunogenicity. *Vaccine, 18*(15), 1473-1484.

Eisenstein, T. K., Killar, L. M., Stocker, B. A., & Sultzer, B. M. (1984). Cellular immunity induced by avirulent Salmonella in LPS-defective C3H/HeJ mice. *J Immunol, 133*(2), 958-961.

Eliasson, D. G., Helgeby, A., Schon, K., Nygren, C., El-Bakkouri, K., Fiers, W., Saelens, X., Lovgren, K. B., Nystrom, I., & Lycke, N. Y. (2011). A novel non-toxic combined CTA1-DD and ISCOMS adjuvant vector for effective mucosal immunization against influenza virus. *Vaccine, 29*(23), 3951-3961.

Elwell, L. P., & Shipley, P. L. (1980). Plasmid-mediated factors associated with virulence of bacteria to animals. *Annu Rev Microbiol, 34*, 465-496.

Endt, K., Maier, L., Kappeli, R., Barthel, M., Misselwitz, B., Kremer, M., & Hardt, W. D. (2012). Peroral ciprofloxacin therapy impairs the generation of a protective immune response in a mouse model for Salmonella enterica serovar Typhimurium diarrhea, while parenteral ceftriaxone therapy does not. *Antimicrob Agents Chemother, 56*(5), 2295-2304.

Endt, K., Stecher, B., Chaffron, S., Slack, E., Tchitchek, N., Benecke, A., Van Maele, L., Sirard, J. C., Mueller, A. J., Heikenwalder, M., Macpherson, A. J., Strugnell, R., von Mering, C., & Hardt, W. D. (2010). The microbiota mediates pathogen clearance from the gut lumen after non-typhoidal Salmonella diarrhea. *PLoS Pathog, 6*(9), e1001097.

Ermak, T. H., Dougherty, E. P., Bhagat, H. R., Kabok, Z., & Pappo, J. (1995). Uptake and transport of copolymer biodegradable microspheres by rabbit Peyer's patch M cells. *Cell Tissue Res, 279*(2), 433-436.

Fagarasan, S., Muramatsu, M., Suzuki, K., Nagaoka, H., Hiai, H., & Honjo, T. (2002). Critical roles of activation-induced cytidine deaminase in the homeostasis of gut flora. *Science, 298*(5597), 1424-1427.

Felmy, B., Songhet, P., Slack, E. M., Muller, A. J., Kremer, M., Van Maele, L., Cayet, D., Heikenwalder, M., Sirard, J. C., & Hardt, W. D. (2013). NADPH oxidase deficient mice develop colitis and bacteremia upon infection with normally avirulent, TTSS-1- and TTSS-2-deficient Salmonella Typhimurium. *PLoS One, 8*(10), e77204.

Ferguson, A. (1977). Intraepithelial lymphocytes of the small intestine. *Gut, 18*(11), 921-937.

Forbes, S. J., Bumpus, T., McCarthy, E. A., Corthesy, B., & Mantis, N. J. (2011). Transient suppression of Shigella flexneri type 3 secretion by a protective O-antigen-specific monoclonal IgA. *MBio, 2*(3), e00042-00011.

Forbes, S. J., Eschmann, M., & Mantis, N. J. (2008). Inhibition of Salmonella enterica serovar typhimurium motility and entry into epithelial cells by a protective antilipopolysaccharide monoclonal immunoglobulin A antibody. *Infect Immun, 76*(9), 4137-4144.

Forbes, S. J., Martinelli, D., Hsieh, C., Ault, J. G., Marko, M., Mannella, C. A., & Mantis, N. J. (2012). Association of a protective monoclonal IgA with the O antigen of Salmonella enterica serovar Typhimurium impacts type 3 secretion and outer membrane integrity. *Infect Immun, 80*(7), 2454-2463.

Fritz, J. H., Rojas, O. L., Simard, N., McCarthy, D. D., Hapfelmeier, S., Rubino, S., Robertson, S. J., Larijani, M., Gosselin, J., Ivanov, II, Martin, A., Casellas, R., Philpott, D. J., Girardin, S. E., McCoy, K. D., Macpherson, A. J., Paige, C. J., & Gommerman, J. L. (2012). Acquisition of a multifunctional IgA+ plasma cell phenotype in the gut. *Nature, 481*(7380), 199-203.

Fukata, M., & Arditi, M. (2013). The role of pattern recognition receptors in intestinal inflammation. *Mucosal Immunol, 6*(3), 451-463.

Gal-Mor, O., Boyle, E. C., & Grassl, G. A. (2014). Same species, different diseases: how and why typhoidal and non-typhoidal Salmonella enterica serovars differ. *Front Microbiol, 5*, 391.

Galan, J. E. (2001). Salmonella interactions with host cells: type III secretion at work. *Annu Rev Cell Dev Biol, 17*, 53-86.

Galan, J. E., & Curtiss, R., 3rd. (1989). Virulence and vaccine potential of phoP mutants of Salmonella typhimurium. *Microb Pathog, 6*(6), 433-443.

Ganguly, N. K., & Kaur, T. (1996). Mechanism of action of cholera toxin & other toxins. *Indian J Med Res, 104*, 28-37.

Gil, D., & Bouche, J. P. (1991). ColE1-type vectors with fully repressible replication. *Gene, 105*(1), 17-22.

Gill, S. R., Pop, M., Deboy, R. T., Eckburg, P. B., Turnbaugh, P. J., Samuel, B. S., Gordon, J. I., Relman, D. A., Fraser-Liggett, C. M., & Nelson, K. E. (2006). Metagenomic analysis of the human distal gut microbiome. *Science, 312*(5778), 1355-1359.

Gisbert, J. P., & Panes, J. (2009). Loss of response and requirement of infliximab dose intensification in Crohn's disease: a review. *Am J Gastroenterol, 104*(3), 760-767.

Glenn, G. M., Francis, D. H., & Danielsen, E. M. (2009). Toxin-mediated effects on the innate mucosal defenses: implications for enteric vaccines. *Infect Immun, 77*(12), 5206-5215.

Grant, A. J., Restif, O., McKinley, T. J., Sheppard, M., Maskell, D. J., & Mastroeni, P. (2008). Modelling within-host spatiotemporal dynamics of invasive bacterial disease. *PLoS Biol, 6*(4), e74.

Haas, A., Zimmermann, K., Graw, F., Slack, E., Rusert, P., Ledergerber, B., Bossart, W., Weber, R., Thurnheer, M. C., Battegay, M., Hirschel, B., Vernazza, P., Patuto, N., Macpherson, A. J., Gunthard, H. F., Oxenius, A., & Swiss, H. I. V. Cohort Study. (2011). Systemic antibody responses to gut commensal bacteria during chronic HIV-1 infection. *Gut, 60*(11), 1506-1519.

Hammarstrom, L., Vorechovsky, I., & Webster, D. (2000). Selective IgA deficiency (SIgAD) and common variable immunodeficiency (CVID). *Clin Exp Immunol, 120*(2), 225-231.

Hammerschmidt, S. I., Friedrichsen, M., Boelter, J., Lyszkiewicz, M., Kremmer, E., Pabst, O., & Forster, R. (2011). Retinoic acid induces homing of protective T and B cells to the gut after subcutaneous immunization in mice. *J Clin Invest, 121*(8), 3051-3061.

Hanson, L. A., & Korotkova, M. (2002). The role of breastfeeding in prevention of neonatal infection. *Semin Neonatol, 7*(4), 275-281.

Hapfelmeier, S., Ehrbar, K., Stecher, B., Barthel, M., Kremer, M., & Hardt, W. D. (2004). Role of the Salmonella pathogenicity island 1 effector proteins SipA, SopB, SopE, and SopE2 in Salmonella enterica subspecies 1 serovar Typhimurium colitis in streptomycin-pretreated mice. *Infect Immun, 72*(2), 795-809.

Hapfelmeier, S., Lawson, M. A., Slack, E., Kirundi, J. K., Stoel, M., Heikenwalder, M., Cahenzli, J., Velykoredko, Y., Balmer, M. L., Endt, K., Geuking, M. B., Curtiss, R., 3rd, McCoy, K. D., & Macpherson, A. J. (2010). Reversible microbial colonization of germ-free mice reveals the dynamics of IgA immune responses. *Science, 328*(5986), 1705-1709.

Hapfelmeier, S., Muller, A. J., Stecher, B., Kaiser, P., Barthel, M., Endt, K., Eberhard, M., Robbiani, R., Jacobi, C. A., Heikenwalder, M., Kirschning, C., Jung, S., Stallmach, T., Kremer, M., & Hardt, W. D. (2008). Microbe sampling by mucosal dendritic cells is a discrete, MyD88-independent step in Delta invG S. Typhimurium colitis. *Journal of Experimental Medicine, 205*(2), 437-450.

Harrison, J. A., Villarreal-Ramos, B., Mastroeni, P., Demarco de Hormaeche, R., & Hormaeche, C. E. (1997). Correlates of protection induced by live Aro- Salmonella typhimurium vaccines in the murine typhoid model. *Immunology, 90*(4), 618-625.

Hassan, J. O., & Curtiss, R., 3rd. (1990). Control of colonization by virulent Salmonella typhimurium by oral immunization of chickens with avirulent delta cya delta crp S. typhimurium. *Res Microbiol, 141*(7-8), 839-850.

Hassan, J. O., & Curtiss, R., 3rd. (1996). Effect of vaccination of hens with an avirulent strain of Salmonella typhimurium on immunity of progeny challenged with wild-Type Salmonella strains. *Infect Immun, 64*(3), 938-944.

He, B., Xu, W., Santini, P. A., Polydorides, A. D., Chiu, A., Estrella, J., Shan, M., Chadburn, A., Villanacci, V., Plebani, A., Knowles, D. M., Rescigno, M., & Cerutti, A. (2007). Intestinal bacteria trigger T cell-independent immunoglobulin A(2) class switching by inducing epithelial-cell secretion of the cytokine APRIL. *Immunity, 26*(6), 812-826.

Helander, A., Miller, C. L., Myers, K. S., Neutra, M. R., & Nibert, M. L. (2004). Protective immunoglobulin A and G antibodies bind to overlapping intersubunit epitopes in the head domain of type 1 reovirus adhesin sigma1. *J Virol, 78*(19), 10695-10705.

Helander, A., Silvey, K. J., Mantis, N. J., Hutchings, A. B., Chandran, K., Lucas, W. T., Nibert, M. L., & Neutra, M. R. (2003). The viral sigma1 protein and glycoconjugates containing alpha2-3-linked sialic acid are involved in type 1 reovirus adherence to M cell apical surfaces. *J Virol, 77*(14), 7964-7977.

Hesseling, A. C., Rabie, H., Marais, B. J., Manders, M., Lips, M., Schaaf, H. S., Gie, R. P., Cotton, M. F., van Helden, P. D., Warren, R. M., & Beyers, N. (2006). Bacille Calmette-Guerin vaccine-induced disease in HIV-infected and HIV-uninfected children. *Clin Infect Dis, 42*(4), 548-558.

Hohmann, E. L., Oletta, C. A., & Miller, S. I. (1996). Evaluation of a phoP/phoQ-deleted, aroA-deleted live oral Salmonella typhi vaccine strain in human volunteers. *Vaccine, 14*(1), 19-24.

Hoiseth, S. K., & Stocker, B. A. (1981). Aromatic-dependent Salmonella typhimurium are non-virulent and effective as live vaccines. *Nature, 291*(5812), 238-239.

Hone, D. M., Tacket, C. O., Harris, A. M., Kay, B., Losonsky, G., & Levine, M. M. (1992). Evaluation in volunteers of a candidate live oral attenuated Salmonella typhi vector vaccine. *J Clin Invest, 90*(2), 412-420.

Hooper, L. V., Littman, D. R., & Macpherson, A. J. (2012). Interactions between the microbiota and the immune system. *Science, 336*(6086), 1268-1273.

Hormaeche, C. E., Mastroeni, P., Harrison, J. A., Demarco de Hormaeche, R., Svenson, S., & Stocker, B. A. (1996). Protection against oral challenge three months after i.v. immunization of BALB/c mice with live Aro Salmonella typhimurium and Salmonella enteritidis vaccines is serotype (species)-dependent and only partially determined by the main LPS O antigen. *Vaccine, 14*(4), 251-259.

Howe, S. E., & Konjufca, V. H. (2015). Per-oral immunization with antigen-conjugated nanoparticles followed by sub-cutaneous boosting immunization induces long-lasting mucosal and systemic antibody responses in mice. *PLoS One, 10*(2), e0118067.

Hutchings, A. B., Helander, A., Silvey, K. J., Chandran, K., Lucas, W. T., Nibert, M. L., & Neutra, M. R. (2004). Secretory immunoglobulin A antibodies against the sigma1 outer capsid protein of reovirus type 1 Lang prevent infection of mouse Peyer's patches. *J Virol, 78*(2), 947-957.

Ibs, K. H., & Rink, L. (2003). Zinc-altered immune function. *J Nutr, 133*(5 Suppl 1), 1452S-1456S.

Iwata, M., Hirakiyama, A., Eshima, Y., Kagechika, H., Kato, C., & Song, S. Y. (2004). Retinoic acid imprints gut-homing specificity on T cells. *Immunity, 21*(4), 527-538.

Janeway, C. A., Jr. (1989). Approaching the asymptote? Evolution and revolution in immunology. *Cold Spring Harb Symp Quant Biol, 54 Pt 1*, 1-13.

Jepson, M. A., Collares-Buzato, C. B., Clark, M. A., Hirst, B. H., & Simmons, N. L. (1995). Rapid disruption of epithelial barrier function by Salmonella typhimurium is associated with structural modification of intercellular junctions. *Infect Immun, 63*(1), 356-359.

Johansen, F. E., Pekna, M., Norderhaug, I. N., Haneberg, B., Hietala, M. A., Krajci, P., Betsholtz, C., & Brandtzaeg, P. (1999). Absence of epithelial immunoglobulin A transport, with increased mucosal leakiness, in polymeric immunoglobulin receptor/secretory component-deficient mice. *J Exp Med, 190*(7), 915-922.

Johansson, M. E., Phillipson, M., Petersson, J., Velcich, A., Holm, L., & Hansson, G. C. (2008). The inner of the two Muc2 mucin-dependent mucus layers in colon is devoid of bacteria. *Proc Natl Acad Sci U S A, 105*(39), 15064-15069.

Johnson, R. A., Uddin, T., Aktar, A., Mohasin, M., Alam, M. M., Chowdhury, F., Harris, J. B., LaRocque, R. C., Bufano, M. K., Yu, Y., Wu-Freeman, Y., Leung, D. T., Sarracino, D., Krastins, B., Charles, R. C., Xu, P., Kovac, P., Calderwood, S. B., Qadri, F., & Ryan, E. T. (2012). Comparison of immune responses to the O-specific polysaccharide and lipopolysaccharide of Vibrio cholerae O1 in Bangladeshi adult patients with cholera. *Clin Vaccine Immunol, 19*(11), 1712-1721.

Jones, B. D., Ghori, N., & Falkow, S. (1994). Salmonella typhimurium initiates murine infection by penetrating and destroying the specialized epithelial M cells of the Peyer's patches. *J Exp Med, 180*(1), 15-23.

Jorgensen, G. H., Gardulf, A., Sigurdsson, M. I., Sigurdardottir, S. T., Thorsteinsdottir, I., Gudmundsson, S., Hammarstrom, L., & Ludviksson, B. R. (2013). Clinical symptoms in adults with selective IgA deficiency: a case-control study. *J Clin Immunol, 33*(4), 742-747.

Kabir, S. (2014). Critical analysis of compositions and protective efficacies of oral killed cholera vaccines. *Clin Vaccine Immunol, 21*(9), 1195-1205.

Kaetzel, C. S., Robinson, J. K., Chintalacharuvu, K. R., Vaerman, J. P., & Lamm, M. E. (1991). The polymeric immunoglobulin receptor (secretory component) mediates transport of immune complexes across epithelial cells: a local defense function for IgA. *Proc Natl Acad Sci U S A, 88*(19), 8796-8800.

Kaetzel, C. S., Robinson, J. K., & Lamm, M. E. (1994). Epithelial transcytosis of monomeric IgA and IgG cross-linked through antigen to polymeric IgA. A role for monomeric antibodies in the mucosal immune system. *J Immunol, 152*(1), 72-76.

Kaiser, P., Regoes, R. R., Dolowschiak, T., Wotzka, S. Y., Lengefeld, J., Slack, E., Grant, A. J., Ackermann, M., & Hardt, W. D. (2014). Cecum lymph node dendritic cells harbor slow-growing bacteria phenotypically tolerant to antibiotic treatment. *PLoS Biol, 12*(2), e1001793.

Kaiser, P., Slack, E., Grant, A. J., Hardt, W. D., & Regoes, R. R. (2013). Lymph node colonization dynamics after oral Salmonella Typhimurium infection in mice. *PLoS Pathog, 9*(9), e1003532.

Karapetian, O., Shakhov, A. N., Kraehenbuhl, J. P., & Acha-Orbea, H. (1994). Retroviral infection of neonatal Peyer's patch lymphocytes: the mouse mammary tumor virus model. *J Exp Med, 180*(4), 1511-1516.

Kaufman, D. R., De Calisto, J., Simmons, N. L., Cruz, A. N., Villablanca, E. J., Mora, J. R., & Barouch, D. H. (2011). Vitamin A deficiency impairs vaccine-elicited gastrointestinal immunity. *J Immunol, 187*(4), 1877-1883.

Kelly, B. G., Vespermann, A., & Bolton, D. J. (2009). Gene transfer events and their occurrence in selected environments. *Food Chem Toxicol, 47*(5), 978-983.

Keusch, G. T., Denno, D. M., Black, R. E., Duggan, C., Guerrant, R. L., Lavery, J. V., Nataro, J. P., Rosenberg, I. H., Ryan, E. T., Tarr, P. I., Ward, H., Bhutta, Z. A., Coovadia, H., Lima, A., Ramakrishna, B., Zaidi, A. K., Hay Burgess, D. C., & Brewer, T. (2014). Environmental enteric dysfunction: pathogenesis, diagnosis, and clinical consequences. *Clin Infect Dis, 59 Suppl 4*, S207-212.

Killar, L. M., & Eisenstein, T. K. (1985). Immunity to Salmonella typhimurium infection in C3H/HeJ and C3H/HeNCrlBR mice: studies with an aromatic-dependent live S. typhimurium strain as a vaccine. *Infect Immun, 47*(3), 605-612.

Kim, J. J., & Khan, W. I. (2013). Goblet cells and mucins: role in innate defense in enteric infections. *Pathogens, 2*(1), 55-70.

Kim, Y. K., Shin, J. S., & Nahm, M. H. (2016). NOD-Like Receptors in Infection, Immunity, and Diseases. *Yonsei Med J, 57*(1), 5-14.

Klemola, T. (1988). Immunohistochemical findings in the intestine of IgA-deficient persons: number of intraepithelial T lymphocytes is increased. *J Pediatr Gastroenterol Nutr, 7*(4), 537-543.

Kong, W., Wanda, S. Y., Zhang, X., Bollen, W., Tinge, S. A., Roland, K. L., & Curtiss, R., 3rd. (2008). Regulated programmed lysis of recombinant Salmonella in host tissues to release protective antigens and confer biological containment. *Proc Natl Acad Sci U S A, 105*(27), 9361-9366.

Korpe, P. S., & Petri, W. A., Jr. (2012). Environmental enteropathy: critical implications of a poorly understood condition. *Trends Mol Med, 18*(6), 328-336.

Lamkanfi, M., & Dixit, V. M. (2014). Mechanisms and functions of inflammasomes. *Cell, 157*(5), 1013-1022.

Langridge, W., Denes, B., & Fodor, I. (2010). Cholera toxin B subunit modulation of mucosal vaccines for infectious and autoimmune diseases. *Curr Opin Investig Drugs, 11*(8), 919-928.

Lécuyer, Emelyne, Rakotobe, Sabine, Lengliné-Garnier, Hélène, Lebreton, Corinne, Picard, Marion, Juste, Catherine, Fritzen, Rémi, Eberl, Gérard, McCoy, Kathy D, Macpherson, Andrew J, Reynaud, Claude-Agnès, Cerf-Bensussan, Nadine, & Gaboriau-Routhiau, Valérie. (2014).

Segmented Filamentous Bacterium Uses Secondary and Tertiary Lymphoid Tissues to Induce Gut IgA and Specific T Helper 17 Cell Responses. *Immunity, 40*(4), 608-620.

Lee, M. R., Seo, G. Y., Kim, Y. M., & Kim, P. H. (2011). iNOS potentiates mouse Ig isotype switching through AID expression. *Biochem Biophys Res Commun, 410*(3), 602-607.

Levine, M. M. (2010). Immunogenicity and efficacy of oral vaccines in developing countries: lessons from a live cholera vaccine. *BMC Biol, 8*, 129.

Levine, M. M., Ferreccio, C., Abrego, P., Martin, O. S., Ortiz, E., & Cryz, S. (1999). Duration of efficacy of Ty21a, attenuated Salmonella typhi live oral vaccine. *Vaccine, 17 Suppl 2*, S22-27.

Levinson, K. J., De Jesus, M., & Mantis, N. J. (2015). Rapid effects of a protective O-polysaccharide-specific monoclonal IgA on Vibrio cholerae agglutination, motility, and surface morphology. *Infect Immun, 83*(4), 1674-1683.

Lievin-Le Moal, V., & Servin, A. L. (2006). The front line of enteric host defense against unwelcome intrusion of harmful microorganisms: mucins, antimicrobial peptides, and microbiota. *Clin Microbiol Rev, 19*(2), 315-337.

Lindh, E. (1975). Increased risistance of immunoglobulin A dimers to proteolytic degradation after binding of secretory component. *J Immunol, 114*(1 Pt 2), 284-286.

Lindner, C., Wahl, B., Fohse, L., Suerbaum, S., Macpherson, A. J., Prinz, I., & Pabst, O. (2012). Age, microbiota, and T cells shape diverse individual IgA repertoires in the intestine. *J Exp Med, 209*(2), 365-377.

Lowe, D. C., Savidge, T. C., Pickard, D., Eckmann, L., Kagnoff, M. F., Dougan, G., & Chatfield, S. N. (1999). Characterization of candidate live oral Salmonella typhi vaccine strains harboring defined mutations in aroA, aroC, and htrA. *Infect Immun, 67*(2), 700-707.

Lycke, N. (2012). Recent progress in mucosal vaccine development: potential and limitations. *Nat Rev Immunol, 12*(8), 592-605.

Mabbott, N. A., Donaldson, D. S., Ohno, H., Williams, I. R., & Mahajan, A. (2013). Microfold (M) cells: important immunosurveillance posts in the intestinal epithelium. *Mucosal Immunol, 6*(4), 666-677.

Maclennan, Calman A. (2014). Antibodies and protection against invasive Salmonella disease. *Frontiers in Immunology, 5*.

Macpherson, A. J., Gatto, D., Sainsbury, E., Harriman, G. R., Hengartner, H., & Zinkernagel, R. M. (2000). A primitive T cell-independent mechanism of intestinal mucosal IgA responses to commensal bacteria. *Science, 288*(5474), 2222-2226.

Macpherson, A. J., Geuking, M. B., & McCoy, K. D. (2005). Immune responses that adapt the intestinal mucosa to commensal intestinal bacteria. *Immunology, 115*(2), 153-162.

Macpherson, A. J., Lamarre, A., McCoy, K., Harriman, G. R., Odermatt, B., Dougan, G., Hengartner, H., & Zinkernagel, R. M. (2001). IgA production without mu or delta chain expression in developing B cells. *Nat Immunol, 2*(7), 625-631.

Macpherson, A. J., & McCoy, K. D. (2013). Stratification and compartmentalisation of immunoglobulin responses to commensal intestinal microbes. *Semin Immunol, 25*(5), 358-363.

Macpherson, A. J., McCoy, K. D., Johansen, F. E., & Brandtzaeg, P. (2008). The immune geography of IgA induction and function. *Mucosal Immunol, 1*(1), 11-22.

Macpherson, A. J., & Uhr, T. (2004a). Compartmentalization of the mucosal immune responses to commensal intestinal bacteria. *Ann N Y Acad Sci, 1029*, 36-43.

Macpherson, A. J., & Uhr, T. (2004b). Induction of protective IgA by intestinal dendritic cells carrying commensal bacteria. *Science, 303*(5664), 1662-1665.

Maier, L., Diard, M., Sellin, M. E., Chouffane, E. S., Trautwein-Weidner, K., Periaswamy, B., Slack, E., Dolowschiak, T., Stecher, B., Loverdo, C., Regoes, R. R., & Hardt, W. D. (2014). Granulocytes impose a tight bottleneck upon the gut luminal pathogen population during Salmonella typhimurium colitis. *PLoS Pathog, 10*(12), e1004557.

Majumder, P. P., Sarkar-Roy, N., Staats, H., Ramamurthy, T., Maiti, S., Chowdhury, G., Whisnant, C. C., Narayanasamy, K., & Wagener, D. K. (2013). Genomic correlates of variability in immune response to an oral cholera vaccine. *Eur J Hum Genet, 21*(9), 1000-1006.

Mantis, N. J., Cheung, M. C., Chintalacharuvu, K. R., Rey, J., Corthesy, B., & Neutra, M. R. (2002). Selective adherence of IgA to murine Peyer's patch M cells: evidence for a novel IgA receptor. *J Immunol, 169*(4), 1844-1851.

Mantis, N. J., & Forbes, S. J. (2010). Secretory IgA: arresting microbial pathogens at epithelial borders. *Immunol Invest, 39*(4-5), 383-406.

Mantis, N. J., McGuinness, C. R., Sonuyi, O., Edwards, G., & Farrant, S. A. (2006). Immunoglobulin A antibodies against ricin A and B subunits protect epithelial cells from ricin intoxication. *Infect Immun, 74*(6), 3455-3462.

Marcobal, A., Southwick, A. M., Earle, K. A., & Sonnenburg, J. L. (2013). A refined palate: bacterial consumption of host glycans in the gut. *Glycobiology, 23*(9), 1038-1046.

Martinoli, C., Chiavelli, A., & Rescigno, M. (2007). Entry route of Salmonella typhimurium directs the type of induced immune response. *Immunity, 27*(6), 975-984.

Mathias, A., Longet, S., & Corthesy, B. (2013). Agglutinating secretory IgA preserves intestinal epithelial cell integrity during apical infection by Shigella flexneri. *Infect Immun, 81*(8), 3027-3034.

Matsui, H., Isshiki, Y., Eguchi, M., Ogawa, Y., & Shimoji, Y. (2015). Evaluation of the live vaccine efficacy of virulence plasmid-cured, and phoP- or aroA-deficient Salmonella enterica serovar Typhimurium in mice. *J Vet Med Sci, 77*(2), 181-186.

Matsui, H., Suzuki, M., Isshiki, Y., Kodama, C., Eguchi, M., Kikuchi, Y., Motokawa, K., Takaya, A., Tomoyasu, T., & Yamamoto, T. (2003). Oral immunization with ATP-dependent protease-deficient mutants protects mice against subsequent oral challenge with virulent Salmonella enterica serovar typhimurium. *Infect Immun, 71*(1), 30-39.

Matter, K., & Balda, M. S. (2014). SnapShot: Epithelial tight junctions. *Cell, 157*(4), 992-992 e991.

Mazanec, M. B., Kaetzel, C. S., Lamm, M. E., Fletcher, D., & Nedrud, J. G. (1992). Intracellular neutralization of virus by immunoglobulin A antibodies. *Proc Natl Acad Sci U S A, 89*(15), 6901-6905.

Mebius, R. E. (2003). Organogenesis of lymphoid tissues. *Nat Rev Immunol, 3*(4), 292-303.

Mellander, L., Bjorkander, J., Carlsson, B., & Hanson, L. A. (1986). Secretory antibodies in IgA-deficient and immunosuppressed individuals. *J Clin Immunol, 6*(4), 284-291.

Michetti, P., Mahan, M. J., Slauch, J. M., Mekalanos, J. J., & Neutra, M. R. (1992). Monoclonal secretory immunoglobulin A protects mice against oral challenge with the invasive pathogen Salmonella typhimurium. *Infect Immun, 60*(5), 1786-1792.

Molenaar, R., Knippenberg, M., Goverse, G., Olivier, B. J., de Vos, A. F., O'Toole, T., & Mebius, R. E. (2011). Expression of retinaldehyde dehydrogenase enzymes in mucosal dendritic cells and gut-draining lymph node stromal cells is controlled by dietary vitamin A. *J Immunol, 186*(4), 1934-1942.

Moon, C., Baldridge, M. T., Wallace, M. A., Burnham, C. A., Virgin, H. W., & Stappenbeck, T. S. (2015). Vertically transmitted faecal IgA levels determine extra-chromosomal phenotypic variation. *Nature, 521*(7550), 90-93.

Moor, K., & Slack, E. (2015). What Makes A Bacterial Oral Vaccine a Strong Inducer of High-Affinity IgA Responses? *Antibodies (Basel), 4*(4), 295.

Moor, K., Wotzka, S. Y., Toska, A., Diard, M., Hapfelmeier, S., & Slack, E. (2016). Peracetic Acid Treatment Generates Potent Inactivated Oral Vaccines from a Broad Range of Culturable Bacterial Species. *Front Immunol, 7*, 34.

Mora, J. R., Iwata, M., Eksteen, B., Song, S. Y., Junt, T., Senman, B., Otipoby, K. L., Yokota, A., Takeuchi, H., Ricciardi-Castagnoli, P., Rajewsky, K., Adams, D. H., & von Andrian, U. H. (2006). Generation of gut-homing IgA-secreting B cells by intestinal dendritic cells. *Science, 314*(5802), 1157-1160.

Mora, J. R., Iwata, M., & von Andrian, U. H. (2008). Vitamin effects on the immune system: vitamins A and D take centre stage. *Nat Rev Immunol, 8*(9), 685-698.

Moreau, M. C., Ducluzeau, R., Guy-Grand, D., & Muller, M. C. (1978). Increase in the population of duodenal immunoglobulin A plasmocytes in axenic mice associated with different living or dead bacterial strains of intestinal origin. *Infect Immun, 21*(2), 532-539.

Mowat, A. M., & Agace, W. W. (2014). Regional specialization within the intestinal immune system. *Nat Rev Immunol, 14*(10), 667-685.

Müller, A. J., Kaiser, P., Dittmar, K. E. J., Weber, T. C., Haueter, S., Endt, K., Songhet, P., Zellweger, C., Kremer, M., Fehling, H. J., & Hardt, W. D. (2012). Salmonella Gut Invasion Involves TTSS-2-Dependent Epithelial Traversal, Basolateral Exit, and Uptake by Epithelium-Sampling Lamina Propria Phagocytes. *Cell Host Microbe, 11*(1), 19-32.

Muramatsu, M., Kinoshita, K., Fagarasan, S., Yamada, S., Shinkai, Y., & Honjo, T. (2000). Class switch recombination and hypermutation require activation-induced cytidine deaminase (AID), a potential RNA editing enzyme. *Cell, 102*(5), 553-563.

Muramatsu, M., Sankaranand, V. S., Anant, S., Sugai, M., Kinoshita, K., Davidson, N. O., & Honjo, T. (1999). Specific expression of activation-induced cytidine deaminase (AID), a novel member of the RNA-editing deaminase family in germinal center B cells. *J Biol Chem, 274*(26), 18470-18476.

Niess, J. H., Brand, S., Gu, X., Landsman, L., Jung, S., McCormick, B. A., Vyas, J. M., Boes, M., Ploegh, H. L., Fox, J. G., Littman, D. R., & Reinecker, H. C. (2005). CX3CR1-mediated dendritic cell access to the intestinal lumen and bacterial clearance. *Science, 307*(5707), 254-258.

Okahashi, N., Yamamoto, M., Vancott, J. L., Chatfield, S. N., Roberts, M., Bluethmann, H., Hiroi, T., Kiyono, H., & McGhee, J. R. (1996). Oral immunization of interleukin-4 (IL-4) knockout mice with a recombinant Salmonella strain or cholera toxin reveals that CD4+ Th2 cells producing IL-6 and IL-10 are associated with mucosal immunoglobulin A responses. *Infect Immun, 64*(5), 1516-1525.

Owen, R. L., Pierce, N. F., Apple, R. T., & Cray, W. C., Jr. (1986). M cell transport of Vibrio cholerae from the intestinal lumen into Peyer's patches: a mechanism for antigen sampling and for microbial transepithelial migration. *J Infect Dis, 153*(6), 1108-1118.

Pabst, O. (2012). New concepts in the generation and functions of IgA. *Nat Rev Immunol, 12*(12), 821-832.

Pabst, O., Cerovic, V., & Hornef, M. (2016). Secretory IgA in the Coordination of Establishment and Maintenance of the Microbiota. *Trends Immunol, 37*(5), 287-296.

Pantazi, E., Marks, E., Stolarczyk, E., Lycke, N., Noelle, R. J., & Elgueta, R. (2015). Cutting Edge: Retinoic Acid Signaling in B Cells Is Essential for Oral Immunization and Microflora Composition. *J Immunol*.

Pati, N. B., Vishwakarma, V., Selvaraj, S. K., Dash, S., Saha, B., Singh, N., & Suar, M. (2013). Salmonella Typhimurium TTSS-2 deficient mig-14 mutant shows attenuation in immunocompromised mice and offers protection against wild-type Salmonella Typhimurium infection. *BMC Microbiol, 13*, 236.

Periaswamy, B., Maier, L., Vishwakarma, V., Slack, E., Kremer, M., Andrews-Polymenis, H. L., McClelland, M., Grant, A. J., Suar, M., & Hardt, W. D. (2012). Live attenuated S. Typhimurium vaccine with improved safety in immuno-compromised mice. *PLoS One, 7*(9), e45433.

Phalipon, A., Cardona, A., Kraehenbuhl, J. P., Edelman, L., Sansonetti, P. J., & Corthesy, B. (2002). Secretory component: a new role in secretory IgA-mediated immune exclusion in vivo. *Immunity, 17*(1), 107-115.

Phalipon, A., Kaufmann, M., Michetti, P., Cavaillon, J. M., Huerre, M., Sansonetti, P., & Kraehenbuhl, J. P. (1995). Monoclonal immunoglobulin A antibody directed against serotype-specific epitope of Shigella flexneri lipopolysaccharide protects against murine experimental shigellosis. *J Exp Med, 182*(3), 769-778.

Praharaj, I., John, S. M., Bandyopadhyay, R., & Kang, G. (2015). Probiotics, antibiotics and the immune responses to vaccines. *Philos Trans R Soc Lond B Biol Sci, 370*(1671).

Reikvam, D. H., Derrien, M., Islam, R., Erofeev, A., Grcic, V., Sandvik, A., Gaustad, P., Meza-Zepeda, L. A., Jahnsen, F. L., Smidt, H., & Johansen, F. E. (2012). Epithelial-microbial crosstalk in polymeric Ig receptor deficient mice. *Eur J Immunol, 42*(11), 2959-2970.

Robinson, J. K., Blanchard, T. G., Levine, A. D., Emancipator, S. N., & Lamm, M. E. (2001). A mucosal IgA-mediated excretory immune system in vivo. *J Immunol, 166*(6), 3688-3692.

Roche, A. M., Richard, A. L., Rahkola, J. T., Janoff, E. N., & Weiser, J. N. (2015). Antibody blocks acquisition of bacterial colonization through agglutination. *Mucosal Immunol, 8*(1), 176-185.

Rochereau, N., Drocourt, D., Perouzel, E., Pavot, V., Redelinghuys, P., Brown, G. D., Tiraby, G., Roblin, X., Verrier, B., Genin, C., Corthesy, B., & Paul, S. (2013). Dectin-1 is essential for reverse transcytosis of glycosylated SIgA-antigen complexes by intestinal M cells. *PLoS Biol, 11*(9), e1001658.

Rogier, E. W., Frantz, A. L., Bruno, M. E., Wedlund, L., Cohen, D. A., Stromberg, A. J., & Kaetzel, C. S. (2014). Secretory antibodies in breast milk promote long-term intestinal homeostasis by regulating the gut microbiota and host gene expression. *Proc Natl Acad Sci U S A, 111*(8), 3074-3079.

Rosenberger, C. M., Gallo, R. L., & Finlay, B. B. (2004). Interplay between antibacterial effectors: a macrophage antimicrobial peptide impairs intracellular Salmonella replication. *Proc Natl Acad Sci U S A, 101*(8), 2422-2427.

Ruggeri, F. M., Johansen, K., Basile, G., Kraehenbuhl, J. P., & Svensson, L. (1998). Antirotavirus immunoglobulin A neutralizes virus in vitro after transcytosis through epithelial cells and protects infant mice from diarrhea. *J Virol, 72*(4), 2708-2714.

Saletti, Giulietta, Çuburu, Nicolas, Yang, Jae Seung, Dey, Ayan, & Czerkinsky, Cecil. (2013). Enzyme-linked immunospot assays for direct ex vivo measurement of vaccine-induced human humoral immune responses in blood. *Nat. Protocols, 8*(6), 1073-1087.

Salzman, N. H., Ghosh, D., Huttner, K. M., Paterson, Y., & Bevins, C. L. (2003). Protection against enteric salmonellosis in transgenic mice expressing a human intestinal defensin. *Nature, 422*(6931), 522-526.

Sansonetti, P. J., Arondel, J., Cantey, J. R., Prevost, M. C., & Huerre, M. (1996). Infection of rabbit Peyer's patches by Shigella flexneri: effect of adhesive or invasive bacterial phenotypes on follicle-associated epithelium. *Infect Immun, 64*(7), 2752-2764.

Sato, A., Hashiguchi, M., Toda, E., Iwasaki, A., Hachimura, S., & Kaminogawa, S. (2003). CD11b+ Peyer's patch dendritic cells secrete IL-6 and induce IgA secretion from naive B cells. *J Immunol, 171*(7), 3684-3690.

Schneider, P. (2005). The role of APRIL and BAFF in lymphocyte activation. *Curr Opin Immunol, 17*(3), 282-289.

Seleznik, G. M., Reding, T., Romrig, F., Saito, Y., Mildner, A., Segerer, S., Sun, L. K., Regenass, S., Lech, M., Anders, H. J., McHugh, D., Kumagi, T., Hiasa, Y., Lackner, C., Haybaeck, J., Angst, E., Perren, A., Balmer, M. L., Slack, E., MacPherson, A., Manz, M. G., Weber, A., Browning, J. L., Arkan, M. C., Rulicke, T., Aguzzi, A., Prinz, M., Graf, R., & Heikenwalder, M. (2012). Lymphotoxin beta receptor signaling promotes development of autoimmune pancreatitis. *Gastroenterology, 143*(5), 1361-1374.

Sheridan, B. S., & Lefrancois, L. (2010). Intraepithelial lymphocytes: to serve and protect. *Curr Gastroenterol Rep, 12*(6), 513-521.

Shroff, K. E., Meslin, K., & Cebra, J. J. (1995). Commensal enteric bacteria engender a self-limiting humoral mucosal immune response while permanently colonizing the gut. *Infect Immun, 63*(10), 3904-3913.

Shulzhenko, N., Morgun, A., Hsiao, W., Battle, M., Yao, M., Gavrilova, O., Orandle, M., Mayer, L., Macpherson, A. J., McCoy, K. D., Fraser-Liggett, C., & Matzinger, P. (2011). Crosstalk between B lymphocytes, microbiota and the intestinal epithelium governs immunity versus metabolism in the gut. *Nat Med, 17*(12), 1585-1593.

Sicinski, P., Rowinski, J., Warchol, J. B., Jarzabek, Z., Gut, W., Szczygiel, B., Bielecki, K., & Koch, G. (1990). Poliovirus type 1 enters the human host through intestinal M cells. *Gastroenterology, 98*(1), 56-58.

Simon, R., Tennant, S. M., Galen, J. E., & Levine, M. M. (2011). Mouse models to assess the efficacy of non-typhoidal Salmonella vaccines: revisiting the role of host innate susceptibility and routes of challenge. *Vaccine, 29*(32), 5094-5106.

Slack, E., Balmer, M. L., Fritz, J. H., & Hapfelmeier, S. (2012). Functional flexibility of intestinal IgA - broadening the fine line. *Front Immunol, 3*, 100.

Slack, E., Balmer, M. L., & Macpherson, A. J. (2014). B cells as a critical node in the microbiota-host immune system network. *Immunol Rev, 260*(1), 50-66.

Slack, E., Hapfelmeier, S., Stecher, B., Velykoredko, Y., Stoel, M., Lawson, M. A., Geuking, M. B., Beutler, B., Tedder, T. F., Hardt, W. D., Bercik, P., Verdu, E. F., McCoy, K. D., & Macpherson, A. J. (2009). Innate and adaptive immunity cooperate flexibly to maintain host-microbiota mutualism. *Science, 325*(5940), 617-620.

Soucy, S. M., Huang, J., & Gogarten, J. P. (2015). Horizontal gene transfer: building the web of life. *Nat Rev Genet, 16*(8), 472-482.

Spits, H., Artis, D., Colonna, M., Diefenbach, A., Di Santo, J. P., Eberl, G., Koyasu, S., Locksley, R. M., McKenzie, A. N., Mebius, R. E., Powrie, F., & Vivier, E. (2013). Innate lymphoid cells--a proposal for uniform nomenclature. *Nat Rev Immunol, 13*(2), 145-149.

Stecher, B., Berry, D., & Loy, A. (2013a). Colonization resistance and microbial ecophysiology: using gnotobiotic mouse models and single-cell technology to explore the intestinal jungle. *FEMS Microbiol Rev, 37*(5), 793-829.

Stecher, B., Chaffron, S., Kappeli, R., Hapfelmeier, S., Freedrich, S., Weber, T. C., Kirundi, J., Suar, M., McCoy, K. D., von Mering, C., Macpherson, A. J., & Hardt, W. D. (2010). Like will to like: abundances of closely related species can predict susceptibility to intestinal colonization by pathogenic and commensal bacteria. *PLoS Pathog, 6*(1), e1000711.

Stecher, B., Denzler, R., Maier, L., Bernet, F., Sanders, M. J., Pickard, D. J., Barthel, M., Westendorf, A. M., Krogfelt, K. A., Walker, A. W., Ackermann, M., Dobrindt, U., Thomson, N. R., & Hardt, W. D. (2012). Gut inflammation can boost horizontal gene transfer between pathogenic and commensal Enterobacteriaceae. *Proc Natl Acad Sci U S A, 109*(4), 1269-1274.

Stecher, B., & Hardt, W. D. (2011). Mechanisms controlling pathogen colonization of the gut. *Curr Opin Microbiol, 14*(1), 82-91.

Stecher, B., Maier, L., & Hardt, W. D. (2013b). 'Blooming' in the gut: how dysbiosis might contribute to pathogen evolution. *Nat Rev Microbiol, 11*(4), 277-284.

Stecher, B., Robbiani, R., Walker, A. W., Westendorf, A. M., Barthel, M., Kremer, M., Chaffron, S., Macpherson, A. J., Buer, J., Parkhill, J., Dougan, G., von Mering, C., & Hardt, W. D. (2007). Salmonella enterica serovar typhimurium exploits inflammation to compete with the intestinal microbiota. *PLoS Biol, 5*(10), 2177-2189.

Stokes, C. R., Soothill, J. F., & Turner, M. W. (1975). Immune exclusion is a function of IgA. *Nature, 255*(5511), 745-746.

Strugnell, R. A., & Wijburg, O. L. (2010). The role of secretory antibodies in infection immunity. *Nat Rev Microbiol, 8*(9), 656-667.

Stubbe, H., Berdoz, J., Kraehenbuhl, J. P., & Corthesy, B. (2000). Polymeric IgA is superior to monomeric IgA and IgG carrying the same variable domain in preventing Clostridium difficile toxin A damaging of T84 monolayers. *J Immunol, 164*(4), 1952-1960.

Sun, D. X., Mekalanos, J. J., & Taylor, R. K. (1990). Antibodies directed against the toxin-coregulated pilus isolated from Vibrio cholerae provide protection in the infant mouse experimental cholera model. *J Infect Dis, 161*(6), 1231-1236.

Suzuki, K., Meek, B., Doi, Y., Muramatsu, M., Chiba, T., Honjo, T., & Fagarasan, S. (2004). Aberrant expansion of segmented filamentous bacteria in IgA-deficient gut. *Proc Natl Acad Sci U S A, 101*(7), 1981-1986.

Svennerholm, A. M., & Holmgren, J. (1976). Synergistic protective effect in rabbits of immunization with Vibrio cholerae lipopolysaccharide and toxin/toxoid. *Infect Immun, 13*(3), 735-740.

Tacket, C. O., Hone, D. M., Curtiss, R., 3rd, Kelly, S. M., Losonsky, G., Guers, L., Harris, A. M., Edelman, R., & Levine, M. M. (1992). Comparison of the safety and immunogenicity of delta aroC delta aroD and delta cya delta crp Salmonella typhi strains in adult volunteers. *Infect Immun, 60*(2), 536-541.

Tacket, C. O., Sztein, M. B., Losonsky, G. A., Wasserman, S. S., Nataro, J. P., Edelman, R., Pickard, D., Dougan, G., Chatfield, S. N., & Levine, M. M. (1997). Safety of live oral Salmonella typhi vaccine strains with deletions in htrA and aroC aroD and immune response in humans. *Infect Immun, 65*(2), 452-456.

Tan, X., Sande, J. L., Pufnock, J. S., Blattman, J. N., & Greenberg, P. D. (2011). Retinoic acid as a vaccine adjuvant enhances CD8+ T cell response and mucosal protection from viral challenge. *J Virol, 85*(16), 8316-8327.

Tennant, S. M., & Levine, M. M. (2015). Live attenuated vaccines for invasive Salmonella infections. *Vaccine, 33 Suppl 3*, C36-C41.

Tezuka, H., Abe, Y., Iwata, M., Takeuchi, H., Ishikawa, H., Matsushita, M., Shiohara, T., Akira, S., & Ohteki, T. (2007). Regulation of IgA production by naturally occurring TNF/iNOS-producing dendritic cells. *Nature, 448*(7156), 929-933.

Tomasello, E., & Bedoui, S. (2013). Intestinal innate immune cells in gut homeostasis and immunosurveillance. *Immunol Cell Biol, 91*(3), 201-203.

Turner, J., Cho, Y., Dinh, N. N., Waring, A. J., & Lehrer, R. I. (1998). Activities of LL-37, a cathelin-associated antimicrobial peptide of human neutrophils. *Antimicrob Agents Chemother, 42*(9), 2206-2214.

Uchiyama, R., Chassaing, B., Zhang, B., & Gewirtz, A. T. (2014). Antibiotic treatment suppresses rotavirus infection and enhances specific humoral immunity. *J Infect Dis, 210*(2), 171-182.

Uddin, T., Aktar, A., Xu, P., Johnson, R. A., Rahman, M. A., Leung, D. T., Afrin, S., Akter, A., Alam, M. M., Rahman, A., Chowdhury, F., Khan, A. I., Bhuiyan, T. R., Bufano, M. K., Rashu, R., Yu, Y., Wu-Freeman, Y., Harris, J. B., LaRocque, R. C., Charles, R. C., Kovac, P., Calderwood, S. B., Ryan, E. T., & Qadri, F. (2014). Immune responses to O-specific polysaccharide and lipopolysaccharide of Vibrio cholerae O1 Ogawa in adult Bangladeshi recipients of an oral killed cholera vaccine and comparison to responses in patients with cholera. *Am J Trop Med Hyg, 90*(5), 873-881.

Uddin, T., Harris, J. B., Bhuiyan, T. R., Shirin, T., Uddin, M. I., Khan, A. I., Chowdhury, F., LaRocque, R. C., Alam, N. H., Ryan, E. T., Calderwood, S. B., & Qadri, F. (2011). Mucosal immunologic responses in cholera patients in Bangladesh. *Clin Vaccine Immunol, 18*(3), 506-512.

Underdown, B. J., & Dorrington, K. J. (1974). Studies on the structural and conformational basis for the relative resistance of serum and secretory immunoglobulin A to proteolysis. *J Immunol, 112*(3), 949-959.

Vishwakarma, V., Pati, N. B., Chandel, H. S., Sahoo, S. S., Saha, B., & Suar, M. (2012). Evaluation of Salmonella enterica serovar Typhimurium TTSS-2 deficient fur mutant as safe live-attenuated vaccine candidate for immunocompromised mice. *PLoS One, 7*(12), e52043.

Vishwakarma, V., Pati, N. B., Ray, S., Das, S., & Suar, M. (2014). TTSS2-deficient hha mutant of Salmonella Typhimurium exhibits significant systemic attenuation in immunocompromised hosts. *Virulence, 5*(2), 311-320.

Vyas, S. P., & Gupta, P. N. (2007). Implication of nanoparticles/microparticles in mucosal vaccine delivery. *Expert Rev Vaccines, 6*(3), 401-418.

Wahid, R., Simon, R., Zafar, S. J., Levine, M. M., & Sztein, M. B. (2012). Live oral typhoid vaccine Ty21a induces cross-reactive humoral immune responses against Salmonella enterica serovar Paratyphi A and S. Paratyphi B in humans. *Clin Vaccine Immunol, 19*(6), 825-834.

Wain, J., Hendriksen, R. S., Mikoleit, M. L., Keddy, K. H., & Ochiai, R. L. (2015). Typhoid fever. *Lancet, 385*(9973), 1136-1145.

Walker, R. I., Schmauder-Chock, E. A., Parker, J. L., & Burr, D. (1988). Selective association and transport of Campylobacter jejuni through M cells of rabbit Peyer's patches. *Can J Microbiol, 34*(10), 1142-1147.

Weiner, H. L., da Cunha, A. P., Quintana, F., & Wu, H. (2011). Oral tolerance. *Immunol Rev, 241*(1), 241-259.

Wiesner, J., & Vilcinskas, A. (2010). Antimicrobial peptides: the ancient arm of the human immune system. *Virulence, 1*(5), 440-464.

Winner, L., 3rd, Mack, J., Weltzin, R., Mekalanos, J. J., Kraehenbuhl, J. P., & Neutra, M. R. (1991). New model for analysis of mucosal immunity: intestinal secretion of specific monoclonal immunoglobulin A from hybridoma tumors protects against Vibrio cholerae infection. *Infect Immun, 59*(3), 977-982.

Wright, A., Lamm, M. E., & Huang, Y. T. (2008). Excretion of human immunodeficiency virus type 1 through polarized epithelium by immunoglobulin A. *J Virol, 82*(23), 11526-11535.

Yan, H., Lamm, M. E., Bjorling, E., & Huang, Y. T. (2002). Multiple functions of immunoglobulin A in mucosal defense against viruses: an in vitro measles virus model. *J Virol, 76*(21), 10972-10979.

Yel, L. (2010). Selective IgA deficiency. *J Clin Immunol, 30*(1), 10-16.

Yutin, N., Puigbo, P., Koonin, E. V., & Wolf, Y. I. (2012). Phylogenomics of prokaryotic ribosomal proteins. *PLoS One, 7*(5), e36972.

CHAPTER 2

-

PERACETIC ACID TREATMENT GENERATES

POTENT INACTIVATED ORAL VACCINES

FROM A BROAD RANGE OF CULTURABLE BACTERIAL SPECIES

Peracetic Acid Treatment Generates Potent Inactivated Oral Vaccines from a Broad Range of Culturable Bacterial Species.

Kathrin Moor[1], Sandra Yvonne Wotzka[1], Albulena Toska[1], Médéric Diard[1], Siegfried Hapfelmeier[2], Emma Slack[1]

[1]Institute for Microbiology, ETH Zürich, Zürich, Switzerland.

[2]Institute for Infectious Disease, University of Bern, Bern, Switzerland.

Published in:

Frontiers in Immunology, 11. February 2016

Abstract

Our mucosal surfaces are the main sites of non-vector-borne pathogen entry, as well as the main interface with our commensal microbiota. We are still only beginning to understand how mucosal adaptive immunity interacts with commensal and pathogenic microbes to influence factors such as infectivity, phenotypic diversity, and within-host evolution. This is in part due to difficulties in generating specific mucosal adaptive immune responses without disrupting the mucosal microbial ecosystem itself. Here, we present a very simple tool to generate inactivated mucosal vaccines from a broad range of culturable bacteria. Oral gavage of 10^{10} peracetic acid-inactivated bacteria induces high-titre-specific intestinal IgA in the absence of any measurable inflammation or species invasion. As a proof of principle, we demonstrate that this technique is sufficient to provide fully protective immunity in the murine model of invasive non-typhoidal Salmonellosis, even in the face of severe innate immune deficiency.

Keywords: oral vaccines, inactivated vaccines, *Salmonella typhimurium*, *Yersinia enterocolytica*, IgA

Introduction

Many immune mechanisms controlling bacterial infection in the blood and systemic secondary lymphoid organs are well described and understood (Bournazos *et al.*, 2015; Vidarsson *et al.*, 2014) As the systemic immune system is exquisitely sensitive to bacterial-derived "pathogen-associated molecular patterns" (PAMPs) and antigens, parenteral introduction of very low concentrations of live or inactivated bacteria induces high titre serum IgG responses and T cell activation in experimental animals (Iwasaki *et al.*, 2015). These simple vaccination protocols have permitted the elucidation of major effector functions, including antibody-mediated enhancement of phagocytosis and pathogen recognition (Bournazos *et al.*, 2015), T cell help to orchestrate appropriate cell-mediated antimicrobial responses (Tubo *et al.*, 2014; Wiesel *et al.*, 2012), and enhancement of the microbicidal activity of the complement system (Vidarsson *et al.*, 2014). Correspondingly, we have been able to identify a large number of mechanisms by which bacterial pathogens subvert and evade systemic immunity and can start to apply this knowledge clinically (Thammavongsa *et al.*, 2015).

By contrast, our knowledge of immune effector function at mucosal surfaces, particularly in the intestinal system, remains incomplete (Azegami *et al.*, 2014; Slack *et al.*, 2014). The mammalian large intestine is home to an extraordinarily dense microbial consortium, known as the microbiota. Among other functions, these microorganisms determine the host nutrient profile (Marcobal *et al.*, 2013), densely occupy intestinal niches providing "colonization resistance" to infection (Stecher *et al.*, 2013), and determine the immune status of the host

(Hooper *et al.*, 2012). Coevolution has produced an intestinal immune system that is both compartmentalized away from the systemic system such that parenteral immunization does not induce robust mucosal immunity (Macpherson *et al.*, 2013) and rather insensitive to locally delivered bacterial PAMPs and antigens in order to coexist with the commensal microbiota (Hapfelmeier *et al.*, 2010; Hooper *et al.*, 2012). In comparison to activation of systemic immunity, it is therefore a considerable challenge to activate the intestinal immune system, in particular to induce high-avidity secretory IgA, the major antibody isotype secreted into the intestinal lumen.

In order to induce strong intestinal immunity, it is necessary to deliver both antigen and appropriate adjuvant-derived signals into the gut-associated lymphoid tissues [recently reviewed in Ref. (Moor *et al.*, 2015)]. The most potent strategies to induce bacteria-specific IgA employ live-attenuated invasive pathogens [e.g., *Salmonella enterica* ssp. *enterica* ser. Typhimurium (Cheminay *et al.*, 2008), *Shigella* species (Wang *et al.*, 2014)]. This had led to the suggestion that some degree of pathogenicity, such as the ability to invade into the epithelium or subvert phagocyte function, is required for induction of intestinal immunity (Abd El Ghany *et al.*, 2007; Galen *et al.*, 2014; Matsui *et al.*, 2015; Peters *et al.*, 2010; Stecher *et al.*, 2010). While mucosal adaptive immunity can easily be activated by these vaccines, the vaccination process itself is often associated with mild inflammation, persistent colonization of secondary lymphoid tissues, and shifts in microbiota composition, due either to live vaccine presence or inflammatory processes (Endt *et al.*, 2010; Kaiser *et al.*, 2014; Stecher *et al.*, 2010). Any major perturbation of the microbiota has the potential to modify a very broad spectrum of host physiological functions (Hooper *et al.*, 2012), necessarily complicating the dissection of effector mechanisms. Furthermore, it is difficult and generally undesirable to generate an invasive pathogen from an apathogenic species in order to study immunity in host–commensal interactions.

An alternative strategy employed by us and others, particularly in the study of commensal microbes, is the gavage of high numbers of live apathogenic bacteria (Macpherson *et al.*, 2004; Manohar *et al.*, 2001; Shroff *et al.*, 1995; Talham *et al.*, 1999). For example, specific IgA is induced by six oral doses of 10^{10} live *Escherichia coli* K-12, which is a lab-adapted strain free of any identifiable virulence mechanisms (Hapfelmeier *et al.*, 2010). This effect can be mimicked by monocolonising germ-free mice with very low numbers of apathogenic bacteria, providing those bacteria grow up to a high density in the otherwise uncolonised intestinal lumen (Hapfelmeier *et al.*, 2010; Shroff *et al.*, 1995). Therefore, pathogenicity is not absolutely necessary for induction of specific IgA responses if high loads of live bacteria are present. Again, the drawback of this method for IgA induction is that the animal tends to be permanently colonized with the vaccination strain from the initiation of vaccination (Macpherson *et al.*, 2004; Manohar *et al.*, 2001; Shroff *et al.*, 1995; Talham *et al.*, 1999). This

makes it very difficult to clearly dissect effects on phenotype, colonization levels, etc. due to niche occupancy and shifts in host physiology. Elegant work with auxotrophic mutations can generate systems where the vaccination strain does not permanently colonize a germ-free mouse, permitting later re-challenge and study (Hapfelmeier *et al.*, 2010; Wang *et al.*, 2013). However, this requires powerful genetic systems in your organism of choice as well as a very detailed knowledge of bacterial metabolism and potential escape mechanisms.

The use of fully inactivated oral vaccines is, therefore, highly attractive as there is potential to induce a specific mucosal immune response without inducing inflammation and without persistently colonizing the intestine and/or associated lymphoid tissues. In the murine system, inactivated oral vaccines have often been found to be ignored by the mucosal immune system (Hapfelmeier *et al.*, 2010; Macpherson *et al.*, 2004). However, inactivated oral vaccines are so far the most successful strategy to induce at least partially protective immunity against enteric bacterial pathogens in humans (Walker, 2005). The human cholera vaccines Shanchol® and Dukoral® rely on oral delivery of more than 10^{10} inactivated *Vibrio cholerae* in the presence or absence of the mucosal adjuvant recombinant cholera toxin B subunit (Kabir, 2014). An enterotoxigenic *E. coli* vaccine currently in clinical trials (Lundgren *et al.*, 2014) is also based on oral delivery of inactivated bacteria along with the heat-labile toxin, a homolog of cholera toxin with known mucosal adjuvant activity. An inactivated *Shigella flexneri* vaccine is also showing promise in humans (Mckenzie *et al.*, 2006). It is, therefore, clear that successful oral vaccination of humans can be achieved in the absence of live bacteria; at least if a known mucosal adjuvant is present.

It is unclear why this discrepancy exists in the dogma between human and murine oral vaccination. Nevertheless, mouse infection/colonization remains the most commonly used system to elucidate biological mechanisms of host–microbe interactions, as experiments can be carried out that are simply not possible in human patients. We hypothesized that previous failure of inactivated oral vaccines in murine systems may be due to quantitatively insufficient delivery of antigens and PAMPs. Our previous work had determined that both the dose and the particulate nature of the vaccine were important to induce specific IgA (Hapfelmeier *et al.*, 2010). Therefore, in order to produce oral vaccines at concentrations of more than 10^{10} inactivated bacteria per 100 µl dose, we needed a drastic inactivation method that nevertheless minimized bacterial lysis. To this end, we made use of the very strong oxidizing agent peracetic acid (Chen, X. *et al.*, 2014; Park *et al.*, 2014; Sudhaus *et al.*, 2012). We were able to fully inactivate a taxonomically diverse range of bacterial species to generate particulate oral vaccines. As a proof of principle, we here demonstrate induction of high-titre IgA responses against a range of Enterobacteriaceae species.

In order to compare this strategy to existing oral vaccines, we made use of the murine model of invasive non-typhoidal Salmonellosis (Kaiser *et al.*, 2012). This is a particularly challenging

model for vaccination-mediated protection as <10 CFU delivered orally results in lethal infection within 5 days (Kaiser *et al.*, 2012), and live-attenuated vaccine strains are known to cause severe pathology in mice with innate immune deficiencies (Felmy *et al.*, 2013). Using our peracetic acid-inactivated *S.* Typhimurium vaccine, we could generate high-titre IgA in the absence of any detectable intestinal pathology, and could observe sterile protection from disease, even in the mouse model of chronic granulomatous disease.

Material and Methods

Ethics Statement

All animal experiments were approved by the legal authorities (licenses 223/2010 and 222/2013; Kantonales Veterinäramt Zürich, Switzerland) and performed according to the legal and ethical requirements.

Mice

SOPF C57BL/6, $J_H^{-/-}$ (Chen, J. *et al.*, 1993), *cybb*$^{-/-}$ (Pollock *et al.*, 1995), IgA$^{-/-}$ (Harriman *et al.*, 1999), and TCRβδ$^{-/-}$ (Mombaerts *et al.*, 1992) mice (all C57BL/6 background) were re-derived by artificial insemination into a specific opportunistic pathogen-free (SOPF) foster colony to normalize the microbiota and bred in full barrier conditions in individually ventilated cages in the ETH Phenomics centre (EPIC), ETH Zürich, for <4 generations. Specific pathogen-free mice (SPF) wild-type C57BL/6 mice were bred at the Rodent centre HCI (RCHCI), ETH Zürich, in individually ventilated cages. Low complex microbiota (LCM) mice (C57BL/6 background) are ex-germ-free mice, which were colonized with a naturally diversified Altered Schaedler flora in 2007 (Stecher *et al.*, 2010) and were bred in individually ventilated cages under strict hygienic isolation at the RCHCI ETH Zürich. All mice were used between 6 and 12 weeks of age. Wherever possible, male and female mice were randomized between groups to permit detection of a gender-specific effect.

Bacterial Strains and Growth Conditions

For infection experiments, the streptomycin-resistant wild-type strain *S. enterica* serovar Typhimurium (SL1344 wild-type clone SB300) or the isogenic *sseD::aphT* SPI2 mutant *S.* Typhimurium (M556) [described previously in Ref. (Hapfelmeier *et al.*, 2004; Hoiseth *et al.*, 1981)] were cultured in LB for 12 h at 37°C and subcultured for 3h as described previously (Barthel *et al.*, 2003). For vaccine production and antibody titering, all strains (Table 1) were cultured overnight in LB medium with aeration to late stationary phase.

Bacterial strains used in this study (Table 1)

Species name	Strain name	Genetic modifications /resistances	Source
Salmonella enterica serovar Typhimurium	SB300	None	Murine passage of the type-strain SL1344 (Barthel *et al.*, 2003)
		Streptomycin resistant	
Salmonella enterica serovar Typhimurium	M2702	Δ*sseD*::Δ*invG*	SB300 derivative (Hapfelmeier *et al.*, 2005)
		Streptomycin resistant	
Salmonella enterica serovar Typhimurium	M556	*sseD::aphT*	SB300 derivative (Hapfelmeier *et al.*, 2005)
		Streptomycin resistant	
		Kanamycin resistant	
Salmonella enterica serovar Typhimurium	SKI10	*wbaP::aphT*	SB300 derivative (Hapfelmeier *et al.*, 2005)
		Streptomycin resistant	
		Kanamycin resistant	
Salmonella enterica serovar Enteritidis	125109	Wild type	(Thomson *et al.*, 2008)
Salmonella enterica serovar Choleraesuis	ATCC25957 (914/99)	Wild type	(Nutter *et al.*, 1970)
Citrobacter rodentium	DSM 16636	Wild type	(Schauer *et al.*, 1995)
Yersinia enterocolitica	JB580	Wild type	Kind gift from Prof. Markus Aebi, ETH Zurich (Kinder *et al.*, 1993)
Klebsiella pneumonia		Human faecal isolate	(Balmer *et al.*, 2014)
E. coli	Nissle 1914	Human isolate	(Stecher *et al.*, 2012)
E. coli	8178	Mouse commensal isolate	(Stecher *et al.*, 2010)
Burkholderia multivorans	AE1064722	Cystic fibrosis patient lung isolate	Kind gift of Dr. A. Endimiani, University of Bern
Moraxella catarrhalis	O35E	Human isolate	(Unhanand *et al.*, 1992)
Staphylococcus aureus	NCTC 8532	Human lung isolate	ATCC
Staphylococcus epidermidis		Human skin isolate	(Haas *et al.*, 2011)
Staphylococcus xylosus		Mouse faecal isolate	(Slack *et al.*, 2009)
Enterococcus faecalis		Mouse faecal isolate	(Slack *et al.*, 2009)
Enterococcus faecalis		Human faecal isolate	(Haas *et al.*, 2011)
Pseudomonas aeruginosa	PA01	Wild-type strain	Institute strain collection
Pseudomonas fluorescens			Institute strain collection

Testing of (a) Paraformaldehyde Fixation, (b) Mild Heat-Treatment, and (c) Hydrogen Peroxide-Mediated Vaccine Inactivation

One litre of LB was inoculated with avirulent *S.* Typhimurium and cultured overnight at 37°C with shaking. The bacteria were concentrated by centrifugation at 16,000 × *g* for 20 min and resuspended in 10 ml D-PBS without Calcium or Magnesium (e.g., 14190-094, Gibco, Waltham, MA, USA). The 500 µl aliquots were then made in 2 ml snap-cap tubes (Sarstedt,

Nümbrecht, Germany). Three aliquots were subjected to the following treatments: (A) heat-treatment (1 h, 60°C with mild agitation in an Eppendorf Thermomixer); (B) PFA fixation [the bacteria were pelleted by centrifugation at 16,000 × g and resuspended in 1 ml of 4% paraformaldehyde (158127, Sigma-Aldrich, St. Louis, MO, USA) in D-PBS and incubated for 1 h at room temperature (RT)]; or (C) H_2O_2 inactivation [the bacteria were transferred to a 50 ml tube to contain the effervescence and 30% H_2O_2 (H-1009, Sigma-Aldrich) was added to a final concentration of 3%. The suspension was incubated for 1 h at RT]. This was compared to peracetic acid mediated inactivation on matched aliquots, as described in the paragraph below. After 1 h, the cultures, along with a control sample in PBS only at RT, were washed three times with 1 ml D-PBS to remove inactivating agents and were then resuspended in 500 µl for analysis. The 100 µl per sample were inoculated into 200 ml LB for overnight culture to determine sterility. The remaining sample was used for bright-field microscopy and FACS counting.

Production of Peracetic Acid-Inactivated Vaccines

Bacteria for peracetic acid-inactivated vaccines were grown overnight to late stationary phase at their respective optimal growth conditions. Bacteria were harvested by centrifugation (16,000 × g, 15 min) and resuspended at a density of 10^9–10^{10} per ml in sterile D-PBS. The 10 ml aliquots were transferred to sterile 50-ml Falcon tubes. Peracetic acid (433241, Sigma-Aldrich) was added to a final concentration of 0.4%. The suspension was mixed thoroughly and incubated for 1 h at RT. The bacteria were washed three times in 50 ml sterile D-PBS, meticulously removing all supernatant after each centrifugation step, and thoroughly resuspending the pellet each time to rapidly remove the peracetic acid. The final pellet was resuspended at a final concentration of 10^{11} particles per ml in sterile D-PBS (determined by OD_{600}) and stored at 4°C for up to 3 weeks. As a quality control, each batch of vaccine was tested before use by inoculating 100 µl of the inactivated vaccine (one vaccine dose) into 200 ml LB and incubating over night at 37°C with aeration to ensure complete inactivation, i.e., a "negative enrichment culture." One microliter of vaccine suspended in 100 µl D-PBS was used for bright-field microscopy. If aggregation was observed, the vaccine was aliquoted into sterile 2-ml tubes (Sarstedt) each with a single sterile 5-mm steal ball [5 mm G80 1.3541, PO8(xq + 8) × B2 beads, Berani Kugellager AG, Uster, Switzerland]. The tubes were then shaken at 25 Hz for 1 min in a Retsch Tissuelyser (Qiagen, Hilden, Germany) to disrupt aggregates.

FACS Quantification of Intact Inactivated Bacterial Particles

In order to quantify the total intact bacterial particles, the OD_{600} of prepared vaccines or control live bacterial suspensions was measured. The suspensions were then diluted to give an approximate OD_{600} of 0.1 and the dilution factor noted. The 150 µl of this culture was then

added to 150 µl of PBS containing and known concentration of Fluoresbrite Multifluorescent 1 µm Microspheres (Polysciences, Warrington, PA, USA) (in the range of 10^8 per ml, which is roughly 50 µl of the delivered bead suspension in 10 ml PBS, as determined by dilution and haemocytometer counting). Samples were acquired on an LSRII Flow cytometer (Becton Dickenson, NJ, USA) with forward- and side-scatter parameters in logarithmic mode and both parameters thresholded on a low value to exclude electronic noise but detect beads and bacteria. Beads were identified based on a "beads only" sample, as highly fluorescent in all channels. Bacteria/vaccine were identified by the absence of fluorescence as compared to the "bead-only" sample. Ten thousand multifluorescent bead events were acquired for each sample and the "counts" of beads and bacteria extracted by analysis in FlowJo (Treestar, Ashland, OR, USA). The background in the bacterial gate acquired with the "beads-only" sample was subtracted from all bacterial counts. The concentration of bacteria was then calculated using the formula Bacterial density = Bead density*bacteria FACS counts/Beads FACS counts.

Oral Vaccination with Peracetic Acid-Inactivated Vaccines

Mice received 10^{10} particles of the respective peracetic acid-inactivated bacteria in 100 µl of D-PBS by oral gavage once per week for 3 weeks. Except where stated in Figure 4, no antibiotics were applied during the vaccination period. Unless otherwise stated, on day 21 after the first gavage (i.e., 7 days after the final gavage), mice were used for analysis of antibody titres or infection experiments. For the data show in Figure C, mice received 0.8 g/kg ampicillin sodium salt (A0839, Applichem, Darmstadt, Germany) in sterile water or 1.0 g/kg gentamicin sulphate (A1104, Applichem) in sterile water by gavage 24 h prior to each dose of vaccine.

Oral Vaccination with Live-Attenuated *Salmonella*

Mice were pretreated with 1 g/kg streptomycin sulphate (A1852, AppliChem) in sterile water by gavage. Twenty-four hours later, the mice were inoculated with 5×10^7 CFU avirulent *S.* Typhimurium *sseD::aphT* (M556) by gavage [as described in Ref. (Endt *et al.*, 2010)].

Analysis of Specific Antibody Titres by Bacterial Flow Cytometry

Specific antibody titres were analysed in mouse serum and intestinal washes by flow cytometry as described previously (Slack *et al.*, 2009). Briefly, intestinal washes were collected by flushing the small intestine with 5 ml of a wash buffer containing PBS, 0.05M EDTA (A1104, Applichem), and 1 µg/ml Soybean trypsin inhibitor (T9128, Sigma-Aldrich). Intestinal washes were centrifuged at $16,000 \times g$ for 30 min and aliquots of the supernatants were stored at −20°C until analysis. Blood was collected into tubes containing clotting activating gel (41.1395.005, Sarstedt) and allowed to clot at RT for 30 min before centrifugation at

16,000 × g for 15 min. Bacterial targets (antigen against which antibodies are to be titered) were grown to late stationary phase and gently pelleted for 2 min at 3000 × g in an Eppendorf minifuge. The pellet was washed with sterile-filtered FACS buffer [PBS, 1% Bovine serum albumin factor V (K41-001, GE Healthcare, Little Chalfront, UK), 0.05% sodium azide (71289, Sigma-Aldrich)] before resuspending at a density of approximately 10^7 bacteria per ml. Intestinal washes and serum were heat-inactivated for 30 min at 56°C and centrifuged again at 16,000 g for 10 min to remove bacterial sized particles that may have been generated by the heat-treatment. Supernatants were used to perform serial dilutions. The 25 µl of the dilutions were incubated with 25 µl bacterial suspension at 4°C for 1 h. Bacteria were washed twice with 200 µl FACS buffer before resuspending in the appropriate antibody cocktail: monoclonal FITC-anti-mouse IgA (10 µg/ml, 559354, Clone C10-3, BD Pharmingen, New Jersey, NY, USA), FITC-anti-mouse IgG2b (5 µg/ml, 406706, Clone RMG2b-1, BioLegend, San Diego, CA, USA), PE-anti-mouse IgG1 (5 µg/ml, 406608, Clone RMG1-1, BioLegend), and APC/Cy7-anti-mouse IgM (5 µg/ml, 406516, Clone RMM-1, BioLegend). After 1 h of incubation, bacteria were washed once with FACS buffer and resuspended in 300 µl FACS buffer for acquisition on FACS LSRII using FSC and SSC parameters in logarithmic mode. Data were analysed using FlowJo (Treestar, Ashland, OR, USA). After gating on bacterial particles and compensation for bleed-through between fluorescence detectors where appropriate, median fluorescence intensities (MFI) were plotted against antibody concentrations for each sample and 4-parameter logistic curves fitted using Prism (Graphpad, La Jolla, CA, USA). Titres were calculated from these curves as the inverse of the antibody concentration giving an above-background signal (see Figure S1 in Supplementary Material).

Challenge of Vaccinated Animals with Wild-Type *S.* Typhimurium

Salmonella infections were performed in individually ventilated cages at the RCHCI, Zurich as described previously (Barthel *et al.*, 2003). Mice were pretreated with 1 g/kg streptomycin sulphate (Applichem) in sterile PBS by gavage. Twenty-four hours later, the mice were inoculated with 5 × 10^5 CFU *S.* Typhimurium SB300 by gavage. As mentioned earlier, 24-h post infection, blood and intestinal lavages were collected for analysis of specific antibody titres. Bacterial loads (CFU) in fresh faecal pellets, mesenteric lymph nodes (mLN), spleen, and cecal content (CC) were determined by plating on MacConkey agar plates containing 50 µg/ml streptomycin sulphate (Applichem).

Histopathological Evaluation

Samples of cecal tissue were embedded in OCT (Sakura, Torrqance, CA, USA) and snap frozen in liquid nitrogen. Five-micrometer cross-sectional tissue sections were cut and stained with haemotoxylin and eosin [as described in Ref. (Barthel *et al.*, 2003)]. Tissue sections were scored for cecal pathology as described (Barthel *et al.*, 2003). Briefly, the cecum pathology

score is based on oedema, polymorphonuclear cell infiltration, reduced numbers of goblet cells, and epithelium disruption with a maximum score of 14.

ELISAs

Lipocalin 2 was detected in faeces homogenized in 500 μl sterile PBS by ELISA using the DuoSet Lipocalin ELISA kit (DY1857, R&D Systems, Minneapolis, MN, USA) according to the manufacturer's instructions. Total concentrations of antibody isotypes in mouse serum or intestinal lavages were determined by sandwich ELISA. Coating antibodies were goat anti-mouse IgA (1040-01, SouthernBiotec, Birmingham, AL, USA), goat-anti-mouse IgG2b (1090-01, SouthernBiotec), goat-anti-mouse IgG1 (1070-01, SouthernBiotec), and goat-anti-mouse IgM (1020-01, SouthernBiotec). Detection antibodies were HRP-conjugated anti-mouse IgA α chain (A4789, Sigma-Aldrich), anti-mouse IgG γ chain (A3673, Sigma-Aldrich), and anti-mouse IgM μ chain (A8786, Sigma-Aldrich). Standards were purified mouse IgA (03101D, Pharmingen) or mouse reference serum (RS10-101, Bethyl, Montgomery, TX, USA).

Statistics

As we were predominantly working with datasets with $N < 10$, non-parametric tests were employed wherever possible. Where two groups of data are compared, analysis was carried out using two-tailed Mann–Whitney U tests with a significance cut-off of 5%. Where more than two groups were compared, data were analysed by Kruskal–Wallis test with Dunns post-test to account for multiple testing. Where more than one variable was tested simultaneously, log-normally distributed data were normalized and tested by two-way ANOVA with Bonferroni post-tests. All statistics were evaluated using Graphpad Prism. The dendrogram was generated by multiple alignment of 16S rDNA sequences using ClustalX and NJPlot (Conway Institute UCD Dublin, Ireland). As very large effects with minimal variation were measured, power calculations were not necessary to determine sample size and we adhered to standard practice of analysing at least five mice per group, wherever possible.

Results

In order to deliver 10^{10} inactivated bacteria orally with a minimal risk of accidental infection, it was essential to have a method that very efficiently kills bacteria at high densities without destroying antigenic structures. To this end, we tested several different standard inactivation procedures, including paraformaldehyde fixation (Mckenzie *et al.*, 2006), pasteurization (Kabir, 2014), and hydrogen peroxide treatment (Slack *et al.*, 2009), as well as a novel peracetic acid treatment, on the broad host-range pathogen *S. enterica* serovar Typhimurium (*S.* Typhimurium). As with many enteric pathogens, virulent *S.* Typhimurium carries a number of super oxide dismutase (SOD) genes (Amanna *et al.*, 2012; Battistoni, 2003), and correspondingly 3% hydrogen peroxide treatment resulted in considerable gaseous oxygen production but very little toxicity (Figures 1A,B). As expected, 4% paraformaldehyde treatment and pasteurization for 1 h result in a 4–6log decrease in viable bacteria, but both methods are insufficient for the 10–11log decrease that we are aiming for (Figures 1A, B). 0.4% peracetic acid, presumably due to the combination of low pH and very strong oxidizing activity, cannot be fully inactivated by SOD enzymes. This treatment results in very minimal gas production and inactivates 10^{10} CFU *S.* Typhimurium to sterility, as determined by plating or enrichment culture (Figures 1A, B). Very little lysis of *S.* Typhimurium was observed with any of the procedures tested (Figure 1C). Light microscopy revealed largely intact bacterial bodies after inactivation (Figure 1D). Sytox-green uptake, determined by microscopy (Figure 1D) or flow cytometry (data not shown), revealed uniform loss of membrane integrity in the peracetic acid-inactivated bacteria.

To demonstrate that the efficiency of peracetic acid treatment was really sufficient for our needs, we used streptomycin pre-treated mice carrying a low-complexity microbiota, which are extremely sensitive to oral infection with streptomycin-resistant *Salmonella* (Maier *et al.*, 2013). Twenty four hours after streptomycin treatment, these mice received just 10 or 100 CFU of live wild-type *S.* Typhimurium [strain SB300 (Barthel *et al.*, 2003)] or 5×10^{10} particles of peracetic acid-inactivated wild-type (SB300) or avirulent [Δ*sseD* Δ*invG* (Hapfelmeier *et al.*, 2005)] *S.* Typhimurium. Three days post-gavage, all mice receiving live *S.* Typhimurium, but 0/10 mice gavaged with peracetic acid-inactivated bacteria had full-blown cecal inflammation (Figures 1E,F) and high counts of *S.* Typhimurium in the intestinal content and mLN (Figures 1G,H). Thus, incubation in 0.4% peracetic acid is sufficient to kill >99.9999999% of all bacteria, preventing any pathological sequelae even when fully virulent wild-type *S.* Typhimurium was used as the vaccination strain.
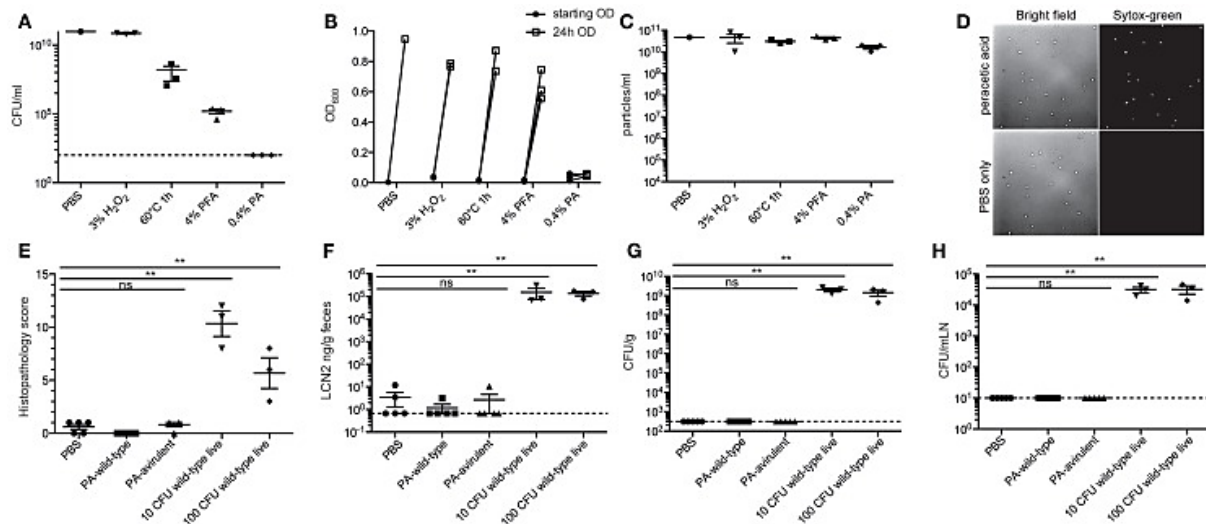
Figure 1 Peracetic acid highly efficiently kills bacteria, with minimal lysis. **(A–D)** Avirulent *S.* Typhimurium was cultured overnight to stationary phase, concentrated, and inactivated by incubating in 3% H_2O_2 for 1 h, heating to 60°C for 1 h, incubating in 4% PFA/PBS for 1 h, or incubating in 0.4% peracetic acid for 1 h. All aliquots were subsequently washed three times to remove fixatives/oxidizing agents before resuspending for CFU analysis by plating **(A)** and total sterility by enrichment culture **(B)**. Lysis was determined by counting bacterial particles by flow cytometry **(C)**. To examine morphology, the bacteria were diluted in PBS containing 0.5 µM Sytox-green and were imaged by bright-field and fluorescence microscopy at 100× magnification **(D)**. One representative experiment of two. **(E–H)** C57BL/6 LCM mice received 1.0 g/kg streptomycin p.o. 24 h before oral gavage of 5×10^{10} particles of peracetic acid-inactivated wild-type *S.* Typhimurium SB300 (PA-wild-type), 5×10^{10} particles of peracetic acid-inactivated avirulent *S.* Typhimurium M2702 (PA-avirulent), or 10 CFU or 100 CFU of wild-type live *S.* Typhimurium SB300. After 72 h, all animals were analysed. **(E,F)** Intestinal pathology as determined by histopathology or faecal Lipocalin 2 (LCN2). Kruskal–Wallis test, $P = 0.0023$ **(G,H)**. Cecal content (Kruskal–Wallis test, $P = 0.0007$) and mesenteric lymph node CFU (Kruskal–Wallis test, $P = 0.0007$). **Dunn's post-test, $P < 0.01$. One experiment with three to five mice per group.

In order to demonstrate that this process is applicable across a range of bacterial species, we aerobically cultured 17 different pathogenic and commensal bacterial species from the *Proteobacteria* and *Firmicutes* phyla and examined their inactivation by peracetic acid (Figure 2A). Full inactivation of dense bacterial suspensions was observed for all species tested. Spontaneous lysis in 0.4% peracetic acid was observed in only one species tested (*Moraxella catarrhalis*). Staphylococci and Enterococci tended to aggregate during inactivation, which is likely to inhibit sampling by the mucosal immune system. However, these aggregates could be easily disrupted by physical force, for example, vigorous shaking with a large steel bead (Figure 2B). The basic protocol we suggest (see Materials and Methods) is, therefore, a 1 h treatment of bacteria suspended at 10^{10} particles per ml in Dulbecco's PBS (D-PBS) with 0.4% peracetic acid. After extensive washing with sterile D-PBS, a small aliquot of bacteria should be examined by standard light microscopy techniques to determine the extent of aggregation (or lysis if this is not macroscopically obvious). If aggregates are present, the vaccine can be homogenized by shaking at 25 Hz in the presence of a large sterile steel bead. The final vaccine preparation is resuspended with at least 10^{10} particles per 100 µl and a full 100 µl is taken into 200 ml appropriate sterile media for overnight culture to determine absolute sterility

(Schematic diagram, Figure 2B). During this time, produced vaccine can be safely stored at 4°C. This is a broadly applicable, highly efficient bacterial inactivation technique that permits working with highly concentrated bacterial slurries in situations where administration of very few live bacteria would be confounding. A useful side-observation from our work is that in the case of vaccine made from *S.* Typhimurium, the inactivated bacteria could be stored as a dense slurry in PBS at 4°C for at least 3 weeks.
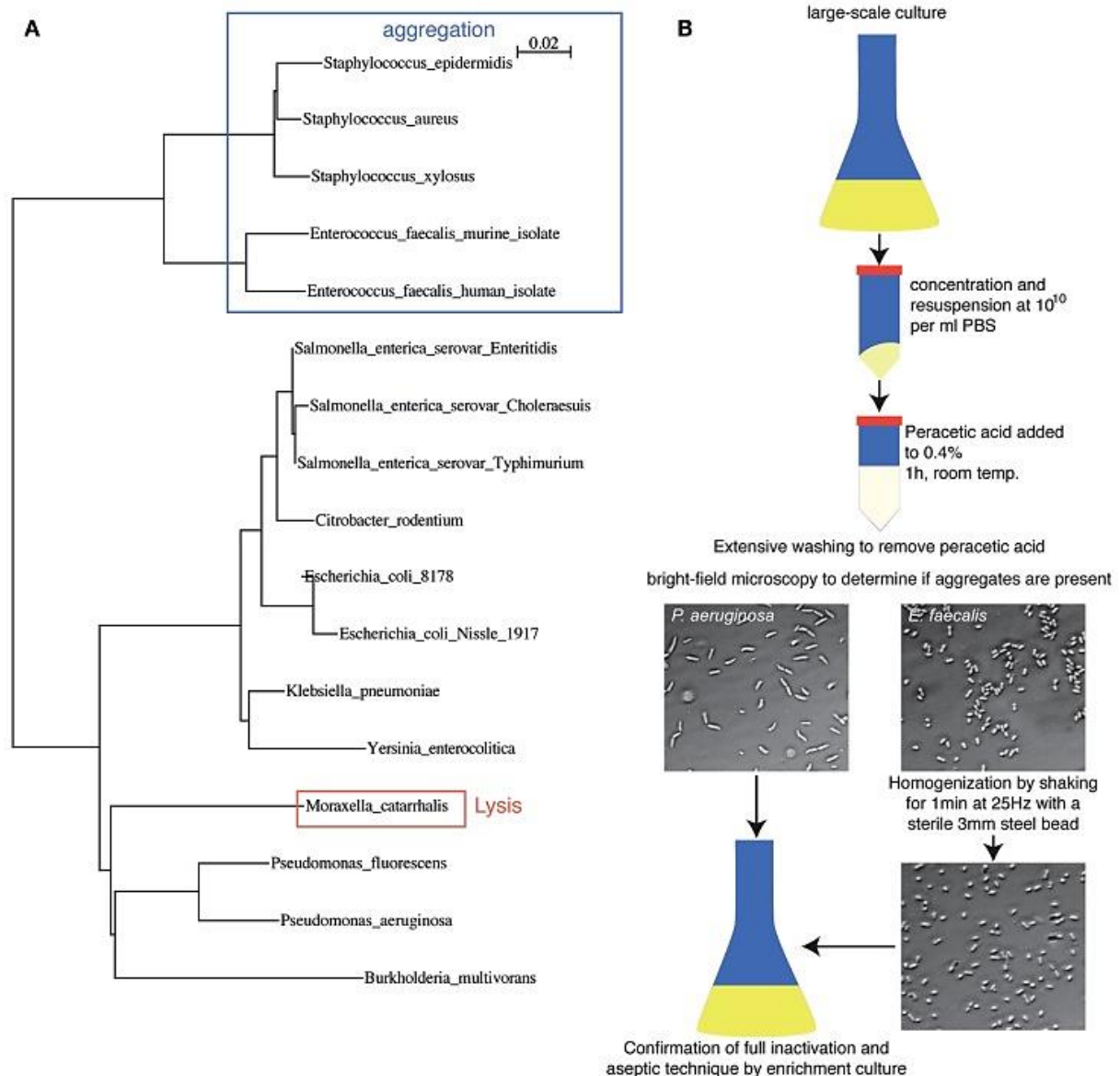

Figure 2 Peracetic acid can be used to inactivate a broad range of bacterial species relevant to intestinal immunology research. **(A)** Dendrogram based on 16S rDNA sequence differences of the species tested so far, highlighting potential pitfalls. Legend refers to the distance score as calculated by ClustalX neighbour-joining multiple alignment. **(B)** Schematic diagram of oral vaccine production, including homogenization to disrupt bacterial clumps produced during inactivation, and expected brightfield images.

We next compared the induction of specific intestinal IgA by orally delivered peracetic acid-inactivated bacteria and a standard live-attenuated *Salmonella* vaccine strain *sseD::aphT* (Endt *et al.*, 2010; Hapfelmeier *et al.*, 2005). When C57BL/6 mice were pre-treated with high-dose streptomycin and then infected with *S.* Typhimurium *sseD::aphT* (Hapfelmeier *et al.*, 2005), they developed a self-limiting intestinal inflammation and robust *S.* Typhimurium-specific intestinal immunity. In parallel, we constructed a peracetic acid-inactivated vaccine from a fully avirulent *S.* Typhimurium mutant, henceforth, referred to as PA.STm (*ΔsseD ΔinvG* – M2702, used to minimize operator risk during vaccine preparation). 10^{10} particles of PA.STm were gavaged once per week for 3 weeks without antibiotic pre-treatment. On day 21 after the vaccination start, PA.STm-treated mice developed a *S.* Typhimurium-specific intestinal IgA titre that is equivalent to that observed at 3 weeks post-infection with the live attenuated strain *S.* Typhimurium M556, as determined by bacterial flow cytometry (Slack *et al.*, 2009) (Figures 3A,B; Figure S1 in Supplementary Material). Serum IgA and IgM responses were also equivalent between the two treatments (Figure S2 in Supplementary Material). Serum IgG2b (Figure 3C) and IgG1 (Figure S2 in Supplementary Material) responses induced by PA.STm are low, but higher than those observed at the same time-point during infection with the live-attenuated vaccine. Mice receiving PA.STm displayed zero detectable intestinal inflammation as determined by histopathology scoring (data not shown), or by quantification of faecal Lipocalin 2 (Figure 3D) (Vijay-Kumar *et al.*, 2010). Furthermore, no live *S.* Typhimurium was recovered from the cecum content or from draining lymphoid tissues of mice receiving high-dose peracetic acid-inactivated bacteria, whereas this is observed in 100% of mice vaccinated with live-attenuated strains at this time-point (Figures 3E, F). To demonstrate that this robust induction of specific IgA is not restricted to *Salmonella* Typhimurium, we tested peracetic acid-inactivated oral vaccines from a range of *Enterobacteriaceae* species *in vivo*. We could demonstrate robust induction of specific IgA against two other non-typhoidal *Salmonella* serovars (Enteritidis – Figure 3G, Choleraesuis – data not shown), as well as the more distantly related species *Yersinia enterocolitica* and *Citrobacter rodentium* (Figures 3H, I).
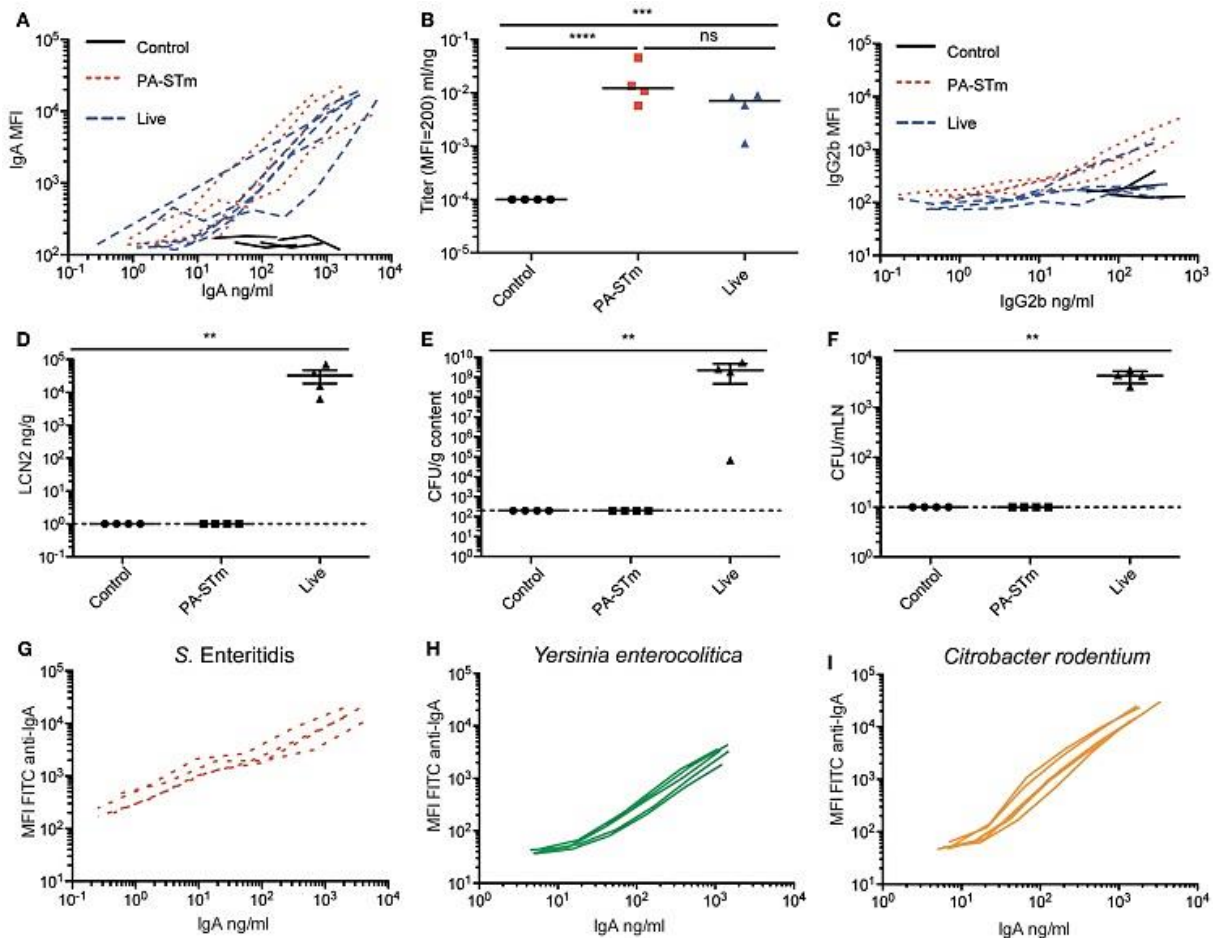
Figure 3 Oral PA.STm is a strong inducer of specific intestinal IgA in the absence of pathology. C57BL/6 SOPF mice were either pre-treated with 1.0 g/kg streptomycin and infected orally with 5×10^7 CFU of the oral vaccination *S.* Typhimurium strain M556 (SB300 Δ*sseD*) ("live") or were gavaged once a week with 10^{10} particles of peracetic acid-killed *S.* Typhimurium ("PA.STm") over 3 weeks. **(A)** Intestinal lavage IgA titre curves and **(B)** intestinal lavage IgA titres, as calculated in Figure S3 in Supplementary Material (Kruskal–Wallis test on log-normalized values, $P < 0.0001$, Pairwise comparisons calculated by Dunn's post-tests). **(C)** Serum IgG2b titre curves at day 21 after the first vaccination/infection, as determined by bacterial flow cytometry. **(D)** Lipocalin 2 in faeces at day 21 after the first vaccination/infection (Kruskal–Wallis test, $P = 0.0054$ with Dunn's post-test). **(E,F)** CFU of live *S.* Typhimurium recovered from the cecal content and mesenteric lymph nodes at the same time-point. One representative experiment of two shown. **(G–I)** Specific IgA induced by vaccination with peracetic acid-killed vaccines generated from with *S.* Enteritidis*, Yersinia enterocolitica*, and *Citrobacter rodentium*. Titres were determined by flow cytometry and ELISA. $N = 5$ mice per vaccine tested.

We next tested the host requirements for induction of specific IgA by peracetic acid-inactivated *Salmonella*. As expected for a high-avidity antibody responses (Hale *et al.*, 2015), induction of high-titre IgA by PA.STm was abrogated in TCRβ$^{-/-}$ TCRδ$^{-/-}$ mice (lacking the entire T cell compartment), even when lower total IgA production was taken into account, indicating that the inactivated vaccine is also capable of eliciting a T follicular helper response facilitating specific IgA production (Figure 4A). Importantly, we observed a strong quantitative effect of different microbiota compositions on *S.* Typhimurium-specific IgA titres, which roughly correlated with hygiene status (Figure 4B). Mice with a very limited microbiota "LCM – low complexity microbiota" (Stecher *et al.*, 2010) (LCM – separate cages, Figure 4B), or mice

recently re-derived into an ultra-clean SOPF foster colony (Figure 3A), produce very high IgA titres with little mouse-to-mouse variation. By contrast, mice bred in a SPF colony that harbours a more diverse microbiota, including low levels of protozoa (SPF – separate cages, Figure 4B), produced lower and more variable IgA titres specific for *S.* Typhimurium when vaccinated in parallel. Cohousing of LCM mice with animals with a diverse SPF microbiota for 3 weeks prior to commencement of vaccination significantly decreased the titre of *S.* Typhimurium-specific IgA produced (co-housed, Figure 4B). Correspondingly, pre-treatment of SPF animals with ampicillin or gentamicin 24 h prior to each vaccination increased final antibody titres (Figure 4C). However, as minimal disruption of the microbiota community was a major aim in developing our inactivated vaccination protocol, antibiotic-mediated augmentation of the vaccination response was not further employed. While it is beyond the scope of the current investigation to determine the exact nature of the "transferrable" microbiota that mediates this effect, it will clearly be critical to control for microbiota composition in all studies employing inactivated oral vaccines.
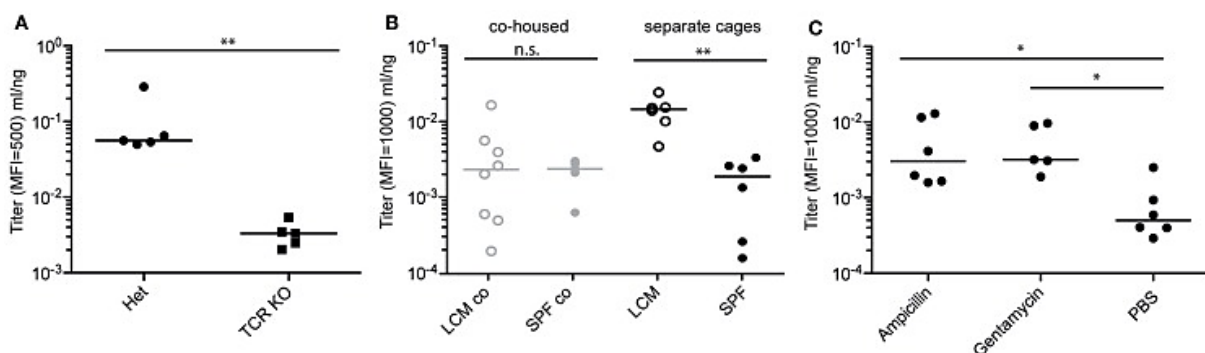

Figure 4 Specific IgA induction by PA.STm is dependent on T cells and the microbiota. **(A)** TCRβδ$^{-/-}$ and matched heterozygote controls were vaccinated three times over 3 weeks with PA.STm. On day 21, after the first vaccination, all mice were euthanized, and IgA in the intestinal lavage analysed by bacterial flow cytometry for *Salmonella* specific IgA, and ELISA for total IgA concentrations. Pooled data from two independent experiments. Mann–Whitney *U* test *P* = 0.0079. **(B)** Female LCM and SPF mice were either co-housed for 3 weeks, or were housed separately under identical conditions. Subsequently, all mice were gavaged three times over 3 weeks with PA.STm. Antibody titres were determined as above on day 21 after the initial vaccination. Pooled data from three independent experiments. Two-way ANOVA *P* (hygiene effect) = 0.0142, *P* (Interaction between housing and hygiene) = 0.0104. **(C)** C57BL/6 SPF mice were pre-treated orally with vehicle only (PBS) or high-dose ampicillin (0.8 g/kg) or gentamycin (1 g/kg) 24 h prior to each PA.STm dose. Three rounds of pre-treatment and vaccination were carried out over 3 weeks. On day 21, antibody titres were determined as in **(A)**. Pooled data from two independent experiments. Kruskal–Wallis *P* = 0.0140 with Dunn's post-test.

We next carried out proof-of-principle experiments to determine whether intestinal responses to peracetic acid-inactivated vaccines are functional. To this end, we made use of the murine model of invasive non-typhoidal Salmonellosis (Kaiser *et al.*, 2012). In this model, SOPF mice received high-dose oral streptomycin 24 h prior to infection to reduce the density

of the microbiota in the large intestinal lumen and generate a permissive niche for *S.* Typhimurium growth. 5×10^5 *S.* Typhimurium were given orally and grew to a density of 10^9–10^{10} CFU per gram intestinal content, filling this niche by day 1 post-infection. Once bacteria reach a sufficiently high density, virulence factor expression is triggered and *Salmonella* can invade into epithelial cells and penetrate to draining lymph nodes and systemic sites (Kaiser *et al.*, 2012). This is a particularly challenging model for vaccine-mediated protection as the lethal infectious dose in C57BL/6 mice is <10 CFU. Previous work in this model using live-attenuated vaccination had demonstrated that O-antigen-specific IgA is a necessary component of any observed protection (Endt *et al.*, 2010). Therefore, we additionally tested the effect of PA.STm in antibody-deficient animals [$J_H^{-/-}$ (Chen, J. *et al.*, 1993)] and the effect of a vaccine produced from a "rough" (i.e., O-antigen-deficient) *S.* Typhimurium strain SKI10 (*wbaP:aphT*) (Ilg *et al.*, 2009). PA.STm vaccinated wild-type mice were completely protected from an oral challenge of 5×10^5 *S.* Typhimurium in the streptomycin pre-treatment model at 24 h post-infection, with no detectable live *S.* Typhimurium recovered from the mLN, despite high levels of cecal colonization (Figures 5A,B). Additionally, no cecal pathology was observed in wild-type mice vaccinated with PA.STm as determined by histopathology (Figure 5C) or faecal Lipocalin 2 (Figure 5D). By contrast, mice vaccinated with a peracetic acid-inactivated strain lacking the O-antigen (PA-SKI10) showed no protection either at the level of cecal pathology or tissue bacterial loads (Figures 5A–D), and no IgA binding to wild-type *Salmonella* (Figure 5E). This was not due to reduced antigenicity of this vaccine as IgA induce by PA-SKI10 was as good as that induced by PA.STm in binding to surface structures of O-sidechain-deficient *S.* Typhimurium mutants (rough or deep-rough strains, Figures 5F,G). Rather, the presence of O-sidechains masks most other relevant antigens on the surface of live bacteria. As would be predicted from previous work (Endt *et al.*, 2010), antibodies were an essential component of the protective response, as PA.STm vaccinated $J_H^{-/-}$ mice, which lack all mature B cells (Chen, J. *et al.*, 1993), show no measurable protection from infection (Figures 5A–E). Furthermore, vaccinated IgA-deficient mice display greatly reduced protection from infection (Figures 5H-J), when compared to IgA heterozygote littermates. Therefore, the main protective immune response induced by PA.STm was O-antigen-specific IgA.
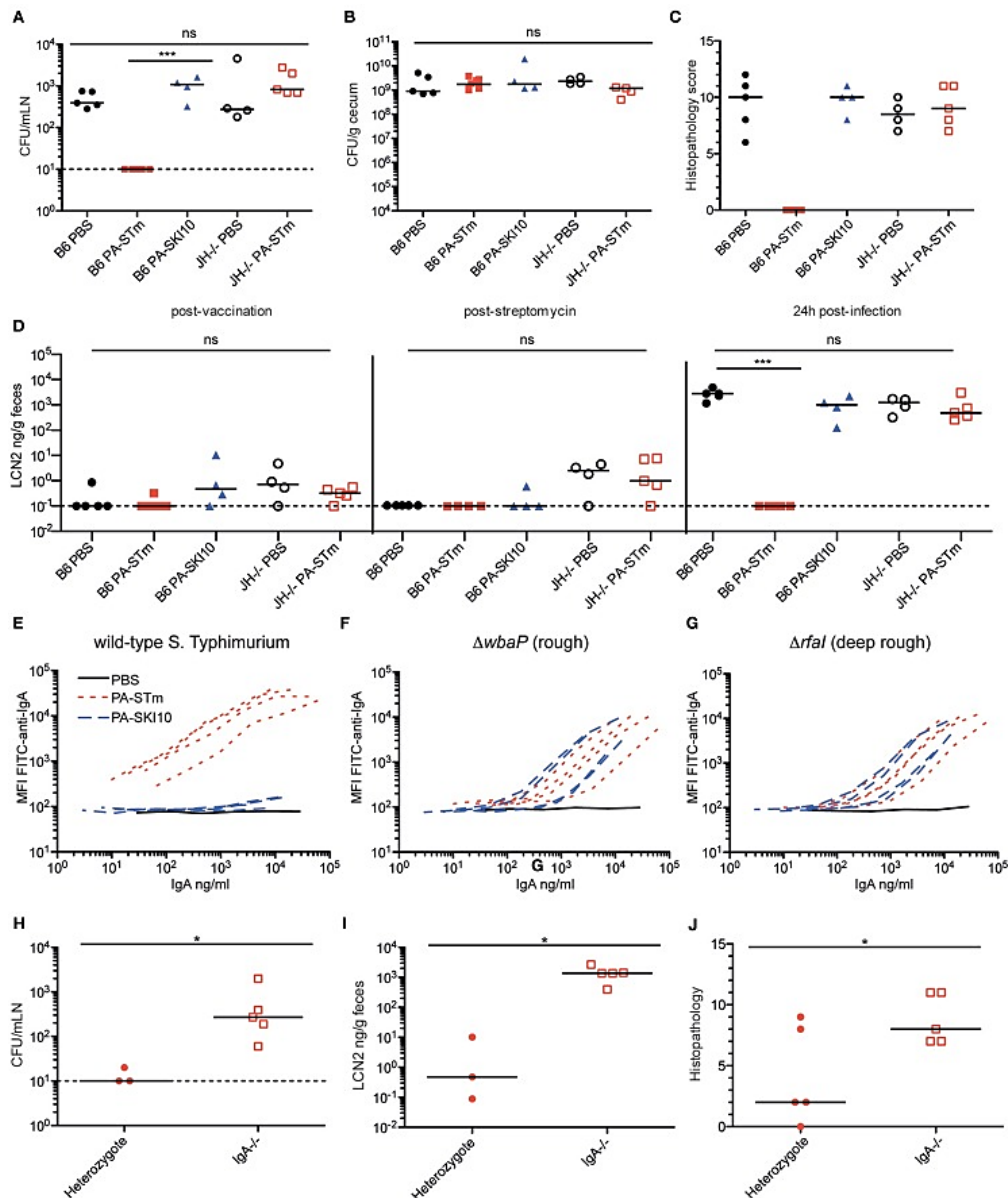
Figure 5 PA.STm provides protection from non-typhoidal Salmonellosis in an O-antigen and antibody-dependent manner. **(A)** C57BL/6 SOPF or JH$^{-/-}$ mice recently rederived into an SOPF colony were vaccinated once per week for 3 weeks with the indicated vaccine (PA.STm: killed O-antigen-sufficient vaccine, PA-SKI10: killed O-antigen-deficient "rough" strain). On day 21, all mice were pre-treated with 1.0 g/kg streptomycin p.o. 24 h later, all mice received 10 CFU of wild-type *S.* Typhimurium SB300 p.o. Mice were euthanized 24-h post-infection. **(A,B)** Live *S.* Typhimurium CFU in the mesenteric lymph nodes (Kruskal–Wallis $P = 0.0009$, with Dunn's post-tests) and cecal content. **(C)** Histopathology of the cecum at 24-h post-infection. (Kruskal–Wallis test $P = 0.0325$) **(D)** Faecal Lipocalin 2 on day 21 post-vaccination, 24 h post streptomycin treatment and 24 h post-challenge (24 h post-challenge, Kruskal–Wallis $P = 0.0006$, with Dunn's post-tests). **(E–G)** Intestinal IgA titre specific for the surface of wild-type *S.* Typhimurium, rough *S.* Typhimurium ($\Delta wbaP$) and deep-rough *S.* Typhimurium ($\Delta rfaI$), as determined by bacterial surface-specific bacterial flow cytometry. **(H–J)** IgA$^{\pm}$ and IgA$^{-/-}$ SOPF littermate mice were vaccinated three times over 3 weeks with PA.STm. All mice were streptomycin pre-treated, followed by infection with 10^5 CFU wild-type *S.* Typhimurium. All parameters were assessed 24-h post-infection. **(H)** CFU of live *S.* Typhimurium in the mesenteric lymph nodes (Mann–Whitney U $P = 0.0358$). **(I,J)** Intestinal pathology as determined by faecal Lipocalin 2 levels (Mann–Whitney U $P = 0.0357$) and histopathology (Mann–Whitney U $P = 0.0336$).

The sterile nature of PA.STm immediately suggested its potential to investigate mucosal immunity in situations of severe innate immune deficiency. Both human patients and mice carrying mutations in the phagocyte NADPH oxidase component gp91phox (*cybb*) are extremely susceptible to invasive Salmonellosis and also develop overt pathology when infected with live-attenuated oral vaccination strains (Burniat *et al.*, 1980; Felmy *et al.*, 2013). In contrast to live-attenuated *Salmonella*, PA.STm was extremely well tolerated in *cybb*-deficient animals with no statistical difference in inflammatory scores or intestinal inflammatory markers between mock-treated and vaccinated mice (Figure 6A, data not shown).

Additionally, the *cybb* pathway is not required for successful responses to the vaccine, as titres of intestinal IgA (Figure 6B) are similar to those of matched wild-type mice. Critically, this adaptive immune response is equally protective in *cybb*-deficient and wild-type mice up to 24 h post-infection with a large inoculum (5×10^5 CFU, Figures 6C-E), and up to at least 80 h post-infection with a small inoculum (50 CFU, Figures 6F-H).
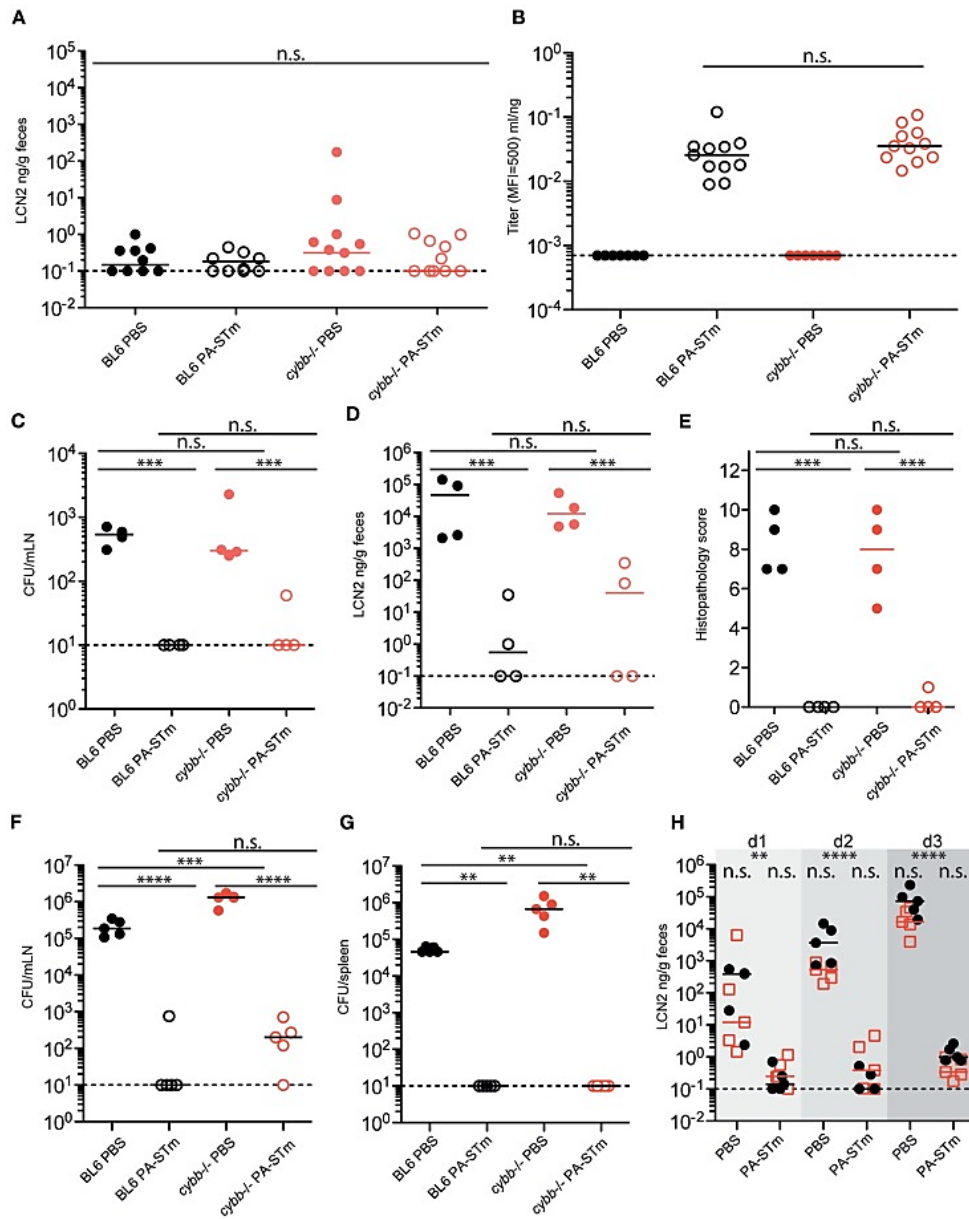
Figure 6 Oral PA.STm is safe for vaccination in *cybb*-deficient mice and provides dose-dependent protection from tissue invasion and pathology up to at least 80-h post-infection in the non-typhoidal Salmonellosis model. C57BL/6 and *cybb*−/− mice recently re-derived into an identical SOPF foster colony were vaccinated three times over 3 weeks with PA.STm or vehicle alone (PBS). **(A,B)** On day 21 after the first vaccination, cecal pathology was determined by faecal Lipocalin 2 ELISA [two-way ANOVA P (genotype) = 0.3583, P (vaccination) = 0.3500, P (Interaction) = 0.3515] **(A)** and intestinal IgA titres were determined by bacterial flow cytometry (Mann–Whitney U test on vaccinated samples only, P = 0.1679) **(B)**. **(C–E)** Mice vaccinated as in A and B were pre-treated with 1 g/kg streptomycin on day 21 after the first vaccination and subsequently infected with 10^5 wild-type *S.* Typhimurium. **(C)** Live *S.* Typhimurium CFU recovered from the mesenteric lymph nodes at 24-h post-infection. **(D,E)**. Intestinal inflammation as determined by faecal Lipocalin 2 **(D)** and histopathology scoring of cecum tissue **(E)**. **(C–E)** were analysed by (two-way ANOVA, ***P (vaccination) <0.001) **(F–H)**. Mice vaccinated as in **(A,B)** were pretreated with 1 g/kg streptomycin on day 21 after the first vaccination and subsequently infected with 50 CFU wild-type *S.* Typhimurium. **(F,G)** Live *S.* Typhimurium CFU recovered from the mesenteric lymph nodes **(F)** [two-way ANOVA. P (genotype) = <0.0001, P (vaccination) <0.0001, P (interaction) = <0.0001] and spleen **(G)** (two-way ANOVA. P (genotype) = 0.0098, P (vaccination) = 0.0038, P (interaction) = 0.0098) at 80-h post-infection. **(H)** Intestinal inflammation as determined by faecal Lipocalin 2 up to 80 h (day 3) post-infection (two-way repeat-measures ANOVA with Bonferroni post-tests on log-normalized data. **P < 0.01, ****P < 0.0001).

64

Discussion

Based on our previous observations with apathogenic species, we devised and tested a highly simplified strategy to generate high dose inactivated oral vaccines, capable of inducing robust specific intestinal IgA responses. The strong oxidizing agent peracetic acid has long been used as a decontaminant in the husbandry of axenic animals (Smith *et al.*, 2007) and in the food industry (Bauermeister *et al.*, 2008; Rajkowski *et al.*, 2009). Here, we demonstrate that the bacterial killing efficiency of 0.4% peracetic acid is considerably higher than those of standard vaccine inactivation protocols (4% paraformaldehyde, pasteurization, or 3% hydrogen peroxide), and can be used on a wide range of bacterial species. This permits the oral application of very high numbers of vaccine particles with close-to-zero risk of inoculating live bacteria (Figures 1 and 2). When sufficient numbers of inactivated bacteria are delivered orally, we can induce a robust T-cell-dependent mucosal IgA response against a range of *Enterobacteriaceae* (Figures 3 and 4). This occurs in the complete absence of intestinal pathology, in the complete absence of live bacteria and in the absence of exogenous mucosal adjuvants (Figure 3), even in situations of severe innate immune deficiency (Figure 6). The immune responses induced can protect from oral infection with virulent *S.* Typhimurium in the mouse model of non-typhoidal Salmonellosis (Figures 5 and 6). This is the first demonstration of phagocyte oxidative burst-independent protection by high-titre IgA in this infectious model. Our observation somewhat goes against a prevailing dogma in mouse vaccination that sterile material delivered orally induces either tolerance or is simply ignored by the immune system (Hapfelmeier *et al.*, 2010; Macpherson *et al.*, 2013; Pabst *et al.*, 2012). While both phenomena can be easily observed, our clear demonstration of immunity highlights the quantitative nature of mucosal immune system stimulation.

The beauty of this strategy is that it permits researchers using well-established animal models of host–microbiota interactions or host–pathogen–(microbiota) interactions to generate high-titre IgA responses in an otherwise largely unperturbed host. Highly controlled infections or colonisations can then be carried out to determine the mechanisms by which IgA alters microbial physiology *in vivo* (for example, bacterial virulence, induction of inflammatory signalling, within-host population dynamics, and within-host evolution). When combined with very rigorous aseptic technique, this methodology should be safe enough to apply in germ-free and gnotobiotic animals without contamination (Smith *et al.*, 2007). Extra caution would need to be applied with species capable of forming spores, which may be highly resistant (Grover *et al.*, 2013) and hard to detect by *in vitro* enrichment culture. Another benefit of the technique is that the antigenic composition of the vaccine is determined by *in vitro* growth and the bacterial phenotype becomes locked at the time of inactivation. Therefore, there is the possibility to grow the vaccination strain under selection to maintain phase-locked states, or to overexpress factors associated with a high metabolic cost. This is almost impossible to

achieve with live vaccines due to rapid out-selection of the fittest strains *in vivo* (Diard *et al.*, 2013). Of note, the more pessimistic reader may spot that this is also a potential disadvantage, as bacteria grown in rich media *in vitro* may be antigenically distinct from those *in vivo* and modification of the culture conditions may be important to generate appropriate responses.

We envisage this technique as being immediately useful to the field of host–microbial interaction in experimental animal models. Based on our previous work, we expect the induced IgA responses to wane quite rapidly after the final vaccine dose (Hapfelmeier *et al.*, 2010) and, therefore, the usefulness in human and veterinary medicine may be limited. However, it should be noted that two licensed human oral vaccines against *V. cholerae* and one vaccine in late-stage clinical trials against ETEC (Lundgren *et al.*, 2014) work on the basis of high numbers of bacteria killed by formalin or heat-treatment (Kabir, 2014). All of these vaccines include an autologous toxin (or subunit thereof) which is a known mucosal adjuvant (Lycke, 2005). It remains unclear whether the absence of long-term-mucosal memory observed with non-adjuvanted mucosal vaccines in the murine system is due to physiological differences, or the absence of adjuvant. The greatly increased efficiency of peracetic acid-mediated inactivation, as compared to paraformaldehyde and heat-treatment, suggests that this process could be used to increase the efficiency of human oral vaccines adjuvanted with cholera toxin B or heat-labile toxin B subunit. It will additionally be interesting to test these adjuvanted vaccines to look for qualitative and quantitative differences in activation of mucosal immunity in animal models. Furthermore, there are a number of clinical situations where highly susceptible patients could benefit from a short-term extremely safe boost in mucosal immunity against diverse bacterial strains, such as prior to myeloablation, in primary innate immune deficiencies, during TNF-blockade, or prior to faecal transplantation. In these situations, the ability to easily produce oral vaccines from a broad range of bacterial species may be of clinical interest.

Currently, we have not tested whether this technique is also suitable for inactivation of strictly anaerobic bacterial species. A further limitation is that we have not investigated the nature of T cell responses induced by peracetic acid-inactivated oral vaccines. Additionally, we observe an effect of microbiota composition on the efficiency of specific IgA induction by peracetic acid-inactivated vaccines, which suggests that there will be lab-to-lab variation in absolute efficacy. Despite these caveats, we feel this technique finally makes it possible to cleanly study the effects of the antibody-mediated intestinal immunity on host-microbial interactions.

Conflict of Interest Statement

The authors declare that the research was conducted in the absence of any commercial or financial relationships that could be construed as a potential conflict of interest.
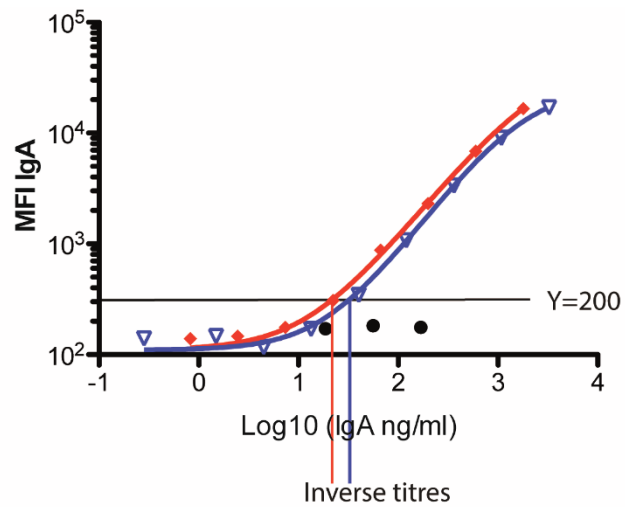
Acknowledgments

Funding

Supplementary Figures

Supplementary Figure 1: Calculation of antibody titres from bacterial flow cytometry data. Live bacterial targets were stained with dilution series of serum or intestinal lavages. Total antibody concentrations in serum and lavages was determined by sandwich ELISA. Median fluorescence intensity (MFI) was calculated for each flow cytometry sample and plotted against the total antibody concentration in each dilution series step (IgA in this example). 4-parameter logistic curves were fitted to each data series using Graphpad Prism by least-squares nonlinear regression. The concentration of total antibody required to achieve a given MFI (in the example =200) was calculated by re-arrangement of the fitted 4-parameter logistic equation for each sample. As this value is low where a strong antibody response is present, the inverse of this value was plotted. Thus, titres are calculated as the inverse total antibody concentration required to achieve a given (MFI). The y-axis value chosen as "above background" necessarily varies between experiments due to the flow cytometer settings, but is constant within any one analysis.
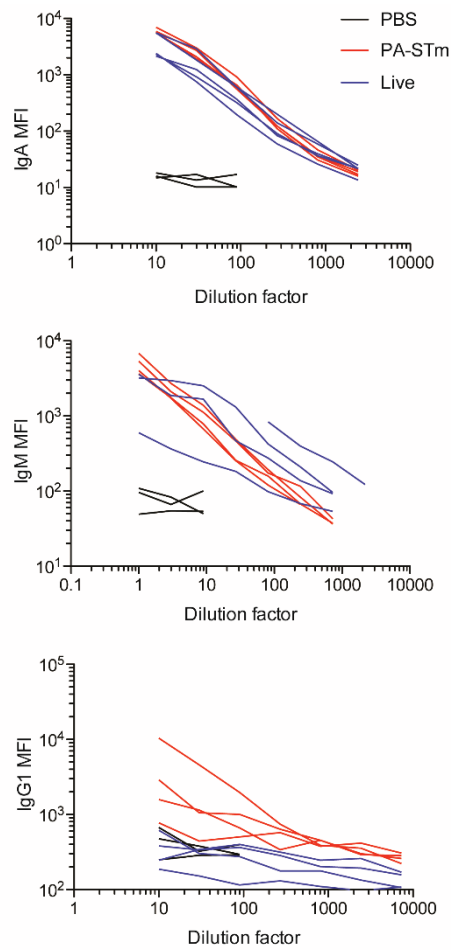
Supplementary Figure 2. Serum antibody titration curves against *S.* Typhimurium **corresponding to Figure 3A-C.** C57BL/6 SOPF mice were either pre-treated with 1.0g/kg streptomycin and infected orally with 5x107 CFU of the oral vaccination *S.* Typhimurium strain M556 (SB300 ΔsseD) ("Live") or were gavaged once a week with 1010 particles of peracetic acid-killed *S.* Typhimurium ("PA.STm") or vehicle only ("PBS") over three weeks. Serum was collected on d21 after the first gavage/infection (d7 after the final PA.STm gavage) and analysed by bacterial flow cytometry.

References

Abd El Ghany, M., Jansen, A., Clare, S., Hall, L., Pickard, D., Kingsley, R. A., & Dougan, G. (2007). Candidate live, attenuated Salmonella enterica serotype Typhimurium vaccines with reduced fecal shedding are immunogenic and effective oral vaccines. *Infect Immun, 75*(4), 1835-1842.

Amanna, I. J., Raue, H. P., & Slifka, M. K. (2012). Development of a new hydrogen peroxide-based vaccine platform. *Nat Med, 18*(6), 974-979.

Azegami, T., Yuki, Y., & Kiyono, H. (2014). Challenges in mucosal vaccines for the control of infectious diseases. *Int Immunol, 26*(9), 517-528.

Balmer, M. L., Slack, E., de Gottardi, A., Lawson, M. A., Hapfelmeier, S., Miele, L., Grieco, A., Van Vlierberghe, H., Fahrner, R., Patuto, N., Bernsmeier, C., Ronchi, F., Wyss, M., Stroka, D., Dickgreber, N., Heim, M. H., McCoy, K. D., & Macpherson, A. J. (2014). The liver may act as a firewall mediating mutualism between the host and its gut commensal microbiota. *Sci Transl Med, 6*(237), 237ra266.

Barthel, M., Hapfelmeier, S., Quintanilla-Martinez, L., Kremer, M., Rohde, M., Hogardt, M., Pfeffer, K., Russmann, H., & Hardt, W. D. (2003). Pretreatment of mice with streptomycin provides a Salmonella enterica serovar Typhimurium colitis model that allows analysis of both pathogen and host. *Infect Immun, 71*(5), 2839-2858.

Battistoni, A. (2003). Role of prokaryotic Cu,Zn superoxide dismutase in pathogenesis. *Biochem Soc Trans, 31*(Pt 6), 1326-1329.

Bauermeister, L. J., Bowers, J. W., Townsend, J. C., & McKee, S. R. (2008). Validating the efficacy of peracetic acid mixture as an antimicrobial in poultry chillers. *J Food Prot, 71*(6), 1119-1122.

Bournazos, S., DiLillo, D. J., & Ravetch, J. V. (2015). The role of Fc-FcgammaR interactions in IgG-mediated microbial neutralization. *J Exp Med, 212*(9), 1361-1369.

Burniat, W., Toppet, M., & De Mol, P. (1980). Acute and recurrent salmonella infections in three children with chronic granulomatous disease. *J Infect, 2*(3), 263-268.

Cheminay, C., & Hensel, M. (2008). Rational design of Salmonella recombinant vaccines. *Int J Med Microbiol, 298*(1-2), 87-98.

Chen, J., Trounstine, M., Alt, F. W., Young, F., Kurahara, C., Loring, J. F., & Huszar, D. (1993). Immunoglobulin gene rearrangement in B cell deficient mice generated by targeted deletion of the JH locus. *Int Immunol, 5*(6), 647-656.

Chen, X., Bauermeister, L. J., Hill, G. N., Singh, M., Bilgili, S. F., & McKee, S. R. (2014). Efficacy of various antimicrobials on reduction of salmonella and campylobacter and quality attributes of ground chicken obtained from poultry parts treated in a postchill decontamination tank. *J Food Prot, 77*(11), 1882-1888.

Diard, M., Garcia, V., Maier, L., Remus-Emsermann, M. N., Regoes, R. R., Ackermann, M., & Hardt, W. D. (2013). Stabilization of cooperative virulence by the expression of an avirulent phenotype. *Nature, 494*(7437), 353-356.

Endt, K., Stecher, B., Chaffron, S., Slack, E., Tchitchek, N., Benecke, A., Van Maele, L., Sirard, J. C., Mueller, A. J., Heikenwalder, M., Macpherson, A. J., Strugnell, R., von Mering, C., & Hardt, W. D. (2010). The microbiota mediates pathogen clearance from the gut lumen after non-typhoidal Salmonella diarrhea. *PLoS Pathog, 6*(9), e1001097.

Felmy, B., Songhet, P., Slack, E. M., Muller, A. J., Kremer, M., Van Maele, L., Cayet, D., Heikenwalder, M., Sirard, J. C., & Hardt, W. D. (2013). NADPH oxidase deficient mice develop colitis and bacteremia upon infection with normally avirulent, TTSS-1- and TTSS-2-deficient Salmonella Typhimurium. *PLoS One, 8*(10), e77204.

Galen, J. E., & Curtiss, R., 3rd. (2014). The delicate balance in genetically engineering live vaccines. *Vaccine, 32*(35), 4376-4385.

Grover, N., Dinu, C. Z., Kane, R. S., & Dordick, J. S. (2013). Enzyme-based formulations for decontamination: current state and perspectives. *Appl Microbiol Biotechnol, 97*(8), 3293-3300.

Haas, A., Zimmermann, K., Graw, F., Slack, E., Rusert, P., Ledergerber, B., Bossart, W., Weber, R., Thurnheer, M. C., Battegay, M., Hirschel, B., Vernazza, P., Patuto, N., Macpherson, A. J.,

Gunthard, H. F., Oxenius, A., & Swiss, H. I. V. Cohort Study. (2011). Systemic antibody responses to gut commensal bacteria during chronic HIV-1 infection. *Gut, 60*(11), 1506-1519.

Hale, J. S., & Ahmed, R. (2015). Memory T follicular helper CD4 T cells. *Front Immunol, 6*, 16.

Hapfelmeier, S., Ehrbar, K., Stecher, B., Barthel, M., Kremer, M., & Hardt, W. D. (2004). Role of the Salmonella pathogenicity island 1 effector proteins SipA, SopB, SopE, and SopE2 in Salmonella enterica subspecies 1 serovar Typhimurium colitis in streptomycin-pretreated mice. *Infect Immun, 72*(2), 795-809.

Hapfelmeier, S., Lawson, M. A., Slack, E., Kirundi, J. K., Stoel, M., Heikenwalder, M., Cahenzli, J., Velykoredko, Y., Balmer, M. L., Endt, K., Geuking, M. B., Curtiss, R., 3rd, McCoy, K. D., & Macpherson, A. J. (2010). Reversible microbial colonization of germ-free mice reveals the dynamics of IgA immune responses. *Science, 328*(5986), 1705-1709.

Hapfelmeier, S., Stecher, B., Barthel, M., Kremer, M., Muller, A. J., Heikenwalder, M., Stallmach, T., Hensel, M., Pfeffer, K., Akira, S., & Hardt, W. D. (2005). The Salmonella pathogenicity island (SPI)-2 and SPI-1 type III secretion systems allow Salmonella serovar typhimurium to trigger colitis via MyD88-dependent and MyD88-independent mechanisms. *J Immunol, 174*(3), 1675-1685.

Harriman, G. R., Bogue, M., Rogers, P., Finegold, M., Pacheco, S., Bradley, A., Zhang, Y., & Mbawuike, I. N. (1999). Targeted deletion of the IgA constant region in mice leads to IgA deficiency with alterations in expression of other Ig isotypes. *J Immunol, 162*(5), 2521-2529.

Hoiseth, S. K., & Stocker, B. A. (1981). Aromatic-dependent Salmonella typhimurium are non-virulent and effective as live vaccines. *Nature, 291*(5812), 238-239.

Hooper, L. V., Littman, D. R., & Macpherson, A. J. (2012). Interactions between the microbiota and the immune system. *Science, 336*(6086), 1268-1273.

Ilg, K., Endt, K., Misselwitz, B., Stecher, B., Aebi, M., & Hardt, W. D. (2009). O-antigen-negative Salmonella enterica serovar Typhimurium is attenuated in intestinal colonization but elicits colitis in streptomycin-treated mice. *Infect Immun, 77*(6), 2568-2575.

Iwasaki, A., & Medzhitov, R. (2015). Control of adaptive immunity by the innate immune system. *Nat Immunol, 16*(4), 343-353.

Kabir, S. (2014). Critical analysis of compositions and protective efficacies of oral killed cholera vaccines. *Clin Vaccine Immunol, 21*(9), 1195-1205.

Kaiser, P., Diard, M., Stecher, B., & Hardt, W. D. (2012). The streptomycin mouse model for Salmonella diarrhea: functional analysis of the microbiota, the pathogen's virulence factors, and the host's mucosal immune response. *Immunol Rev, 245*(1), 56-83.

Kaiser, P., Regoes, R. R., Dolowschiak, T., Wotzka, S. Y., Lengefeld, J., Slack, E., Grant, A. J., Ackermann, M., & Hardt, W. D. (2014). Cecum lymph node dendritic cells harbor slow-growing bacteria phenotypically tolerant to antibiotic treatment. *PLoS Biol, 12*(2), e1001793.

Kinder, S. A., Badger, J. L., Bryant, G. O., Pepe, J. C., & Miller, V. L. (1993). Cloning of the YenI restriction endonuclease and methyltransferase from Yersinia enterocolitica serotype O8 and construction of a transformable R-M+ mutant. *Gene, 136*(1-2), 271-275.

Lundgren, A., Bourgeois, L., Carlin, N., Clements, J., Gustafsson, B., Hartford, M., Holmgren, J., Petzold, M., Walker, R., & Svennerholm, A. M. (2014). Safety and immunogenicity of an improved oral inactivated multivalent enterotoxigenic Escherichia coli (ETEC) vaccine administered alone and together with dmLT adjuvant in a double-blind, randomized, placebo-controlled Phase I study. *Vaccine, 32*(52), 7077-7084.

Lycke, N. (2005). Targeted vaccine adjuvants based on modified cholera toxin. *Curr Mol Med, 5*(6), 591-597.

Macpherson, A. J., & McCoy, K. D. (2013). Stratification and compartmentalisation of immunoglobulin responses to commensal intestinal microbes. *Semin Immunol, 25*(5), 358-363.

Macpherson, A. J., & Uhr, T. (2004). Induction of protective IgA by intestinal dendritic cells carrying commensal bacteria. *Science, 303*(5664), 1662-1665.

Maier, L., Vyas, R., Cordova, C. D., Lindsay, H., Schmidt, T. S., Brugiroux, S., Periaswamy, B., Bauer, R., Sturm, A., Schreiber, F., von Mering, C., Robinson, M. D., Stecher, B., & Hardt, W. D. (2013).

Microbiota-derived hydrogen fuels Salmonella typhimurium invasion of the gut ecosystem. *Cell Host Microbe, 14*(6), 641-651.

Manohar, M., Baumann, D. O., Bos, N. A., & Cebra, J. J. (2001). Gut colonization of mice with actA-negative mutant of Listeria monocytogenes can stimulate a humoral mucosal immune response. *Infect Immun, 69*(6), 3542-3549.

Marcobal, A., Kashyap, P. C., Nelson, T. A., Aronov, P. A., Donia, M. S., Spormann, A., Fischbach, M. A., & Sonnenburg, J. L. (2013). A metabolomic view of how the human gut microbiota impacts the host metabolome using humanized and gnotobiotic mice. *ISME J, 7*(10), 1933-1943.

Matsui, H., Isshiki, Y., Eguchi, M., Ogawa, Y., & Shimoji, Y. (2015). Evaluation of the live vaccine efficacy of virulence plasmid-cured, and phoP- or aroA-deficient Salmonella enterica serovar Typhimurium in mice. *J Vet Med Sci, 77*(2), 181-186.

McKenzie, R., Walker, R. I., Nabors, G. S., Van De Verg, L. L., Carpenter, C., Gomes, G., Forbes, E., Tian, J. H., Yang, H. H., Pace, J. L., Jackson, W. J., & Bourgeois, A. L. (2006). Safety and immunogenicity of an oral, inactivated, whole-cell vaccine for Shigella sonnei: preclinical studies and a Phase I trial. *Vaccine, 24*(18), 3735-3745.

Mombaerts, P., Clarke, A. R., Rudnicki, M. A., Iacomini, J., Itohara, S., Lafaille, J. J., Wang, L., Ichikawa, Y., Jaenisch, R., Hooper, M. L., & et al. (1992). Mutations in T-cell antigen receptor genes alpha and beta block thymocyte development at different stages. *Nature, 360*(6401), 225-231.

Moor, K., & Slack, E. (2015). What Makes A Bacterial Oral Vaccine a Strong Inducer of High-Affinity IgA Responses? *Antibodies (Basel), 4*(4), 295.

Nutter, R. L., Bullas, L. R., & Schultz, R. L. (1970). Some properties of five new Salmonella bacteriophages. *J Virol, 5*(6), 754-764.

Pabst, O., & Mowat, A. M. (2012). Oral tolerance to food protein. *Mucosal Immunol, 5*(3), 232-239.

Park, E., Lee, C., Bisesi, M., & Lee, J. (2014). Efficiency of peracetic acid in inactivating bacteria, viruses, and spores in water determined with ATP bioluminescence, quantitative PCR, and culture-based methods. *J Water Health, 12*(1), 13-23.

Peters, S. E., Paterson, G. K., Bandularatne, E. S., Northen, H. C., Pleasance, S., Willers, C., Wang, J., Foote, A. K., Constantino-Casas, F., Scase, T. J., Blacklaws, B. A., Bryant, C. E., Mastroeni, P., Charles, I. G., & Maskell, D. J. (2010). Salmonella enterica serovar typhimurium trxA mutants are protective against virulent challenge and induce less inflammation than the live-attenuated vaccine strain SL3261. *Infect Immun, 78*(1), 326-336.

Pollock, J. D., Williams, D. A., Gifford, M. A., Li, L. L., Du, X., Fisherman, J., Orkin, S. H., Doerschuk, C. M., & Dinauer, M. C. (1995). Mouse model of X-linked chronic granulomatous disease, an inherited defect in phagocyte superoxide production. *Nat Genet, 9*(2), 202-209.

Rajkowski, K. T., & Ashurst, K. (2009). Use of 1% peroxyacetic acid sanitizer in an air-mixing wash basin to remove bacterial pathogens from seeds. *Foodborne Pathog Dis, 6*(9), 1041-1046.

Schauer, D. B., Zabel, B. A., Pedraza, I. F., O'Hara, C. M., Steigerwalt, A. G., & Brenner, D. J. (1995). Genetic and biochemical characterization of Citrobacter rodentium sp. nov. *J Clin Microbiol, 33*(8), 2064-2068.

Shroff, K. E., Meslin, K., & Cebra, J. J. (1995). Commensal enteric bacteria engender a self-limiting humoral mucosal immune response while permanently colonizing the gut. *Infect Immun, 63*(10), 3904-3913.

Slack, E., Balmer, M. L., & Macpherson, A. J. (2014). B cells as a critical node in the microbiota-host immune system network. *Immunol Rev, 260*(1), 50-66.

Slack, E., Hapfelmeier, S., Stecher, B., Velykoredko, Y., Stoel, M., Lawson, M. A., Geuking, M. B., Beutler, B., Tedder, T. F., Hardt, W. D., Bercik, P., Verdu, E. F., McCoy, K. D., & Macpherson, A. J. (2009). Innate and adaptive immunity cooperate flexibly to maintain host-microbiota mutualism. *Science, 325*(5940), 617-620.

Smith, K., McCoy, K. D., & Macpherson, A. J. (2007). Use of axenic animals in studying the adaptation of mammals to their commensal intestinal microbiota. *Semin Immunol, 19*(2), 59-69.

Stecher, B., Berry, D., & Loy, A. (2013). Colonization resistance and microbial ecophysiology: using gnotobiotic mouse models and single-cell technology to explore the intestinal jungle. *FEMS Microbiol Rev, 37*(5), 793-829.

Stecher, B., Chaffron, S., Kappeli, R., Hapfelmeier, S., Freedrich, S., Weber, T. C., Kirundi, J., Suar, M., McCoy, K. D., von Mering, C., Macpherson, A. J., & Hardt, W. D. (2010). Like will to like: abundances of closely related species can predict susceptibility to intestinal colonization by pathogenic and commensal bacteria. *PLoS Pathog, 6*(1), e1000711.

Stecher, B., Denzler, R., Maier, L., Bernet, F., Sanders, M. J., Pickard, D. J., Barthel, M., Westendorf, A. M., Krogfelt, K. A., Walker, A. W., Ackermann, M., Dobrindt, U., Thomson, N. R., & Hardt, W. D. (2012). Gut inflammation can boost horizontal gene transfer between pathogenic and commensal Enterobacteriaceae. *Proc Natl Acad Sci U S A, 109*(4), 1269-1274.

Sudhaus, N., Pina-Perez, M. C., Martinez, A., & Klein, G. (2012). Inactivation kinetics of spores of Bacillus cereus strains treated by a peracetic acid-based disinfectant at different concentrations and temperatures. *Foodborne Pathog Dis, 9*(5), 442-452.

Talham, G. L., Jiang, H. Q., Bos, N. A., & Cebra, J. J. (1999). Segmented filamentous bacteria are potent stimuli of a physiologically normal state of the murine gut mucosal immune system. *Infect Immun, 67*(4), 1992-2000.

Thammavongsa, V., Kim, H. K., Missiakas, D., & Schneewind, O. (2015). Staphylococcal manipulation of host immune responses. *Nat Rev Microbiol, 13*(9), 529-543.

Thomson, N. R., Clayton, D. J., Windhorst, D., Vernikos, G., Davidson, S., Churcher, C., Quail, M. A., Stevens, M., Jones, M. A., Watson, M., Barron, A., Layton, A., Pickard, D., Kingsley, R. A., Bignell, A., Clark, L., Harris, B., Ormond, D., Abdellah, Z., Brooks, K., Cherevach, I., Chillingworth, T., Woodward, J., Norberczak, H., Lord, A., Arrowsmith, C., Jagels, K., Moule, S., Mungall, K., Sanders, M., Whitehead, S., Chabalgoity, J. A., Maskell, D., Humphrey, T., Roberts, M., Barrow, P. A., Dougan, G., & Parkhill, J. (2008). Comparative genome analysis of Salmonella Enteritidis PT4 and Salmonella Gallinarum 287/91 provides insights into evolutionary and host adaptation pathways. *Genome Res, 18*(10), 1624-1637.

Tubo, N. J., & Jenkins, M. K. (2014). CD4+ T Cells: guardians of the phagosome. *Clin Microbiol Rev, 27*(2), 200-213.

Unhanand, M., Maciver, I., Ramilo, O., Arencibia-Mireles, O., Argyle, J. C., McCracken, G. H., Jr., & Hansen, E. J. (1992). Pulmonary clearance of Moraxella catarrhalis in an animal model. *J Infect Dis, 165*(4), 644-650.

Vidarsson, G., Dekkers, G., & Rispens, T. (2014). IgG subclasses and allotypes: from structure to effector functions. *Front Immunol, 5*, 520.

Vijay-Kumar, M., Aitken, J. D., Carvalho, F. A., Cullender, T. C., Mwangi, S., Srinivasan, S., Sitaraman, S. V., Knight, R., Ley, R. E., & Gewirtz, A. T. (2010). Metabolic syndrome and altered gut microbiota in mice lacking Toll-like receptor 5. *Science, 328*(5975), 228-231.

Walker, R. I. (2005). Considerations for development of whole cell bacterial vaccines to prevent diarrheal diseases in children in developing countries. *Vaccine, 23*(26), 3369-3385.

Wang, S., & Curtiss, R., 3rd. (2014). Development of Vaccines Using Live Vectors. *Vaccines (Basel), 2*(1), 49-88.

Wang, S., Kong, Q., & Curtiss, R., 3rd. (2013). New technologies in developing recombinant attenuated Salmonella vaccine vectors. *Microb Pathog, 58*, 17-28.

Wiesel, M., & Oxenius, A. (2012). From crucial to negligible: functional CD8(+) T-cell responses and their dependence on CD4(+) T-cell help. *Eur J Immunol, 42*(5), 1080-1088.

CHAPTER 3

-

ANALYSIS OF BACTERIAL SURFACE-SPECIFIC ANTIBODIES

IN BODY FLUIDS USING BACTERIAL FLOW CYTOMETRY

Analysis of bacterial surface-specific antibodies in body fluids using bacterial flow cytometry

Kathrin Moor[1+], Jehane Fadlallah[2+], Albulena Toska[1+], Delphine Sterlin[2], Maria L Balmer[3,4], Andrew J Macpherson[3], Guy Gorochov[2], Martin Larsen[2*], Emma Slack[1*]

1. Institute for Microbiology, ETH Zurich, Vladimir Prelog-Weg 4-10, 8093 Zurich, Switzerland

2. Université Pierre et Marie Curie, Centre de Recherche CIMI,

UPMC UMRS CR7 - Inserm U1135, 83 Bvd. de l'Hopital, 75013 Paris, France

3. Maurice Müller Laboratories (DKF), Universitätsklinik für Viszerale Chirurgie und Medizin Inselspital, University of Bern, Murtenstrasse 35, 3010 Bern, Switzerland

4. Department of Biomedicine, University Hospital Basel, Switzerland

+ These authors contributed equally to this manuscript.

Author Contributions:

K.M., J.F., A.T., D.S. generated data shown in Figures 1-11. M.B.L generated data shown in Figure13. A.J.M. provided support during the development of the method and reviewed the manuscript. G.G. provided support for adaption of the method to clinical scenarios and reviewed the manuscript. M.L. further developed the method for application to human research, generated data shown in Figure 1-11 and wrote the manuscript. E.S. established the methodology and analysis protocols, generated data shown in Figures 1-12 and wrote the manuscript.

ABSTRACT

Anti-bacterial antibody responses targeting surfaces of live bacteria or secreted toxins are likely to be relevant in controlling bacterial pathogenesis. The ability to specifically quantify bacterial surface-binding antibodies is therefore highly attractive as a quantitative correlate of immune protection. Here, binding of antibodies from various body fluids to pure-cultured live bacteria is made visible with fluorophore-conjugated secondary antibodies and measured by flow cytometry. We demonstrate the necessary controls to exclude non-specific binding and also a cross-adsorption technique to determine the extent of cross-reactivity. This technique has numerous advantages over standard ELISA and western blotting techniques due to the independence from scaffold binding, exclusion of cross-reactive elements from lysed bacteria, and ability to visualize bacterial subpopulations. Additionally, minute quantities of both bacteria and antibodies are required. The technique requires 3-4 hours of hands-on experimentation and analysis. Moreover, it can be combined with automation and multiplexing for high-throughput applications.

INTRODUCTION

This protocol describes a technique to quantify bacterial surface-binding antibody titres in a variety of body fluids, using cultivated bacteria as a binding "matrix". We have used this extensively to study host-microbiota and host-pathogen interactions in both murine models and clinical research (Balmer *et al.*, 2014; Endt *et al.*, 2010; Haas *et al.*, 2011; Hapfelmeier *et al.*, 2010; Seleznik *et al.*, 2012; Slack *et al.*, 2009). The technique builds on basic concepts developed for the analysis of pneumococcal vaccine responses (Brown *et al.*, 2002; Cohen *et al.*, 2013; Hyams *et al.*, 2010) and antibody responses to *Candida albicans*(Leibundgut-Landmann *et al.*, 2007)*.* The role of antibodies in host-bacterial interactions is clearly critical in both protection from pathogenic infection (Maclennan, 2014) and in influencing mutualistic interactions with the microbiota (Slack *et al.*, 2014). Quantification of functionally relevant bacterial-binding antibodies has mainly been carried out by ELISA/ELISPOT techniques against purified components or whole cells (e.g. (Lécuyer *et al.*, 2014; Porsch-Özcürümez *et al.*, 2004)), or semi-quantitative techniques such as western blotting or dot blotting (e.g. (Endt *et al.*, 2010; Karlsson *et al.*, 1989; Macpherson *et al.*, 2004)). While all of these techniques can yield useful data, they are subject to a number of pitfalls, including high levels of cross-reactivity between highly conserved bacterial cytosolic proteins (Yutin *et al.*, 2012), variable binding to plastic or membrane scaffolds or the need to purify components to homogeneity (Cooper *et al.*, 1981). This flow cytometry-based technique enables quantitative analysis of host immunity to any culturable bacterial species in any available body fluid

Most laboratory animals are raised in highly controlled environments with zero known pathogen exposure (Smith *et al.*, 2007). Although conventional (i.e. not germ-free) animals are colonized by a dense bacterial microbiota on all body surfaces, strong compartmentalization of the blood and mucosal immune systems renders the blood of these animals effectively ignorant of any bacterial exposure (Macpherson *et al.*, 2013). In these cases, parenteral vaccination or deliberate infection generates a specific immune response in the blood that can be evaluated against a near-zero background level of bacteria-specific immunity (Slack *et al.*, 2009). In contrast, antibodies isolated from the mucosal surfaces of conventional animals will always contain immunoglobulins induced by the presence of the microbiota (Macpherson *et al.*, 2004), via either T-dependent or T-independent B cell responses (Bunker *et al.*, 2015). Here, the issue of high level cross-reactivity between bacterial cytosolic components can make it extremely challenging to quantify the immune response of interest using techniques based on bulk lysed bacteria.

This technique represents a simple way to quantify exclusively antibodies binding to bacterial surface-exposed epitopes using flow cytometry. The ability to gate on whole bacteria automatically excludes lysed bacteria and fragments. Further, the system is extremely sensitive, has a broad dynamic range, requires only minute quantities of immunoglobulins, and requires only very low densities of bacterial targets allowing analysis of responses against fastidious species.

Overview of the procedure

In its simplest form, this technique incubates 10^5 bacterial cells from a pure culture with an antibody-containing bodily fluid (serum, plasma, intestinal/bronchial/vaginal lavage, purified antibodies from saliva, breast milk etc.). After washing, bound antibody is visualized with appropriate secondary reagents (Figure 1A). The bacteria are then washed, recovered in an appropriate buffer, and quantified on any standard flow cytometer with the settings adapted for bacterial cell recognition (Figure 1B). Median fluorescence intensities, relative to the dilution factor or antibody concentrations can then be analysed to generate titres (Figure 1C). As such, it is very similar to any other flow cytometry staining. However, the success of the technique depends critically on the ratio of bacterial cells to antibody, and on avoiding contaminations.
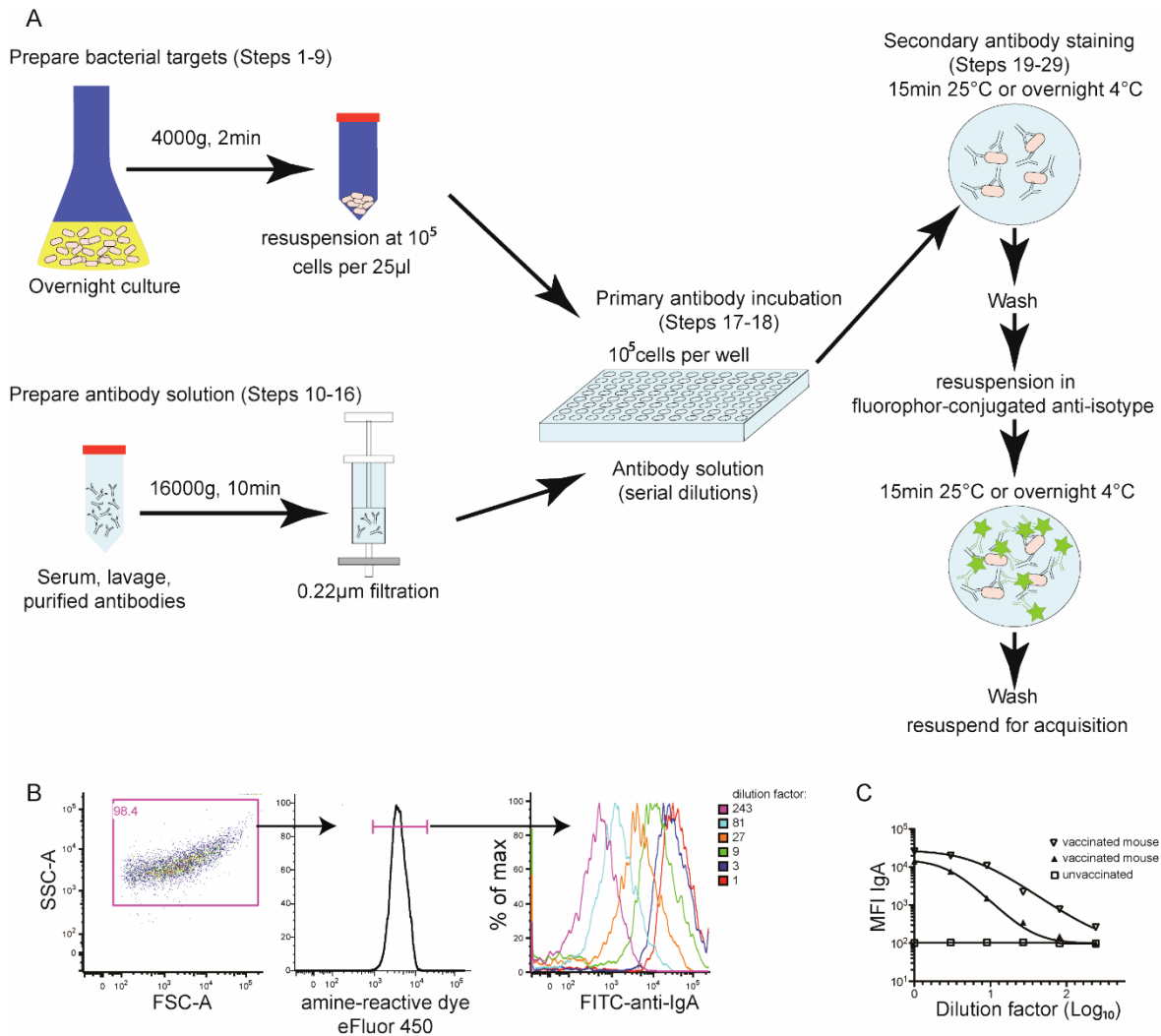
Figure 1: Overview of the protocol. A. Diagrammatic representation of how a basic bacterial flow cytometry experiment is carried out. B. Intestinal lavage was collected from a mouse which had been orally vaccinated against *Salmonella* Typhimurium (Moor *et al.*, 2016). Typical dot plots and gating of whole *Salmonella* Typhimurium labelled with an amine-reactive dye, and overlaid histograms of the dilution series. C. Typical titration curves obtained by plotting the median fluorescence intensity (MFI) of *Salmonella* staining against the sample dilution factor for intestinal lavages from two C57BL/6 mice vaccinated orally and one lavage from an unvaccinated mouse.

Applications of the protocol

This protocol quantifies bacterial surface-binding antibodies. As such it is extremely useful to track the success of bacterial vaccination, and to determine immunologically relevant exposure to defined bacterial species (Balmer *et al.*, 2014; Endt *et al.*, 2010; Haas *et al.*, 2011; Hapfelmeier *et al.*, 2010; Seleznik *et al.*, 2012; Slack *et al.*, 2009). The technique may also be used to quantitatively study changes in bacterial biochemistry that alter surface antibody binding (Hyams *et al.*, 2010; Moor *et al.*, 2016). This protocol may also be used for a wider range of applications such as screening of monoclonal antibodies and cell sorting (Bunker *et al.*, 2015; Cullender *et al.*, 2013; Palm *et al.*, 2014). Potentially the protocol may be expanded

to other cultivable microorganisms, such as fungi (e.g. *Candida albicans* (Leibundgut-Landmann *et al.*, 2007)) or eukaryotic parasites, as well as to whole purified microbiota.

Quantification of bacterial surface-binding antibodies, when combined with cross-adsorption (i.e. removal of specific antibodies by saturating out-titration with the same bacterial strain or related strains of interest, see Box 1), permits definition of the species specificity of a response with much greater certainty than other techniques. It is therefore also particularly useful in quantifying antibody titres in situations where other techniques yield high background (Balmer *et al.*, 2014; Endt *et al.*, 2010; Haas *et al.*, 2011). Additionally, this technique has many advantages over more traditional scaffold-based analyses, particularly for scientists working with fastidious bacterial strains or scarce antibody samples. The antigenic targets are required only at a sufficient number that bacteria can be reliably differentiated from electronic noise/contamination in the flow cytometer (10^5 bacteria per sample). An average assay uses between 0.1 and 100µg of total antibody (e.g. up to 10µl serum for IgG1), as opposed to much larger quantities needed for western blotting applications. The quantities of antibodies required are similar to those typically used for ELISA, but the possibility to multiplex the flow cytometry based analysis for multiple bacterial species further increases the efficiency. The readout is immediately quantitative and numerical analysis can calculate standard antibody titres.

Limitations of the protocol

A major requirement of this technique is that you require access to a flow cytometer and operational knowledge to run the cytometer for bacterial analysis. Further, it is also necessary to have fluorescently labelled monoclonal or polyclonal antibodies against the immunoglobulin of interest. It is also unsuitable for bacteria expressing high-avidity antibody-binding proteins on their surfaces (e.g. *Staphylococcal* protein A (Bouvet, 1994; Tashiro *et al.*, 1995)), as this yields non-specific staining. We have not attempted to apply this technique to strains producing very large amounts of capsular polysaccharide(s). However, work from the pneumococcal vaccine field suggests that with the appropriate controls, useful data may also be obtained with such strains (Chimalapati *et al.*, 2011; Hyams *et al.*, 2010).

An additional limitation is that bacterial culture conditions may alter the surface phenotype of your bacterial strain of interest (Avraham *et al.*, 2015; Mouslim *et al.*, 2014; Van Der Woude, 2011), or the strain may display other types of phenotypic diversity such as phase variation (Van Der Woude, 2011). Whilst it is possible to alter the culture conditions for some bacterial strains in order to influence this (e.g. temperature, media constituents, different growth phases), it is close to impossible to accurately replicate *in vitro* the growth conditions *in vivo*. In some cases, this may lead to over- or under-estimation of specific antibody responses.

Additionally, in its current form, this protocol is designed for use with culturable bacterial species. While the fraction of microbiota species that can be successfully cultivated *in vitro* is continuously expanding (Goodman *et al.*, 2011), further development of the protocol will be required to work with mixed bacterial populations (e.g. from faeces).

We would like to point out that there is considerable variation in light-scattering characteristics between bacterial species and subspecies, as well as in sedimentation efficiencies and tendency to agglutinate. Therefore, even when bacterial cell number is extremely well controlled, it is not appropriate to compare absolute binding values from a single antibody sample against two or more different species (i.e. it would be inappropriate in isolation to deduce that antibodies from donor A bind with a higher titre to bacterial species x than to bacterial species y). However, relative binding patterns for sets of antibody donors; a donor plus appropriate controls; or cross-adsorbed samples (see Box 1), binding to different strains can be compared. For example, donor A has a higher titre against species x than against species y, whereas donor B has a higher titre against species y than species x. This concept is particularly important when using this technique to probe bacterial biochemistry affecting the nature of surface epitopes.

Finally, it should be noted that this technique was conceived specifically for the analysis of exposed surface epitopes. This does not encompass all biologically relevant epitopes (e.g. most secreted toxins cannot be analysed). Although antibodies binding to the live bacterial surface are likely to be relevant in *in vivo* protection, the assay does not provide any direct evidence of functional protection.

Comparison with other methods

Many different assays have been developed to measure bacterial species-specific antibodies, including plate-based assays for binding to purified surface carbohydrates, toxins or whole bacteria (e.g. (Lécuyer *et al.*, 2014; Saletti *et al.*, 2013)), or gel/membrane based techniques such as dot-blotting and western blotting (e.g. (Endt *et al.*, 2010; Macpherson *et al.*, 2004)). Some of these technologies require higher amounts of antibody, which may be unobtainable from certain body fluids. Additionally, even comparing between strains of the same species can yield complex results due to physical properties such as resistance to lysis and scaffold binding. Further, with other methods it can be difficult to exclude the detection of reactivity to bacterial cytosolic proteins. By specifically analysing only intact bacteria, in the absence of any other scaffold, bacterial flow cytometry avoids many of these issues.

An additional benefit of this protocol is that by using live bacteria as the adsorptive matrix ("cross-adsorption") we can demonstrate the specificity of the responses measured, as well as the nature of the epitopes recognized. This is demonstrated in Figure 2 ((Moor *et al.*, 2016))
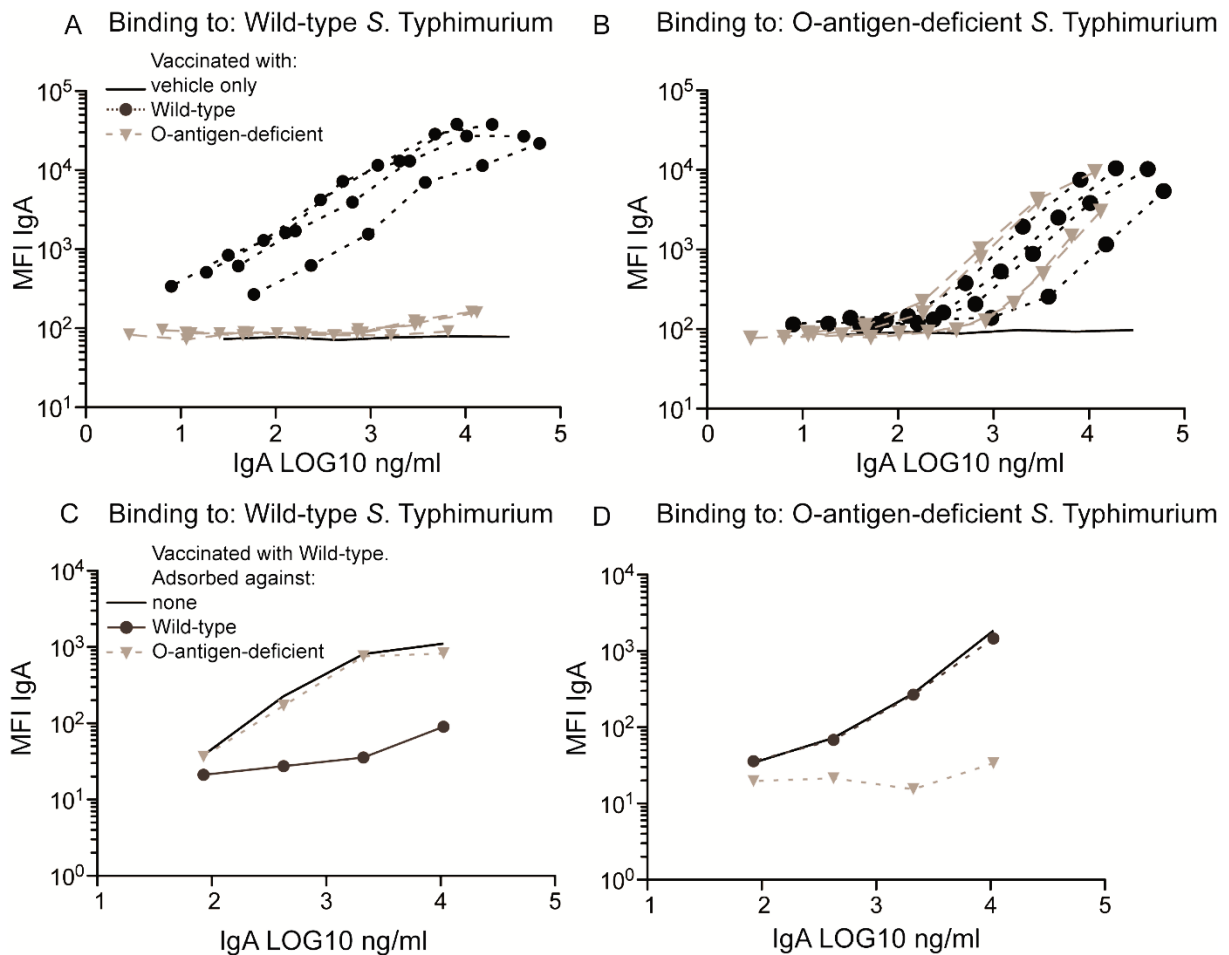

Figure 2: Detailed analysis of surface epitopes. A and B. Taken from Frontiers in Immunology 2016 (Moor *et al.*, 2016) and reproduced under the Creative Commons License. C57BL/6 (wild-type) mice were vaccinated once per week for three weeks with an oral inactivated *Salmonella* vaccine constructed from either wild-type *Salmonella* Typhimurium (black circles) or an O-antigen-deficient strain (*ΔwbaP*, grey triangles), lacking the major surface carbohydrates, or with vehicle alone (PBS, no symbols). On d21 after the first vaccination, intestinal IgA was collected by lavage and used to stain either wild-type (A) or O-antigen-deficient *Salmonella* (B). C and D. A single sample generated as in A and B was cross-adsorbed against buffer only (no symbols), live wild-type *Salmonella* (black circles) or O-antigen-deficient *Salmonella* (grey triangles). The cross-adsorbed samples were then used for bacterial flow cytometry staining of wild-type (C) and O-antigen deficient (D) *Salmonella*. All animal experiments were approved by the legal authorities (licenses 223/2010 and 222/2013; Kantonales Veterinäramt Zürich, Switzerland) and performed according to the legal and ethical requirements.

Here we used bacterial flow cytometry and cross-adsorption to examine the intestinal IgA response induced by oral vaccination with inactivated wild-type *Salmonella enterica subspecies enterica* serovar Typhimurium SB300 (*S.* Typhimurium) and O-antigen-deficient *S.* Typhimurium SB300 Δ*wbaP* (Moor *et al.*, 2016) which lacks the major surface carbohydrate

epitope. Although these strains are isogenic apart from deletion of the galactosyltransferase *wbaP*, IgA induced by the O-antigen-deficient vaccination binds only to the surface of O-antigen-deficient bacteria (Figure 2A and B) (Moor *et al.*, 2016). IgA raised by oral vaccination with the wild-type vaccine binds to both strains (Figure 2A and B). This suggested that O-antigen shields all other major epitopes on the surface of wild-type *Salmonella* strains. As a confirmation, we could demonstrate that cross-adsorption of the IgA induced by wild-type *S.* Typhimurium against wild-type bacteria abrogates binding to the wild-type strain, but not the O-antigen-deficient strain (Figure 2C and D) indicating that the majority of surface-exposed non-O-antigen epitopes are indeed shielded. Vice versa, cross-adsorption of IgA induced by vaccination with wild-type *S.* Typhimurium against O-antigen deficient *S.* Typhimurium abrogates binding to the O-antigen-deficient strain, but not to the wild-type. We can therefore conclude that oral vaccination with an inactivated *S.* Typhimurium vaccine induces IgA with specificity for both O-antigen and other surface antigens. However, on live *S.* Typhimurium the major exposed epitope visible to IgA is the O-antigen. Thus bacterial flow cytometry can be used to interrogate the antigenic specificity of antibody responses and the nature of surface-exposed antibody epitopes in intact bacteria.

Experimental design

Bacterial number. The most important consideration when setting up a bacterial flow cytometry experiment is that bound antibodies are measured per bacterium. Therefore, in contrast to bulk assays such as western blotting or ELISA, using high numbers of bacteria per well actually dilutes rather than maximizes the specific signal. In fact, increasing the number of bacteria per sample is exactly equivalent to diluting the antibody solution (Figure 3). We have therefore developed this protocol to stain only 10^5 bacteria per sample - at least 100-fold fewer than has previously been used in pneumococcal antibody assays (Cohen *et al.*, 2013). This delivers high levels of sensitivity with very low volumes of antibody-containing body fluids.

Minimizing contamination and noise. Another major consideration is that in the basic version of this protocol, bacteria are identified entirely based on their flow cytometry determined light scattering features. This means that any bacteria, or bacterial-sized particles in solutions (including dead bacteria in autoclaved solutions), or in cytometer tubing, will contaminate the final data file. This problem can be minimized by thoroughly cleaning the flow cytometer prior to use and by passing all buffers and media through sterile 0.22μm filters prior to use (note that optically clear solutions can contain 10^6 bacteria per ml). Figure 4 demonstrates the likely effects of such contaminations on the final conclusions drawn from the analysis. It should be noted that contaminants can be antibody positive (Figure 4B, E and H) or negative (Figure 4C,

F and I), and can be mixed with the antibody solutions, in which case they dilute out with titrations (Figure 4H) or mixed with the bacterial targets or present in the flow cytometer (Figure 4I), in which case they are present in all samples at equal concentrations. In the worst cases, excessive noise signal may render a positive signal undetectable without complex data analysis (Figure 4I). In all cases, data displaying these staining patterns are unreliable (see TROUBLESHOOTING section steps 31-32) and the experiment should be re-run with further purification steps.
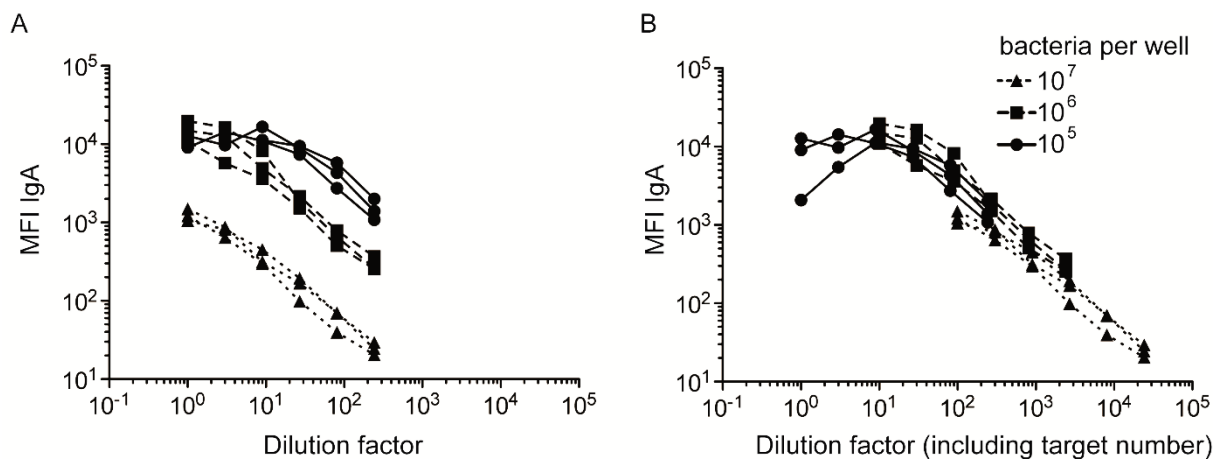

Figure 3: Increasing the target cell number is equivalent to increasing the dilution factor. Intestinal lavages from *Salmonella* Typhimurium vaccinated-mice (as in Figure 2 (Moor *et al.*, 2016)) were used to stain the surface of *Salmonella* Typhimurium at a density of either 10^5, 10^6 or 10^7 cells per well as indicated. Identical data is plotted in A and B. However in B, the x-axis dilution factor is corrected to include the increased number of bacteria per well. All animal experiments were approved by the legal authorities (licenses 223/2010 and 222/2013; Kantonales Veterinäramt Zürich, Switzerland) and performed according to the legal and ethical requirements.

An alternative solution to minimize noise is to use fluorescently labelled target bacteria, allowing specific gating. In the case of genetically tractable organisms, fluorescent protein expression is a simple and effective approach. It is highly recommended that those carrying out bacterial flow cytometry for the first time include a sample with *E. coli* K-12 engineered to express an easily detectable fluorescent protein (e.g. green fluorescent protein in cytometers with a 488nm laser) to confidently set up the flow cytometer to detect bacteria.

For organisms that cannot easily be induced to take up plasmids and/or express fluorescent proteins, it is possible to utilize cell-permeable amine-binding dyes (Figure 1B) or covalent surface labelling with NHS-biotin compounds and fluorescent streptavidin conjugates. For multiplexing several bacterial strains, the very low off-rate of biotin-streptavidin interactions may be used with NHS-Biotin labelling prior to mixing different target populations. A disadvantage of NHS-biotinylation of the target strain surface is that dense chemical modification of the bacterial surface may interfere with epitope recognition.
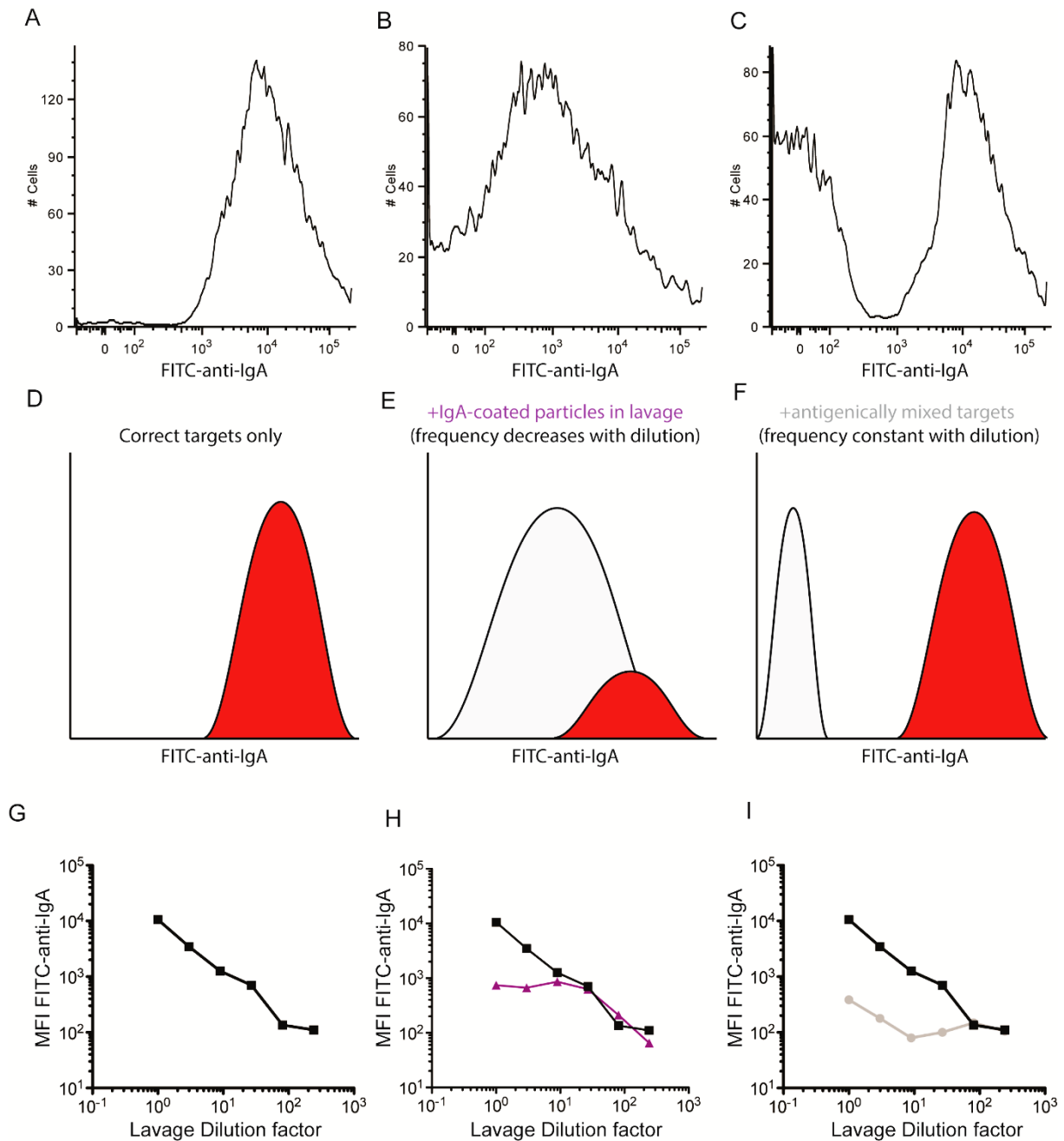
Figure 4: The effects of different contamination sources on acquired data. A-C: A single intestinal lavage from a *S.* Typhimurium-vaccinated mouse was fully cleared by centrifugation and filtration (A and C), or was left uncleared (B). This was then used to stain a pure preparation of *S.* Typhimurium (A and B) or *S.* Typhimurium mixed 1:1 with *E. coli* 8178 (C). Histograms of IgA staining. D-F: Schematic representations of the effects of contaminations on the appearance of histograms at a high-specific IgA concentration. Red - specific signal due to IgA bound to *S.* Typhimurium, Grey- non-specific signal due to contamination. G-I. Effect of different types of contamination on the titration curves generated by plotting median fluorescence intensity against dilution factor. Black squares - non-contaminated sample. Purple triangles - contamination with IgA-dim events present in the intestinal lavage. Grey circles - contamination with IgA-negative events present in the bacterial targets. All animal experiments were approved by the legal authorities (licenses 223/2010 and 222/2013; Kantonales Veterinäramt Zürich, Switzerland) and performed according to the legal and ethical requirements.

Choice of body fluid, purifications and time-points for analysis. The exact choice of body fluids and time-points to analyse for antibody responses depends strongly on the scientific objective. In order to illustrate best practice, we here give four typical situations.

Induction of serum antibodies: whole bacterium intravenous vaccination in mice (Slack *et al.*, 2009). This is an example of a robust serum antibody response induced by a very strong stimulus at a defined time-point. In this case, it is well documented that a peak antibody response is observed roughly three weeks after initial exposure. The antibodies induced are present at high concentrations in blood serum. As serum is easily accessible and blood can be repeatedly sampled, one would most logically sample prior to vaccination and then weekly for 3-5 weeks after vaccination (Slack *et al.*, 2009). As only a few microliters of serum are required per assay, 50μl of blood per time-point is sufficient for a full analysis. Unless the serum samples have a very high fat content, it will be possible to use 0.22μm-filtered serum directly for bacterial staining.

Induction of serum antibodies: during documented *Klebsiella pneumoniae* septicemia. A patient presented with *Klebsiella pneumoniae* sepsis, secondary to a lung infection. We followed the *Klebsiella pneumoniae*-specific serum IgG (Figure 5A) and serum IgA (Figure 5B) responses longitudinally. Serum dilutions were adjusted in order to work with single total IgG and IgA concentrations of 10μg/ml. As a control, the IgG and IgA responses of the same individual were tested against an irrelevant strain (*Enterococcus faecalis*). These remain low and at stable over the course of infection, suggesting that the *Klebsiella*-binding activity we detected was indeed *Klebsiella*-specific, or *Klebsiella*-related. This longitudinal study highlights a typical three-week kinetic in induction of specific IgG, but a much faster kinetic of IgA induction. As the IgA response is predominantly primed at mucosal surfaces, the observed response may actually have been initiated during the primary lung infection (Figure 5B).

Analysis of bacterial binding IgA in intestinal lavage of ex-germ-free mice after recolonization with a single apathogenic strain (Slack *et al.*, 2009). This is an example of a relatively weak immune stimulus given at a defined time-point. The bacteria are given into the intestine and stimulate the mucosal immune system predominantly to induce an IgA response. Although specific IgA will be measurable in serum, the majority of IgA is secreted across the host mucosal membranes and the strongest signal will therefore be measurable in an intestinal lavage (Hapfelmeier *et al.*, 2010; Slack *et al.*, 2009). Based on published literature (Hapfelmeier *et al.*, 2010; Macpherson *et al.*, 2004), specific IgA is measurable from approximately 2 weeks post colonization with a titre that increases over time.
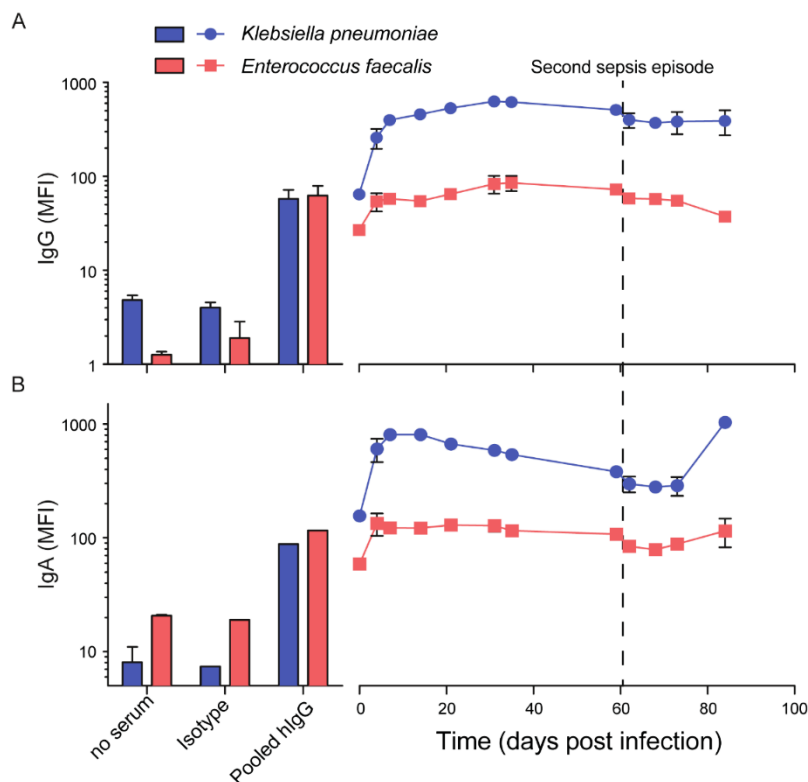
Figure 5: Timing of serum IgG and IgA induction after confirmed *Klebsiella pneumoniae* sepsis, secondary to a lung infection. Blood samples were collected from a patient admitted to the hospital with a systemic *Klebsiella pneumoniae* infection from day 0 until day 84. A second infection with the same strain occurred during the follow-up at day 62. IgG (A) and IgA (B) responses against *Klebsiella pneumoniae* (blue line, circles) and *Enterococcus faecalis* (red line, squares) were determined at a single normalized Ig concentration (10μg/ml). Negative control MFI levels (no primary antibodies, Isotype control) as well as a standard control of pooled hIgG from healthy donors, are represented as bars. IgG and IgA median fluorescence intensity levels are plotted for each time point. All human samples were obtained following acquisition of the study participants' and/or their legal guardians' written informed consent. The study protocol was reviewed and approved by the local ethics committees (Comité de Protection des Personnes Ile de France VI).

Analysis of bacterial binding IgA in human breast milk and faecal water. As these fluids are potentially viscous with a high fat content, we strongly recommend avidity-based purification of IgA prior to analysis to avoid high levels of non-specific background (as detailed in Box 2). These purified IgA solutions can then be used to stain the bacterial species of choice using the standard protocol. In the given examples IgA specific for a human *E. coli* isolate could be detected in faecal water. *B. adolescentis*-binding IgA was found in breast milk. In contrast, IgA specific for *Bacteroides dorei* were not detected in either of these donors/fluids. Non-specific binding of the primary and secondary reagents to these bacterial strains was assessed in parallel (Figure 6A and B).
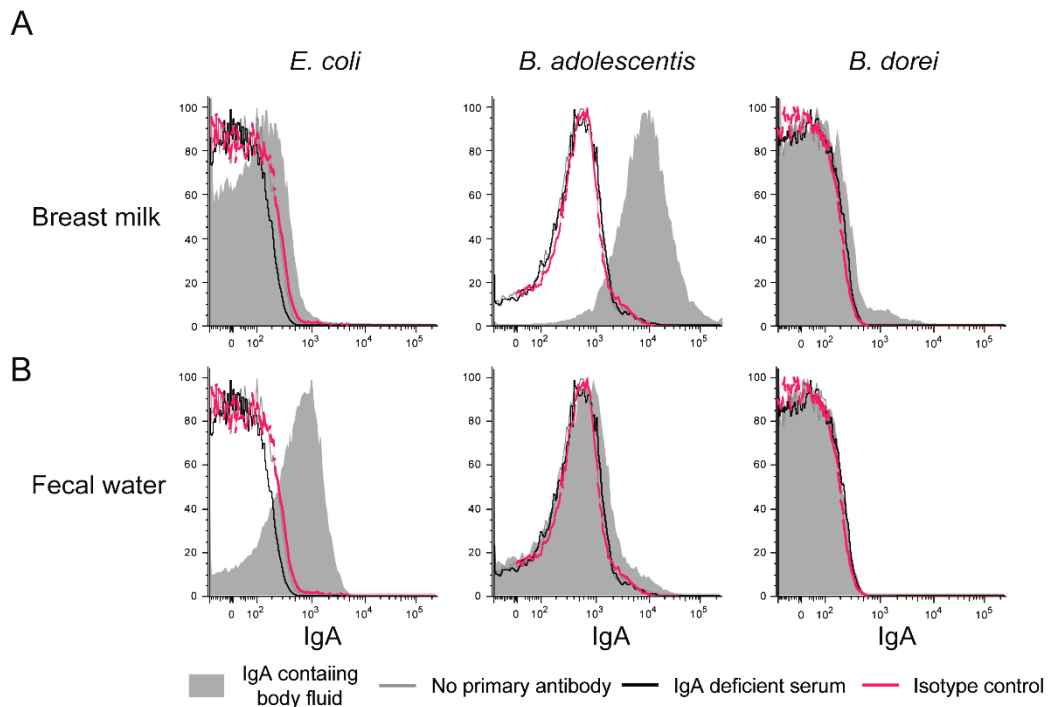
Figure 6: Bacterial flow cytometry with purified IgA from human breast milk and faecal water. A. Secretory IgA purified from breast milk (grey filled histogram) and B. Secretory IgA purified from faecal water (grey-filled histogram) from two independent donors were tested for binding to *E. coli* (human isolate), *Bifidobacterium adolescentis* and *Bacteroides dorei* at a fixed, normalized, concentration (10µg/mL). Monoclonal IgA isotype control (pink line), no primary antibody (grey line) and IgA-deficient serum (black line) are included as negative controls. Binding is revealed by anti-human IgA-FITC. All human samples were obtained following acquisition of the study participants' and/or their legal guardians' written informed consent. The study protocol was reviewed and approved by the local ethics committees (Comité de Protection des Personnes Ile de France VI).

Choice of bacterial targets and preparation methods. The species, subspecies and serovar of bacteria chosen for analysis, as well as the growth conditions employed may dramatically alter the pattern of bacterial antibody binding observed. Two bacteria of the same species (for example *Salmonella enterica* subspecies *enterica* serovar Typhimurium and *Salmonella enterica* subspecies *enterica* serovar Choleraesuis) share almost no exposed surface epitopes (Liu *et al.*, 2014). Additionally, many bacterial species display considerable phenotypic variation due to growth phase, environmental influences and quorum sensing (Van Der Woude, 2011). We therefore advise to choose the bacterial strains for analysis very carefully, to generate frozen stocks of these strains and to regularly check for contamination by standard microbiological techniques. Additionally, it may be of interest to initially screen a range of culture media and growth conditions to optimize relevant antigen expression.

For organisms with higher biosafety containment requirements, it may be necessary to fix the bacteria prior to staining. Although paraformaldehyde fixation before staining very slightly reduces the specific signal for the strains we have tested, it tends to do so equally for all

antibody samples, and therefore does not alter the final interpretation of relative titres (Figure 7A and B). It is also possible to fix samples at the end of staining with no alteration in signal (data not shown).
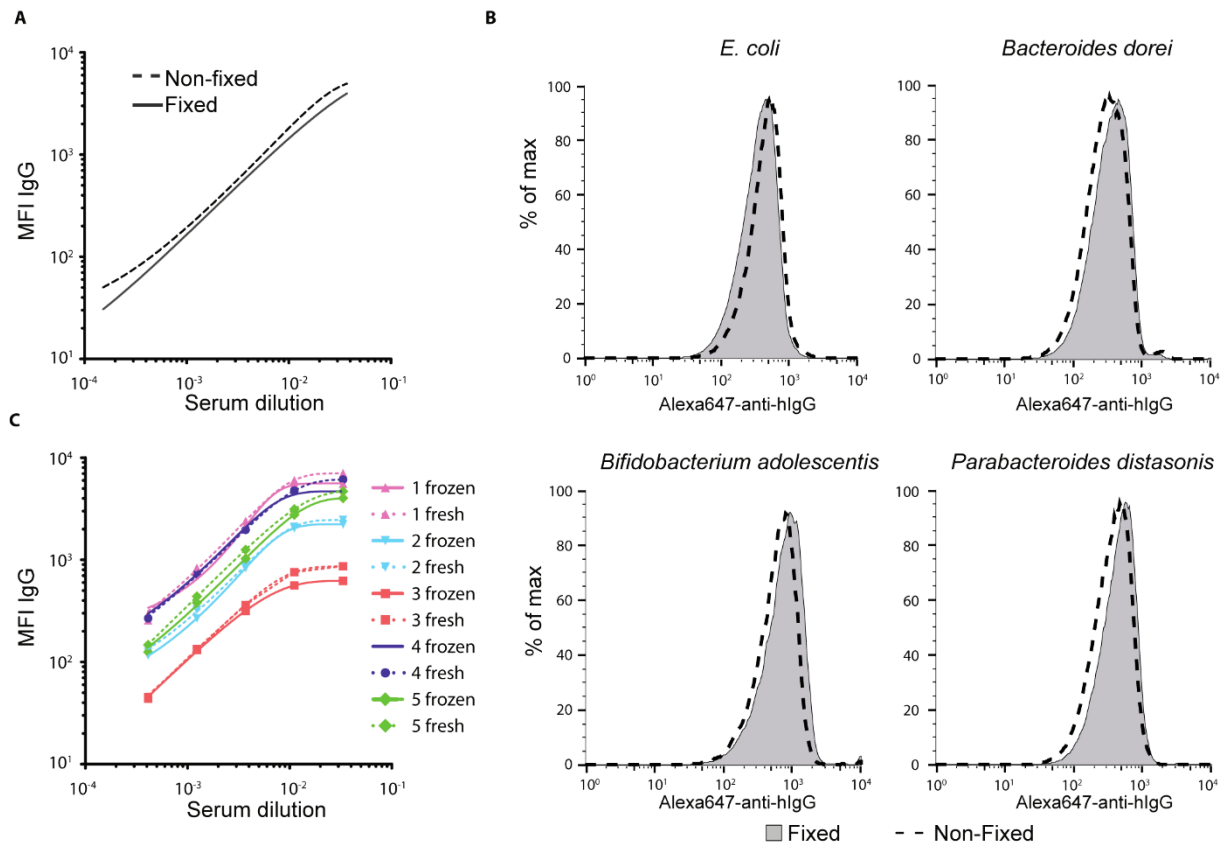

Figure 7: Effects of bacterial cryo-preservation and fixation on IgG binding. A. Analysis of healthy donor serum IgG responses against paraformaldehyde fixed and live (non-fixed) freshly grown *Klebsiella pneumoniae*. B. A similar analysis of *Escherichia coli, Bacteroides dorei, Bifidobacterium adolescentis* and *Parabacteroides distasonis* stained with 10µg/ml pooled healthy donor serum IgG. C Analysis of IgG responses from 5 healthy donors against either fresh (dotted lines) or frozen (solid lines) *Klebsiella pneumoniae*. All human samples were obtained following acquisition of the study participants' and/or their legal guardians' written informed consent. The study protocol was reviewed and approved by the local ethics committees (Comité de Protection des Personnes Ile de France VI).

Typically the experiment size in basic research is small and samples can be measured in a single batch. For this, freshly cultured bacteria can easily be used as targets. However, there are several situations where it is important to have a bulk stock of bacterial targets. Typically, longitudinal clinical studies may follow patient responses to a particular strain over several years. Ideally effects of bacterial growth conditions and genetic drift in the bacterial stocks should be excluded. Additionally, some fastidious strains may require growth conditions that are unavailable at the scientists' host institution, requiring culture off-site. We have therefore established a protocol for preparation of large batches of cryo-preserved bacterial targets

(Box 3), and have demonstrated only minor uniform effects of freezing on antibody binding, which again was equal across all samples we have tested (Figure 7C). This generates both a "plug and play" system, where bacteria are always available for experiments, and much better reproducibility of experiments over time.

Controls. The value of this technique rests on the use of good controls for non-specific binding and contamination. Bacterial species that interact with mammalian hosts have experienced selective pressure from adaptive immunity and some have the ability to non-specifically bind antibodies (Bouvet, 1994; Pack, 2001; Tashiro *et al.*, 1995). Additionally it is important to include sufficient controls to distinguish "natural antibody" binding, background priming levels, and antibody complexes, from real signals.

Testing for antibody Fc binding should be carried out before starting any experiments on the bacterial strain of interest. Monoclonal antibodies with irrelevant specificities (isotype controls) are the ideal controls. These are widely available in the mouse, rat and rabbit systems. In the human setting, purified Fc fragments, or clinical humanized antibodies specific for cytokines can be used. Figure 8A and B show examples where either the whole population (*Staphylococcus aureus*) or a small subpopulation (*Klebsiella pneumoniae* Isolate 1) display strong binding to human IgG Fc. If this test is positive, it may be worth screening related isolates or genetic mutants to find one lacking Fc-binding activity (Figure 8C). It is important to use identical secondary staining reagents to those planned for the main experiments when investigating non-specific binding to also exclude non-specific binding of the secondary antibody (Figure 8D).

"Natural" broadly cross-reactive antibody responses and background priming can be identified using appropriate negative controls. In the murine system (and other experimental animal models), it is usually possible to obtain negative control samples from animals never exposed to the bacterium of interest (Figure 9). If significant antibody-binding is observed here, even if this is lower than in actively immunized animals, it may be worth obtaining appropriate antibody preparations from germ-free animals to exclude the role of microbiota-driven responses (Figure 9A and B, (Bunker *et al.*, 2015)).
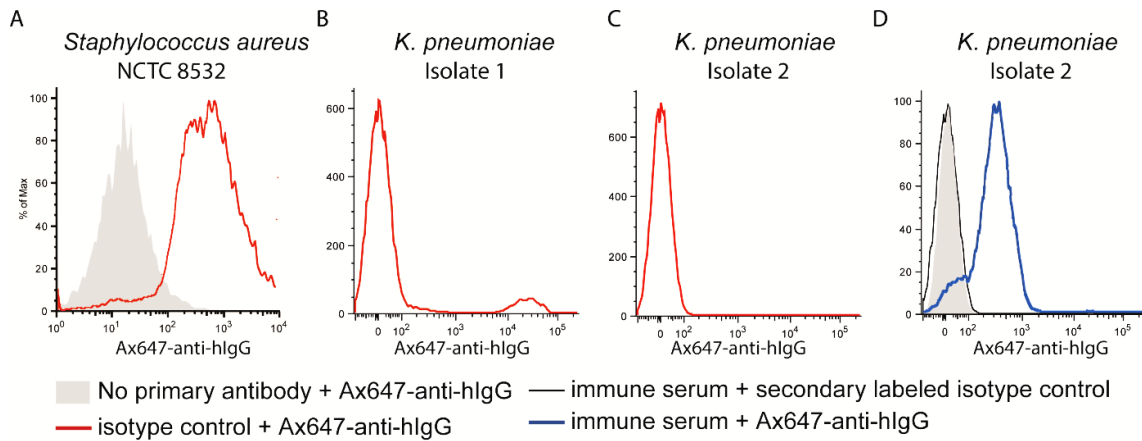
Figure 8: Non-specific antibody binding. *Staphylococcus aureus* strain NCTC 8532 (A) and two primary isolates of *Klebsiella pneumoniae* (B and C) and were stained without primary anti-sera ("no primary antibody", grey shading) or were incubated with a humanized anti-TNF IgG monoclonal antibody ("isotype control", red). Staining was detected with Alexa 647-conjugated polyclonal goat-anti-human IgG. D. For *K. pneumoniae* isolate 2, an additional positive control (serum from a patient with documented *K. pneumoniae* sepsis ("immune serum", blue) and negative control (serum from an IgA-deficient patient, black line) is shown. All human samples were obtained following acquisition of the study participants' and/or their legal guardians' written informed consent. The study protocol was reviewed and approved by the local ethics committees (Comité de Protection des Personnes Ile de France VI).
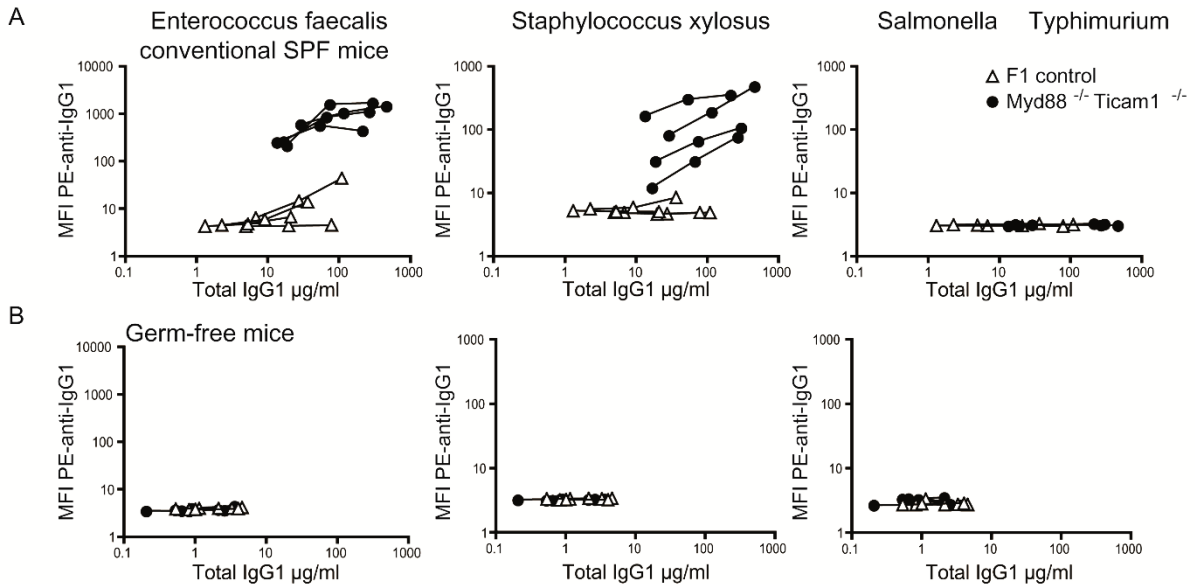
Figure 9: Use of irrelevant bacterial species and germ-free mice as negative controls in the murine system. Reproduced with permission from reference (Slack *et al.*, 2009). Serum from conventionally housed *MyD88-/-Ticam1-/-* mice (black circles) and F1 control mice (open triangles) (A) was used to stain two autologous aerobically culturable microbiota species, *Enterococcus faecalis* and *Staphylococcus xylosus,* as well as the irrelevant bacterial strain *Salmonella* Typhimurium (to which they had never been exposed). B. Serum from germ-free *MyD88-/-Ticam1-/-* mice and F1 control mice was used to stain the same bacterial strains.

Technical controls for adequate clearance of antibody solutions and buffers, as well as biological controls for pre-existing specific antibodies are essential to demonstrate the reliability of data generated using this technique. Large antibody complexes can sometimes form in antibody solutions, and if the sample was insufficiently cleared prior to the bacterial staining, these may be hard to distinguish from bacteria (Figure 4B). The best control for sufficient sample preparation is to examine the presence of positive antibody-binding signal against a bacterial strain to which the host is highly unlikely to have a functional antibody response. In mice, this can be any strain excluded under the definition of hygienic housing in the local facility (e.g. *Salmonella enterica* serovar Typhimurium, Figure 9A and B) (Slack *et al.*, 2009). In humans, we have previously used a plant pathogen *B. japonicum*, as a negative control (Haas *et al.*, 2011). Ideally these bacteria should be stained in parallel with the test species, so that exactly the same antibody preparation is used.

In clinical scenarios, appropriate controls are harder to obtain. Microbial exposure is universal and highly variable making biological negative controls almost impossible for most experimental purposes. The best controls for Fc- or light-chain binding available are therefore isotype controls - typically monoclonal antibodies of known irrelevant specificity such as the humanized antibodies used clinically for cytokine blockade (Figure 8, Figure 10A and B). Correspondingly, for most species there are no active human immunizations to generate positive controls. However, positive controls can be obtained in cases of recent and documented infections with the bacterium of interest, or a strain of identical serotype (see Figure 5, Figure 10A and B). While, this will not always be possible for practical reasons, introduction of such positive controls greatly improves data interpretation. A further advantage of such positive control samples is that they can be used as internal standards to facilitate data comparisons in longitudinal measurements.

Pooled polyclonal human IgG (either replacement therapy Ig (IVIg) or human reference serum for research purposes) and IgA (human reference serum) may also be used as standard controls. These are also useful tools allowing a global assessment of the average healthy population status (Figure 10A and B). Cross-adsorption, as shown in Figure 2, may also be applied in the human system to generate appropriate negative controls.
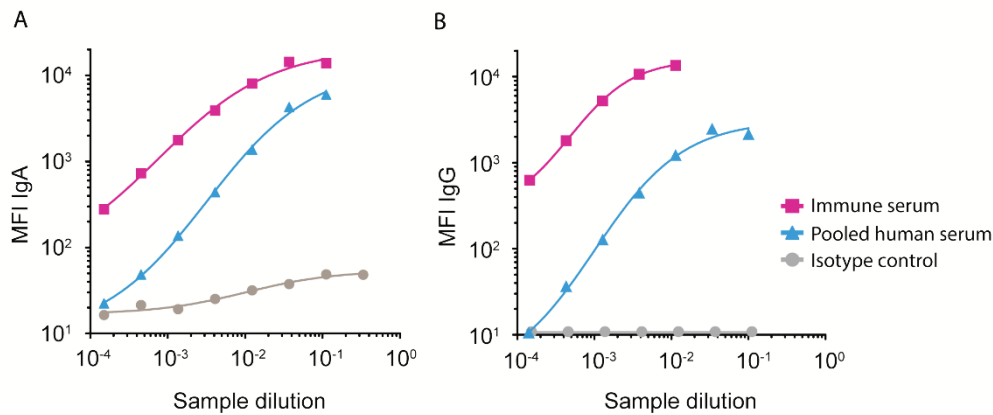
Figure 10: Controls in the human system. Serum from a patient with *Klebsiella pneumoniae* sepsis "immune serum" (purple squares), "Pooled human serum" (Blue triangles) and humanized monoclonal IgA or IgG Isotype controls (grey circles) were used to stain *Klebsiella pneumoniae* (isolate 2, non-Fc-binding) followed by detection with human IgA- and IgG-specific reagents. All human samples were obtained following acquisition of the study participants' and/or their legal guardians' written informed consent. The study protocol was reviewed and approved by the local ethics committees (Comité de Protection des Personnes Ile de France VI).

A final essential set of controls is required to determine appropriate flow cytometer settings and compensation for fluorescence spill over. Ideally these controls should be generated using the same bacterial species as the main analysis to account for background fluorescence. For each fluorophore you should generate a pair of samples: one stained with positive control antibodies and one stained with negative control antibodies, as detailed in the main protocol below (steps 1-28). These samples are then stained with a single fluorophore-conjugated secondary antibody to generate single stained controls. For highly complex stainings, cocktails of secondary antibodies can be generated for "fluorescence-minus-one" controls. In the case that no positive control is available, a last resort is to use cytometer set-up beads to determine cytometer settings, but given the very different size and scatter characteristics of beads and bacteria, this is only really suitable for fluorophores with little or no spectral overlap. A further control for longitudinal experiments where data must be compared over several different days of analysis is the use of fixed gating templates and calibration beads. When the first samples are run, the calibration beads should be run on the fully set-up cytometer and the file saved. A "gate" can then be drawn on each bead population in the fluorescence channels of interest and this gating template and statistics can be saved. As the bead fluorescence remain constant over time, exactly replicating the distribution of beads in the saved gates can generate fully comparable cytometer settings (Koch *et al.*, 2013).

Choice of FACS machine. Samples can theoretically be acquired on any flow cytometer with the laser/filter compatible with the chosen fluorophores. The procedures suggested here have been used successfully to analyse samples on a FACSCalibur (BD) a LSRII (BD), FACS CANTO II (BD) and a FACSArray (BD). It is beyond the scope of this protocol to provide instructions for all possible flow cytometers, and considerable differences exist between older and newer

machines. Rather, we suggest contacting the manufacturer or local experts to determine an appropriate set-up protocol for bacterial detection on your specific flow cytometer, as well as advice on how best to generate comparable data on different days.

How detailed an analysis is planned? Full titration curves versus single antibody concentrations. ELISA-based techniques to measure antibody titres typically measure either the total signal for a given antibody concentration, or generate a full titration curve by applying serially diluted sample to an antigen-coated plate. Exactly the same types of quantitative data can be generated by bacterial flow cytometry. The requirement for both types of analysis depends on the experiment aim.

When serially diluted antibody-containing solutions are used to stain the bacterial strain of interest, the resulting fluorescence intensities can be plotted against the dilution factor and will form a 4-parameter logistic curve. (Figure 11A and B, Supplementary data 1). This generates a very data-rich data set that can be further interpreted. Typically, the horizontal displacement of curves is used to determine the relative titre. Where a monoclonal antibody of known specificity for the strain of interest is analysed in parallel, this permits the calculation of a titre as the concentration of surface-binding antibodies present in the sample (Figure 11C, Supplementary data 1). It should be noted that avidity and epitope availability will also affect the shift when comparing a monoclonal to a polyclonal response, so this is not an entirely accurate description of the read-out. It is also possible to calculate relative titres in the absence of a monoclonal control (Figure 11D-F, Supplementary data 1). Note that although the units and values differ from the absolute values calculated in Figure 5C, the proportional difference between the "test" and "control" values are identical.

For very large sample sets, analysis of full titration curves increases the workload multiplicatively for each titration step and generates complex statistical issues relating to curve fitting and multiple testing. In these cases, it may be more reasonable to carry out pilot dilution-series stainings on positive control samples to determine a total antibody concentration giving binding levels around the inflection point of the logistic curve (pseudo-linear range) (Figure 11G). All samples can then be diluted to exactly this total antibody concentration and a single well analysed for each donor (Figure 11H and I). The disadvantage of this approach is that it will consider a reasonably narrow window of high-titre responses, it may miss quantitative differences between samples showing saturating binding at these concentrations, and it will score all low-titres as "zero". Nevertheless, this can generate almost equivalent data with considerably lower cost, lab-hours and computer-hours.
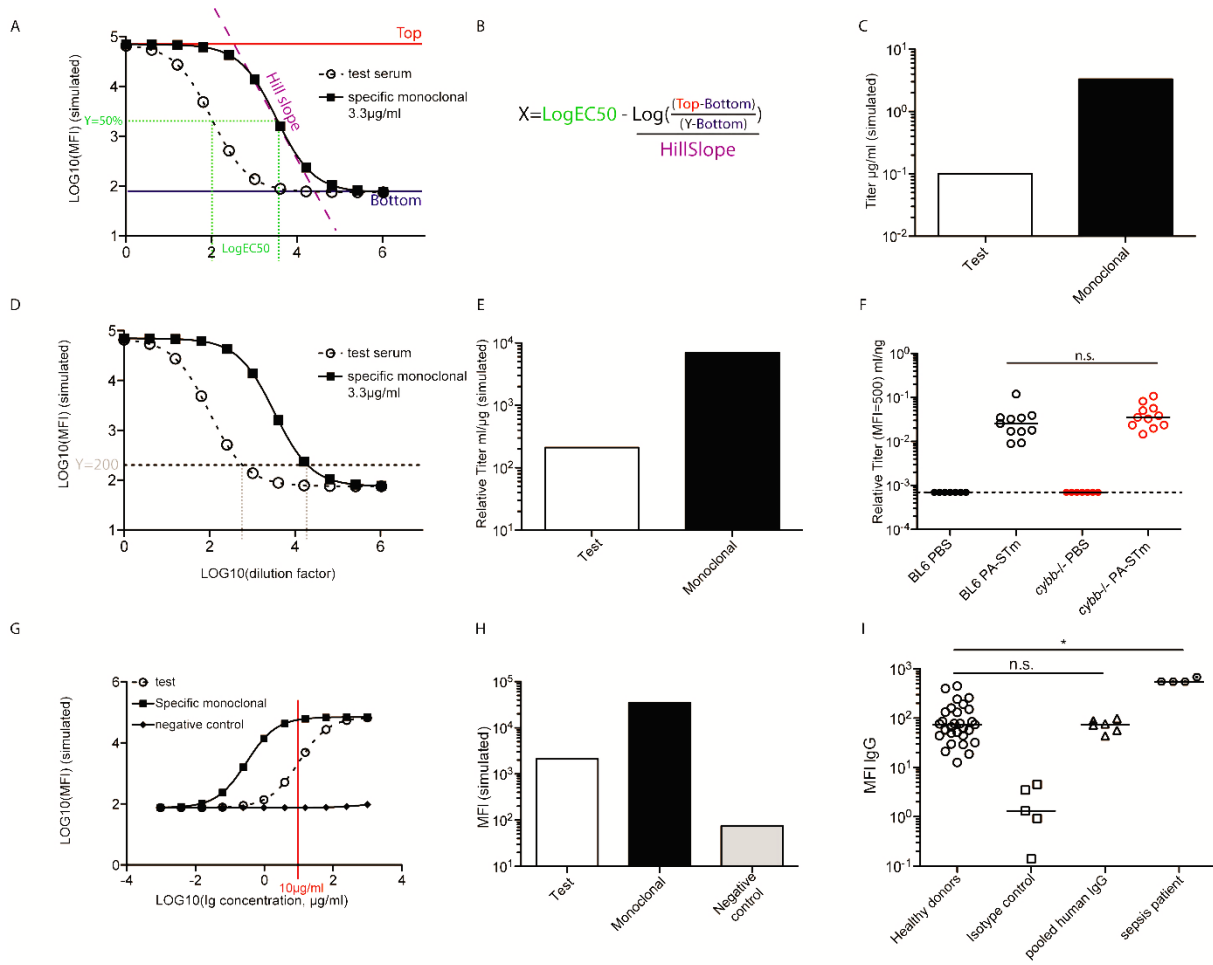
Figure 11: Data analysis methods. A, Two *in silico*-generated "perfect" data sets for a monoclonal antibody of known specificity and a test sample fitted using the 4-parameter logistic equation to demonstrate the meaning of all parameters generated by the non-linear regression. B. The 4-parameter logistic equation rearranged to give X in Y. C. Simulated absolute titres calculated from the curves in A. D. *In silico* generated curves, as in A, showing the setting of a Y axis limit for the calculation of relative titres. E. Relative titres calculated from curve shown in D. F. Taken from Frontiers in Immunology 2016 (Moor *et al.*, 2016). Relative titres calculated using the method shown in panels D and E for IgA in the intestinal lavages of orally vaccinated (PA.STm) or mock vaccinated (PBS) wild-type (B6) and gp91Phox-deficient mice (*cybb$^{-/-}$*) against *S.* Typhimurium. Statistics: 2-way Anova. n.s.- not significant G. Use of single immunoglobulin concentration measurements to simplify data acquisition and analysis. From full titration curves (simulated as in A and D) a value can be identified that gives a good window for detection of positive and negative signals (10μg/ml in this case). Plotting the MFI values for this total concentration gives the graph shown in H. Binding of 10μg/ml IgG of the indicated sources to *Klebsiella pneumoniae.* Kruskal-Wallis test with Dunn's post-test. * p< 0.05. n.s. not significant. All human samples were obtained following acquisition of the study participants' and/or their legal guardians' written informed consent. The study protocol was reviewed and approved by the local ethics committees (Comité de Protection des Personnes Ile de France VI).

In conclusion, when designing a bacterial flow cytometry experiment the following steps should be considered:

1) Determine the optimal time-points, body fluids to collect, and whether antibody purification will be required.

2) Identify the bacterial species of interest and obtain pure frozen bacterial stocks. Establish robust culture protocols for this species and whether fresh or frozen targets are most appropriate. Establish whether fixation is necessary for practical or biosafety reasons.

3) Before any experiment starts, it is crucial to exclude Fc binding by the bacterial strain of interest by use of isotype controls.

4) Establish the relevant positive and negative control antibody solutions and bacterial strains.

5) Decide whether full titrations or single concentrations will be analysed. If single concentrations are to be used, establish the optimal concentration in pilot experiments.

REAGENTS

- Phosphate-buffered Saline (PBS) pH 7.4 no Calcium or Magnesium (standard lab reagent or 10X-PBS, CS3PBS01-01 Eurobio, France. Diluted to 1x with distilled water)
- Bovine serum albumin factor V ("BSA") (K41-001, GE Healthcare, Little Chalfront, UK)
- Sodium azide (71289, Sigma-Aldrich,St. Louis, Missouri, USA)
  CAUTION! This is a hazardous chemical. Avoid contact with skin, eyes and airways.
- Paraformaldehyde (PFA): 158127 (Sigma-Aldrich)
  CAUTION! Paraformaldehyde is toxic and flammable. When weighing the crystalline solid or preparing solutions, work should be performed in a fume hood.
- Human blood, breast milk, faeces or other fluid of interest, collected in the context of an approved clinical trial or from an approved biobank.
  CAUTION! For human studies informed consent must be obtained from all study subjects.
  CAUTION! For studies using human or animal samples, all experiments must be conducted according to the relevant guidelines and official permissions/ethical approval must be obtained.
  CAUTION! Potential infection hazard. Handle at an appropriate biosafety level.
- Murine blood, intestinal lavage, faeces or other fluid of interest collected in the course of ethically approved animal experiments.
  CAUTION! For studies using human or animal samples, all experiments must be conducted according to the relevant guidelines and official permissions/ethical approval must be obtained.
  CAUTION! Potential infectious hazard. Handle at an appropriate biosafety level.
- Appropriate liquid bacterial culture media. e.g. Lysogeny Broth medium (e.g. liquid medium, MP Biomedicals, 3001-031), Brain-Heart Infusion broth (CM1135, Oxoid, Germany)
  CAUTION! Many liquid media contain components potentially harmful to human health. Follow the manufacturer's instructions for safe handling.
- Appropriate solid bacterial culture media. e.g. Columbia agar + 5% sheep blood (43049, Petri dishes, Biomerieux, France), LB Agar (22700-025, Thermo-Fischer, Life Technologies, NY, USA).
  CAUTION! Many solid media contain components potentially harmful to human health. Follow the manufacturer's instructions for safe handling.
- Frozen stocks of the bacteria of interest (For example *Klebsiella pneumoniae* (ATCC® BAA-1705™), American Type Culture Collection (ATCC) , VA, USA)
  CAUTION! Potential infectious hazard. Handle according to the appropriate biosafety regulations for the species in question.

- Appropriate liquid disinfectant (e.g. Clidox 95120F, 96120F, Pharmacal, CT, USA)

Table 1: Suitable secondary reagents

Target	Clone name/ polyclonal	Supplier	Cat. number	Conjugate	Tertiary	Working conc.
Mouse IgA	C10-3	BD, NJ, USA	559354	FITC	NA	10µg/ml
Mouse IgA	RMA-1	Biolegend CA, USA	407004	Biotin	Pacific blue-streptavidin Invitrogen, S-11222. 2µg/ml	10µg/ml
Mouse IgG2a/c	RMG2a-62	Biolegend	407106	FITC (others not tested)	NA	5µg/ml
Mouse IgG2b	RMG2b-1	Biolegend	406706	FITC (others not tested)	NA	5µg/ml
Mouse IgG3	RMG3-1	Biolegend	406803	Biotin	Pacific blue-streptavidin Invitrogen, S-11222. 2µg/ml	5µg/ml
Mouse IgM	RMM-1	Biolegend	406509	Allophycocyanin (APC-Cy7 also tested)	NA	4µg/ml
Human IgM (Fcµ)	Donkey polyclonal	Jackson Immuno-research, UK	709-116-073	PE	NA	7µg/ml
Human IgG (Fc☐)	Goat polyclonal	Jackson Immuno-research	109-605-098	Alexa®647	NA	7µg/ml
Human IgA (Fc☐)	Goat polyclonal	Jackson Immuno-research	109-095-011	FITC	NA	7.5µg/ml

These reagents can be combined where fluorophores are compatible, permitting analysis of multiple antibody isotypes in parallel.

There are many suppliers and many possibilities for secondary reagents that should encompass almost any host species. The optimal concentration for reagents not listed here should be determined by testing a range of concentrations on a known positive control sample.

- 16Ss rDNA primers (Microsynth AG, Switzerland)

  FD1: 5'-AGAGTTTGATCCTGGCTCAG-3

  FD2: 5'-AGAGTTTGATCATGGCTCAG-3'

  RC1: 5'-ACGGGCGGTGWGTRCAA-3'

- Taq PCR kit (e.g. Promega GoTaq® Green, M7122, Promega, WI, USA)
- Agarose LE (e.g. V3125, Promega)
- 1x TE buffer (e.g. V6232, Promega)
- Gel extraction kit (e.g. Wizard® SV Gel and PCR Clean-Up System, A9281, Promega)
- ACD tubes (Cat no 364606, BD-Vacutainer)
- Lymphocytes separation medium (Cat no CMSMSL0101, Eurobio)
- 1.2ml Serum activating gel tubes (41.1395.005, Sarstedt, Germany)
- 0.5M EDTA (A1104, Applichem, Germany)

  CAUTION! Irritant. Wear suitable personal protective equipment while handling.
- Soybean trypsin inhibitor (T9128, Sigma-Aldrich)
- Easylink-NHS-PEG4-Biotin (21330 Thermofischer, Life Technologies, NY, USA)
- Glycine (A1067, AppliChem)
- Cell proliferation dye eFluor 450 (65-0842-85, eBiosciences, CA, USA)
- Fixable Viability Dye eFluor780 (65-0863-14, eBiosciences)
- LIVE/DEAD Fixable Dead cell Stain kit (Green L-23101, Life Technologies)
- CellTraceTM CFSE (C34554, Life technologies)
- Critical: We have noticed that the Aqua version of LIVE/DEAD Fixable Dead cell Stain kit (L-34957, Life Technologies) is inefficient for bacterial staining. Similarly, CFSE is efficient only for a subset of bacterial species. As dye loading is heavily dependent on bacterial biochemistry, optimal dye-type, concentration, and loading conditions should be determined for each bacterial species tested.
- IgA binding peptides: Peptide M / Agarose (gel-pdm-2, Invivogen), Immobilized Jacalin (20395, THERMO SCIENTIFIC)

  Critical: M-peptide binds IgA1 and IgA2 whereas Jacalin binds only IgA1 (and IgD)
- Elution buffers:

  Peptide M: 100mM Glycine pH 2-3 (A1067, AppliChem)

  Jacalin: 0.1 M α-D-Galactose (G0625, Sigma-Aldrich)
- Neutralization buffer: 1M TRIS HCl pH 7.5 (e.g. 15567-027, Life Technologies)
- Human reference serum (RS10-101, Bethyl, Montgomery, TX, USA)
- Pooled human IgG (Hizentra, CSL Behring laboratories)
- Infliximab (monoclonal chimeric IgG1 anti human TNF alpha, Janssen biotech)
- Chimeric IgA anti hRSV protein F (A1Trsv11, B cell Design)
- Glycerol (G7757, Sigma-Aldrich)

- Fluorescent calibration beads (e.g. Rainbow Calibration Particles 8 peaks, 3.0 - 3.4 μm. 559123. Becton Dickinson, USA)
- Flow-count fluorospheres beads (A91346, Beckman Coulter)
- ELISA kits to determine total concentrations of your antibody isotypes of interest (e.g. Human IgG ELISA Quantitation Set, E80-104, Bethyl, TX, USA)

EQUIPMENT

- Polypropylene 96-well V-bottom plates (e.g. 732-2620, VWR)
- Library tubes, 1.2ml PP, 5.8x47.4mm (077210, Milian SA, Switzerland)
- Sterile serological pipettes (e.g. 86.1254.001 Sarstedt)
- Syringes
- 0.22μm bottle-top filters (rapid FILTERMAX, 0.22μm PES, 99505, TPP, Switzerland)
- 0.22μm syringe filters (>1ml, PES 0.22μm, 99722, TPP)
- 0.22μm syringe filters (<1ml, Millex-GV, 0.22μm PVDF, 4mm, SLGVR04NL, Merck Millipore, USA)
- 1.5ml snap-cap tubes, autoclaved 121°C, 12min (e.g. 72.695.500 Sarstedt)
- Sterile pipette tips
- Petri dishes (e.g. 82.1472, Sarstedt)
- Sterile inoculation loops (e.g. I7648-1PAK, Nunc, Sigma-Aldrich,St. Louis, Missouri, USA)
- Parafilm (P7793-1EA, Sigma-Aldrich)
- For filtration of very small volumes
  0.2μm centrifugation columns (82031-356 VWR, PA, USA)
- For IgA purification:
  Disposable gravity-flow columns (e.g. 29925, Pierce, Life Technologies)
  Amicon Ultra centrifugal filters 100kDa cut-off (UCF910096, Merck Millipore, Germany)
- For anaerobic bacterial culture:
  Glass Bacterial culture flasks/tubes with rubber stoppers and aluminium seals (e.g. CLS-4209-01, Chemglass life sciences, NJ, USA)
- Any flow cytometer with appropriate laser/detector combinations for the fluorophores used. E.g. LSRII (Becton Dickinson, USA) 488, 405 and 633nm lasers and with 9 detectors. Associated computer running acquisition software, for example FACS Diva (BD)
  CAUTION! Class I laser product.
- Robotic sample loaders for the flow cytometer (not essential)

- Bench-top centrifuge capable of centrifuging 96 well plates. E.g. Eppendorf 5810 R, A-4-81 rotor
- Refrigerated minifuge for 1.5-2ml tubes: e.g. Eppendorf 5417R with rotor FA-45-30-11.
- Multichannel pipettes (e.g. Gilson pipetmanL Multichannel 12x 20-200µl FA10012).
- Laminar flow cabinet certified up to biosafety level II (e.g. Scanlaf Safe 1200, 61200-LAB, Vitaris, Switzerland)
- Fume hood
- For anaerobic culture of targets: Anaerobic tent (e.g. Type B Vinyl Anaerobic Chamber, Coy, Michigan, USA) supplied with gas mixture (e.g. 10% H2, 5% CO2, 85% N2) for anaerobic culture.
- For anaerobic culture of targets ONLY: Anaerobic culture Jar (e.g. HP0011 Oxoid)
- Stationary incubator (e.g. Heraeus B12, Thermo Scientific)
- Shaking incubator (e.g. Kuhner shaker ISF-1-W, Adolf Kühner AG, Switzerland)
- Micropipettes
- Aspirator pump (e.g. Vacusafe, Vitaris, Switzerland)
- Waterbath or thermomixer programmable to 37°C and 56°C
- Orbital shaker
- Spectrophotometer capable of measuring OD_{600nm}. (e.g. Agilent 8543, Agilent Technologies)
- PCR machine (e.g. T100™ Thermal Cycler, Bio-rad, CA, USA)
- Agarose gel equipment and power pack (e.g. 1704467 and PowerPac™ Universal Power Supply, Bio-rad)
- Analysis computers running FlowJo (Treestar), Excel (Microsoft) and Prism (Graphpad). It would be possible to run all analysis in the "R" statistical programming language, and open-source flow cytometry analysis solutions (Flow https://galen.dulci.duhs.duke.edu/flow/ or Bioconductor http://bioconductor.org/) and thus to have an open-source software solution. However, we have not currently implemented this solution.

REAGENT SETUP

Bacterial flow cytometry buffer

- PBS, 2% w/v BSA, 0.02% w/v Sodium azide, sterile-filtered. Store at room temperature (RT 20-25°C) for up to 1 year.

  CAUTION! Sodium azide is harmful. Avoid contact with skin, eyes or airways. Wear suitable personal protective equipment when handling the solid or solutions containing this chemical.

4% Paraformaldehyde w/v in PBS

- Dissolve paraformaldehyde powder with heating at high pH. Correct to pH7 using hydrochloric acid. Pass the solution through a sterile 0.22µm filter. Aliquot and store at -20°C for up to 3 months

  CAUTION! Paraformaldehyde is toxic and flammable. When weighing the crystalline solid or preparing solutions, work should be performed in a fume hood.

Collecting antibody-containing body fluids

Collect Serum/Plasma using any standard protocol. Serum and plasma should be separated away from blood cells rapidly after collection and stored at -80°C until use (indefinite storage at -80°C).

- Mouse intestinal lavages as described (Macpherson *et al.*, 2004). Make Intestinal lavage buffer less than 1h before use: 1x PBS, 5mM EDTA, 1mg/ml Soybean trypsin inhibitor. Dissect the entire intestine from stomach to sigmoid colon. Inject 5ml of intestinal lavage buffer into the duodenal lumen over a petri-dish. Collect the fluid into a petri dish by cutting open the cecum. Transfer the fluid to a 50ml falcon tube and clear by centrifugation at 16000g for 30min. The supernatant can be stored aliquoted at -80°C for several years.

- To obtain human faecal water, homogenize 0.2g faeces in 1ml PBS. Centrifuge the suspension at 21000 g for 15 min, 4°C. Carefully collect the supernatant by micropipetting. Add a second 1ml of PBS, homogenize and centrifuge again. Pool this supernatant with that collected initially and store at -80°C until required.

  CAUTION! For human studies informed consent must be obtained from all study subjects.

  CAUTION! For studies using human or animal samples, all experiments must be conducted according to the relevant guidelines and official permissions/ethical approval must be obtained.

  CAUTION! Potential infection hazard. Handle at an appropriate biosafety level.

Preparation of secondary staining reagents

Make up all secondary staining solutions less than 1h before use in bacterial flow cytometry buffer, as indicated in Table 1.

Critical step: Filter all staining solutions through a 0.22µm syringe filter immediately before use to remove antibody complexes.

Preparation of bacterial agar plates

Make up and autoclave the solid bacterial media according to the manufacturer's instructions. In a clean environment, pour 25ml agar per petri dish. Close the plates with the lids and allow to set at room-temperature. Follow the manufacturer's guidelines on agar plate storage. For anaerobic bacterial culture, it is recommended to pre-reduce the plates by incubation in an anoxic environment for 3-7 days prior to inoculation.

Preparation of liquid bacterial culture media

Make up, sterilize and store liquid bacterial culture media according to the manufacturers' instructions. Follow the manufacturer's guidelines on media storage.

Critical step: Most rich liquid culture media contain poorly defined ingredients such as yeast extract and may contain dead bacterial particles. In order to avoid these as a source of incorrect target material, all liquid media should be first autoclaved and then filtered through a sterile 0.22µm filter to clear any of these particles. If correct aseptic technique is then used, all bacterial-sized particles present in the final culture will be your species of interest.

Optional: For anaerobic bacterial culture, it is recommended to reduce the media prior to use by incubating in an anoxic environment for at least 7 days prior to inoculation.

Cell freezing buffer

1xPBS 20% vol/vol glycerol. Filter through a sterile 0.22µm filter into a sterile sealable vessel. As along as good aseptic technique is followed, this solution may be stored at 4°C for up to 6 months.

EQUIPMENT SET-UP

For users of a FACSCalibur (BD) a LSRII (BD), FACS CANTO II (BD) and a FACSArray (BD), bacteria are easily visualized by changing the standard cytometer settings. Firstly both forward-scatter and side-scatted parameters should be acquired on logarithmic scales. Secondly, standard flow cytometer settings "threshold" the acquired events to only record data from particles of mammalian cell size or higher (typically electronically discarding all values with a low forward-scatter value). Bacterial cells have low values for both side scatter and forward scatter. We therefore recommend to "threshold" the acquisition on both forward-scatter and side-scatter at a very low, but non-zero value (e.g. FSc=200, SSc=200 on LSRII and FACS CANTO II). The thresholds should be combined with an "AND" logic gate.

Critical step: Ensure that flow cytometer is clean by acquiring a tube containing 0.22μm-filtered 1x-PBS or water prior to commencing acquisition. If more than 100 events are acquired in 1 min, re-clean the machine and repeat.

PROCEDURE

Preparation of bacterial targets. Timing: 2-7 days

1. Work in sterile conditions (e.g. laminar flow cabinet). Streak out the bacterial target strain from a frozen stock onto solid media using a sterile inoculation loop (Media as suggested in Table 2, or appropriate to your strain of interest).
   Critical step: If the strain is an anaerobe, carry out this procedure in an anaerobic tent using pre-reduced agar plates and inoculation loops.
   CAUTION! Potential biohazard. Wear personal protective equipment and follow local guidelines for biosafety level 1 or 2.
2. Incubate the inverted plates at an appropriate temperature and in an appropriate atmosphere (e.g. sealed in anaerobic culture jars for anaerobes or unsealed for aerobes in a 37°C incubator) until single colonies are visible. Typically 16-48h for aerobes, 48h or longer for anaerobic strains.
3. Prepare an appropriate sterilized bacterial culture vessel containing 5ml of 0.22μm filtered bacterial culture media (see Table 2) using good aseptic technique.
   Critical step: for anaerobes, pre-reduce this media for 1 week by incubating unsealed at RT in an anaerobic tent.
4. Inoculate a single colony from Step 2 into the 5ml of culture media from Step 3 using good aseptic technique under an appropriate atmosphere.
5. Incubate the culture at 37°C (or the appropriate temperature) under an appropriate atmosphere until stationary phase growth is reached.

Critical step: Growth phase, media and oxygen availability may affect the expression of relevant surface antigens. Carry out pilot experiments to determine the optimal growth conditions for detection of antibody binding.

Critical step: For further details on anaerobic culture see reference (Speers *et al.*, 2005).

CAUTION!: Potential infectious hazards. Always wear appropriate personal protective equipment. Handle bacterial strains according to their designated biocontainment risk level.

?TROUBLESHOOTING

6. Centrifuge 1ml culture at 4000g, 4°C, 2mins to gently pellet only whole bacteria (bacterial fragments will bind antibodies but will be later lost from the analysis so may reduce the specific signal). It is possible to label the bacteria with an amine-reactive dye or NHS-biotin (see Anaerobic and aerobic strains may be handled identically from this step onwards. Optionally, it is also possible to label the bacteria with an amine-reactive dye or NHS-biotin at this stage (see Box 4).

It is advised to freeze an aliquot of this culture in cell freezing medium for later confirmation of culture purity (see Box 5).

?TROUBLESHOOTING

Critical step: Bacterial species vary enormously in size, shape and resistance to physical force. While centrifugation speeds given in this protocol have worked for all species listed in Table 2, you should experimentally determine optimal speeds to give full sedimentation without excessive toxicity for all other species.

7. Resuspend in 1ml bacterial flow cytometry buffer and determine the bacterial density. For *E. coli* and *Salmonella* cultures, a 1ml pathlength OD_{600nm} measurement of 1.0 roughly corresponds to 5×10^8 bacterial CFU/ml. For other species it will be necessary to test the relationship between CFU and OD_{600nm} by measurement and plating. Alternatively bacteria may be quantified by flow cytometry counting, i.e. mixing a known density of counting beads with the bacterial sample and determining the ratio of beads to bacteria in the cytometer. Optionally, it is possible to prepare large batches of frozen, aliquoted bacteria for longitudinal experiments at this stage (Box 3).

?TROUBLESHOOTING

8. Optional: To reduce operator risk, it is possible to paraformaldehyde-fix bacteria at this stage, although it should be considered that chemical modification of surface epitopes by paraformaldehyde may alter antibody binding. To do so, centrifuge at 4000g, 2min, 4°C and resuspend in 1ml freshly thawed 4% PFA. Incubate 20min RT (20-25°C). Centrifuge at 4000g, 2min, 4°C and resuspend in 1ml bacterial flow cytometry buffer.

9. Adjust the bacterial concentration to 5×10^6 per ml with bacterial flow cytometry buffer.

PAUSE POINT. Bacterial suspension can be stored at 4°C for up to 72h before flow cytometry.

Table 2: Typical bacterial growth conditions of species currently tested in bacterial flow cytometry

Strain	Growth medium	Incubation
Facultative/obligate aerobes		
Escherichia coli K-12*, Escherichia coli* Nissle 1913, human and mouse primary *Escherichia coli* isolates, *Salmonella enterica* species*, Klebsiella pneumoniae, Enterococcus faecalis, Streptococcus epidermidis, Streptococcus pneumoniae, Moraxella catarrhalis, Lactococcus lactis,* Altered schaedler flora *Lactobacllli* strains. *Citrobacter rodentium, Yersinia enterocolitica, Burkholderia cepacia* complex*,*	Liquid: Lysogeny Broth medium, or Brain-heart infusion medium Solid: LB Agar plates or Columbia agar + 5% sheep blood	Tubes and flasks of liquid media 37°C for 18h in a standard shaking incubator. Plates 37°C, 18h in a standard incubator.
Strict anaerobes		
Clostridium perfringens, Altered Schaedler flora *Clostridia* species*, Bifidobacterium adolescentis, Bifidobacterium infantis, Bifidobacterium longum, Mucispirillum schaedleri*	Liquid: Brain-heart infusion medium Solid: Columbia agar + 5% sheep blood	Both plates and liquid cultures at 37°C stationary for 18h-48h in anaerobic atmosphere (85% N_2, 10% H_2, 5% CO_2)
Anaerobic or microaerophilic		
Bacteroides dorei, Bacteroides fragilis, Bacteroides thetaiotamicron, Bacteroides vulgatus, Parabacteroides distasonis,	Liquid: Brain-heat infusion medium Solid: Columbia agar + 5% sheep blood	Liquid media at 37°C with gentle shaking for 18-36h in anaerobic atmosphere (85% N_2, 10% H_2, 5% CO_2) Plates, 48h, 37°C in anaerobic atmosphere (85% N_2, 10% H_2, 5% CO_2)

Preparation of antibody-containing body fluids. Timing: 1h

10. Thaw antibody-containing fluids rapidly at 37°C in an incubator or water-bath.

11. Dilute the solution to twice the desired starting concentration in bacterial flow cytometry buffer (see Table 3). The total volume required depends on the number of assays being performed. We recommend 50µl multiplied by the number of bacterial strains to be analysed. Be sure to include sufficient volume for positive and negative control samples required for the cytometer set-up.
    ?TROUBLESHOOTING

12. Inactivate complement and other heat-labile antimicrobials by heating the antibody solution to 56°C for 30min in a water-bath or heating block.

13. Centrifuge the solution at 16000g for 5min to pellet all bacterial-sized particles and antibody complexes.

14. Carefully remove the supernatant and pass through at 0.22µm syringe filter (if >500µl total volume) or 0.22µm spin filter column (if <500µl total volume).
    Critical step: Fluids containing a high fat concentration or with a high viscosity give high background in this assay even after 0.22µm filtration. These fluids (e.g. breast milk, faecal water) must be purified (as described in Box 2) before continuing.
    Critical step: For specificity testing by cross-adsorption, see Box 1.
    ?TROUBLESHOOTING

15. Make serial dilutions in bacterial flow cytometry buffer, as suggested in Table 3.
    ?TROUBLESHOOTING
    Critical step: The exact scale and number of titration steps ideal for your experiment will vary depending on the experiment type and the values given in Table 3 should be considered as suggestions only.

16. Transfer 25µl of the titrated antibodies into V-bottom 96 well plates.
    Critical step: The exact volume of antibody solution will vary with the exact details of the experiment. 25µl is our suggested minimum volume.

Table 3: Recommended titration schemes

Sample type	Expected response strength	Suggested starting concentration	Dilution step size	Number of steps
Mouse serum	Strong IgG response (e.g. after IV vaccination)	≤100µg/ml IgG.	4-fold	6-8
Mouse Intestinal lavage	Strong IgA response	≤5µg/ml IgA	3-fold	6-8
Mouse serum	weak/endogenous response	≤1mg/ml IgG	3-fold	6-8
Human serum (sepsis)	Strong response	≤100µg/ml IgG ≤100µg/ml IgA	3-fold	6-8
Human serum (unknown)	Unknown	<200µg/ml IgG <50µg/ml IgA	3-fold	6-8
Human faecal water	Weak response	50µg/ml IgA	3-fold	6-8
Human breast milk	Weak response	100µg/ml IgA	3-fold	6-8
Human serum/purified antibodies	Strong response where a single concentration should be analysed across multiple donors	10µg/ml IgA or IgG	NA	NA

Primary antibody incubation. Timing: 45min-overnight

17. The minimum number of bacteria that can be reasonably detected in a single sample is 10^5. We therefore suggest as a minimum to mix 25µl of bacterial suspension at 5×10^6 bacteria per ml (from step 9) with 25µl of antibody-containing solutions (from step 16) prepared according to Table 3 with in a 96-well V-bottom plate.

    Critical step: If higher numbers of bacterial targets are used, the volume of antibody-containing solution must be correspondingly increased.

    ?TROUBLESHOOTING

18. Incubate the samples at room temperature for 15min, or at 4°C for 1h to overnight. (these incubation times give equivalent results and can be adapted for convenience)

Primary antibody washing. Timing: 30min

19. Add 200µl of sterile Bacterial flow cytometry buffer to each well and centrifuge the plates at 4000g, 10min, 4°C in a bench-top centrifuge (e.g. Eppendorf centrifuge 5810 R, A-4-81 rotor).

    CAUTION! If potential infectious material is present, seal the plates with parafilm prior to centrifugation to prevent aerosol formation.

    Critical step: You should not see any cell pellets with 10^5 bacteria per well.

20. Remove the supernatant by decanting

CAUTION! - Decant potentially infectious samples in a biosafety flow cabinet into a large vessel of disinfectant, and not directly into the sink.

21. Add a second 200µl of Bacterial flow cytometry buffer to each well, without active resuspension, and centrifuge as above (step 19) to remove all residual antibody solution. Remove the supernatant by decanting as above (step 20)

Secondary incubation. Timing: 30min-overnight

22. Add 50µl of secondary staining reagent, made up as in Table 1, to each well.
23. Actively resuspend the bacteria by pipetting.

    Critical step: Vortexing or shaking are not recommended for this as resuspension is poor by these methods, and there is a high risk of contamination between wells.

24. Wrap the plates in parafilm and incubate in the dark at RT for 15min or 4°C for 1h to overnight (with equivalent results)

Secondary antibody wash. Timing: 30min

25. Repeat Steps 19-21.

Tertiary reagent staining (e.g. streptavidin-fluorophore conjugates). Timing: 30min-overnight

    CRITICAL: These steps are optional, if not used, skip to step 29

26. Make up the tertiary reagent solution (typically 2µg/ml fluorophore-streptavidin in bacterial flow cytometry buffer) and add 50µl per well. Actively resuspend the bacteria by pipetting. Incubate at RT for 30min or 4°C overnight **(**these incubations yield identical results and can be adapted to the available time-schedule).

27. Add 200µl of bacterial flow cytometry buffer to each well and the centrifuge plates at 4000g 10min, 4°C in a bench-top centrifuge, as above**[(**step 19-21)

28. Optional: If the bacteria are not already fixed, and samples must conform to Biosafety level 1 for cytometry analysis, resuspend the pellet in 200µl 2% PFA in 1x PBS, 0.22µm filtered. Incubate for 20min, RT in the dark. Centrifuge at 4000g 10min, 4°C in a bench-top centrifuge, as above (step 19)

29. Remove supernatant by decanting, as above (step 20)

Resuspension for acquisition. Timing: 10min per plate

30. Resuspend the samples in a minimum of 300µl bacterial flow cytometry buffer or 2% PFA (depending on local flow cytometry recommendations) for acquisition. For acquisition on a FACSArray or another cytometer with plate-loading capacity, the stained bacteria plus buffer can be left in the 96 well plates and directly loaded into the machine. For flow cytometers without plate-loading capabilities, we recommend transferring the samples into 1.2ml library tubes, which can be arrayed with the identical arrangement to the 96 well plates, avoiding extensive tube labelling.

Cytometer set-up and acquisition. Timing: 20s per sample

Critical step: The exact set-up procedure will depend on the model of flow cytometer used. The steps below are suggested for LSRII (BD) and FACS CANTO II (BD) machines. For other cytometers, we recommend to contact the local support team to establish an optimal set-up for bacteria detection.

31. Using the cytometer set-up described in "Equipment setup", first acquire positive control single-stained samples to set PMT voltages and compensation matrices. It is recommended to acquire less than 2000 events per second even on cytometers capable of detecting mammalian cells at five times this rate. Optionally, for longitudinal analyses, it may be beneficial to work with a fixed gating template and calibration beads. In this case, acquire calibration beads and adjust the cytometer settings so that the beads fall into the pre-determined gates (Koch *et al.*, 2013).
?TROUBLESHOOTING

32. Acquire all samples. For robust statistics, it is recommended to acquire a minimum 10000 positively identified target events per sample. Plate-loaders should be set up to acquire this sample size, according to the manufacturer's instructions.
?TROUBLESHOOTING

Data analysis: Example workflow using FlowJo, Excel and Graphpad Prism. Timing: 30min per plate

Critical step: this could be implemented entirely in open-source frameworks by anyone familiar with these tools (Flow https://galen.dulci.duhs.duke.edu/flow/ or Bioconductor http://bioconductor.org/, the R project, https://adsorp.r-project.org/)

33. Import raw data from the flow cytometer (ideally.fcs3 files) into FlowJo (this analysis is functional in all FlowJo versions)

Draw a gate on the main bacterial population based on Fsc/Ssc. Optionally, carry out software compensation based on single-stained positive control samples, if this was not performed during acquisition (Szaloki *et al.*, 2015).

Critical step: Generate a layout displaying all fluorescence parameters for each sample to screen for errors in data acquisition, multiple peaks, and evidence of contaminations. Omitting this step may lead to misinterpretation of the data. ?TROUBLESHOOTING.

34. Calculate median fluorescence intensity (MFI) for each sample and each fluorophore/isotype combination present.

    Critical step: Arithmetic mean should not be used due to the log-normal distribution of fluorescence data, as well as the presence of potentially more complex distributions (multiple peaks etc.). For purely log-normal distributions (i.e. clean log-symmetrical single peak data), geometric mean will be identical to the median. However, as all parametric statistics are more sensitive to low numbers of outliers with very high or even negative values, we recommend to use the median as a robust single value read-out of fluorescence intensity.

35. Export MFI values to Excel. If a single antibody concentration was used, this is the end result and can be statistically evaluated between groups.

    Critical step: Where multiple isotypes are quantified in parallel, statistical significance levels must be corrected for multiple testing, for example using Bonferroni corrections or 1-way ANOVA of normalized values to analyse the data.

36. If titrations were generated, rearrange the data to generate a table in which the first column contains the dilution factor and each adjacent column contains the MFI titration values for a single sample. Generate the Log_{10} values of the entire table.

37. Import this data into Graphpad Prism as a xy dot-plot. Inspect this plot for smooth logistic dilution curves.

    ?TROUBLESHOOTING.

38. Use the non-linear regression function with the least-squares method to fit a 4-parameter logistic equation.

$$Y = Bottom + \frac{Top - Bottom}{1 + 10^{(LogEC50-X)*HillSlope}}$$

Critical step: At least 5 points, plus a base-line need to be present to fit with reasonable accuracy. Constrain the bottom of the curve to a single value for all samples (typically the MFI of the negative control). It may be necessary to limit the top asymptote if titrations do not reach saturation to avoid nonsensical results. Optionally, the MFI values may also be plotted against the total antibody concentration for each sample

dilution, rather than the dilution factor. This is particularly important when no further analysis is planned, as differences between curves, as revealed by dilution values, may be due simply to changes in total antibody concentrations.

?TROUBLESHOOTING

39. Export the results of the curve fitting back to Excel. For each curve you should have values for "top", "bottom", "logEC50" and "Hill slope". The "logEC50" is the log10 of the dilution factor at the curve inflexion point.

40. Rearrange the 4-parameter logistic equation to give x in y

$$X = LogEC50 - \left(\frac{Log \left(\frac{Top - Y}{Y - Bottom} \right)}{HillSlope} \right)$$

and use this with your above exported parameters ("Top", "Bottom", "LogEC50" and "Hillslope") to calculate the dilution factor (x) giving a defined "above-background" MFI (y) for all data sets (See figure 5, Supplementary data 1). This is your titre in terms of the dilution factor. As long as "y" falls within the pseudolinear range of the fitted curves, the actual value you choose to set for Y should not dramatically affect the relative data interpretation.

?TROUBLESHOOTING

41. To generate relative titres, divide the total antibody concentration (as determined by commercial sandwich ELISA following the manufacturer's instructions) by the titre in terms of dilution factor. This reveals the total antibody concentration required to give the chosen level of bacterial coating for each sample/donor. As this value is necessarily low with a high titre response, and this is often confusing to readers, the inverse of this value is usually plotted i.e. a value in ng^{-1}ml.

42. As an alternative, titres giving an approximate idea of the concentration of specific antibodies per ml can be calculated by reference to binding of a defined monoclonal antibody (Figure 5, Supplementary data 1). It should be noted that this is not quite an accurate description as the shift in binding curve depends not only on the number but also the avidity/avidity of antibodies, but it can be a more intuitive read-out where such standards are available. Here, the value in ng/ml is calculated as:

$$Titer = (concentration\ of\ monoclonal) * \frac{dilution\ factor\ for\ MFI = N : Sample}{dilution\ factor\ for\ MFI = N : Monoclonal}$$

TIMING

- Steps 1 to 9: 2-7 days depending on bacterial growth characteristics
- Steps 10 to 16: 1h
- Step 17 to18: 45 min to overnight-PAUSE POINT
- Steps 19 to 21: 30 min
- Steps 22 to 24: 30 min to overnight-PAUSE POINT
- Steps 25 to 26: 30 min
- Steps 27 to 29: Optional, 30 min to overnight-PAUSE POINT
- Step 30: 10 min per plate
- Step 31-32: Data acquisition: 20s per sample
- Step 33-43: Data analysis: 30min per plate

TROUBLESHOOTING

Troubleshooting advice can be found in Table 4.

ANTICIPATED RESULTS

If this protocol is carefully followed, clean data on species-specific antibodies can be generated in a wide range of situations. The technique has been successfully used in a range of publications both in murine model systems and in the human system (Balmer *et al.*, 2014; Endt *et al.*, 2010; Haas *et al.*, 2011; Hapfelmeier *et al.*, 2010; Seleznik *et al.*, 2012; Slack *et al.*, 2009).

In the first published example, taken from (Moor *et al.*, 2016) C57BL/6 SPF mice received either three oral doses of 10^{10} peracetic acid inactivated *S.* Typhimurium over three weeks, or were orally infected with a live-attenuated *S.* Typhimurium vaccination strain. 3 weeks after the initiation of vaccination, the intestinal IgA response was quantified from intestinal lavages (Figure 12A and B) and serum IgG2b (Figure 12C), IgG1 and IgM (data not shown) were quantified from serum. This demonstrates the effective induction of a mucosal IgA response by the inactivated and live oral vaccines, with minimal induction of serum IgG at these time-points. The data analysis leading from the raw data in panel A to the analysed data in panel B is described in detail in Supplementary data file 1.
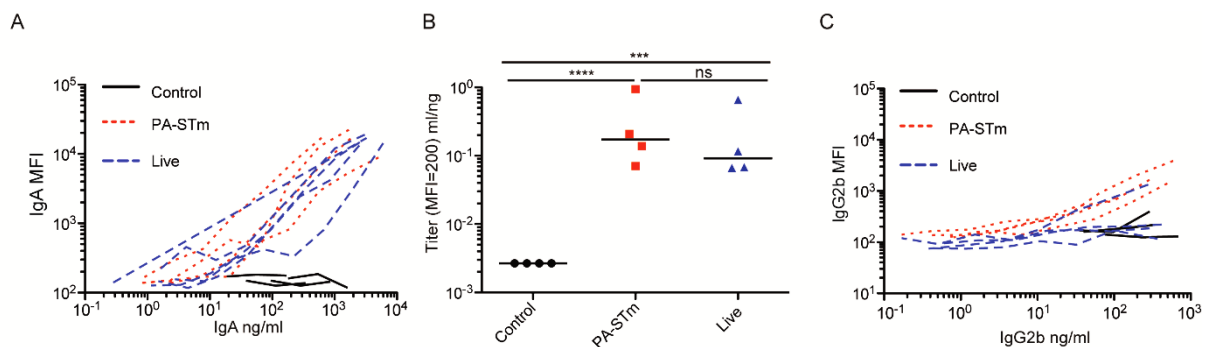

Figure 12: Vaccination with oral peracetic acid-inactivated *S.* Typhimurium and infection with live-attenuated *S.* Typhimurium induce a similar magnitude of intestinal IgA response. Reproduced under the Creative Commons license from Frontiers in Immunology 2016 (Moor *et al.*, 2016) . C57BL/6 SOPF mice were either pre-treated with 1.0g/kg streptomycin and one day later infected orally with 5×10^7 CFU of the oral vaccination *S.* Typhimurium strain M556 (SB300 *ΔsseD*) ("Live"), or were gavaged once a week with 10^{10} particles of peracetic acid-killed *S.* Typhimurium ("PA.STm") over three weeks. A. Intestinal lavage IgA titre curves and B. intestinal lavage IgA titres, as calculated in Figure 11D-E (Kruskal-Wallis test on log-normalized values, P < 0.0001. Pairwise comparisons calculated by Dunn's posttests). C. serum IgG2b titre curves at d21 after the first vaccination/infection, as determined by bacterial flow cytometry. All animal experiments were approved by the legal authorities (licenses 223/2010 and 222/2013; Kantonales Veterinäramt Zürich, Switzerland) and performed according to the legal and ethical requirements.

In the second published example, taken from ref. (Balmer *et al.*, 2014), bacterial flow cytometry was used to quantify serum antibody responses against a panel of anaerobic intestinal microbiota species in patients with varying stages of metabolic liver disease and

healthy donors. Relative titres were calculated for each sample/species combination (Figure 13A) and the final large data set analysed by hierarchical clustering (Figure 13B). In this example we could demonstrate elevated microbiota-directed serum IgG responses in patients with metabolic liver diseases, independent of disease stage. This suggested that increased immune exposure to the intestinal microbiota is an early event in the progression of metabolic diseases.
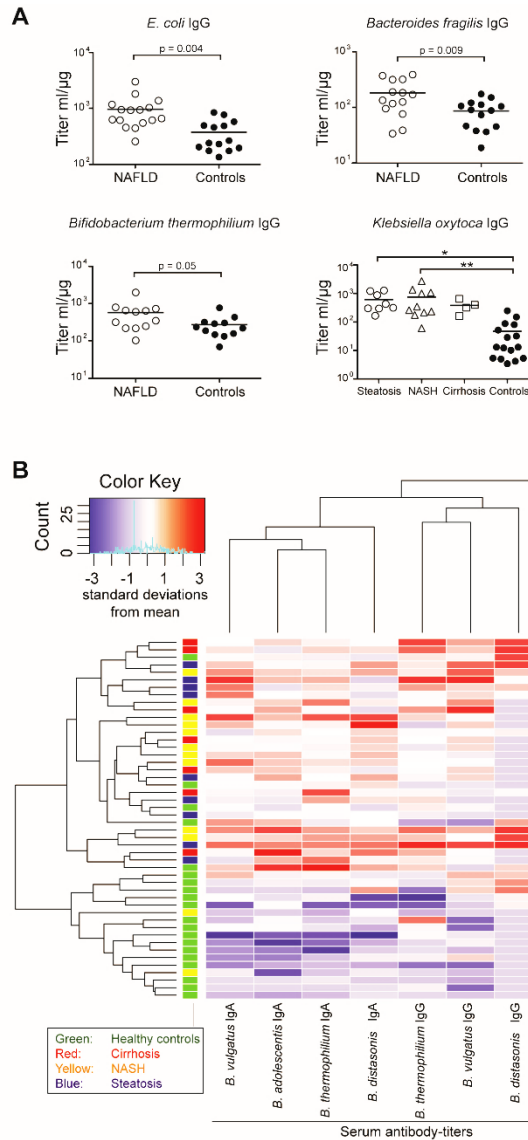
Figure 13: Bacterial flow cytometry reveals increased microbiota-specific serum antibodies in metabolic liver disease. Reproduced with permission from Science Translational Medicine 2014 (Balmer *et al.*, 2014). (**A**) Serum IgG titres against the indicated bacteria in NAFLD patients (open symbols) compared to age- and sex-matched healthy controls (filled dots). Pure cultures of the indicated bacteria were stained with dose-titrations of serum from patients or controls. Serum antibody coating of bacteria was visualised using monoclonal DyLight647-conjugated anti-human IgG and quantified per bacterium by flow cytometry. Resulting MFI was plotted against total IgG added to the assay as determined by ELISA and IgG-titres calculated by fitting 4-parameter logistic curves to each donor and determining the concentration of IgG required to give a median fluorescence intensity binding of 80. The inverse of this IgG concentration is shown, for ease of interpretation. Each point represents an individual subject and lines show means. Unpaired t-test or one-way ANOVA and Tukey post-test were used to compare the groups; *, $p \leq 0.05$, **; $p \leq 0.01$. (**B**) Cluster-analysis from Basel NAFLD patients with different stages of liver disease (steatosis = blue, NASH = yellow, cirrhosis = red) and age- and sex-matched healthy controls (green). Heatmaps were generated using an euclidean distance function with complete linkage clustering in the statistical package R using the package "gplots version 2.8.0", function "heatmap.2". Red indicates increased and blue decreased titres compared to the mean of the entire population.

Box 1: Cross-adsorption for specificity testing

These antibody preparation steps should be carried out when you wish to test the specificity of a response. By first incubating the antibody-containing solution with a high number of a known bacterial species, and looking for loss of signal, it is possible to distinguish non-specific binding (which will depend only on the total immunoglobulin concentration and will be unaffected by this treatment) from specific binding (which should be completely removed by this process).

1. Cross-adsorption needs to be carried out in reasonably large volumes to permit efficient clearance and re-filtration, therefore it is suggested to dilute the samples with bacterial flow cytometry buffer to a concentration giving high, but non-saturating, binding in the bacterial flow cytometry assays (determine this in a pilot experiment).

2. Prepare (n+1) x 500µl of the diluted sample to be cross-adsorbed, as detailed in Steps 11-14 of the Procedure where "n" is the number of bacterial species against which cross-adsorption is planned.

3. Aliquot 500µl of this solution into 1.5ml snap-cap tubes.

4. From stationary-phase cultures of your species of interest, centrifuge sufficient volume to pellet 10^9 bacteria. Resuspend at 10^9 bacteria per ml in bacterial flow cytometry buffer.

5. Add 500µl bacterial flow cytometry buffer to the control aliquot of your antibody solution.

6. To all other aliquots, add 500µl of the bacterial suspensions.

7. Incubate at 4°C for 1h with gentle shaking

8. Centrifuge all tubes at 16000g, 4°C, 15min to sediment all bacteria.

9. Recover the supernatants and filter through a 0.22µm filter into fresh 1.5ml tubes to remove any remaining bacteria.

10. Proceed with staining, from step 17.

    Critical step: The "bacterial flow cytometry buffer only" cross-adsorbed sample must be included as a dilution control.

Box 2: Purification of IgA from viscous or fatty samples

Purification of antibodies using Fc-specific gel-filtration is extremely helpful for fluids with a very high viscosity or fat content, for example faecal water or breast milk. As these tend to be mucosal-associated fluids, IgA is normally the target isotype for purification, and it should be noted that this isotype does not bind to either Protein A or Protein G standard immunoglobulin purification reagents. We therefore recommend the following procedure:

1. Pre-dilute the samples in PBS to achieve a workable viscosity and pH>7 and a volume of between 1 and 10ml.
2. Clear the suspensions by centrifugation (16000g, +4° for 5 minutes).
3. Filter the samples through a 0.22μm syringe filter
   Critical step: This is essential to avoid purification column blockage and complete loss of the sample.
4. For each sample, prepare a gravity flow column containing either Peptide M / Agarose or Immobilized Jacalin avidity gel according to the manufacturer's instructions: typically degas both the agarose and washing buffer, then carefully load the agarose on top of a membrane filter avoiding air bubbles. Wash through with 10 column volumes of wash buffer. Column size and IgA binding protein quantities should be adjusted to the expected IgA concentration in the sample of interest. Binding capacity Peptide M: 4-6 mg/ml. Binding capacity Jacalin: 1-3mg/ml.
   Critical step: Peptide-M binds IgA1 and IgA2 whereas Jacalin binds only IgA1 (and IgD)
5. Equilibrate columns with 10ml PBS
6. Add the sample and allow to fully enter the matrix.
7. Wash with 20 column volumes of PBS.
8. Elute in 10ml elution buffer (0.1M Glycine pH 2-3 for Peptide M, 0.1M Alpha-D-Galactose for Jacalin).
9. After elution in 0.1M Glycine pH 2-3, use 1M TRIS pH 7.5 to neutralize the solution. As dimeric secretory IgA has a molecular mass of >300kDa, buffer exchange can be easily performed by filtration through a 100kDa ultrafiltration membrane (as per the manufacturer's instructions) and resuspension in flow cytometry buffer.
10. These antibody solutions can be aliquoted and frozen at -20°C for several months of -80°C for several years.
    Critical step: Re-filter the solution through a 0.22μm syringe filter prior to use, in order to remove any precipitates that may have formed during the preparation process.

Box 3: Cryo-preserving and thawing aliquoted bacterial targets

1. Cultivate bacteria and quantify density as described in Steps 1-7 of the procedure. Calculate the volume of media prepared and inoculated to permit production of sufficient aliquots of frozen cells for the entire experiment series (e.g. *E. coli* typically grows to a maximum density of 10^9CFU/ml in aerobic culture in rich media. To generate 200 aliquots of 10^8 CFU will require 20ml of overnight culture).

2. Centrifuge 10-50ml culture 4°C, 4000-8000g, 5 min. Resuspend in 10-50ml sterile PBS.

3. Centrifuge again at 4°C, 4000-8000g, 5 min.

4. Resuspend the pellet in cell freezing medium to a final concentration of 5×10^8 - 10^9CFU/ml. Make 100µl aliquots and freeze immediately in liquid nitrogen.
   PAUSE POINT Aliquots may be stored for up to 2 years at -80°C.

5. To perform experiments, thaw sufficient bacterial aliquots at RT, 15min.

6. Pool all aliquots and add 1ml 1xPBS
   Critical step: PBS should be at 4°C, 0.22µm filtered

7. Centrifuge at 4000-8000g, 10min at 4°C.

8. Thaw an aliquot of 4% PFA solution.

9. Resuspend the cell pellet from Step 7 of this box in 4% PFA (Optional: + amine-reactive dye - see Box 4) at a density of 10^9 cells per ml. Incubate in the dark at 4°C for 20min.

10. Add 1 volume 1x PBS and centrifuge (4000g, 4°C, 2min) to gently pellet only whole bacteria.

11. Resuspend the bacteria at 5×10^6 cells per ml in bacterial flow cytometry buffer and use within 72h (store at 4°C). PAUSE POINT

12. Continue with the protocol from Step 10.

Box 4: Amine-reactive dye or NHS-Biotin labelling for target identification and multiplexing.

These procedures can be used to chemically fluorescently label bacterial targets, either to positively gate these away from debris in the flow cytometer or to be able to mix multiple bacterial species to multiplex the analysis.

Amine-reactive dyes

1. Either prepare fresh live bacterial targets as in Steps 1-6 of the Procedure, or thaw frozen bacterial targets as described in Box 3.
2. Centrifuge at 4000-8000g, 2min, 4°C.
3. Thaw a fresh aliquot of 4% PFA (1ml per 10^9 CFU) and add an amine-binding dye to the recommended concentration (e.g. e-Fluor 450 Cell proliferation dye 20μM), 0.22μm filter the solution.
4. Resuspend the bacterial pellet in the dye solution and incubate 20min room temperature in the dark with shaking to ensure even dye labelling.
   ?TROUBLESHOOTING
5. Centrifuge at 4000-8000g, 2min, 4°C. Resuspend in 1ml bacterial flow cytometry buffer and proceed to adjust the bacteria density to $5x10^6$ per ml, at described in Step 7 of the Procedure.

Surface NHS-Biotin labelling

1. Prepare fresh, live bacterial targets as described in Steps 1-6 of the Procedure. Measure the OD_{600nm} and adjust the density to $5x10^8$ bacteria/ml with bacterial flow cytometry buffer. Determine the volume of this suspension required for the experiment (0.25μl per well to be analysed).
2. Make up an equal volume of Easylink-NHS-PEG4-Biotin as per the manufacturer's instructions to 2mM in 1xPBS
3. Mix the NHS-biotin solution 1:1 with the bacterial suspension.
4. Incubate at RT, 1h, with shaking (500rpm, orbital shaker)
5. Centrifuge at 4000-8000g, 5min, 4°C and discard supernatant.
6. Resuspend pellet in 1ml 1xPBS 100mM glycine to quench staining.
7. Centrifuge at 4000-8000g, 5min, 4°C and discard supernatant.
8. Resuspend in 1ml bacterial flow cytometry buffer. Repeat washing steps of this box (7 and 8) in bacterial flow cytometry buffer twice.
9. Resuspend in 1ml fluorophore-streptavidin conjugate solution in bacterial flow cytometry buffer (e.g. Pacific Blue-streptavidin, 2μg/ml). Incubate for 30min, RT, in the dark.

10. Wash 3 times by centrifugation at 4000-8000g, 4°C and resuspension in 1ml bacterial flow cytometry buffer to remove all un-bound streptavidin.

11. Bacterial targets labelled with different colours of streptavidin conjugates may then be pooled and the final concentration adjusted to $5x10^6$ bacteria of each species per ml bacterial flow cytometry buffer.

12. Proceed from Step 9 of the main protocol.

Critical Step: Check that surface labelling is homogenous by running a small aliquot (25µl of the $5x10^6$ CFU per ml final suspension, diluted to 300µl with bacterial flow cytometry buffer) through the flow cytometer. A single fluorescent peak should be visible in the relevant fluorescence channel. If multiple peaks are observed, the targets should not be analysed further.

?TROUBLESHOOTING

Table 4. Troubleshooting

Step	Problem	Probable cause	Solution
1-5	No bacterial growth	Stock too old/dead	Obtain fresh bacterial frozen stock
		Inappropriate growth conditions	Check recommended growth conditions
			Check culture identity (See Box 5)
	Unexpectedly rapid bacterial growth	Stock or media contaminated	Re-sterilize glassware. Re-prepare and sterilize culture media.
			Obtain fresh bacterial frozen stocks
6	Poor sedimentation after centrifugation at 4000g, 2min	Small/boyant bacteria	Increase centrifugation speed and time
	Sticky pellet after centrifugation	Fragile bacteria may lyse if pelleted with excessive force releasing DNA	Decrease centrifugation speed
7	Highly variable OD_{600} readings after overnight culture	Culture conditions are not constant.	Check media and gas compositions. Check incubator temperatures are constant.
		OR	
		$OD600$ readings are affected by bacterial aggregation.	Decrease centrifugation speeds to avoid bacterial lysis. Try disrupting aggregates by physical force, or consider counting by flow cytometry.
11	Extensive precipitates and very high viscosity in antibody-containing body fluids	Cell debris or lipids present in the fluid	If this is hard to clear by centrifugation and filtration, consider antibody purification prior to analysis (see Box 2)
11	Insufficient antibody to follow recommended concentrations in Table 3	NA	Use undiluted samples with minimum numbers of bacterial targets to maximize the chance of observing specific signal.
14	Frequent blockage of 0.22μm syringe filters during antibody-containing fluid preparation	Large quantities of cell debris or precipitated biomolecules in solutions	Increased length of 16000g centrifugation step prior to filtration
			Use larger volume 0.22μm filters
			Consider antibody purification (see Box 2)
31	High event numbers in the cytometer when	Contamination in cytometer tubing or sheath fluid	Thoroughly clean the cytometer with bleach- and detergent-containing solutions

	running 0.22µm filtered water or PBS		0.22µm filter in-house produced sheath fluid If this does not solve the issue, the flow cell may be damaged. Ideally this should be replaced. However, an alternative solution is to chemically fluorescently label the bacterial targets (see Box 4) to permit specific gating.
31-32	Zero events in flow cytometer	Incorrect cytometer settings	Ensure that threshold values are not set too high resulting in exclusion of all bacteria-sized events
		Cytometer blocked or mis-functioning	Check for normal detection of set-up beads. Clean the machine to remove blockages. If this fails, contact manufacturer's support engineers.
31-32	No bacteria observable in cytometer	Insufficient cells	Check relationship between OD_{600nm} and CFU
		Centrifugation failure	Include one well with high CFU number to check centrifugation has pelleted cells
		Incorrect cytometer settings	Obtain a fluorescently-labelled bacterial sample (e.g. brightly GFP-positive *E. coli*, or chemically-stained cells) at reasonably high density (e.g. $5x10^7$/ml). Alter cytometer settings until the population is visible.
31-32	Very low fluorescence signal in positive control sample	Incorrect bacterial strain or growth conditions	Streak out bacterial culture and pick a single colony. Confirm the species by biochemistry and genetics (see Box 5).
		To many CFU per well	Re-check the relationship between OD_{600nm} and CFU/ml. Correct such that only 10^5 bacteria are loaded per well.
31-32	High background in negative control	Fc- or non-specific binding	Check binding of isotype controls. Test closely related strains to identify one without Fc binding activity.
		Antibody complex contamination	Ensure all antibody solutions are filtered through 0.22µm filters prior to adding to the bacterial targets.
Box 4	Multiple peaks after chemical labelling	Insufficient mixing after dye addition	Repeat chemical labelling with gentle vortexing.
31-32	Multiple peaks	Phenotypic variation or stochastic gene expression in targets	Alter culture conditions or try to work with phase-locked variants, if genetically accessible.

		Inefficient detection by cytometer (typically second peaks appear on the axes)	Decrease acquisition rate
		Contamination	See Box 5. Obtain fresh bacterial stocks, culture media and sterile culture vessels.
37	"Bell-shaped" dilution curves when MFI is plotted against dilution factor	Toxicity and/or massive agglutination at very high antibody concentrations	Exclude all values with high total antibody concentrations to permit a curve-fit. As efficient agglutination is what antibodies "do" at high concentrations, this is unavoidable. Consider repeating the measurements with lower starting antibody concentrations.
38	Poor r^2 value for curve fitting, or unable to fit 4-parameter logistic equation	No antibody binding detected	You cannot fit a flat horizontal line. In this case, the calculated titre is at the detection limit (typically the inverse undiluted antibody concentration)
		Sample contamination	Examine scatter plots in FlowJo for evidence of multiple peaks. See troubleshooting for multiple peaks (Steps 31-32)
		Bell-shaped curve	See troubleshooting for bell-shaped dilution curves (Step 37)
40-42	No mathematical solution for relative titre calculations	Top of the curve does not reach the chose Y axis value.	Check that your chosen Y axis value is reasonable (i.e. falls in the pseudolinear part of the curve for the positive control samples). If this is OK, then samples that do not reach this value have a titre at the detection limit.

Conflict of Interest Statement

The authors declare that they have no competing financial interests.

SUPPLEMENTARY DATASET

4-parameter logistic curve values to simulate, based on real values

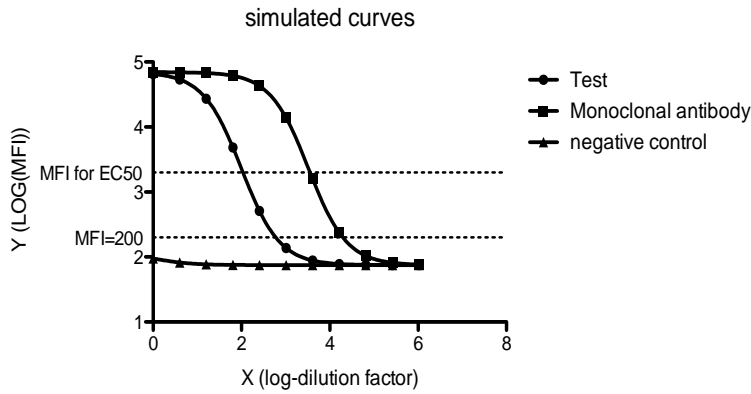|	test	monoclonal antibody
Lower limit Log10(MFI)	1.875	1.875
Upper limit Log10(MFI)	4.8451	4.8451
LogEC50	2	3.51851394
HillSlope	-1	-1
EC50	100	3300

Calculate simulated MFI values based on the 4-parameter logistic equation

$$Y = Bottom + \frac{Top - Bottom}{1 + 10^{(LogEC50 - X) * HillSlope}}$$

Dilution	X (log10-dilution factor)	test	monoclonal antibody
1	0	4.81569307	4.844200242
4	0.602059991	4.73086538	4.841504237
16	1.204119983	4.43543103	4.830768999
64	1.806179974	3.68603659	4.788593936
256	2.408239965	2.70929775	4.631279528
1024	3.010299957	2.13924377	4.141727567
4096	3.612359948	1.94578408	3.200220389
16384	4.214419939	1.89301808	2.372933855
65536	4.816479931	1.87952511	2.017386687
262144	5.418539922	1.87613257	1.911924285
1048576	6.020599913	1.87528322	1.884317952

Anti-logged values to plot

Dilution	test	monoclonal antibody
1	65417.3684	69855.44158
4	53810.2964	69423.13751
16	27254.0491	67728.1166
64	4853.29383	61460.19528
256	512.032765	42783.81696
1024	137.798272	13858.8619
4096	88.2640965	1585.697675
16384	78.1660342	236.0118749
65536	75.774854	104.0846502
262144	75.1852367	81.64400213
1048576	75.038341	76.61573141

simulated curves

Calculating absolute titers by comparing the horizontal displacement of the "test" curve to the "monoclonal antibody" curve where the concentration is known:

Monoclonal positive control concentration µg/ml	3.3	
Dilution giving 50% binding (EC50) test	100	
Dilution giving 50% binding (EC50) monoclonal	3300	
Concentration of specific antibodies in test µg/ml	0.1	=[concentration of monoclonal µg/ml] x [dilution factor for MFI=N, sample] / [dilution factor for MFI=N, monoclonal]

Calculating relative titers for Y=200 using the re-arranged 4-parameter logistic equation and curve fitting parameters derived from non-linear regression

$$X = LogEC50 - \left(\frac{Log\left(\frac{Top - Y}{Y - Bottom} \right)}{HillSlope} \right)$$

	Data from curve-fitting, imported from the relevant software				
	Bottom Log10(MFI)	Top Log10(MFI)	LogEC50	HillSlope	EC50
Test	1.875	4.8451	2	-1	100
Monoclonal antibody	1.875	4.8451	3.51851394	-1	3300

	Calculated values				
	LOG10 dilution factor giving MFI=200	Dilution MFI=200	Total Liga conc µg/ml	IgA giving MFI=200	Titre ng-1.ml
Test	2.77608888	597.1574843	3.3	0.00552618	180.9568134
Monoclonal antibody	4.29460282	19706.19698	3.3	0.00016746	5971.574843

126

References

Avraham, R., Haseley, N., Brown, D., Penaranda, C., Jijon, H. B., Trombetta, J. J., Satija, R., Shalek, A. K., Xavier, R. J., Regev, A., & Hung, D. T. (2015). Pathogen Cell-to-Cell Variability Drives Heterogeneity in Host Immune Responses. *Cell, 162*(6), 1309-1321.

Balmer, M. L., Slack, E., de Gottardi, A., Lawson, M. A., Hapfelmeier, S., Miele, L., Grieco, A., Van Vlierberghe, H., Fahrner, R., Patuto, N., Bernsmeier, C., Ronchi, F., Wyss, M., Stroka, D., Dickgreber, N., Heim, M. H., McCoy, K. D., & Macpherson, A. J. (2014). The liver may act as a firewall mediating mutualism between the host and its gut commensal microbiota. *Sci Transl Med, 6*(237), 237ra266.

Bouvet, J. P. (1994). Immunoglobulin Fab fragment-binding proteins. *Int J Immunopharmacol, 16*(5-6), 419-424.

Brown, Jeremy S., Hussell, Tracy, Gilliland, Sarah M., Holden, David W., Paton, James C., Ehrenstein, Michael R., Walport, Mark J., & Botto, Marina. (2002). The classical pathway is the dominant complement pathway required for innate immunity to Streptococcus pneumoniae infection in mice. *Proceedings of the National Academy of Sciences, 99*(26), 16969-16974.

Bunker, Jeffrey¬†J, Flynn, Theodore¬†M, Koval, Jason¬†C, Shaw, Dustin¬†G, Meisel, Marlies, McDonald, Benjamin¬†D, Ishizuka, Isabel¬†E, Dent, Alexander¬†L, Wilson, Patrick¬†C, Jabri, Bana, Antonopoulos, Dionysios¬†A, & Bendelac, Albert. (2015). Innate and Adaptive Humoral Responses Coat Distinct Commensal Bacteria with Immunoglobulin A. *Immunity, 43*(3), 541-553.

Chimalapati, Suneeta, Cohen, Jonathan, Camberlein, Emilie, Durmort, Claire, Baxendale, Helen, de Vogel, Corné, van Belkum, Alex, & Brown, Jeremy S. (2011). Infection with Conditionally Virulent Streptococcus pneumoniae Δpab Strains Induces Antibody to Conserved Protein Antigens but Does Not Protect against Systemic Infection with Heterologous Strains. *Infection and Immunity, 79*(12), 4965-4976.

Cohen, Jonathan M., Wilson, Robert, Shah, Pranali, Baxendale, Helen E., & Brown, Jeremy S. (2013). Lack of cross-protection against invasive pneumonia caused by heterologous strains following murine Streptococcus pneumoniae nasopharyngeal colonisation despite whole cell ELISAs showing significant cross-reactive IgG. *Vaccine, 31*(19), 2328-2332.

Cooper, M. D., Wannemuehler, M. J., Miller, R. D., & Fedyk, M. F. (1981). Role of outer envelope contamination in protection elicited by ribosomal preparations against Neisseria gonorrhoeae infection. *Infect Immun, 32*(1), 173-179.

Cullender, Tyler C, Chassaing, Benoit, Janzon, Anders, Kumar, Krithika, Muller, Catherine E, Werner, Jeffrey J, Angenent, Largus T, Bell, M. Elizabeth, Hay, Anthony G, Peterson, Daniel A, Walter, Jens, Vijay-Kumar, Matam, Gewirtz, Andrew T, & Ley, Ruth E. (2013). Innate and Adaptive Immunity Interact to Quench Microbiome Flagellar Motility in the Gut. *Cell Host & Microbe, 14*(5), 571-581.

Endt, K., Stecher, B., Chaffron, S., Slack, E., Tchitchek, N., Benecke, A., Van Maele, L., Sirard, J. C., Mueller, A. J., Heikenwalder, M., Macpherson, A. J., Strugnell, R., von Mering, C., & Hardt, W. D. (2010). The microbiota mediates pathogen clearance from the gut lumen after non-typhoidal Salmonella diarrhea. *PLoS Pathog, 6*(9), e1001097.

Goodman, A. L., Kallstrom, G., Faith, J. J., Reyes, A., Moore, A., Dantas, G., & Gordon, J. I. (2011). Extensive personal human gut microbiota culture collections characterized and manipulated in gnotobiotic mice. *Proc Natl Acad Sci U S A, 108*(15), 6252-6257.

Haas, A., Zimmermann, K., Graw, F., Slack, E., Rusert, P., Ledergerber, B., Bossart, W., Weber, R., Thurnheer, M. C., Battegay, M., Hirschel, B., Vernazza, P., Patuto, N., Macpherson, A. J., Gunthard, H. F., Oxenius, A., & Swiss, H. I. V. Cohort Study. (2011). Systemic antibody responses to gut commensal bacteria during chronic HIV-1 infection. *Gut, 60*(11), 1506-1519.

Hapfelmeier, S., Lawson, M. A., Slack, E., Kirundi, J. K., Stoel, M., Heikenwalder, M., Cahenzli, J., Velykoredko, Y., Balmer, M. L., Endt, K., Geuking, M. B., Curtiss, R., 3rd, McCoy, K. D., &

Macpherson, A. J. (2010). Reversible microbial colonization of germ-free mice reveals the dynamics of IgA immune responses. *Science, 328*(5986), 1705-1709.

Hyams, Catherine, Camberlein, Emilie, Cohen, Jonathan M., Bax, Katie, & Brown, Jeremy S. (2010). The Streptococcus pneumoniae Capsule Inhibits Complement Activity and Neutrophil Phagocytosis by Multiple Mechanisms. *Infection and Immunity, 78*(2), 704-715.

Karlsson, M., Mollegard, I., Stiernstedt, G., & Wretlind, B. (1989). Comparison of Western blot and enzyme-linked immunosorbent assay for diagnosis of Lyme borreliosis. *Eur J Clin Microbiol Infect Dis, 8*(10), 871-877.

Koch, Christin, Günther, Susanne, Desta, Adey F., Hübschmann, Thomas, & Müller, Susann. (2013). Cytometric fingerprinting for analyzing microbial intracommunity structure variation and identifying subcommunity function. *Nat. Protocols, 8*(1), 190-202.

Lécuyer, Emelyne, Rakotobe, Sabine, Lengliné-Garnier, Hélène, Lebreton, Corinne, Picard, Marion, Juste, Catherine, Fritzen, Rémi, Eberl, Gérard, McCoy, Kathy D, Macpherson, Andrew J, Reynaud, Claude-Agnès, Cerf-Bensussan, Nadine, & Gaboriau-Routhiau, Valérie. (2014). Segmented Filamentous Bacterium Uses Secondary and Tertiary Lymphoid Tissues to Induce Gut IgA and Specific T Helper 17 Cell Responses. *Immunity, 40*(4), 608-620.

LeibundGut-Landmann, Salome, Grosz, Olaf, Robinson, Matthew J., Osorio, Fabiola, Slack, Emma C., Tsoni, S. Vicky, Schweighoffer, Edina, Tybulewicz, Victor, Brown, Gordon D., Ruland, Jurgen, & Reis e Sousa, Caetano. (2007). Syk- and CARD9-dependent coupling of innate immunity to the induction of T helper cells that produce interleukin 17. *Nat Immunol, 8*(6), 630-638.

Liu, Bin, Knirel, Yuriy A., Feng, Lu, Perepelov, Andrei V., Senchenkova, Sof'ya N., Reeves, Peter R., & Wang, Lei. (2014). Structural diversity in Salmonella O antigens and its genetic basis. *FEMS Microbiology Reviews, 38*(1), 56-89.

Maclennan, Calman A. (2014). Antibodies and protection against invasive Salmonella disease. *Frontiers in Immunology, 5*.

Macpherson, A. J., & McCoy, K. D. (2013). Stratification and compartmentalisation of immunoglobulin responses to commensal intestinal microbes. *Semin Immunol, 25*(5), 358-363.

Macpherson, A. J., & Uhr, T. (2004). Induction of protective IgA by intestinal dendritic cells carrying commensal bacteria. *Science, 303*(5664), 1662-1665.

Moor, K., Wotzka, S. Y., Toska, A., Diard, M., Hapfelmeier, S., & Slack, E. (2016). Peracetic Acid Treatment Generates Potent Inactivated Oral Vaccines from a Broad Range of Culturable Bacterial Species. *Front Immunol, 7*, 34.

Mouslim, C., & Hughes, K. T. (2014). The effect of cell growth phase on the regulatory cross-talk between flagellar and Spi1 virulence gene expression. *PLoS Pathog, 10*(3), e1003987.

Pack, T. D. (2001). Purification of human IgA. *Curr Protoc Immunol, Chapter 2*, Unit 2.10B.

Palm, N. W., de Zoete, M. R., Cullen, T. W., Barry, N. A., Stefanowski, J., Hao, L., Degnan, P. H., Hu, J., Peter, I., Zhang, W., Ruggiero, E., Cho, J. H., Goodman, A. L., & Flavell, R. A. (2014). Immunoglobulin A coating identifies colitogenic bacteria in inflammatory bowel disease. *Cell, 158*(5), 1000-1010.

Porsch-Özcürümez, Mustafa, Kischel, Nele, Priebe, Heidi, Splettstösser, Wolf, Finke, Ernst-Jürgen, & Grunow, Roland. (2004). Comparison of Enzyme-Linked Immunosorbent Assay, Western Blotting, Microagglutination, Indirect Immunofluorescence Assay, and Flow Cytometry for Serological Diagnosis of Tularemia. *Clinical and Diagnostic Laboratory Immunology, 11*(6), 1008-1015.

Saletti, Giulietta, Çuburu, Nicolas, Yang, Jae Seung, Dey, Ayan, & Czerkinsky, Cecil. (2013). Enzyme-linked immunospot assays for direct ex vivo measurement of vaccine-induced human humoral immune responses in blood. *Nat. Protocols, 8*(6), 1073-1087.

Seleznik, G. M., Reding, T., Romrig, F., Saito, Y., Mildner, A., Segerer, S., Sun, L. K., Regenass, S., Lech, M., Anders, H. J., McHugh, D., Kumagi, T., Hiasa, Y., Lackner, C., Haybaeck, J., Angst, E., Perren, A., Balmer, M. L., Slack, E., MacPherson, A., Manz, M. G., Weber, A., Browning, J. L., Arkan, M. C., Rulicke, T., Aguzzi, A., Prinz, M., Graf, R., & Heikenwalder, M. (2012). Lymphotoxin beta

receptor signaling promotes development of autoimmune pancreatitis. *Gastroenterology, 143*(5), 1361-1374.

Slack, E., Balmer, M. L., & Macpherson, A. J. (2014). B cells as a critical node in the microbiota-host immune system network. *Immunol Rev, 260*(1), 50-66.

Slack, E., Hapfelmeier, S., Stecher, B., Velykoredko, Y., Stoel, M., Lawson, M. A., Geuking, M. B., Beutler, B., Tedder, T. F., Hardt, W. D., Bercik, P., Verdu, E. F., McCoy, K. D., & Macpherson, A. J. (2009). Innate and adaptive immunity cooperate flexibly to maintain host-microbiota mutualism. *Science, 325*(5940), 617-620.

Smith, K., McCoy, K. D., & Macpherson, A. J. (2007). Use of axenic animals in studying the adaptation of mammals to their commensal intestinal microbiota. *Semin Immunol, 19*(2), 59-69.

Speers, Allison M., Cologgi, Dena L., & Reguera, Gemma. (2005). Anaerobic Cell Culture *Current Protocols in Microbiology*: John Wiley & Sons, Inc.

Szaloki, G., & Goda, K. (2015). Compensation in multicolor flow cytometry. *Cytometry A, 87*(11), 982-985.

Tashiro, M., & Montelione, G. T. (1995). Structures of bacterial immunoglobulin-binding domains and their complexes with immunoglobulins. *Curr Opin Struct Biol, 5*(4), 471-481.

van der Woude, M. W. (2011). Phase variation: how to create and coordinate population diversity. *Curr Opin Microbiol, 14*(2), 205-211.

Yutin, N., Puigbo, P., Koonin, E. V., & Wolf, Y. I. (2012). Phylogenomics of prokaryotic ribosomal proteins. *PLoS One, 7*(5), e36972.

CHAPTER 4

-

VACCINATION PREVENTS INFLAMMATION-MEDIATED BACTERIOPHAGE-TRANSFER BETWEEN *SALMONELLA* SPP.

Vaccination prevents inflammation-mediated bacteriophage-transfer between *Salmonella* spp.

Médéric Diard*[1], Kathrin Moor[#1], Mikael Sellin[#1], Abram Aertsen[2], Martin Ackermann[3], Emma Slack[#1], Wolf-Dietrich Hardt*[1]

[#]: contributed equally

[*]: corresponding authors

[1]Institute of Microbiology, ETH Zurich, Switzerland

[2]Centre for Food and Microbial Technology, KU Leuven, Belgium

[3]Department of Environmental Systems Science, ETH Zurich, and Department of Environmental Microbiology, Eawag, Switzerland

Manuscript in revision

Abstract

Bacteriophage-transfer (lysogenic conversion) is an important driver of bacterial virulence evolution. There are no practical means to prevent this. This is attributable (at least in part) to our limited understanding of the lysogenic conversion dynamics within infected hosts. Here, we used the murine *Salmonella* Typhimurium (*S*. Tm) diarrhoea model to study the transfer of SopEΦ, a prophage from S. Tm SL1344, to S. Tm ATCC14028S. Gut inflammation triggered >60% lysogenic conversion of ATCC14028S within 3 days. Without inflammation, SopEΦ-transfer was reduced by 105-fold. This was traced to the lack of inflammation-, SOS-response- and tum-mediated induction of SopEΦ lytic cycle and established that enteric disease boosts phage-transfer. In keeping, anti-S. Tm-vaccination, prevented not only enteric disease, but also diminished SopEΦ-transfer. Vaccination might be a general strategy for blocking disease-driven bacteriophage-transfer and pathogen evolution.

Introduction

Bacteriophages (phages) encode many prominent virulence factors and are recognized as important facilitators of bacterial pathogen evolution (Brussow *et al.*, 2004). This also holds true for pathogenic enterobacteriaceae, including the more than 200 strains of *Salmonella enterica* subspecies 1 serovar Typhimurium (*S*. Tm). *S*. Tm genomes typically harbour several prophages (Figueroa-Bossi *et al.*, 2001). Phage-transfer (lysogenic conversion) is a key source of genomic diversification between closely related enterobacteriaceae and thought to allow rapid adaptation to new host species, i.e. by re-assorting the virulence factor repertoire (Brussow *et al.*, 2004; Frost *et al.*, 2005). Phage-transfer has been studied extensively *in vitro*. This research has generated a wealth of knowledge about its molecular basis and delivered numerous tools of immense value for contemporary molecular biology. However, there is still a severe lack of information about the factors controlling phage-transfer *in vivo*.

Therefore, we have developed an experimental approach to analyse phage-transfer dynamics *in vivo*. To this end, we studied the transfer of SopEΦ between two well-established *S*. Tm strains (SL1344 and ATCC14028S) which are commonly used in virulence studies (Fig. S1A, B). SopEΦ belongs to the P2 family of temperate phages (Mirold *et al.*, 1999; Pelludat *et al.*, 2003). Its tail-fibre region carries a gene cassette ("moron") encoding SopE, a virulence factor that can enhance host cell invasion by *S*. Tm and exacerbate gut disease pathology (Hardt *et al.*, 1998; Wood *et al.*, 1996). Lysogenic conversion by *sopE*-encoding phages has been observed during epidemic strain evolution (Petrovska *et al.*, 2016) and a SopEΦ lysogen of ATCC14028S elicits stronger enteropathy in the bovine gut than the isogenic parental strain (Zhang *et al.*, 2002). Based on these observations, it has been speculated that phage mediated *sopE*-transfer may promote expansion of epidemic *Salmonella* strains (Ehrbar *et al.*, 2005; Hardt *et al.*, 1998;

Petrovska *et al.*, 2016). However, we do know nothing about the pace of SopEΦ transfer *in vivo* and the ecological factors that could influence the transfer-dynamics.

Results

Efficient lysogenic conversion of *S*.Tm ATCC14028S *in vivo*

To study SopEΦ-transfer dynamics of *in vivo*, SL1344 served as the donor. This strain naturally carries the SopEΦ prophage inserted at the 3'-end of the *ssrA* gene (Pelludat *et al.*, 2003). Specifically, we employed a variant of this strain harbouring a modified version of the prophage encoding a kanamycin resistance cassette (*aphT*) downstream of the *sopE* gene (SL1344 [SopEΦ*aphT*]; Fig. 1A; Fig. S1A; Table 1 strains). This allows quantifying lysogenic conversion by selective plating (Zhang *et al.*, 2002). *S*. Tm ATCC14028S ("14028S" from here on) was chosen as recipient because it does not carry any bacteriophage at the integration site (*attB*) targeted by the integrase of SopEΦ (Fig. 1A; Fig. S1A; (Jarvik *et al.*, 2010)). Moreover, this strain is well known to colonize the gut lumen in the murine *Salmonella* diarrhoea model (Maier *et al.*, 2014a)) which makes it an ideal recipient strain for *in vivo* phage-transfer experiments.

Mice were first infected with 200 CFU of the donor (SL1344 [SopEΦ*aphT*]; kan^R; amp^R; Table 1) and immediately thereafter with 200 CFU of the recipient (14028S; *marT*::*cat*; cm^R, amp^R; Table 1). The sequential inoculation ensured that phage transfer could only occur *in vivo*. Donors and recipients colonized the gut lumen with comparable efficiencies (mean CI$_{donor\ vs\ recipient}$ day 1p.i.= -0.10 +/- 0.13; not significantly different from 0 (t test p=0.475)) (Fig. 1B) and all infected mice developed pronounced intestinal inflammation (Fig. 1C). Phage-transfer (i.e. recipient lysogens; denoted as 14028S [SopEΦ*aphT*]; Fig. 1A) was detected already by 24h p.i. (10^4 to 10^8 CFU/g of faeces; Fig. 1B) and verified by multiplex PCR (Fig S1B, Table 2). The recipient lysogen frequency continued to rise and 14028S [SopEΦ*aphT*] outnumbered the parental recipient in half of the animals by day 3 p.i. (median = 58% of the total 14028S population; Fig. 1B). Equivalent results were obtained in a second mouse strain (129 SvEv; *Nramp1$^+$*) which is resistant to lethal systemic pathogen spread and can therefore be infected for longer periods while maintaining intestinal inflammation (Fig. S1C, D). In all of these mice, 14028S [SopEΦ*aphT*] had completely replaced the recipient population by day 15 p.i. (Fig. S1C). Thus, phage-transfer proceeds independent of the mouse line employed. Moreover, its high efficiency should permit deeper experimental analysis *in vivo*.
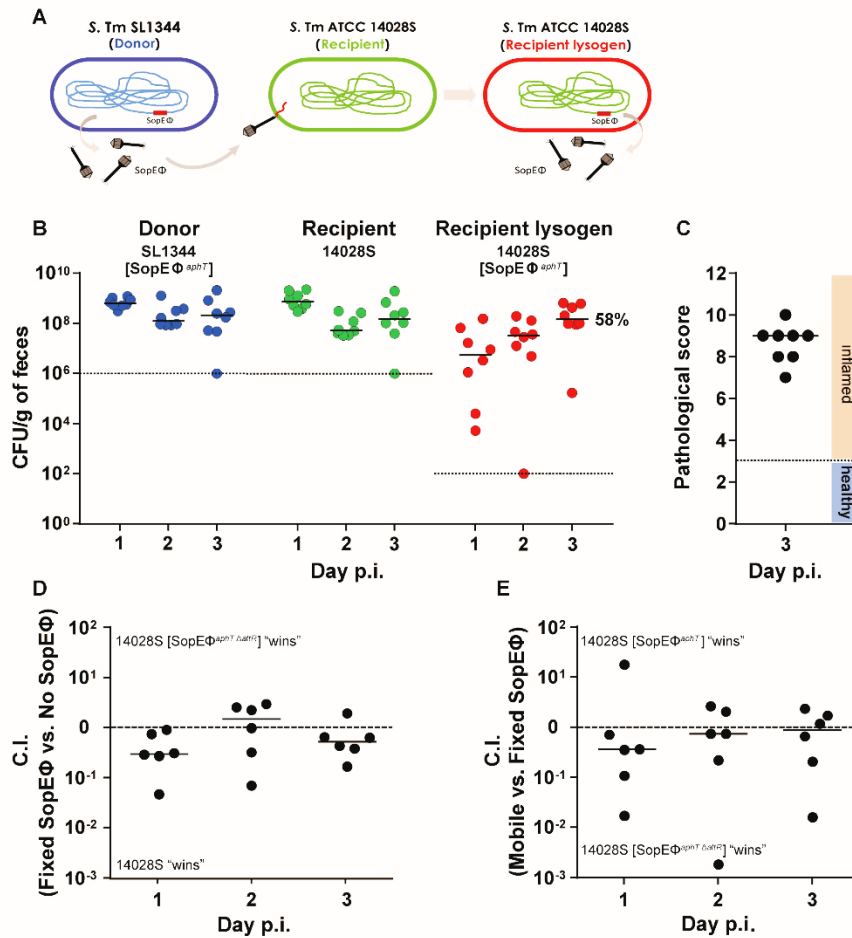
Figure 1 *In vivo*, the bacteriophage SopEΦ is efficiently transferred between two *S*. Tm strains. A. Phage transfer experiment. SopEΦ^{aphT} from the donor strain SL1344 infects the recipient 14028S and yields the recipient lysogen 14028S [SopEΦ^{aphT}] ("lysogenic conversion"). B, *S*. Tm populations as determined by plating of faeces from mice that were sequentially infected with the donor (SL1344 [SopEΦ^{aphT}]; kan^R; amp^R; Table 1) and the recipient (14028S; *marT*::*cat*; cm^R, amp^R; Table 1) Stippled lines: detection limits of the selective plating procedure. 58% of 14028S bacteria were lysogens by day 3 p.i. (median value). C, Gut inflammation at day 3 p.i.. D, Control experiment 1: Competitive infection with a 1:1 mixture of 14028S [SopEΦ^{aphTΔattR}] (kan^R; amp^R) and 14028S (*marT*::*cat*; cm^R, amp^R; Table 1). E, Control experiment 2: Competitive infection with a 1:1 mixture of 14028S [SopEΦ^{aphTΔattR}] and 14028S [SopEΦ^{aphT}] (*marT*::*cat*; cm^R, Kan^R, amp^R). D, E, Stippled lines: Competitive Index null, both strains are equally represented (see also Material and Methods). In all experiments, strains were inoculated by sequential gavage each at about 200 CFU.

Competitive infections assessed if fitness benefits would bias our analysis of the phage-transfer dynamics. First we addressed if 14028S [SopEΦ^{aphT}] might out-compete the ancestral recipient strain 14028S. The prophage was "locked" in the recipient lysogen by deleting the *attR* site (14028S [SopEΦ^{aphTΔattR}]; Fig. S1A), thus prohibiting prophage excision (and thereby any *de novo* phage transfer). In competitive infections, both strains remained at a 1:1 ratio through days 1-3 p.i. (Fig 1D). Equivalent observations were made in competitive infections with 14028S SopEΦ^{aphT} (here, the prophage can be excised) vs. 14028S [SopEΦ^{aphTΔattR}] (locked prophage; resistant to superinfection by SopEΦ^{aphT}) thereby excluding significant effects of

lytic induction on the overall fitness of the lysogen population (Fig 1E). Thus, SopEΦ-transfer does indeed proceed at high rates in the gut without conferring any detectable advantage or fitness cost to its carriers. The system is therefore well suited to identify factors affecting phage-transfer dynamics *in vivo*.

Does the SOS-response control SopEΦ^{aphT} transfer *in vivo*?

Next, we analysed factors controlling the phage-transfer dynamics. Based on established *in vitro* data, we reasoned that "re-activation" (lytic induction) might be of key importance: Temperate phages like SopEΦ are typically lodged in the chromosome where they are replicated along with the bacterial genome. Prophages are however re-activated by stress-induced SOS-response of the host bacterium (at least *in vitro*; (Oppenheim *et al.*, 2005)), excise from the genome, and form new phage particles that can go on to infect new recipient bacteria. Much less is known about lytic induction *in vivo*. However, previous work had established that the mucosal response elicited by *S*. Tm includes massive antimicrobial peptide secretion into the gut lumen, observed that many *S*. TM cells are targeted by these peptides, and discovered that large numbers of *S*. TM cells get killed in the lumen of the inflamed gut (Cullen *et al.*, 2015; Maier *et al.*, 2014b; Miki *et al.*, 2012; Stelter *et al.*, 2011). Thus, we hypothesized that damage inflicted by the host's mucosal immune defence may stimulate *S*.Tm's SOS-response and thereby trigger lytic induction and subsequent transfer of SopEΦ. Based on this hypothesis, we made three testable predictions: a) disrupting the signalling from SOS-response to SopEΦ's lytic induction should diminish phage transfer, b) *S*. Tm mutants failing to elicit gut inflammation should show poor phage-transfer and, c) Interventions preventing enteropathy should prevent phage-transfer. If true, this may point the way towards controlling the rates of pathogen evolution.

To test our first hypothesis, we employed a transcriptional reporter and a SopEΦ-derivative that is "blind" for the bacterial SOS response. The SopEΦ-encoded *tum*-gene was chosen to design the transcriptional reporter. This gene is homologous to the *tum*-genes from related temperate bacteriophages (i.e. coliphage 186 and Fels-2 (Brumby *et al.*, 1996; Bunny *et al.*, 2002; Shearwin *et al.*, 1998)), which encode Tum, a protease linking the bacterial SOS response to the lytic induction of the prophage (Fig. 2A; (Butala *et al.*, 2009)). Indeed, mitomycin C, a well-known inducer of DNA-damage, SOS-response and prophages lytic cycle, enhanced not only SopEΦ-release and phage-transfer (Fig. S2A-B), but also the *gfp*-expression by the *tum*-reporter plasmid *in vitro* (pP*tum*GFP; Fig. S2C, D, E). Infection experiments established that *tum* is also expressed *in vivo* (Fig. 2B, C). Of note, GFP-positive bacteria were only detected if mice were infected with *S*.Tm strains eliciting gut inflammation (i.e. SL1344 [SopEΦ^{aphT}] and 14028S carrying pP*tum*GFP; Fig. 2B, C). No GFP was detected in mice infected

with avirulent *S*. Tm mutants that fail to elicit disease (i.e. Δ*invG* Δ*sseD* derivatives of SL1344 [SopEΦ*aphT*] and 14028S carrying pP*tum*GFP; data not shown). These observations supported that SopEΦ's lytic cycle is induced in response to intestinal inflammation.
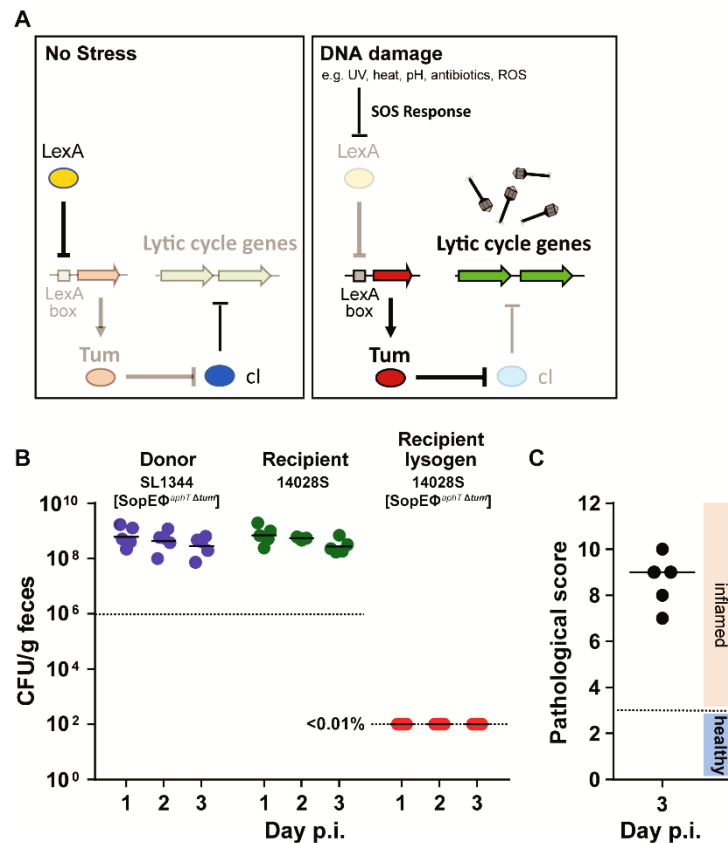

Figure 2. Tum controls phage-transfer *in vivo*. A, Regulation of lytic induction as established *in vitro*. B,C The P*tum* controlled *gfp* expression in the gut contents from mice infected for 24h with SL1344 [SopEΦ*aphT*] pP*tum*GFP (200 CFU by gavage) was analysed by light microscopy. B, left panel: bright field (BF); right panel: GFP; white arrow indicates a filamenting GFP-positive bacterium, black arrow-heads indicate *Salmonella*-shaped bacteria negative for GFP. C, left panel: anti-*S*. Tm LPS antibody staining; middle panel: GFP; right panel: overlay; bars = 10 μm. Arrow indicates the GFP-positive bacterium counter-stained with an anti-LPS antiserum. D, *S*. Tm populations as determined by plating of faeces from mice that were sequentially infected with the donor (SL1344 [SopEΦ*aphTΔtum*]; kan^R; amp^R; Table 1) and the recipient (14028S; *marT*::*cat*; cm^R, amp^R; Table 1); 200 CFU each, by gavage. Less than 0.01% of 14028S bacteria were lysogens by day 3 p.i. (median value). Stippled lines: detection limits of the selective plating procedure. E. Gut inflammation at day 3 p.i.

To assess the relevance of *tum*-induction for the phage-transfer *in vivo*, we constructed a SopEΦ variant that carried a *tum* deletion (SL1344 [SopEΦ*aphTΔtum*]; Fig. S1A, Table 1). In *in vivo* phage-transfer experiments using SL1344 [SopEΦ*aphTΔtum*] as the donor and 14028S as acceptor, both strains colonized the gut, the infection triggered pronounced gut inflammation, but no phage-transfer was detectable in any of the mice tested (Fig. 2D, E). This indicates that the bacterial SOS-response is a central regulator of SopEΦ transfer *in vivo*.

Gut inflammation promotes SopEΦ^{aphT} transfer *in vivo*.

In order to test our second hypothesis about the impact of inflammation on phage-transfer dynamics, we constructed isogenic, avirulent variants of the donor and the recipient strains by disrupting the Type III secretion systems 1 and 2 (T1 and T2) (ΔinvG ΔsseD; SL1344^{avir} [SopEΦ^{aphT}]; 14028S^{avir}; Table 1). Such T1/T2 double-mutants are incapable of triggering inflammation although they can normally colonize the intestinal lumen in our mouse model (Endt *et al.*, 2010; Hapfelmeier *et al.*, 2005; Stecher *et al.*, 2007). Accordingly, when mice were sequentially inoculated with SL1344^{avir} [SopEΦ^{aphT}] as the donor and 14028S^{avir} as the recipient (200 CFU each, by gavage), both strains efficiently colonized the intestinal lumen (Fig. 3A; open blue and open green symbols). However, in sharp contrast to the virulent control strains, the mice did not develop gut inflammation (median pathological score of 1 vs. 9, Fig. 3B; compare open and closed symbols) and yielded much lower numbers of recipient lysogens (14028S^{avir} [SopEΦ^{aphT}]; ≈10^3/g vs. up to 10^9/g of faeces; Fig. 3A, compare open and closed red symbols). This indicated that gut inflammation was an important stimulus of phage-transfer.

To substantiate this, we tested if re-establishing gut inflammation would suffice to rescue phage-transfer from (or into) the avirulent strains. This was done by replacing either the donor or the recipient with the original virulent strain. Indeed, the sequential infection with either the avirulent donor (SL1344^{avir} [SopEΦ^{aphT}]) plus the virulent recipient (14028S) or the virulent donor (SL1344 [SopEΦ^{aphT}]) plus the avirulent recipient (14028S^{avir}) elicited not only pronounced gut inflammation but also allowed for efficient phage-transfer (up to 10^9/g recipient lysogens (14028S [SopEΦ^{aphT}] or 14028S^{avir} [SopEΦ^{aphT}]); Fig. S3A, B). These data verified that intestinal inflammation was required for efficient phage-transfer.

Vaccination prevents SopEΦ-transfer *in vivo*

Finally, we addressed if interventions preventing disease would reduce SopEΦ-transfer *in vivo*. To test this hypothesis, we employed a recent vaccination protocol that can prevent intestinal inflammation even in the face of high gut luminal *S.* Tm loads (Moor *et al.*, 2016). The vaccination protocol consists in three oral gavages with peracetic acid-killed *S.* Tm (see Materials and Methods). Immunization induces production of Immunoglobulin-A (IgA) directed against the O-side chain of *Salmonella* LPS. It protects vaccinated mice from disease in challenge infections with virulent strains of *S.* Tm but still allows gut luminal pathogen growth at densities of 10^9 CFU/g stool (Moor *et al.*, 2016). This protocol should therefore provide an ideal assay system for asking if vaccination can limit the inflammation-dependent phage-transfer.
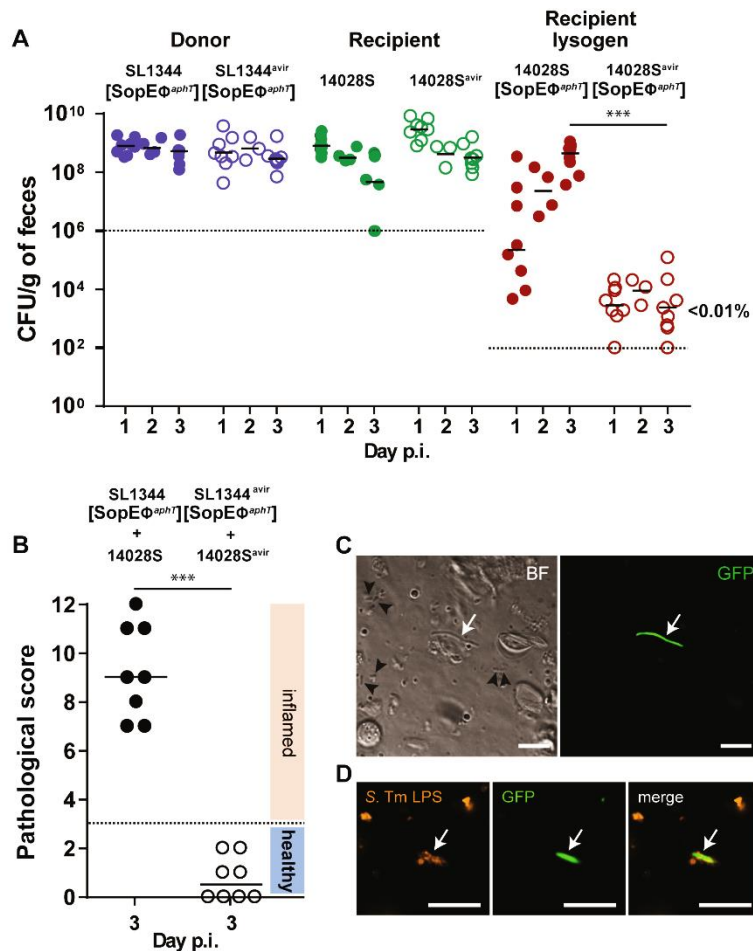
Figure 3. Phage transfer is reduced in the absence of intestinal inflammation. A, *S.* Tm populations as determined by plating of faeces from mice that were sequentially infected with the avirulent donor (open blue symbols; SL1344^{avir} [SopEΦ^{aphT}]; kan^R; amp^R; Table 1) and the avirulent recipient (open green symbols; 14028S^{avir}; *marT*::*cat*; cm^R, amp^R) or (as control) with the virulent donor (closed blue symbols; SL1344 [SopEΦ^{aphT}]; kan^R; amp^R; Table 1) and the virulent recipient (closed green symbols; 14028S; *marT*::*cat*; cm^R, amp^R; Table 1; 200 CFU each, by gavage). Red symbols: faecal loads of recipient lysogens (open symbols: 14028S^{avir} [SopEΦ^{aphT}]; closed symbols: 14028S [SopEΦ^{aphT}]). Less than 0.01% of 14028S bacteria were lysogens by day 3 p.i. (median value). Stippled lines: detection limits of the selective plating procedure. B. Gut inflammation at day 3 p.i.. ***: Mann Whitney U-test p<0.001.

Vaccinated mice or mock-vaccinated "naïve" controls were sequentially infected with the donor (SL1344 [SopEΦ^{aphT}]; Table 1) and the recipient (14028S *marT*::*cat* Table 1; 200 CFU each, by gavage). Both strains efficiently colonized the intestinal lumen of naïve and of vaccinated mice (Fig. 4A; closed and open, blue and green symbols). In sharp contrast to the naïve controls, the vaccinated mice were not only protected from disease for up to 3 days (Fig. 4B), but also yielded much lower numbers of recipient lysogens (14028S [SopEΦ^{aphT}]; Fig. 4A, compare closed vs. open red symbols). In fact, in half of the mice, recipient lysogens remained below the detection limit throughout the entire experiment. This was in line with our hypothesis and indicated that vaccination can dramatically reduce phage-transfer. It is

interesting to note that half of the vaccinated mice developed some degree of mucosal inflammation by day 3 p.i. and that these mice also yielded recipient lysogens (Fig. 4A, B; marked in grey). This supported that the gut inflammation controls the phage-transfer kinetics.

In conclusion, these data establish that the enteric disease elicited in the host's intestine is an important stimulus of phage transfer and that vaccination provides an efficient means to interfere with this process.
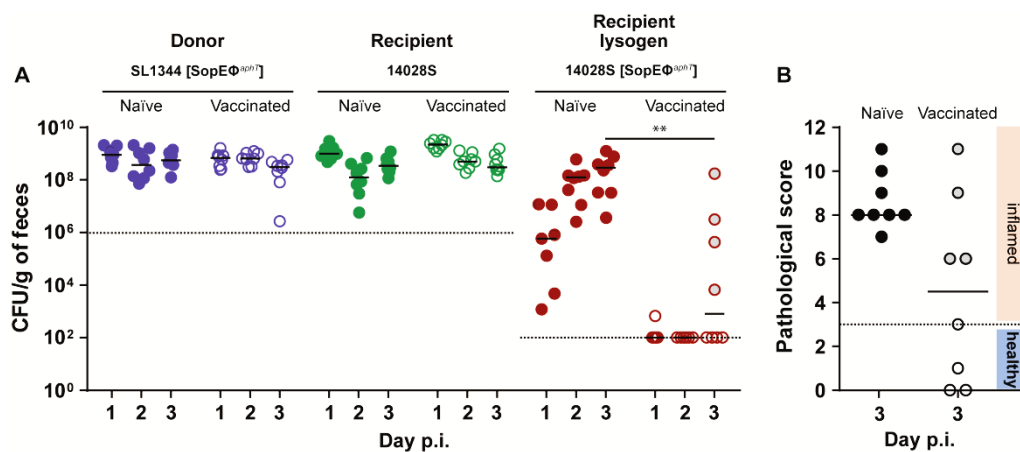

Figure 4. Vaccination prevents gut inflammation and phage-transfer. For vaccination, mice were treated four weeks before infection with gavages of peracetic acid-killed *S*. Tm while naïve mice received PBS (Material and Methods). A, *S*. Tm populations as determined by plating of faeces from naïve (closed symbols) and vaccinated (open symbols) mice that were sequentially infected with the donor (SL1344 [SopEΦ^{aphT}]; kan^R; amp^R; Table 1) and the recipient (14028S; *marT*::*cat*; cm^R, amp^R, Table 1, 200 CFU each, by gavage). Stippled lines: detection limits of the selective plating procedure. B, Gut inflammation at day 3 p.i. Open symbols highlighted with light grey: four vaccinated mice that featured detectable densities of recipient lysogens and some degree of mucosal inflammation. **: Mann Whitney test p<0.005.

Conclusion and Discussion

The factors controlling phage-transfer *in vivo* had remained poorly understood. Our analysis of SopEΦ establishes that this process can be highly efficient in the host's gut. This was attributable to *tum*, a phage-encoded regulator linking the lytic induction to the bacterial SOS response which is elicited by gut inflammation. The mechanism is novel and clearly distinct from inflammation-boosted rates of plasmid-transfer (see supplement, Fig. S5). Importantly, this requirement for inflammation explains why vaccination (i.e. the pathogen's failure to cause enteropathy in the gut of a vaccinated host) prohibits phage transfer and thereby slows down pathogen evolution.

Thus, from the pathogen's perspective, the elicitation of gut inflammation has (at least) two different beneficial effects. First, *S*. Tm growth is favoured by the environmental conditions provided by the inflamed gut, i.e. the availability of terminal electron acceptors, energy-rich carbon sources, iron and zinc (Santos *et al.*, 2009; Stecher *et al.*, 2007; Winter *et al.*, 2010). As shown here, the inflammation also stimulates phage-transfer. This accelerates the re-assortment of the pathogen's virulence factor repertoire, which might increase the chance for successful interactions with new hosts. Thus, enteric disease could be regarded as a driver of *Salmonella enterica* evolution.

Boosting of phage transfer in the inflamed host intestine may be of broad relevance for enter pathogenic bacteria. This seems plausible, as the regulatory circuits controlling the lytic induction of temperate phages are generally linked to the bacterium's SOS-response. Furthermore, the innate mucosal immune response to enteropathogen infection includes the release of large amounts of bacteriotoxic compounds, including high concentrations of antimicrobial proteins and reactive oxygen species (Duerkop *et al.*, 2009; Maier *et al.*, 2014b). This should stimulate the microbial SOS response. It is tempting to speculate that the disease-accelerated phage transfer may explain why enter pathogenic bacteria do harbour so many prophages, including *Salmonella* spp., *Vibrio cholerae* (Waldor *et al.*, 1996), or Shiga-toxin-producing *E. coli* strains (Schmidt, 2001). It would be interesting to determine if such disease-driven spread of temperate phages might also affect the microbiota (e.g. by accelerating the emergence of strains with increased virulence) in patients suffering from inflammatory bowel diseases.

In conclusion, phage-transfer is a dynamic process occurring in *vivo* with variable frequencies. The host's immune response was identified as a key factor determining its pace. Strikingly, the innate and the adaptive immune response of the infected host do have opposing effects. While gut inflammation (elicited by the innate response of the naïve host) boosts phage-transfer, adaptive immunity slows it down. This is an unexpected advantage of vaccination over antibiotic therapy which is known to stimulate phage-transfer and generalized transduction (Bearson *et al.*, 2015). This important beneficial aspect should receive particular attention in future vaccination trials.

Materials and Methods

S. Tm strains and plasmids used in this study. All strains are listed in table 1. Donor and recipient strains derived respectively from SL1344 (Hoiseth *et al.*, 1981) and ATCC 14028S (Jarvik *et al.*, 2010).

The pM975 (Hapfelmeier *et al.*, 2005) plasmid conferred resistance to ampicillin to all strains used in this study. Targeted deletions were performed using the lambda Red-recombinase method as described in (Datsenko *et al.*, 2000) with primers indicated in Table 2 ("Del" primers were used for generation of recombinogenic fragments and "Ver" primers or Right_up/ attBF for PCR verification of the *tum* deletion or of the attR deletion, respectively (Fig. S1)).

Deletions of *tum* and attR were transferred after constructions in the appropriate genetic background by P22 HT105/1 *int-201* mediated transductions as described in (Sternberg *et al.*, 1991).

The *pPtum::GFP* plasmid was constructed by integrating the promoter region of *tum* in front of *gfp* in pM965 (Stecher *et al.*, 2004) in replacement of P*rpsM*. The restriction sites BamH1 and XbaI were used to cut open pM965, excise P*rpsM* and to clone PCR amplified copies of P*tum* (primers P*tum*SopEphi_up/P*tum*SopEphi_dw). A promoter-less plasmid derivative of pM965 was constructed by treating the BamH1 / XbaI digested plasmid with Klenow fragment before ligation without insert.

When specified, antibiotics were added in liquid cultures or agar plates (chloramphenicol 10 µg/ml, kanamycin 50 µg/ml, ampicillin 100 µg/ml) (AppliChem).

Table 1. Strains and Plasmids

Strain name	Relevant genotype info.	Resistance	Reference
14028S	*marT::cat* (or *lpfED::aphT*)*	Cm or Kan	This work, (Diard *et al.*, 2014)
SL1344[avir]	Δ*invG* Δ*sseD*		(Maier *et al.*, 2013)
14028S[avir]	Δ*invG* Δ*sseD* *marT::cat* (or *lpfED::aphT*)*	Cm or Kan	This work, (Diard *et al.*, 2014)
SL1344 [SopEΦ[aphT]]		Kan	This work
SL1344[avir] [SopEΦ[aphT]]	Δ*invG* Δ*sseD*	Kan	This work
SL1344 [SopEΦ[aphTΔtum]]	Δ*tum*	Kan	This work
14028S [SopEΦ[aphT]] (M30)		Kan	(Zhang *et al.*, 2002)
14028S [SopEΦ[aphTΔattR]]	Δ*attR*	Kan	This work
Plasmid name			

141

		Cm	(Stecher *et al.*, 2012)
pCol1B9*cat*	*cat*		
pM975	*bla*	Amp	(Hapfelmeier *et al.*, 2005)
pM965	*bla*	Amp	(Stecher *et al.*, 2004)
pP*tum*GFP	*bla*	Amp	This work
pNoPGFP	*bla*	Amp	This work

* Resistance cassette used in plasmid transfer experiments.

Table 2. Primers

Primer name	Sequence
36R	GGATCAAGAGAGGTCAAAC
Left_dw	TCCCTGCAGCTCGCTG
attBF	GTGCTACGGGGCTTCG
Right_up	GGGATATCTTAGACCAATTAG
Right_dw	AGTCCCATCATAGTCCGC
Del_attR_up	AGGAGATAGTGAGCGTTTATCAACTGACAGATTTTTACAAGCTAGTGTGTAGGCTGGAGCTGCTTC
Del_attR_dw	CTCATTGAAGTTACAGGCTTTTTTAAGGTTCATGATGCATCATGACATATGAATATCCTCCTTAG
Del_*tum*_up	GCAACGTTCCTTAGTGCAGCCAGCTGTCGTCCTCCCAGACTGTGTAGGCTGGAGCTGCTTC
Del_*tum*_dw	AGGAGGGAAGATGCAGGACTATCTTTTGGAGTCGTTGAAGCATATGAATATCCTCCTTAG
Ver_*tum*_up2	CACTAAAGCCTCGCCTTG
Ver_*tum*_dw2	GTCAGGGCTATCTAATTGAC
P*tum*SopEphi_up	CCATTCTCTAGATAAGCAATGCGGAAGTGGA
P*tum*SopEphi_dw	TATGCAGGATCCCTTCCCTCCTTTCACTGC
2772_4_up	GATGAGCTGCAGAAGGTTGA
2772_118_dw	CGCTGCATCCTGATATTCTG
oriT_nikA	AGTTCCTCATCGGTCATGTC
oriT_nikA_rev	GAAGCCATTGGCACTTTCTC
attleft_up	AGACTGACTAAGCATGTAGTAC
attleft_dw	GGCTACGTTTTCACGTAACC

Infection experiments. All mice were kept under specified pathogen free barrier conditions in individually ventilated cages at the RCHCI facility of ETH Zürich. The experiments were reviewed and approved by the responsible legal body (Tierversuchskommission, Kantonales Veterinäramt Zürich, license 222/2013). 8 to 12 weeks old 129 SvEv mice (naturally *nramp+*, thus surviving long term *S*. Tm infection) or sensitive C57BL/6 mice were pretreated with 20

mg ampicillin *per os* 24h before inoculation to alleviate the colonization resistance. Bacteria were grown in LB supplemented with the appropriate antibiotic for 12h at 37°C and cultured to late-log phase for 4h in the same medium without antibiotic (these conditions induce expression of T1). Approximately 200 bacteria from a given strain, washed and diluted in PBS, were inoculated by gavage. Population sizes of *Salmonella* were monitored by plating serial dilutions of fresh faeces on McConkey agar plates (Difco) supplemented with appropriate antibiotics. The competitive index (C.I.) was calculated as the Log10 of the ratio of competitors population sizes at a particular time point corrected by the initial ratio in the inoculum.

Fluorescence microscopy. Live confocal fluorescence microscopy was employed to analyse P*tum*::*gfp* expression by the indicated strains. *S.* Tm cultures grown for 12h in LB +/- Mitomycin C (0.25 µg/ml), or fresh cecal content from infected mice, were serially diluted in phosphate-buffered saline. Samples of suitable density were transferred to glass slides and imaged on a Zeiss Axiovert 200m microscope equipped with a 100X oil objective, a spinning disc confocal unit (Visitron), and dual Evolve512 EMCCD cameras (Photometrics). *S.* Tm LPS was immunodetected using rabbit-anti-*S.*Tm LPS O-antigen group B (Difco) and Cy3-coupled goat-anti-rabbit-IgG (Jackson Laboratories). Images were adjusted for brightness and contrast post-capture with the Visiview software (Visitron). GFP channel images presented side-by-side were generated using identical laser settings, exposure times, and post-capture processing. Bright field images were corrected for illumination unevenness by subtraction of an empty sample image.

Oral Vaccination. An inactivated oral *S.* Tm vaccine ("PA.STm") was generated as described in (Moor *et al.*, 2016). Briefly, late stationary-phase *S.* Tm cultured aerobically in LB were concentrated to 10^9 CFU/ml in PBS, then peracetic acid (433241, Sigma-Aldrich) was added to 0.4% v/v and the suspension was incubated for 1h at room temperature. The inactivated bacteria were extensively washed with sterile PBS to remove any traces of the acid and finally resuspended at a density of 10^{11} particles per ml in sterile PBS. Each vaccine batch was tested by enrichment culture for complete inactivation and the vaccines was stored at 4°C for up to three weeks. Mice received 100µl of vaccine per os, once per week for three weeks.

In vitro phage transfer experiments. Donors (SL1344 [SopEΦ^{aphT}]; kan^R; amp^R) and recipients 14028S (*marT*::*cat*, Cm^R, Amp^R) were cultivated overnight at 37°C in LB supplemented by the appropriate antibiotics then sub-cultivated in LB for 4 hours after 1/20 dilution. Cells were then washed in PBS and diluted 10^5 times before inoculation (about 200 CFU of each strains)

in LB 100 μg/ml ampicillin supplemented if specified with 0.25 μg/ml Mitomycin C. Cells were incubated overnight at 37°C with mixing, diluted and plated on selective McConkey agar plates.

Bacteriophages isolation and quantification. Samples from *in vitro* phage transfer experiments were harvested and centrifuged 3 minutes at 8500 g. The supernatants were filtered on Spin-X 0.45μm centrifuge tube filters (Costar) and supplemented with 10% PEG 8000 and NaCl 1M (Sigma). After incubation overnight on ice, free bacteriophage particles were then harvested by centrifugation (20.000 g for 1h at 4°C) and re-suspended in 100 μl of the DNase I buffer (Roche). Samples were treated by 10 U of DNase I (Roche) for 1h at 37°C and the enzyme was inactivated by incubation at 95°C for 30 minutes.

The relative amount of free SopEΦ^{aphT} DNA obtained in presence or in absence of Mitomycin C was evaluated by qrtPCR using the specific primers pair 2772_4_up/2772_118_dw (Table 2) on treated samples diluted 10 times. A control qrtPCR for chromosomal DNA was performed using primers attleft_up/attleft_dw. Standard curves made from serial dilutions of purified PCR products generated with primers 2772_4_up/2772_118_dw or attleft_up/attleft_dw (Table 2), using SL1344 [SopEΦ^{aphT}] DNA as template, served to calculate the number of copies in the samples. The qrtPCR was performed with the FastStart Universal SYBR Green Master kit (Roche) in the Rotor-gene RG3000 thermocycler (Corbett Research).

Statistical analysis. Statistical tests were performed using GraphPad Prism version 5.00 for Windows (http://www.graphpad.com).
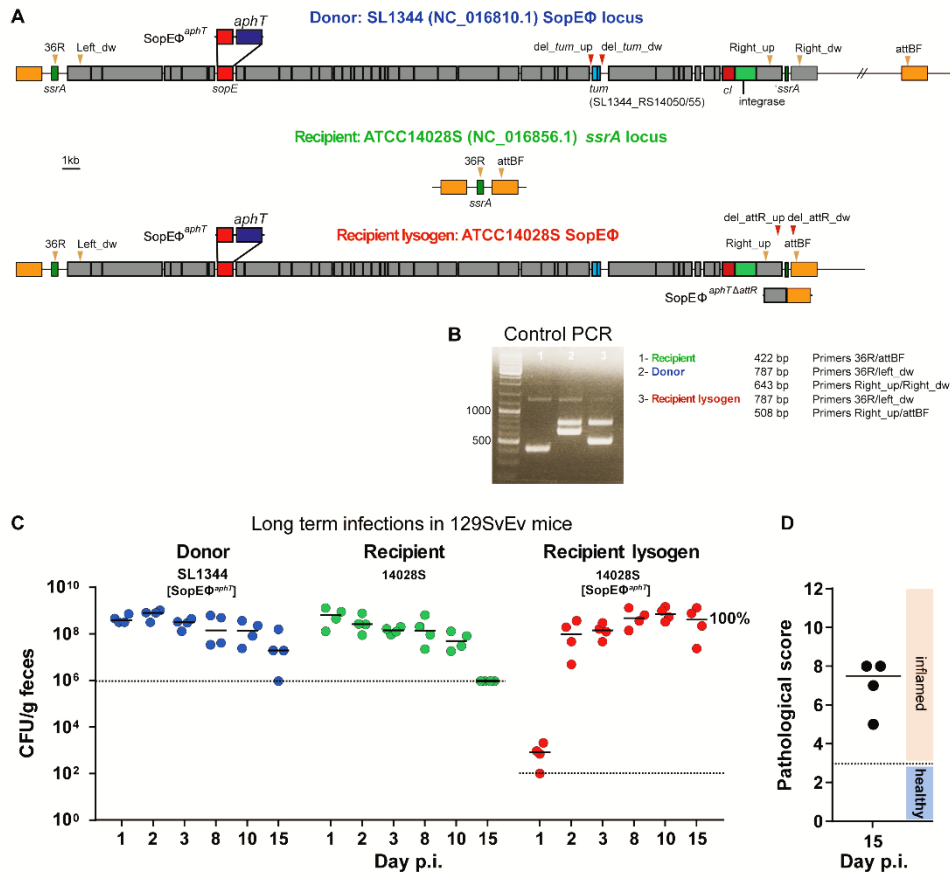
144

Supplementary Figures

Figure S1. Genetic maps, multiplex control PCR and long term *in vivo* phage transfer. A. Maps of the SopEΦ prophage in the *ssrA* locus of SL1344 (i.e., Donor), its derivative SopEΦ*aphT*, of the "empty" *ssrA* locus in 14028S (i.e., Recipient) and of the SopEΦ*aphT* prophage in the *ssrA* locus of 14028S (i.e., Recipient lysogen). Yellow and red arrowheads respectively mark the position of primers used for verification and for the construction of prophage-variants. B, Multiplex PCR assay for verifying the insertion of SopEΦ*aphT* in *S*. Tm SL1344 and in recipient lysogens (for primer binding sites and sequences, see panel A and Table 2. C, *S*. Tm populations as determined by plating of faeces from 129 SvEv mice that were sequentially infected with the donor (SL1344 [SopEΦ*aphT*]; kan[R]; amp[R]; Table 1) and the recipient (14028S; *marT*::*cat*; cm[R], amp[R]; Table 1; 200 CFU each, by gavage). 100% of 14028S bacteria were lysogens by day 15 p.i. (median value). Stippled lines: detection limits of the selective plating procedure. D, Gut inflammation at day 15 p.i.
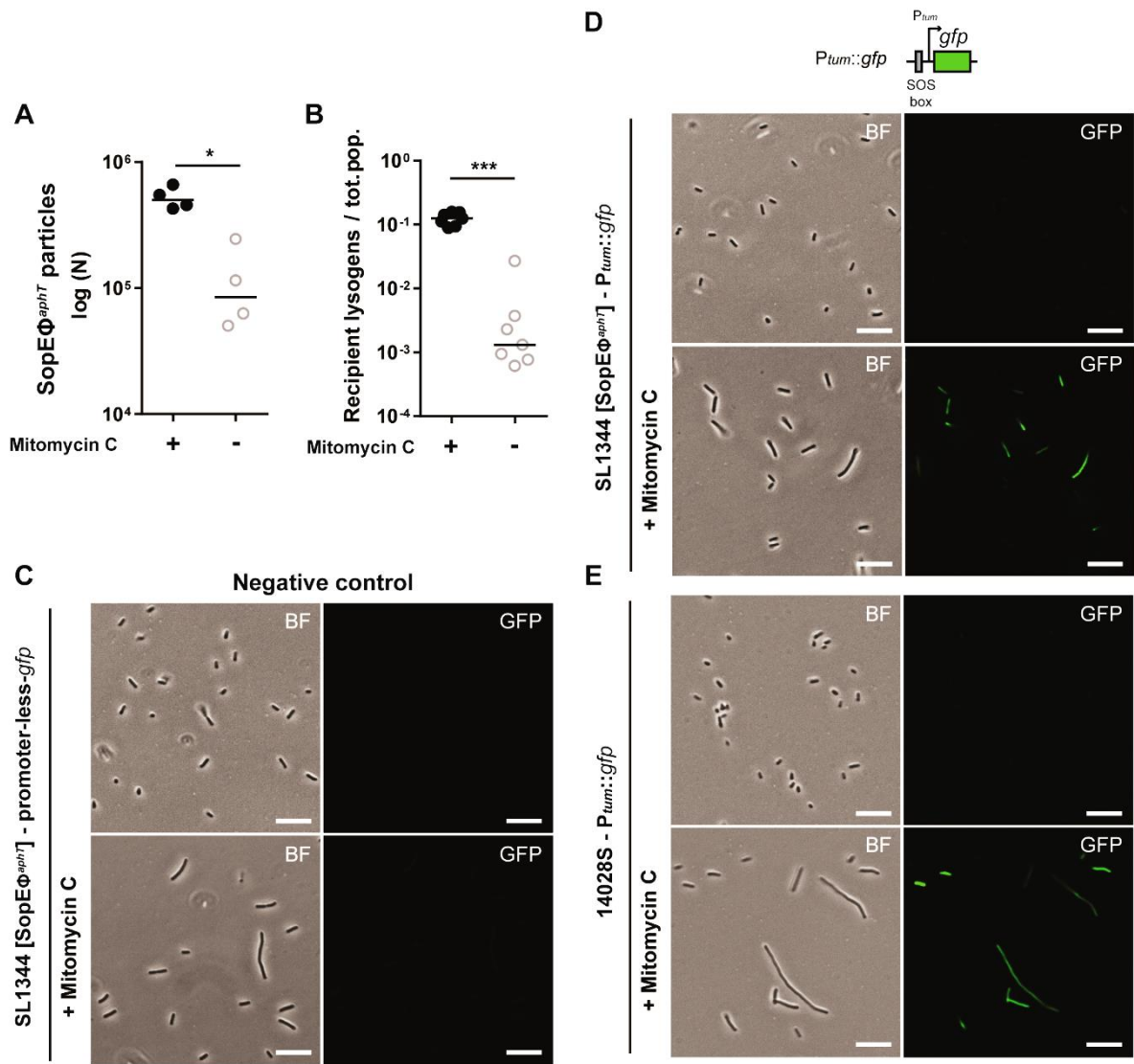
Figure S2. *In vitro* verification of SOS-mediated prophage induction and pP*tum*GFP expression. A, Mitomycin C induces the SopEΦ*aphT* lytic cycle. The donor strain SL1344 [SopEΦ*aphT*] was grown *in vitro* in LB overnight in the presence or absence of 0.25 μg/ml Mitomycin C. Phage particles were purified from the culture supernatants and the relative numbers of free SopEΦ particles was determined by qrtPCR (see Material and Methods). B, *In vitro* SopEΦ*aphT*-transfer experiment testing the effect of Mitomycin C. *S*. Tm populations as determined by plating of LB broth that had been inoculated with the donor (SL1344 [SopEΦ*aphT*]; kan[R]; amp[R]; Table 1) and the recipient (14028S; *marT*::*cat*; cm[R], amp[R]; Table 1; 200 CFU each) and incubated for 24h in the presence (filled symbols) or absence (open symbols) of 0.25 μg/ml Mitomycin C. Mitomycin C significantly increased the yield of recipient lysogens. Mann Whitney U-test * p<0.05; ***p<0.001. C, D, Mitomycin C induces *in vitro* the expression of GFP under the control of the *tum* promoter. LB cultures were inoculated with 200 CFU of SL1344 [SopEΦ*aphT*] carrying either a promoter-less *gfp* control plasmid (C) or pP*tum*GFP (D) in the presence or absence of 0.25 μg/ml Mitomycin C and analysed by light microscopy. Left panels: bright field (BF); right panels: GFP fluorescence; bar = 10 μm. E, *tum* is induced by the SOS response independent of other SopEΦ encoded genes. To obtain further evidence of the direct SOS-mediated control of *tum* expression, the recipient strain (14028S; *marT*::*cat*) carrying pP*tum*GFP was grown *in vitro* in the presence or absence of 0.25 μg/ml Mitomycin C and analysed by light microscopy. Left panels: bright field (BF); right panels: GFP fluorescence; bar = 10 μm. The P*tum*::*gfp* construction is depicted on panel D.
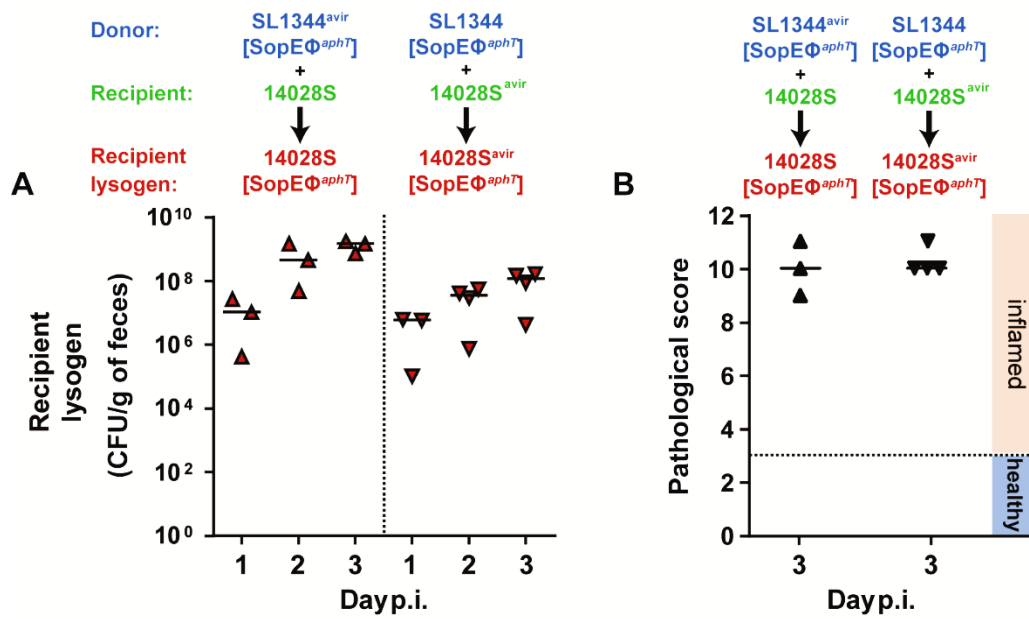
Figure S3. Co-infection with virulent strains restores SopEΦ^{aphT} phage transfer dynamics. A, Recipient lysogen populations (triangles: 14028S [SopEΦ^{aphT}]; inverted triangles: 14028S^{avir} [SopEΦ^{aphT}]) as determined by plating of faeces from mice that were sequentially infected by gavage with either the avirulent donor (SL1344^{avir} [SopEΦ^{aphT}]; 200 CFU, kan^R; amp^R; Table 1) and the virulent recipient (14028S; 200 CFU, *marT*::*cat*; cm^R, amp^R) or with the virulent donor (SL1344 [SopEΦ^{aphT}]; 200 CFU, kan^R; amp^R; Table 1) and the avirulent recipient (14028S^{avir}; 2000 CFU, *marT*::*cat*; cm^R, amp^R; Table 1). Note that the fitness of the avirulent recipient was reduced in the inflamed intestine, in presence of the virulent donor. This had to be compensated by adding 10 times more avirulent recipients than virulent donors in the inoculum in order to reach a 1:1 donor:recipient ratio at 24h p.i. and to restore fully efficient lysogenic conversion. B. Gut inflammation at day 3 p.i.
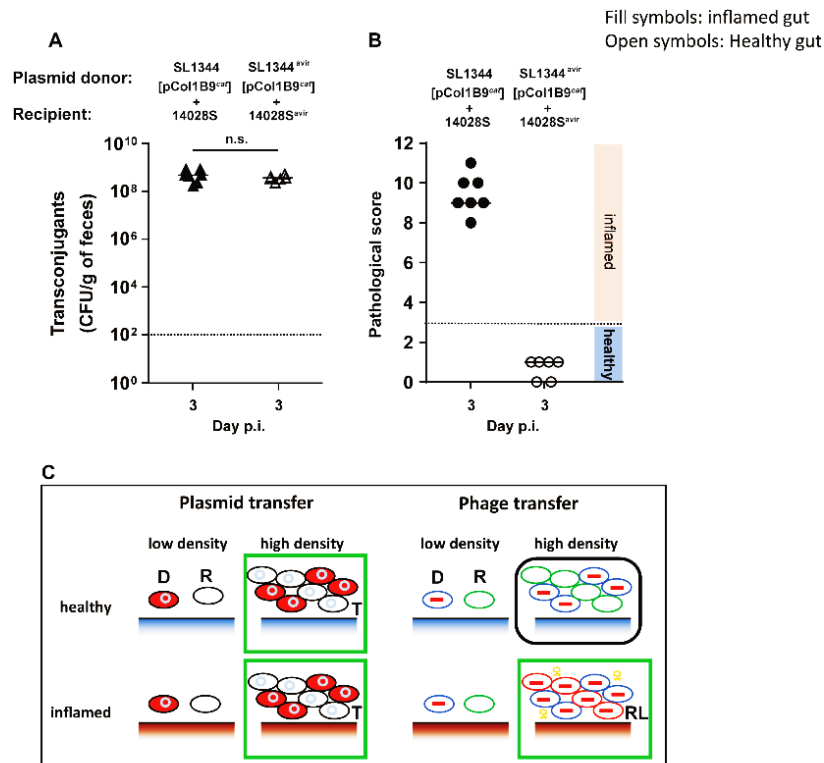
Figure S4. Plasmid-transfer has a different disease-requirement than phage-transfer. Our donor strain (*S*. Tm SL1344) harbours both, the prophage SopEΦ and pCol1B9 (Hoiseth *et al.*, 1981) while the recipient strain (14028S) harbours neither SopEΦ, nor pCol1B9 (Jarvik *et al.*, 2010). This was verified by PCR (primers oriT_nikA and oriT_nikA_rev for pCol1B9, see Table 2). We performed infection assays to analyse the effects of gut inflammation and of vaccination on plasmid-transfer. In these experiments, we used as donor SL1344 (or SL1344^{avir}) carrying pCol1B9^{cat}, an isogenic derivative of pCol1B9 conferring resistance to chloramphenicol (Stecher *et al.*, 2012)). As recipient, we used 14028S (*lpfED*::*aphT*, Kan^R, Amp^R) or its avirulent derivative 14028S^{avir} (Δ*invG* Δ*sseD lpfED*::*aphT*, Kan^R, Amp^R) (Table 1). A, To analyse the effect of gut inflammation, mice were infected with virulent (closed symbols; SL1344 pCol1B9^{cat} and 14028S) or avirulent (open symbols; SL1344^{avir} pCol1B9^{cat} and 14028S^{avir}) pairs of donor and recipient (200 CFU each; by gavage). Transconjugant formation (i.e. 14028S pCol1B9^{cat} or 14028S^{avir} pCol1B9^{cat} respectively) was analysed by plating faeces at day 3 p.i.. B, Gut inflammation at day 3 p.i. C, To analyse the effect of vaccination, mice were vaccinated for 4 weeks (open symbols) or mock-vaccinated with PBS (closed symbols) as described in Fig. 4. Then, the mice were infected with SL1344 pCol1B9^{cat} and 14028S (200 CFU each; by gavage). Transconjugant formation (i.e. 14028S pCol1B9^{cat}) was analysed by plating faeces at day 3 p.i.. D, Gut inflammation at day 3 p.i. These data verify that plasmid-transfer occurs with high efficiency even in the absence of gut inflammation. This differs strikingly from the phage-transfer data (compare to Fig. 3A and Fig. 4A). Stippled lines in A and C: detection limits of the selective plating procedure. n.s. = not significant as analysed by the Mann Whitney U-test p>0.05. E. Schematic depicting key differences between phage- and plasmid transfer. Plasmids and temperate phages are main vehicles of horizontal gene transfer in enterobacteriaceae. Interestingly, the *in vivo* phage-transfer differs in important aspects from the plasmid-transfer described in earlier work: For plasmid-transfer (i.e. pCol1B9 from *S*. Tm SL1344 to commensal *E. coli* (Stecher *et al.*, 2012)) high donor- and acceptor densities are necessary <u>and</u> sufficient. Thus, at high donor- and acceptor densities it does not matter if gut inflammation is present or not (for experimental data, see Fig. S5A-B). This is in striking contrast to the phage-transfer dynamics discovered in the current paper. For phage-transfer, high donor- and recipient densities are necessary, but <u>not</u> sufficient. In the absence of inflammation, phage-transfer does not occur even if high donor and recipient densities have been reached. This is explained by the mechanistic link of lytic induction (via *tum*) to the stress-induced SOS response (Fig. 2). Thus, phage transfer requires high donor densities, high acceptor densities <u>and</u> mucosal disease. This has important consequences. Vaccines that protect from disease (without reducing gut luminal colonization levels) prevent phage- (Fig. 4), but not plasmid transfer (Fig. S5C, D). Key: D: Donor, R: Recipient, T: Transconjugant, RL: Recipient Lysogen. Green box: efficient transfer, black box: inefficient transfer.

References

Bearson, B. L., & Brunelle, B. W. (2015). Fluoroquinolone induction of phage-mediated gene transfer in multidrug-resistant *Salmonella*. *Int. J. Antimicrob. Agents, 46*(2), 201-204.

Brumby, A. M., Lamont, I., Dodd, I. B., & Egan, J. B. (1996). Defining the SOS operon of coliphage 186. *Virology, 219*(1), 105-114.

Brussow, H., Canchaya, C., & Hardt, W. D. (2004). Phages and the evolution of bacterial pathogens: from genomic rearrangements to lysogenic conversion. *Microbiol Mol. Biol. Rev., 68*(3), 560-602.

Bunny, K., Liu, J., & Roth, J. (2002). Phenotypes of *lexA* mutations in *Salmonella enterica*: evidence for a lethal lexA null phenotype due to the Fels-2 prophage. *J. Bacteriol., 184*(22), 6235-6249.

Butala, M., Zgur-Bertok, D., & Busby, S. J. (2009). The bacterial LexA transcriptional repressor. *Cell. Mol. Life Sci., 66*(1), 82-93.

Cullen, T. W., Schofield, W. B., Barry, N. A., Putnam, E. E., Rundell, E. A., Trent, M. S., Degnan, P. H., Booth, C. J., Yu, H., & Goodman, A. L. (2015). Gut microbiota. Antimicrobial peptide resistance mediates resilience of prominent gut commensals during inflammation. *Science, 347*(6218), 170-175.

Datsenko, K. A., & Wanner, B. L. (2000). One-step inactivation of chromosomal genes in *Escherichia coli* K-12 using PCR products. *Proc. Natl. Acad. Sci. U S A, 97*(12), 6640-6645.

Diard, M., Sellin, M. E., Dolowschiak, T., Arnoldini, M., Ackermann, M., & Hardt, W. D. (2014). Antibiotic treatment selects for cooperative virulence of *salmonella* typhimurium. *Curr. Biol., 24*(17), 2000-2005.

Duerkop, B. A., Vaishnava, S., & Hooper, L. V. (2009). Immune responses to the microbiota at the intestinal mucosal surface. *Immunity, 31*(3), 368-376.

Ehrbar, K., & Hardt, W. D. (2005). Bacteriophage-encoded type III effectors in *Salmonella* enterica subspecies 1 serovar Typhimurium. *Infect. Genet. Evol., 5*(1), 1-9.

Endt, K., Stecher, B., Chaffron, S., Slack, E., Tchitchek, N., Benecke, A., Van Maele, L., Sirard, J. C., Mueller, A. J., Heikenwalder, M., Macpherson, A. J., Strugnell, R., von Mering, C., & Hardt, W. D. (2010). The microbiota mediates pathogen clearance from the gut lumen after non-typhoidal *Salmonella* diarrhea. *PLoS Pathog., 6*(9), e1001097.

Figueroa-Bossi, N., Uzzau, S., Maloriol, D., & Bossi, L. (2001). Variable assortment of prophages provides a transferable repertoire of pathogenic determinants in *Salmonella*. *Mol. Microbiol., 39*(2), 260-271.

Frost, L. S., Leplae, R., Summers, A. O., & Toussaint, A. (2005). Mobile genetic elements: the agents of open source evolution. *Nat. Rev. Microbiol., 3*(9), 722-732.

Hapfelmeier, S., Stecher, B., Barthel, M., Kremer, M., Muller, A. J., Heikenwalder, M., Stallmach, T., Hensel, M., Pfeffer, K., Akira, S., & Hardt, W. D. (2005). The Salmonella pathogenicity island (SPI)-2 and SPI-1 type III secretion systems allow Salmonella serovar typhimurium to trigger colitis via MyD88-dependent and MyD88-independent mechanisms. *J Immunol, 174*(3), 1675-1685.

Hardt, W. D., Chen, L. M., Schuebel, K. E., Bustelo, X. R., & Galan, J. E. (1998). S. typhimurium encodes an activator of Rho GTPases that induces membrane ruffling and nuclear responses in host cells. *Cell, 93*(5), 815-826.

Hoiseth, S. K., & Stocker, B. A. (1981). Aromatic-dependent Salmonella typhimurium are non-virulent and effective as live vaccines. *Nature, 291*(5812), 238-239.

Jarvik, T., Smillie, C., Groisman, E. A., & Ochman, H. (2010). Short-term signatures of evolutionary change in the *Salmonella enterica* serovar typhimurium 14028 genome. *J. Bacteriol., 192*(2), 560-567.

Maier, L., Barthel, M., Stecher, B., Maier, R. J., Gunn, J. S., & Hardt, W. D. (2014a). *Salmonella* Typhimurium strain ATCC14028 requires H2-hydrogenases for growth in the gut, but not at systemic sites. *PLoS One, 9*(10), e110187.

Maier, L., Diard, M., Sellin, M. E., Chouffane, E. S., Trautwein-Weidner, K., Periaswamy, B., Slack, E., Dolowschiak, T., Stecher, B., Loverdo, C., Regoes, R. R., & Hardt, W. D. (2014b). Granulocytes Impose a Tight Bottleneck upon the Gut Luminal Pathogen Population during *Salmonella* Typhimurium Colitis. *PLoS Pathog., 10*(12), e1004557.

Maier, L., Vyas, R., Cordova, C. D., Lindsay, H., Schmidt, T. S., Brugiroux, S., Periaswamy, B., Bauer, R., Sturm, A., Schreiber, F., von Mering, C., Robinson, M. D., Stecher, B., & Hardt, W. D. (2013). Microbiota-derived hydrogen fuels Salmonella typhimurium invasion of the gut ecosystem. *Cell Host Microbe, 14*(6), 641-651.

Miki, T., Holst, O., & Hardt, W. D. (2012). The bactericidal activity of the C-type lectin RegIIIbeta against Gram-negative bacteria involves binding to lipid A. *J. Biol. Chem., 287*(41), 34844-34855.

Mirold, S., Rabsch, W., Rohde, M., Stender, S., Tschape, H., Russmann, H., Igwe, E., & Hardt, W. D. (1999). Isolation of a temperate bacteriophage encoding the type III effector protein SopE from an epidemic *Salmonella* typhimurium strain. *Proc. Natl. Acad. Sci. U.S.A., 96*(17), 9845-9850.

Moor, K., Wotzka, S. Y., Toska, A., Diard, M., Hapfelmeier, S., & Slack, E. (2016). Peracetic Acid Treatment Generates Potent Inactivated Oral Vaccines from a Broad Range of Culturable Bacterial Species. *Front Immunol., 7*, 34.

Oppenheim, A. B., Kobiler, O., Stavans, J., Court, D. L., & Adhya, S. (2005). Switches in bacteriophage lambda development. *Annu. Rev. Genet., 39*, 409-429.

Pelludat, C., Mirold, S., & Hardt, W. D. (2003). The SopEPhi phage integrates into the *ssrA* gene of *Salmonella enterica* serovar Typhimurium A36 and is closely related to the Fels-2 prophage. *J. Bacteriol., 185*(17), 5182-5191.

Petrovska, L., Mather, A. E., AbuOun, M., Branchu, P., Harris, S. R., Connor, T., Hopkins, K. L., Underwood, A., Lettini, A. A., Page, A., Bagnall, M., Wain, J., Parkhill, J., Dougan, G., Davies, R., & Kingsley, R. A. (2016). Microevolution of Monophasic *Salmonella* Typhimurium during Epidemic, United Kingdom, 2005-2010. *Emerg. Infect. Dis., 22*(4), 617-624.

Santos, R. L., Raffatellu, M., Bevins, C. L., Adams, L. G., Tukel, C., Tsolis, R. M., & Baumler, A. J. (2009). Life in the inflamed intestine, Salmonella style. *Trends Microbiol., 17*(11), 498-506.

Schmidt, H. (2001). Shiga-toxin-converting bacteriophages. *Res. Microbiol., 152*(8), 687-695.

Shearwin, K. E., Brumby, A. M., & Egan, J. B. (1998). The Tum protein of coliphage 186 is an antirepressor. *J. Biol. Chem., 273*(10), 5708-5715.

Stecher, B., Denzler, R., Maier, L., Bernet, F., Sanders, M. J., Pickard, D. J., Barthel, M., Westendorf, A. M., Krogfelt, K. A., Walker, A. W., Ackermann, M., Dobrindt, U., Thomson, N. R., & Hardt, W. D. (2012). Gut inflammation can boost horizontal gene transfer between pathogenic and commensal Enterobacteriaceae. *Proc Natl Acad Sci U S A, 109*(4), 1269-1274.

Stecher, B., Hapfelmeier, S., Muller, C., Kremer, M., Stallmach, T., & Hardt, W. D. (2004). Flagella and chemotaxis are required for efficient induction of Salmonella enterica serovar Typhimurium colitis in streptomycin-pretreated mice. *Infect Immun, 72*(7), 4138-4150.

Stecher, B., Robbiani, R., Walker, A. W., Westendorf, A. M., Barthel, M., Kremer, M., Chaffron, S., Macpherson, A. J., Buer, J., Parkhill, J., Dougan, G., von Mering, C., & Hardt, W. D. (2007). *Salmonella enterica* serovar typhimurium exploits inflammation to compete with the intestinal microbiota. *PLoS Biol., 5*(10), 2177-2189.

Stelter, C., Kappeli, R., Konig, C., Krah, A., Hardt, W. D., Stecher, B., & Bumann, D. (2011). *Salmonella*-induced mucosal lectin RegIIIbeta kills competing gut microbiota. *PLoS One, 6*(6), e20749.

Sternberg, N. L., & Maurer, R. (1991). Bacteriophage-mediated generalized transduction in *Escherichia coli* and *Salmonella* typhimurium. *Methods Enzymol., 204*, 18-43.

Waldor, M. K., & Mekalanos, J. J. (1996). Lysogenic conversion by a filamentous phage encoding cholera toxin. *Science, 272*(5270), 1910-1914.

Winter, S. E., Thiennimitr, P., Winter, M. G., Butler, B. P., Huseby, D. L., Crawford, R. W., Russell, J. M., Bevins, C. L., Adams, L. G., Tsolis, R. M., Roth, J. R., & Baumler, A. J. (2010). Gut inflammation provides a respiratory electron acceptor for Salmonella. *Nature, 467*(7314), 426-429.

Wood, M. W., Rosqvist, R., Mullan, P. B., Edwards, M. H., & Galyov, E. E. (1996). SopE, a secreted protein of *Salmonella dublin*, is translocated into the target eukaryotic cell via a sip-dependent mechanism and promotes bacterial entry. *Mol. Microbiol., 22*(2), 327-338.

Zhang, S., Santos, R. L., Tsolis, R. M., Mirold, S., Hardt, W. D., Adams, L. G., & Baumler, A. J. (2002). Phage mediated horizontal transfer of the sopE1 gene increases enteropathogenicity of *Salmonella enterica* serotype Typhimurium for calves. *FEMS Microbiol. Lett., 217*(2), 243-247.

CHAPTER 5

-

IgA PROTECTS THE INTESTINE BY ENCHAINING RAPIDLY DIVIDING BACTERIA

IgA protects the intestine by enchaining rapidly dividing bacteria

Kathrin Moor[1], Médéric Diard[1], Mikael E. Sellin[1,2], Boas Felmy[1], Sandra Y. Wotzka[1], Albulena Toska[1], Alma Dal Co[3,4], Tom Völler[1], Florence Bansept[5], Erik Bakkeren[1], Andrea Minola[7], Blanca Fernandez-Rodriguez[6], Gloria Agatic[7], Sonia Barbieri[6], Luca Piccoli[6], Costanza Casiraghi[6†], Davide Corti[6,7], Antonio Lanzavecchia[6,7,1], Roland R. Regoes[8], Claude Loverdo[5], Roman Stocker[9], Douglas R. Brumley[9*], Wolf-Dietrich Hardt[1*], Emma Slack[1*].

1. Institute of Microbiology, ETH Zürich, 8093 Zürich, Switzerland.

2. Department of Cell and Molecular Biology, and Department of Medical Biochemistry and Microbiology, Uppsala University, 75124 Uppsala, Sweden.

3. Department of Environmental Systems Science, ETH Zurich, Zürich, Switzerland.

4. Department of Environmental Microbiology, Eawag, Swiss Federal Institute of Aquatic Science and Technology, Dübendorf, Switzerland

5. Laboratoire Jean Perrin (UMR 8237), CNRS - UPMC, 75005 Paris, France

6. Institute for Research in Biomedicine, Bellinzona, Switzerland.

7. Humabs BioMed SA, 6500 Bellinzona, Switzerland.

8. Institute of Integrative Biology, ETH Zürich, 8092 Zürich, Switzerland.

9. Institute of Environmental Engineering, Department of Civil, Environmental, and Geomatic Engineering, ETH Zürich, 8093 Zurich, Switzerland

† Current address: Department of Experimental, Diagnostic and Specialty Medicine, University of Bologna, Bologna, Italy

*Corresponding authors

Manuscript in review

Opening paragraph

Intestinal IgA is a dimeric antibody-class devoid of classical bactericidal functionality (Woof *et al.*, 2011). It is not well understood how high-affinity IgA protects from bacterial enteropathogens (Pabst, 2012). Here we demonstrate that the dominant effect of IgA in vivo is to enchain the progeny of dividing bacteria into clonal or oligoclonal clumps in the intestinal lumen (enchained growth). Enchained growth has three far-reaching consequences for our understanding of mucosal immune function: Firstly, enchained bacterial clumps cannot participate in tissue invasion. The observed reduction in planktonic bacteria was sufficient to explain all vaccine-mediated protection in a non-Typhoidal Salmonellosis model (NTS). Secondly, enchained growth leads to the loss of entire bacterial clones en bloc from the fecal stream, reducing the genetic diversity of the luminal population. Thirdly, spatial separation of enchained bacterial clones inhibits conjugative transfer of antibiotic-resistance plasmids. IgA-mediated enchained growth was also observed for Escherichia coli. Therefore, enchained growth appears to be a general mechanism by which cross-linking antibodies modify the behavior and evolution of intestinal pathogens and commensals, with broad implications for infection medicine.

Results

In the antibiotic pre-treatment model of NTS*, Salmonella enterica* subspecies *enterica* serovar Typhimurium (*S.* Tm) grows exponentially in the dysbiotic murine large intestine to a carrying capacity of 10^9-10^{10} CFU/g (Extended Data Fig. 1) (Kaiser *et al.*, 2011). Subsequently, virulence factor expression is initiated, driving invasion into the intestinal mucosa and leading to profound large intestinal inflammation and lethal systemic disease (Ackermann *et al.*, 2008; Kaiser *et al.*, 2011). To study the function of high-avidity IgA in this model, mice were orally vaccinated with peracetic acid-inactivated *S.* Tm (PA-STm) (Moor *et al.*, 2016). High-affinity IgA induced by PA-STm vaccination efficiently coated the *S.* Tm population in the cecum lumen in an O-antigen-dependent manner (Extended Data Fig.2a and b). IgA coating did not effect the overall *S.* Tm growth kinetics in the gut lumen (Extended Data Fig. 3a), but protected from intestinal pathology and tissue invasion (Extended Data Fig. 3b-f (Moor *et al.*, 2016)).

Strikingly, protection correlated with IgA-dependent clumping of the bacteria. Clumps often consisted of more than 50 bacteria, leaving less than 2% *S.* Tm in a planktonic state (18h post-infection; Fig. 1a and b, Extended Data Fig. 3g-h). These observations were consistent with immune exclusion by classical agglutination (Levinson *et al.*, 2015; Mcclelland *et al.*, 1972; Pabst, 2012; Roche *et al.*, 2015; Slack *et al.*, 2014). However, collision-dependent agglutination requires two planktonic *S.* Tm to meet: a rare event at the low bacterial densities that are typically encountered during natural intestinal infections (Kiørboe, T, 2008). In contrast, the

progeny of a dividing bacterium are necessarily in contact. We therefore hypothesized that IgA should efficiently cross-link bacteria during division: a process we named enchained growth.

To test this, vaccinated mice were co-infected with *S.* Tm expressing red or green fluorescence proteins. Consistent with enchained growth into clonal microcolonies, we observed exclusively single-color clumps as long as the total bacteria density remained below 10^8 CFU/g (Fig. 1c-f). This is quite different from the mixing expected if agglutination would dominate clump formation (Fig. 1g). The probability to see mixed clumps increased at higher bacterial densities (Fig. 1c-f) consistent with the co-existence of enchained growth and classical agglutination (Fig. 1f and g, Supplementary Information). However, even at these higher *S.* Tm densities, cell lineages remained clearly visible (Fig. 1f).
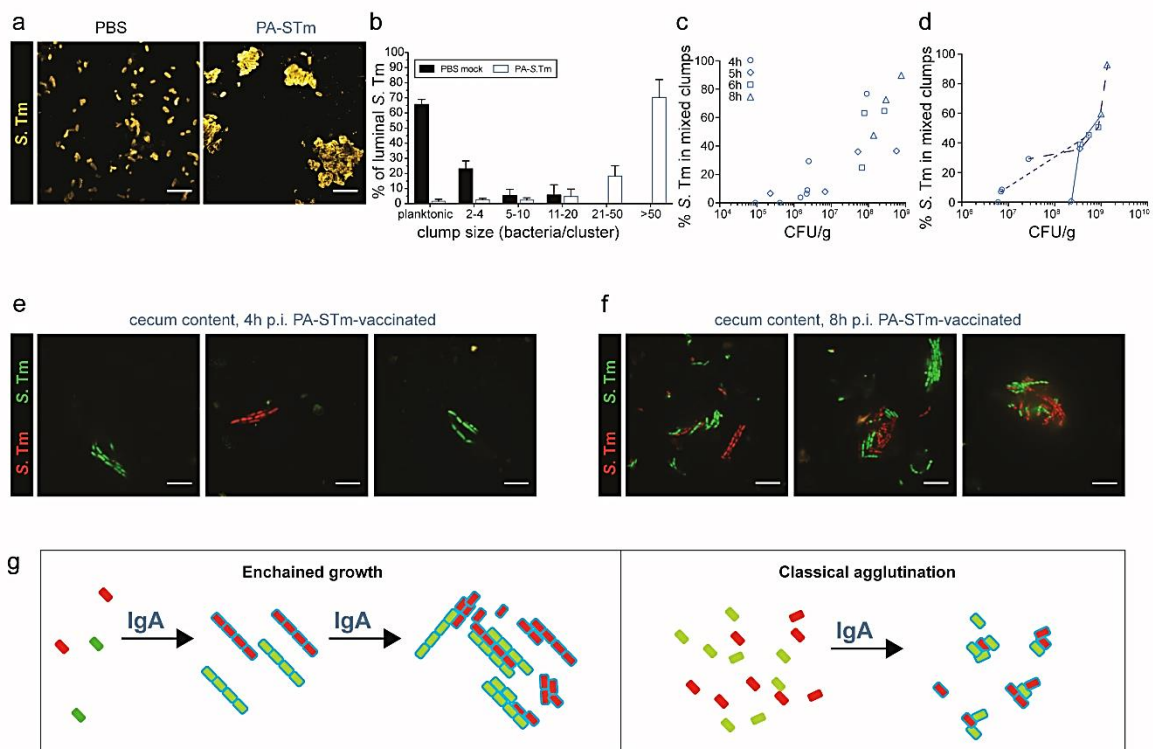

Figure 1. High avidity IgA enchains luminal bacterial into clonal microcolonies. a. Confocal micrographs of cecal content stained for *S.* Tm O-antigen at 18h post-infection with 10^5 CFU of *S.* Tm^wt in mock-vaccinated (PBS) and vaccinated (PA-STm) streptomycin pre-treated C57BL/6 mice. **b.** Quantification of bacteria per clump in mock-vaccinated and vaccinated mice, as in (a). N=5 mice per group. N=8 images per mouse, pooled from two independent experiments. Repeat-measures ANOVA (interaction between vaccination and clump size): p<0.0001. **c-f.** mock-vaccinated and vaccinated, ampicillin pre-treated mice were infected with 10^7 CFU of a 1:1 mixture *S.* Tm^avir constitutively expressing GFP (green) or mCherry (red). **c.** mice were euthanized and live cecal content imaged at the indicated time point, or **d.** mice were terminally anaesthetized and artificially ventilated from 4h post-infection and cecum content sampled for imaging at the indicated time-points. % of total counted *S.* Tm present in mixed clumps by manual image analysis (n=25 images per animal/time-point) is plotted against *S.* Tm density in the cecal content sample. Lines connect points from a single animal. **e and f.** Representative images of the data shown in (c) **g.** Schematic diagrams of bacterial clumping by enchained growth and classical agglutination.

We next asked whether enchained growth was sufficient to explain protection from disease. Confocal intravital microscopy of the cecum at 18h p.i. revealed abundant planktonic *S.* Tm cells swimming in the gut lumen and cecal crypts of naive mice (which lack high-avidity anti-*S.* Tm IgA), but not vaccinated animals (Fig. 2a and b). In fact, enchained *S.* Tm are likely confined ≥100μm away from the epithelial border (Extended Data Fig. 5), too deep inside the cecal lumen of vaccinated mice to be directly imaged by confocal intravital microscopy through the cecum wall (Muller *et al.*, 2012). *S.* Tm lodged in IgA-enchained clumps could therefore no longer participate in tissue invasion. However, a low number of planktonic, potentially infectious, *S.* Tm were still observed in the cecum lumen of vaccinated mice (Fig. 1a-f). The size of this planktonic population may determine the efficacy of protection.

A strong indicator of protection in NTS is a reduced rate of bacterial translocation to the mesenteric lymph nodes. The translocation rate can be quantified by combining mathematical analysis (Fig. 2c) with recovery of barcoded *S.* Tm strains (Wild-type isogenic tagged strains - WITS (Grant *et al.*, 2008; Kaiser *et al.*, 2013)) from the mesenteric lymph nodes (Fig. 2d). The total translocation rate (μG) is a product of the number of infectious luminal *S.* Tm (G) and the translocation rate per infectious *S.* Tm (μ). If μ is unchanged by vaccination, we can derive the infectious lumenal population size (G) required to see the observed translocation rate. This accurately predicted the 1.5log reduction in the planktonic infectious population in the lumen, as determined by microscopy (Fig. 2e). Whilst we do not want to imply that enchained growth is the only function of IgA in this situation, this demonstrates that clumping is of a sufficient magnitude to explain all of the observed tissue protection.

We therefore developed a model to predict the major determinants of the planktonic population size in vaccinated mice (Supplementary Information). Our model predicts that the planktonic population density reaches a true equilibrium during exponential growth due to balanced generation, by escaping enchained growth, and removal, by collision-dependent agglutination (Extended Data Fig. 6, Supplementary Information). Supporting the model, the number of planktonic bacteria remains low and constant as the total enchained population grows exponentially in the gut lumen (Fig. 2f). Our model predicted that the absolute density of the planktonic *S.* Tm population at equilibrium was critically dependent on the strength of IgA cross-linking, and the speed at which the bacteria moved due to swimming and fluid motion of the surroundings (Fig. 2g, Supplementary Information). Interestingly, high avidity IgA prevents *S.* Tm swimming (Extended Data Fig. 7a). While this appears to be a minor contributor to protection (Extended Data Fig. 7b-g), loss of swimming movement actually slightly increased the predicted size of the planktonic population (Fig. 2g).
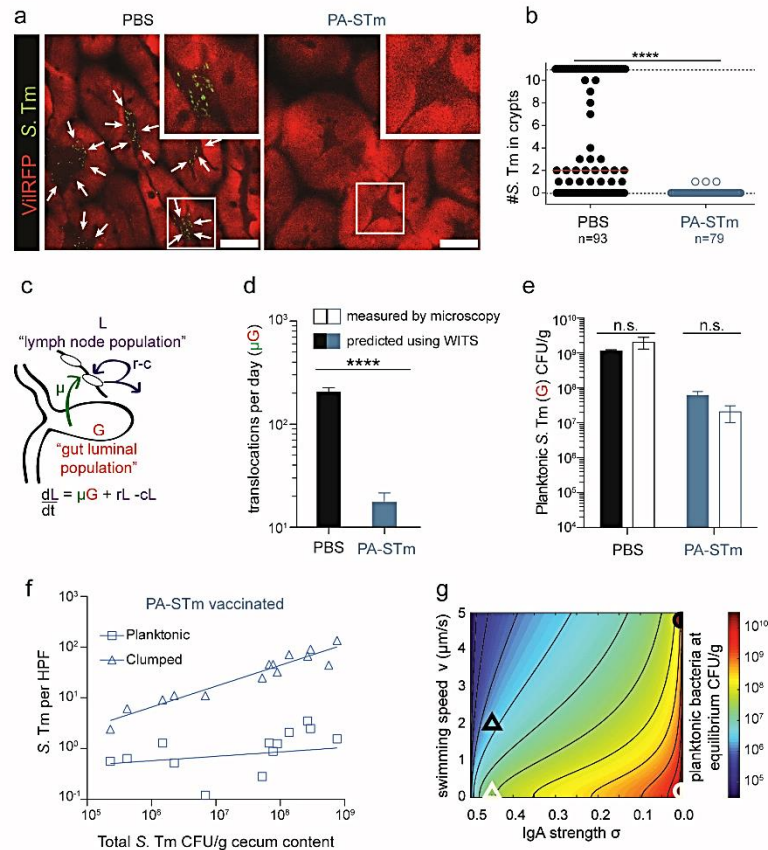
Figure 2. Enchained growth reduces the effective luminal population size capable of tissue invasion. a. Mock-vaccinated (PBS) and vaccinated (PA-STm) VilRFP mice were streptomycin pre-treated and infected with 10^5 *S*. Tm^{avir} constitutively expressing GFP (green). Intravital confocal microscopy of the cecum at 18h. Insets are 2-fold expansions of the highlighted regions. Arrows indicate *S.* Tm in cecum crypts. Scale bar 50μm **b.** Quantification of data shown in (a). Crypts containing more than 11 GFP-expressing bacteria were scored with an upper detection-limit. **** Kruskall-Wallis p<0.0001. Data pooled from three independent experiments **c.** Schematic diagram and deterministic function used for mathematical analysis of barcoded *S.* Tm invasion to the mesenteric lymph nodes. L = Lymph node *S.* Tm population size, G = Gut lumen *S.* Tm population size, μ = migration rate per gut luminal bacterium, r-c = net replication rate in the mesenteric lymph nodes. **d.** Mock-vaccinated and PA-STm vaccinated C57BL/6 mice were streptomycin pre-treated and infected with 10^5 of an *S.* Tm^{wt} inoculum containing genetically barcoded "Wild-type isogenic tagged strains (*S.* Tm^{wt} WITS). Mean+/-standard deviation of bacterial translocations per day from the gut lumen to the mesenteric lymph nodes determined by fitting to a stochastic model based on (c). N = 12 mice per group. 2-tailed T test, p<0.0001. **e.** Infectious *S.* Tm population size in the cecum, determined by scoring free bacteria at 18h p.i. by microscopy (N=10 high-power fields per mouse, N=5 mice per group) or by estimating the expected luminal population size "G" based on the bacterial translocation rate calculated in (d). 2-way ANOVA with Bonferroni post-tests: "Measured" vs "Predicted" - not significant; "PBS vs PA-STm" p=0.0024. **f.** Planktonic versus Clumped bacteria quantified by live microscopy of cecum content sampled at 4-8h post infection with 10^7 *S.* Tm^{avir} constitutively expressing GFP and RFP, correlated to bacterial density, as determined by plating. Spearman's rank correlation coefficients: r(Planktonic) = 0.45, r(Clumped)=0.97. Pooled data from 4 independent experiments **g.** Prediction (based on Supplementary Information) of how the equilibrium planktonic population size (color scale) depends on the speed of bacterial swimming (v) and the IgA strength (σ). Circles= Naive mice, Triangles= Vaccinated mice. Black outlines = motile *S.* Tm, White outlines = non-motile *S.* Tm: Predicted values based on measured average population swimming speeds and hypothetical IgA strength.

By considering the kinetics of bacteria growing in spatially restricted clonal microcolonies, we could predict two important and so far unexpected consequences of high-avidity IgA, beyond straightforward protection.

Populations of bacteria in the large intestine can be sufficiently large to permit extremely rapid evolution. However, enchained growth forces the progeny of an individual bacterial clone to remain physically associated and therefore to be retained or lost from the cecum as a single unit. If enchained growth were perfect, over time we would expect the intestinal population diversity to become reduced to one single clone, leading to a massive loss of genetic diversity (Extended Data Fig. 8). We quantified clonal extinction in situations dominated by either enchained growth (i.e. a low, realistic, bacterial inoculum) or classical agglutination (i.e. a high bacterial inoculum). As predicted, vaccination drives increased clonal extinction (i.e. decreased "evenness" (Maier *et al.*, 2013)) only where enchained growth dominates (Fig. 3). Direct toxicity of intestinal IgA was excluded by *in vitro S.* Tm cultures in the presence of saturating concentrations of purified intestinal IgA (Extended Data Fig. 9). These data further support the existence of enchained growth, and revealed a novel benefit of oral vaccination: IgA-mediated enchained growth is expected to slow the emergence of *S.* Tm variants (e.g. strains with increased epidemic potential) by reducing the pathogen's population diversity.
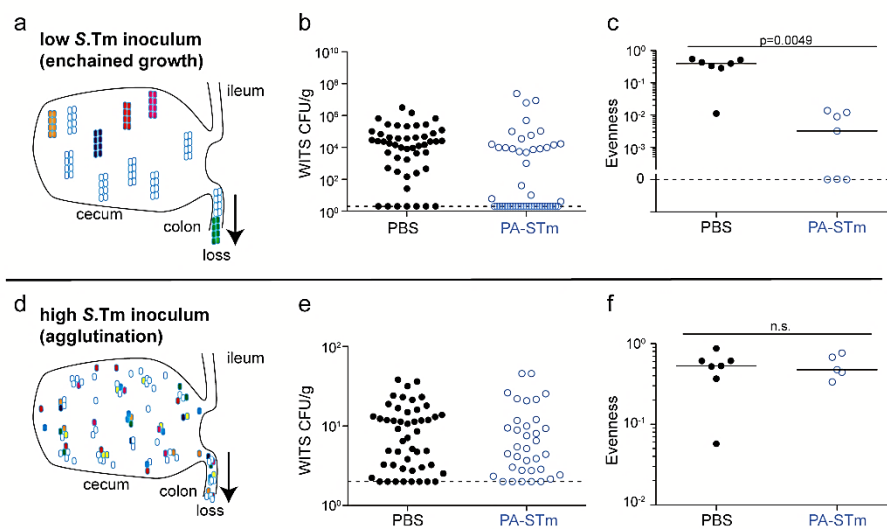

Figure 3. Enchained growth accelerates clonal extinction in the gut lumen. a-f) C57BL/6 mice were orally vaccinated with PA-STm or PBS only. On d21, all mice were streptomycin pre-treated and 24h later infected with 10^5 (**a-c**) or 10^{10} (**d-f**) S. Tm^{avir} carrying 10 CFU of each of seven barcoded strains (S. Tm^{avir} WITS). **a and d.** Schematic diagrams of clonal loss during enchained growth and classical agglutination. Each colour represents a different neutral tagged bacterium. **b and e.** Raw data CFU of each barcoded strain analysed. Dotted line = detection limit. **c and f**. Evenness, 2-tailed Mann Whitney U statistics are shown. Dotted line = Evenness = 0 (≤1 WITS recovered).

The mammalian large intestine is an important site for spread of antimicrobial resistances, often carried on plasmids (Stecher *et al.*, 2013). We predicted that enchained growth would affect plasmid-transfer by conjugation, as enchained donor clones and enchained recipient clones would be spatially isolated. To test this, vaccinated and naive mice were infected with plasmid donor (SL1344 P2^{Cat}) and recipient (14028) *S.* Tm (Stecher *et al.*, 2012), both of which were strongly bound by vaccine-induced IgA (Extended Data Fig. 10). We observed a significant IgA-mediated delay in plasmid transfer in situations where enchained growth should dominate (low inoculum) (Fig. 4a, Extended Data Fig. 10). The delay in plasmid transfer was reduced or eliminated where classical agglutination dominated the IgA effect (high inoculum, *in vitro* conjugation, Fig. 4b and c, Extended Data Fig. 10). This was not attributable to IgA-mediated loss of motility (Extended Data Fig. 10). Thus, these data supported that enchained growth affects conjugative plasmid transfer in the gut of a vaccinated host.
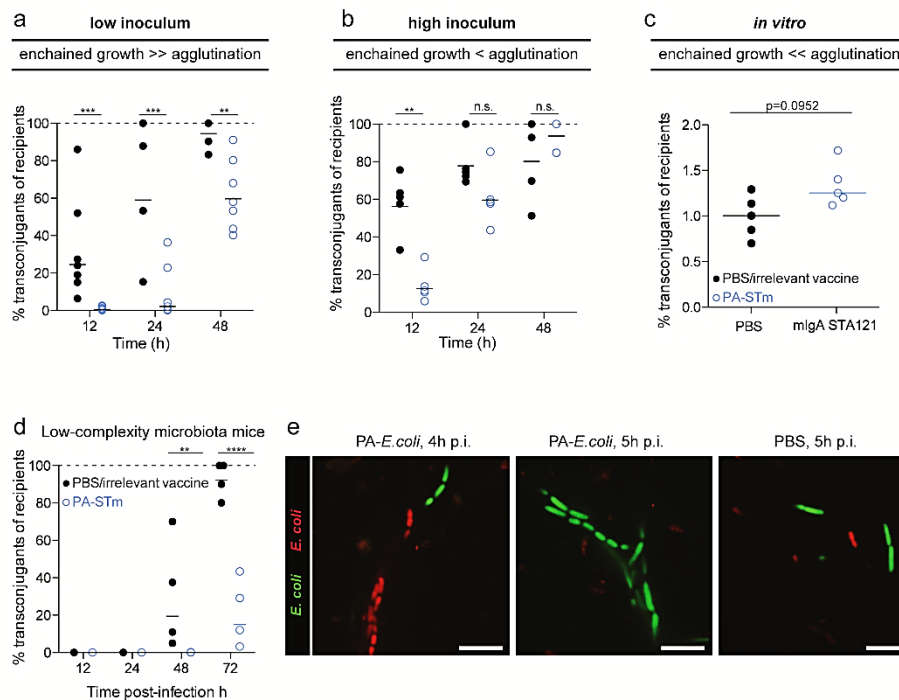

Figure 4. IgA-mediated enchained-growth inhibits conjugative plasmid transfer, and is also observed for *E. coli*.
a. Vaccinated (PA-STm) and mock-vaccinated (PBS/irrelevant vaccine) C57BL/6 mice were ampicillin pre-treated and sequentially infected with 10^2 CFU of plasmid "donor" (SL1344 P2$_{Cat}$), immediately followed by 10^2 CFU of "recipient" (14028) *S.* Tm. Percentage transconjugants of total 14028 *S.* Tm, as determined by selective plating of feces. Repeat-measured ANOVA with Bonferroni post-tests. ** p<0.01, *** p<0.001 **b.** Mice were vaccinated and pre-treated as in (a) received 10^{10} CFU of plasmid "donor" (SL1344 P2$_{Cat}$), immediately followed by 10^{10} CFU of "recipient" (14028) S. Tm. Percentage transconjugants of total 14028 bacteria as in (a). Repeat-measured ANOVA with Bonferroni post-tests. ** p<0.01, n.s. = not significant. **c.** *In vitro* plasmid transfer during 60min in the presence or absence of bacterial coating with murinized monoclonal dimeric IgA specific for the *S.* Tm O-antigen (mSTA121). Mann-Whitney U not significant. **d.** Low complexity microbiota mice were vaccinated and infected as in (a) without any antibiotic pre-treatment. Percentage transconjugants as in (a). Repeat-measured ANOVA with Bonferroni post-tests. ** p<0.01, **** p<0.0001. **e.** PA-*E. coli* CFT073-vaccinated wild-type mice were ampicillin pre-treated and infected with a 1:1 ratio of *E. coli* CFT073 constitutively expressing mCherry (red) or GFP (green). Representative images of n=5 mice per group.

Enchained growth should be even more dominant in a situation where the intestinal niche for *S.* Tm growth is restricted and the bacterial density does not reach the threshold for efficient collision-dependent agglutination. Correspondingly, plasmid transfer was blocked for up to three days post-infection in non-pre-treated gnotobiotic mice harboring a low complexity microbiota (LCF (Endt *et al.*, 2010)) where *S.* Tm grows to a carrying capacity of <10^9 CFU/g (Fig. 4d, Extended Data Fig. 10). This confirms a strong effect of enchained growth at low pathogen densities and suggests that oral vaccination may help to reduce plasmid transfer between intestinal bacteria.

Finally, as enchained growth is based on very generic principles of IgA binding and bacterial growth, we predicted it should function with other bacterial species. We therefore carried out oral vaccinations with an inactivated uropathogenic *E. coli* strain CFT073. When vaccinated mice were intestinally colonized with a mixture of green- and red-fluorescence-protein expressing CFT073, we observed clonal clump formation indicative of enchained growth (Fig. 4e).

Conclusion and Discussion

These observations fundamentally alter the way in which we consider both endogenous and vaccine-induced intestinal IgA function.

High-avidity endogenous IgA binds to a subfraction of intestinal microbiota species with higher "colitogenic potential" (Bunker *et al.*, 2015; Palm *et al.*, 2014; Planer *et al.*, 2016), but may only enchain these species and restrict their freedom when a microenvironment shift fuels their growth. In keeping with this, antibiotic-resistant *E. faecalis* aggregates are only observed in the intestinal lumen during antibiotic-induced dysbiosis (Hendrickx *et al.*, 2015) and IgA-deficient mouse pups poorly control *E. coli* overgrowth at weaning (Mirpuri *et al.*, 2014). Enchained growth, which requires only the oligomeric structure of secretory antibody (but no *bona fide* effector function), targets fast-growing bacterial species to decrease pathogenic potential, genetic diversity and plasmid transfer.

Enchained growth is of considerable interest in the design and application of oral vaccines. Indeed, inactivated oral vaccines against cholera, as well as *Shigellosis* and enterotoxogenic *E. coli* (Chakraborty *et al.*, 2016; Kabir, 2014; Lundgren *et al.*, 2016), are increasingly of interest as low-cost vaccination strategies and are good inducers of high avidity anti-O-antigen IgA responses (Kabir, 2014). However, variable protection has often been observed in cholera-endemic regions, where *vibrio cholera* exposure levels are often high (Azegami *et al.*, 2014; Qadri *et al.*, 2016). As the intestinal density of *vibrio cholera* is maximally 10^8 CFU/g, our models predict that efficient protection will only be achieved where pathogen populations expand in the intestinal lumen: i.e. where the infectious dose is well below the intestinal

carrying capacity. Vaccination with the aim of inducing bacterial surface-specific IgA is therefore only expected to protect efficiently if levels of exposure are kept low by concomitant public health measures.

Finally, this work hints that oral vaccination may hold additional and unexpected benefits by altering the within-host evolution of pathogen populations. This may be particularly important in livestock reservoirs of zoonotic pathogens. Protection from disease by oral vaccines clearly decreases the requirement for antibiotic usage (Lipsitch *et al.*, 2016). Additionally, vaccine-induced IgA may directly decelerate bacterial evolution and slow the spread of antimicrobial resistances often carried on conjugative plasmids.

Material and Methods

Ethics statement

All animal experiments were approved by the legal authorities (licenses 223/2010 and 222/2013; Kantonales Veterinäramt Zürich, Switzerland) and performed according to the legal and ethical requirements.

Mice

Unless otherwise stated, all experiments used recently re-derived SOPF C57BL/6 mice. VilRFP (B6.B6-Gt(ROSA)26Sortm1Hjf x B6.SJL-Tg(Vil-cre)997Gum/J) (Müller *et al.*, 2012), $J_H^{-/-}$ (Chen *et al.*, 1993), IgA$^{-/-}$ (Harriman *et al.*, 1999), PIgR$^{-/-}$ (Shimada *et al.*, 1999) (all C57BL/6 background) were recently re-derived into a specific opportunistic pathogen-free (SOPF) foster colony to normalize the microbiota and bred under full barrier conditions in individually ventilated cages in the ETH Phenomics center (EPIC), ETH Zürich. Low complex microbiota (LCM) mice (C57BL/6) are ex-germfree mice, which were colonized with a naturally diversified Altered Schaedler flora in 2007 (Stecher *et al.*) and were bred in individually ventilated cages under strict hygienic isolation in Rodent Center at ETH. Vaccinations were started between 5 and 6weeks of age, and males and females were randomized between groups to obtain identical ratios wherever possible. As strong phenotypes were expected, we adhered to standard practice of analysing at least 5 mice per group. Researchers were not blinded to group allocation.

Bacterial strains and growth conditions

All bacterial strains used in this study are listed in Table 1. Unless otherwise stated, for infection experiments, wild type *Salmonella enterica* serovar Typhimurium (SL1344 wildtype clone SB300) or the respective mutants were cultured in LB containing the appropriate antibiotics for 12h at 37°C, diluted 1:20 and sub-cultured for 3h in 0.3M NaCl supplemented LB without antibiotics (Barthel *et al.*, 2003).

The recipient^{avir} is the result of two P22 transductions (*invG::cat*, *ssaV::kan*) into 14028S followed by flipping out of the antibiotic resistance cassettes by the flipase encoded on pCP20. The *lpfED::aphT* tag was added by P22 transduction (Diard *et al.*, 2014). The recipient$^{fliGHI::Tn10}$ is the result of P22 transductions (*fliGHI::*Tn*10*) into 14028S

Table 1. Bacterial strains in this study

Strain	Description	Resistances*	Source or Reference
S. Tm^{wt}	SB300 *S.* enterica serovar Typhimurium SL1344 (wildtype)	Sm	(Hoiseth *et al.*, 1981)
S. Tm^{avir}	SB300 derivate, Δ*invG*, Δ*sseD*	Sm	(Maier *et al.*, 2013)
S. Tm^{wt} WITS	Wildtype isogenic tagged versions of SB300	Sm, Km	(Grant *et al.*, 2008)

S. Tm[avir] WITS	Wildtype isogenic tagged versions of *S.* Tm[avir]	Sm, Km	(Maier *et al.*, 2014)
M913	P22-mediated transduction of *fliGH::tn10* into SB300	Sm, Tet	(Stecher *et al.*, 2004)
M933	P22-mediated transduction of *fliGH::tn10* into *S.* Tm[avir]	Sm, Tet, Km	*(Endt et al., 2010)*
SB300 Δ*wbaP*	SB300 derivate lacking O antigen	Sm, Km	(Hapfelmeier *et al.*, 2005)
PII Donor	SB300 derivative carrying pCol1B9[cat] (PII)	Sm, Cm	This study
Recipient	14028S derivative, *lpfED*::*aphtT*	Km	This study
PII Donor[avir]	M2702 derivative carrying pCol1B9[cat]	Sm, Cm	This study
Recipient[avir]	14028S derivative Δ*invG*, Δ*ssaV* *lpfED*::*aphtT*	Km	This study
PII Donor [fliGHI::Tn10]	M913 derivative carrying pCol1B9[cat]	Sm, Tet	This study
Recipient [fliGHI::Tn10]	14028S derivative *fliGHI::*Tn*10*	Sm, Tet	This study
S. Enteritidis (M1513)	*S. enterica* serovar Enteritidis 1251059 Δ*ssa*V::*cat*	Sm, Cm	*(Endt et al., 2010)*
S. Choleraesuis	*S. enterica* serovar Choleraesuis ATCC25957 (914/99)		(Nutter *et al.*, 1970)
E. coli CFT073	Extraintestinal pathogenic *E. coli* that colonizes the mouse intestine as a commensal species.		(Mobley *et al.*, 1990)

*Sm: Streptomycin 50µg/ml, Km: Kanamycin 50µg/ml, Cm: Chloramphenicol 6µg/ml, Tet: Tetracycline 12.5µg/ml

Plasmids used in this study

All plasmids used in this study are listed in Table 2. pBADGFPmut2 was constructed by insertion of a EcoRI gfp-mut2 fragment from pM979 (Stecher *et al.*, 2004) into pBAD24, digested by EcoRI (Fermentas) and dephosphorylated (shrimp alkaline phosphatase, NEB).

Table 2. Plasmids used in this study

Plasmids	Description	Resistances	Ref
pM975	P*ssaG*::*gfp*mut2	Amp	(Müller *et al.*, 2012)
pM965	P*rpsM*::*gfp*mut2	Amp	(Stecher *et al.*, 2004)
pFPV25.1	P*rpsM*::mCherry	Amp	(Drecktrah *et al.*, 2008)
pAM34	ColE type vector requiring IPTG for replication primer production	Amp	(Gil, D. *et al.*, 1991b)
pBADGFPmut2	pBADGFPmut2	Amp	This study
pCol1B9[cal] (PII)	Conjugative plasmid	Cm	(Stecher *et al.*, 2012)

Production of peracetic acid killed vaccines

Peracetic acid killed vaccines were produced as previously described in (Moor *et al.*, 2016). Briefly, bacteria for peracetic acid killed vaccines were grown overnight to late stationary phase. Bacteria were harvested by centrifugation and resuspended at a density of 10^9-10^{10} per ml in sterile PBS. Peracetic acid (Sigma-Aldrich) was added to a final concentration of 1%. The suspension was mixed thoroughly and incubated for 60min at room temperature. Bacteria were washed once in 40ml of sterile 10x PBS and subsequently three times in 50ml sterile 1x PBS. The final pellet was resuspended at a concentration of 10^{11} particles per ml in sterile PBS (determined by OD600) and stored at 4°C for up to three weeks. As a quality control, each batch of vaccine was tested before use by inoculating 100µl of the killed vaccine (one vaccine dose) into 300ml LB and incubating over night at 37°C with aeration. Vaccine lots were released for use only when a negative enrichment culture had been confirmed.

Oral vaccination with peracetic acid killed

Mice was vaccinated as described (Moor *et al.*, 2016). Briefly, mice received 10^{10} particles of the respective peracetic acid killed bacteria in PBS by oral gavage once per week for three weeks. On day 21 after the first gavage, mice were used for infection experiments.

Challenge infections with *S.* Typhimurium

All infections were performed in individually ventilated cages at the RCHCI, Zurich as described previously (Barthel *et al.*, 2003). Unless otherwise stated, mice were pretreated with either 1g/kg streptomycin sulfate or 0.8 g/kg ampicillin sodium salt in sterile PBS by gavage. Twenty-four hours later, the mice were inoculated with the indicated CFU and strain by gavage. For determination of total bacterial loads, fresh fecal pellets, mesenteric lymph nodes, spleen and cecal content were plated on MacConkey agar plates containing 50µg/ml streptomycin.

For IgA-outtitration, mice received one dose (10^{10} particles) of peracetic-acid killed vaccine 20min before infection and a second dose of peracetic-acid killed bacteria or PBS, directly after infection.

For conjugative pCol1B9[cat] (PII) plasmid transfer experiments, ampicillin pretreated SOPF C57BL/6 mice or untreated LCM mice were sequentially infected with equal inoculum of donor and recipient strains (Table 1 and 2) (at 10^2 or 10^{10} CFU each). Both strains were carrying additional plasmids conferring resistance to ampicillin and coding for fluorescence proteins (conditional expression (pM975), or constitutive expression (pM965 and pFPV25.1)). Fecal population sizes of donors, recipients and transconjugants were evaluated by selective plating (MacConkey agar plates containing 50µg/ml streptomycin, 50µg/ml kanamycin, 6µg/ml chloramphenicol or combinations thereof).

Determination of bacterial growth rates in the gut lumen

pAM34 is a colicin-like vector in which the replication primer promoter is under the control of the LacI repressor such that plasmid replication only occurs in the presence of IPTG (Gil, D *et al.*, 1991a). *S.* Tm^{avir} carrying the pAM34 plasmid was therefore cultured overnight in the presence of 1mM IPTG in LB and in the absence of antibiotics, to avoid selection of IPTG-independence. Subsequently, the culture was diluted 1:20 into fresh LB and cultured at 37°C for 3h. The inocula were prepared by centrifugation of sufficient culture to give the desired CFU and resuspended in 50µl of sterile PBS. SOPF C57BL/6 mice that had received 1g/kg streptomycin p.o. 24h previously, were infected orally with either 5x10^3, 5x10^5 or 5x10^7 CFU of the pAM34-carrying inoculum. Simultaneously, the inoculum was serially diluted into LB without IPTG and cultured overnight to determine the relationship between bacterial generations and plasmid loss for each experiment. pAM34 carriage was determined by plating feces and overnight culture on MacConkey agar plates containing 50µg/ml streptomycin only (total CFU) or 100µg/ml ampicillin and 1mM IPTG (pAM34-carrying CFU). The overnight culture total CFU and inoculum CFU were used to calculate fold expansion, and therefore generation number (assuming zero death) for each sample. This was plotted against the log-base-2 of the fraction of pAM34-carrying bacteria and linear regression carried out to determine the relationship between plasmid loss and generations. The copy number of the plasmid is equivalent to 2^(intercept - Log2(100)), as there is no production of plasmid-negative bacteria until the plasmid copy number has been diluted to close to to n=1 per cell. The equation derived by linear regression was then used to back-calculate bacterial generations between the inoculum and fecal bacteria.

Analysis of specific antibody titers by bacterial flow cytometry

Specific antibody titers in mouse intestinal washes were measured by flow cytometry as described (Moor *et al.*, 2016; Slack *et al.*, 2009). Briefly, intestinal washes were collected by flushing the small intestine with 5ml PBS, centrifuged at 16000g for 30min and aliquots of the supernatants were stored at -20°C until analysis. Bacterial targets (antigen against which antibodies are to be titered) were grown to late stationary phase and gently pelleted for 2 min at 3000g. The pellet was washed with sterile-filtered FACS buffer before resuspending at a density of approximately 10^7 bacteria per ml. After thawing, intestinal washes were centrifuged again at 16000g for 10 min. Supernatants were used to perform serial dilutions. 25µl of the dilutions were incubated with 25µl bacterial suspension at 4°C for 1h. Bacteria were washed twice with 200µl FACS buffer before resuspending in 25µl FACS buffer containing monoclonal FITC-anti-mouse IgA (BD Pharmingen, 10µg/ml). After 1h of incubation, bacteria were washed once with FACS buffer and resuspended in 300µl FACS buffer for acquisition on FACS LSRII using FSC and SSC parameters in logarithmic mode. Data were analysed using FloJo (Treestar). After gating on bacterial particles, median fluorescence intensities (MFI) were

plotted against antibody concentrations for each sample and 4-parameter logistic curves fitted using Prism (Graphpad, USA). Titers were calculated from these curves as the inverse of the antibody concentration giving an above-background signal.

Production of monoclonal human IgA and IgG and murinized monoclonal IgA

Memory B cells were isolated from cryopreserved PBMCs by magnetic cell sorting with anti-CD22-FITC antibodies (BD Pharmingen) and anti-FITC microbeads (Miltenyi Biotec), followed by flow cytometry sorting. The B cells were immortalized with Epstein–Barr virus (EBV) in the presence CpG-DNA (2.5µg/ml) and irradiated feeder cells, as described previously (Traggiai *et al.*, 2004). Two weeks post-immortalization, culture supernatants were tested for binding to formaldehyde-treated heat-inactivated *S.* Tm cells by ELISA and FACS analysis as above. STA5 supernatant containing anti-*S.* Tm O-antigen IgG was filtered and used directly. To generate murinized monoclonal IgA, cDNA was synthesized from the mSTA121 positive culture and both heavy chain and light chain variable regions were sequenced. The murine IgA heavy chain and J chain were cloned by reference to the IMGT database. mSTA121 monoclonal antibody was produced recombinantly as murine dimeric IgA by transient transfection of HEK 293 Freestyle Cells (Invitrogen) using polyethylenimine (PEI), and purified by antibody affinity chromatography (CaptureSelect LC-lambda (Hu) Affinity Matrix, Thermo Fisher Scientific).

Purification of Intestinal IgA for *in vitro* assays

Small intestinal lavages from mice that were either vaccinated with PA-STm or PBS-only, were collected as described above and stored at -80°C until usage. Intestinal lavages were thawed and centrifuged at 16000g for 10min. The supernatants were diluted in LB media, sterile filtered (0.22µm filter) and loaded onto a 100kDa cut-off filter column (Amicon Ultra UFC910096). The columns were centrifuged at 6340g for 1h (Heraeus Megafuge 1.0 R) and the flow through was discarded. The collected liquid was resuspended in 0.5ml LB medium per 2ml starting intestinal lavage.

In vitro IgA-agglutination assays and determination of growth rates

S. Typhimurium carrying an arabinose inducible GFP on the plasmid pBADGFPmut2 was grown overnight in LB containing 100µg/ml ampicillin. The overnight culture was diluted 1:100 in LB with ampicillin (100µg/ml) and 1%w/v arabinose, and subcultured for 3h to fully induce the reporter. Subsequently bacteria were thoroughly washed and diluted into LB supplemented with purified intestinal IgA (3mg/ml total IgA). Samples were analysed by plating for total CFU determination and flow cytometry for GFP dilution, as previously (Helaine *et al.*, 2010).

For competitive growth, *S.* Typhimurium and *S.* Enteritidis were grown separately overnight in LB supplemented with the respective antibiotics. The *S.* Typhimurium and *S.* Enteritidis cultures were mixed 1:1 and diluted 1:100 into LB without antibiotics, supplemented with

purified intestinal IgA 3mg/ml. Approximately 10^4 - 10^5 CFU of the *S*. Typhimurium/*S*. Enteritidis mix were added to wells of a 96-well plate (TPP 92096) and bacteria were incubated at 37°C without agitation. Every hour, the top half of the bacterial culture was removed and fresh LB supplemented with purified IgA was added to maintain saturating levels during growth. Samples were collected every 0.5-1h for plating and FACS analyses. IgA coating was verified by flow cytometry. Before plating on selective LB agar and analysis by bacterial flow cytometry, the bacterial culture was bead-beaten at $25s^{-1}$ for 1min to disrupt aggregates.

Confocal microscopy of fixed ceca

Whole ceca were fixed in PBS 4% paraformaldehyde/4% sucrose, saturated in PBS/20% sucrose, embedded in OCT (optimum cutting temperature medium; Tissue-Tek), flash-frozen, and stored at −80°C. 10–20µm cryosections were air-dried, rehydrated in PBS for 1min, permeabilized in PBS/0.5% Triton X-100 for 3min, and blocked in PBS/10% Normal Goat Serum for ≥15min. Sections were incubated with the indicated antibodies for ≥15min each, washed with PBS, and mounted with Mowiol (Calbiochem). For quantification of *S*. Tm in tissue, 20µm cross-sections were stained with α-ICAM-1/CD54 (clone 3E2, Becton Dickinson), anti-hamster-Cy3 (Jackson), AlexaFluor647-conjugated phalloidin (Molecular Probes), and DAPI (Sigma Aldrich). Tissue-residing *S*. Tm were identified by expression of the p*ssaG-GFPmut2* reporter, and were enumerated at 40×–100×, as previously described (Sellin *et al.*, 2014) with a scientist blinded for sample identity. Data presented are mean values of 6-9 non-consecutive tissue sections / mouse. For quantification of *S*. Tm in the cecal lumen 10µm cross-sections were stained with rabbit α-*S*. Tm LPS (antigen group B factor 4-5; Difco), anti-rabbit-Cy3 or anti-rabbit-Cy5 (both from Jackson) and DAPI. Imaging was done using a Zeiss Axiovert 200m microscope with a 100× oil-objective, a spinning disc confocal laser unit (Visitron), and two Evolve 512 EMCCD cameras (Photometrics). Post-capture processing and analysis employed Visiview (Visitron) and Image J ×64.

To quantify the "infectious population size", the number of single and paired bacteria was determined for 10 high power fields per mouse based on the *S*. Tm LPS-staining. The percentage of non-aggregated IgA-negative bacteria in the PA-STm vaccinated mice was determined by complete absence of the anti-IgA staining. 10 high power fields containing non-aggregated bacteria per PA-STm vaccinated mouse were scored.

Live confocal microscopy of cecal content.

Vaccinated or control mice were pretreated with 0.8g/kg ampicillin sodium salt in sterile PBS. 24h later, mice received 10^7 CFU of a 1:1 mix of mCherry-(pFPV25.1) and GFP-(pM965) expressing avirulent *S.* Tm M2702 or *E. coli* CFT073. For sequential sampling of the cecal content, mice were anesthetized, intubated and respired with oxygen containing 1.8%–1.9%

isoflurane as described in (Müller *et al.*, 2012; Sellin *et al.*, 2014). The cecum was exposed, a small piece of the cecum was tied off with fine thread, cut open for removal of the sample, immediately sealed with Histoacryl® glue (B. Braun)) and placed back into the abdominal cavity until the next sampling. For imaging, cecum content was diluted gently 1:10 w/v in sterile PBS containing 6µg/ml chloramphenicol, avoiding heavy mixing. 200µl of the suspension were transferred to an 8-well Nunc Lab-Tek Chambered Coverglass (Thermo Scientific) and imaged at 100x using the Zeiss Axiovert 200m microscope. To determine *S.* Tm motility, ampicillin-pretreated mice were infected with 10^5 CFU M2702pM695 for 18h, before preparing cecal content as above. The heating chamber of the microscope was set to 37°C and all images were taken with an exposure time of 1s. Swimming distances were determined by measuring individual bacterial trajectories in ImageJ. To determine the distribution of bacteria in aggregates, n=25 high power fields per mouse were randomly selected and imaged for mCherry and GFP fluorescence. The images were merged in Visiview (Visitron) and individual bacteria scored manually as either planktonic, present in a single-color aggregate or present in a mixed aggregate.

Intravital two-photon microscopy

Intravital microscopy was performed similarly to previously published (Müller *et al.*, 2012; Sellin *et al.*, 2014). Briefly, anesthetized, intubated mice were respired with oxygen containing 1.8%–1.9% isoflurane. After exposing the cecum and submerging it in ringer/lactate solution, images were acquired using a Leica SP8 DMI6000B microscope equipped with a HC PL IRAPO 403/1.10 water immersion objective, emission filters for GFP (525/50) and RFP (585/40), and nondescanned Hybrid detectors (Leica). GFP and RFP was excited using a two-photon MaiTai XF Laser (Spectra-Physics) tuned to 920nm (pulsed at 80MHz with pulse width <80fs). The microscope was operated using the Leica application suite at ScopeM (ETHZ). The distance measurement was performed using the orthogonal view function of Fiji (based on ImageJ 1.49h). Z-distance was 7.5µm per section. For measurement of the location of 25µm beads, 10µl of 25µm YG latex beads (Polysciences) were injected directly into the cecum lumen of an intubated mouse and were allowed to equilibrate for 30mins. The tissue was sealed using Histoacryl® glue (B. Braun) and imaged as described above.

***In vitro* plasmid transfer**

Overnight cultures of donor (*S.* Tm SB300 pII) and recipient strains (14028) were diluted 1:50, subcultured for 4 hours in LB without antibiotics. The resulting cultures were washed with PBS. 45µl of donor and recipient PBS-washed subcultures were separately incubated with 60µg/ml of monoclonal dimeric IgA specific for the *S.* Tm O-antigen (mIgA STA121) for 5min at room temperature. Donor and recipient strains were then mixed and loaded onto a 0.025µm MF-Millipore mixed cellulose ester membrane using a syringe. Membranes were

placed on LB agar without antibiotics and incubated for 1 hour at 37°C. Membranes were then each bead-beaten in 1ml PBS at 25Hz for 1min. Resuspended mixtures were diluted and plated on selective McConkey agar plates. IgA coating was confirmed by bacterial flow cytometry as described above.

Basic statistics

Where two groups were compared, Mann Whitney U non-parametric tests were employed. Where more than two groups were compared, Kruskal-Wallis tests with Dunn's post-tests were used to correct for multiple testing. Where time-courses were compared with two different groups, data was transformed to approximate a Normal distribution and repeat-measures ANOVA used to determine significance. All correlation analysis was carried out using a Spearman's rank correlation coefficient calculation (non-parametric).

Mathematical modelling

Modelling of translocation to the mesenteric lymph nodes. This was carried out as described previously, using seven "WITS" tags (Grant *et al.*, 2008) at 1:35 of the total 10^5 CFU inoculum. At this dilution, more than 2500 clones of each WITS reach the cecum lumen of vaccinated mice, so clonal loss is not measurable. The distribution of WITS-tagged strains reaching the mesenteric lymph nodes was quantified by plating, enrichment culture and qPCR as described (Kaiser *et al.*, 2013). This distribution was then used to parameterize a stochastic model of translocation to the mesenteric lymph nodes. The number of translocations per day is in fact the product of G (the size of the infectious luminal population) and μ (the translocation rate per infectious luminal bacterium). If we assume that μ is constant in the vaccinated and naive cases, we can derive G by simple division of the total daily translocation rate by μ.

Calculating clonal loss from the cecum lumen. Vaccinated and naive mice were infected with either 10^5 CFU or 10^{10} CFU *S.* Tm^avir, spiked with an average of 10 copies of each of seven *S.* Tm^avir WITS strains. WITS frequencies were determined by plating, enrichment culture and qPCR as described previously (Kaiser *et al.*, 2013; Maier *et al.*, 2014). The loss of evenness was calculated as described previously (Maier *et al.*, 2014).

To estimate the effect of caged growth on clonal loss, a simple scenario was simulated: at the initial time, a single bacterium of each of 7 neutrally-tagged strains is present in the cecum, along with 8 untagged bacteria. In the naive mice, each bacterium duplicates deterministically every 20min, and then each individual of this new population is eliminated with a probability p = 0.15 (based on reasonable estimates for cecal content turnover). In the vaccinated mice, we consider the simple case for which each new offspring remains enchained and the IgA cross-linking is perfect, so that we can keep track of the 15 different clones rather than each individual bacterium. Every 20min, the size of each clump doubles and each of them is

eliminated with a probability p = 0.15. In both cases, the evenness of the tagged bacteria distribution is calculated at each time step. This process is iterated 3000 times and the resulting mean evenness as a function of time is computed.

Mathematical modelling of the planktonic population kinetics in the presence of high-avidity IgA : See supplementary manuscript below.

Supplementary Figures
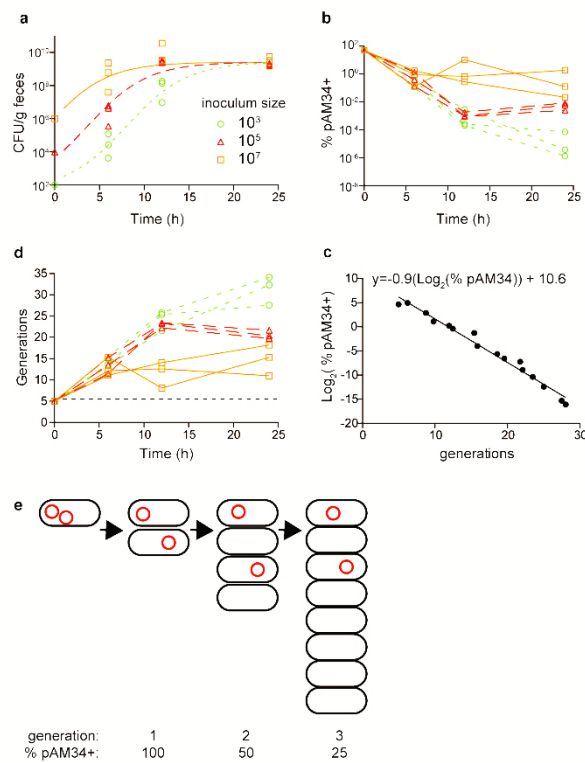
Extended Data Figure 1 | *S.* Tm growth in streptomycin-treated murine large intestine. Naive C57BL/6 SOPF mice received 25mg streptomycin per os. 24h later mice were infected with the indicated CFU of *S*. Tm[avir] carrying the IPTG-addicted plasmid pAM34. **a**. CFU/g feces with fitted logistic (S-shaped) growth curves. **b**. Percentage of the fecal population retaining ampicillin resistance at the indicated time-points. Different inoculum sizes led to identical growth rates, but varied growth periods. **c**. Calculation of a standard curve linking percentage plasmid carriage with generation number derived from serial dilution of the inoculum and overnight cultures *in vitro.* Note that the gradient is shallower than the expected value of 1. This is likely explained by low levels of residual plasmid replication. The y-intercept is considerably greater than $\log_2(100)=6.64$ due to the relatively high starting copy number (c. n=16) of the plasmid. **d**. Calculated numbers of generations in the cecum based on the data shown in b and c. **e**. Schematic diagram of expected plasmid loss with a starting copy number of n=2 (red circles = pAM34).
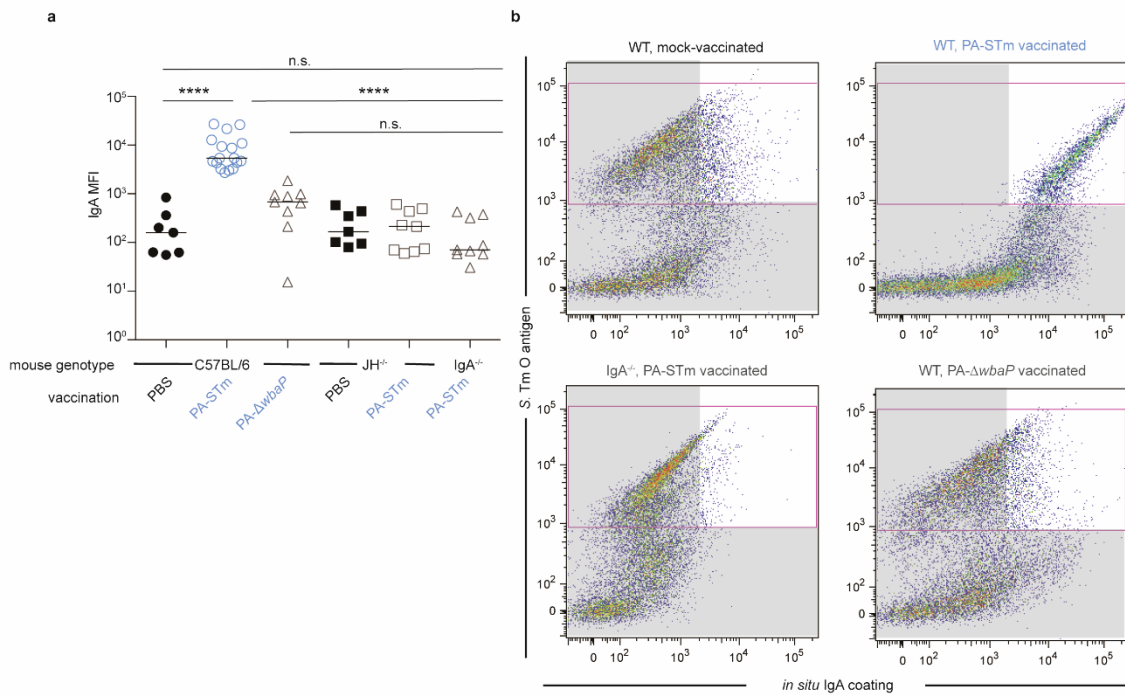
Extended Data Figure 2 | IgA elicited by the PA-STm vaccine coats *S.* Tm in the murine cecum at 24h post-infection. a. C57BL/6, JH^{-/-} and IgA^{-/-} mice were orally vaccinated with vehicle only (PBS), an inactivated O-antigen-deficient *S.* Tm strain (PA-Δ*wbaP*), or inactivated wild-type *S.* Tm (PA-STm). On d21 after the first vaccination, mice were pre-treated with 25mg streptomycin p.o. and 24h later infected with 10^5 wild-type *S.* Tm. Cecum content bacteria were analysed by flow cytometry at 18h post-infection. Median fluorescence intensity of IgA staining on the luminal *S.* Tm population, as determined by flow cytometry analysis of total cecal content. p<0.0001 by ANOVA of log-normalized data. **b**. Representative dot-plots showing *S.* Tm O-antigen (human IgG-anti-O12, Alexa647-anti-hIgG) and IgA staining (Biotin-anti-mouse IgA: Pacific Blue-Streptavidin) of cecal content bacteria. Non-shaded quadrant contains IgA-coated *S.* Tm.
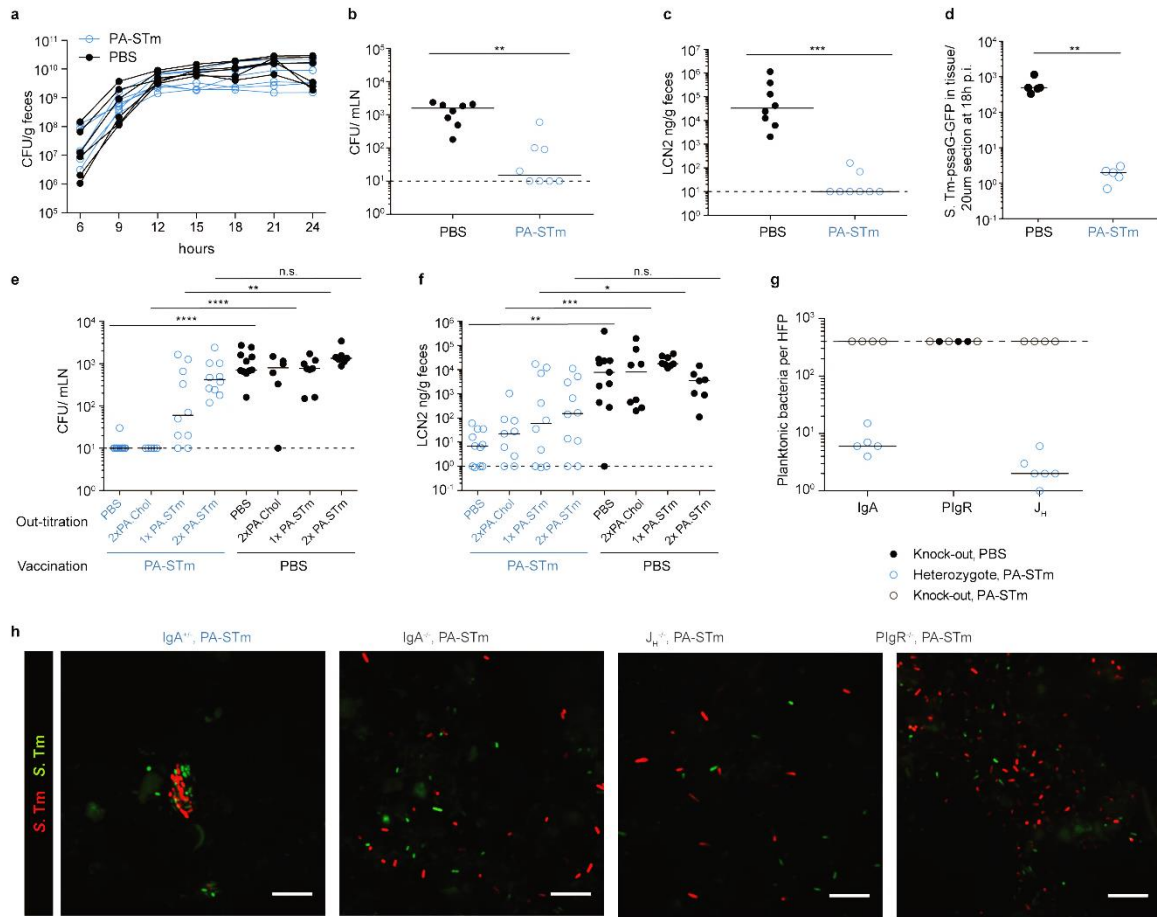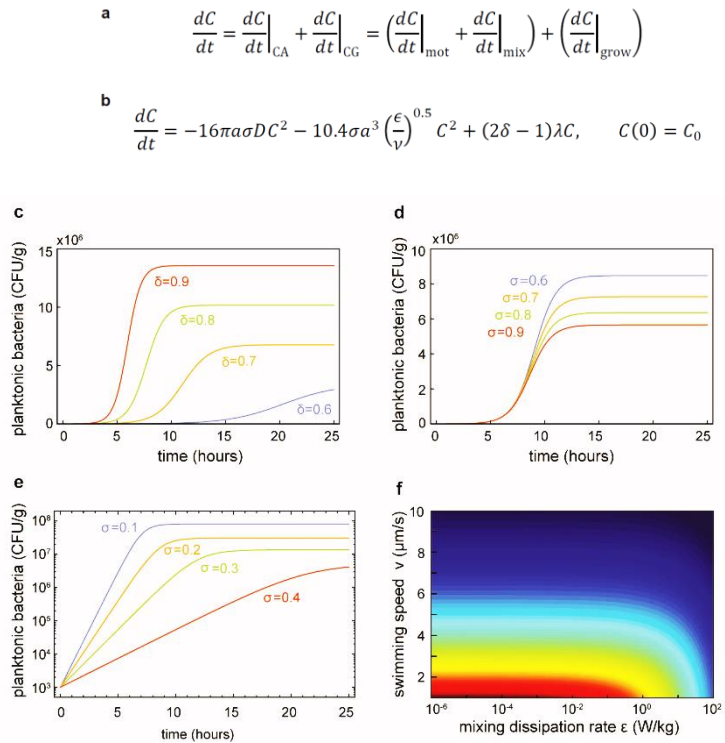
Extended Data Figure 3 | IgA and O-antigen dependence of protection and aggregation: a. Vaccinated (PA-STm) or mock-vaccinated (PBS) C57BL/6 mice received 25mg streptomycin per os and 24h later were infected with 10^5 CFU *S*. Tm^{avir}. Avirulent *S*. Tm was used to avoid growth differences attributable to inflammation. Fecal CFU were determined at the indicated time-points post-infection by plating after bead-beating (see Extended Data Figure 4). Repeat-measures ANOVA with Bonferroni post-tests: not significant. **b** and **c**. Mice vaccinated and pre-treated as in (a) were infected with 10^5 CFU *S*. Tm^{wt}. Mesenteric lymph node CFU at 24h post-infection. **Mann Whitney U p=0.0018. **c**. Intestinal inflammation, as assessed by fecal lipocalin 2. ***Mann Whitney U p=0.0007. **d**. Mice were vaccinated and pretreated as in (a). Subsequently, they received 10^5 *S*.Tm^{wt} pssaG-GFP (GFP reporter expressed after invasion of epithelial cells). Mean bacterial tissue invasion events of 8 sections per mouse at 18h pi. ** Mann-Whitney U p<0.01. **e-f**: Mice were vaccinated and pre-treated as in (a). 23.5h after antibiotic treatment, luminal IgA was out-titrated by gavaging mice with either PBS, 10^{10} particles of PA-STm, or 10^{10} particles of peracetic acid-inactivated *S*. Choleraesuis (PA-Chol, unrelated O-antigen structure). 30min later, all mice were infected with 105 CFU *S*. Tm^{wt}, directly followed by a repeat of the out-titration treatment (PBS, 2x PA-STm, 2x PA-Chol) or PBS alone (1x PA-STm). **e**. Bacterial load in the mLN was determined by plating 24h p.i. **f**. Intestinal inflammation as assessed by fecal Lipocalin 2 at 24h p.i. 2-way ANOVA with Bonferroni post-tests on log-normalized data. **** p<0.0001, *** p<0.001, ** p<0.01, *p<0.05, n.s.=p>0.05. **g-h**. Mixed litters of IgA$^{-/-}$ and $^{+/-}$ mice, JH$^{-/-}$ and $^{+/-}$ mice and PIgR$^{-/-}$ mice were orally vaccinated with PA-STm or PBS only and were pre-treated as in (a). All mice were subsequently infected with 10^5 CFU of a 1:1 mix containing GFP and mCherry-expressing *S*. Tm^{avir}. **g**. Quantification of non-aggregated bacteria per high-power field-of-view. **h**. Representative images of cecal content at 24h post-infection. Scale bar: 10μm

173
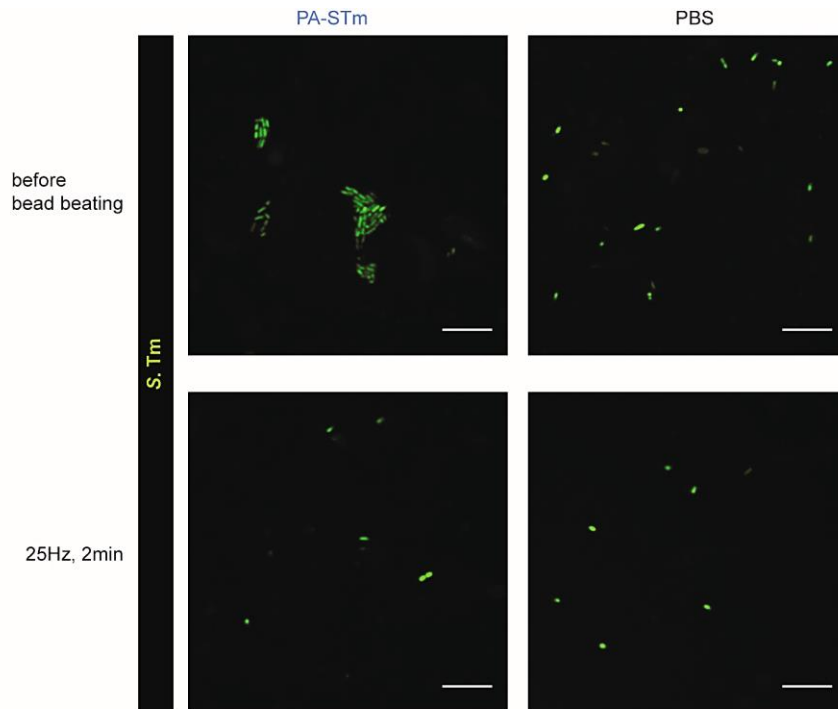
Extended Data Figure 4 | Bead-beating intestinal content or feces disrupts clusters and thereby allows gut luminal growth analysis by CFU determination. C57BL/6 mice were orally vaccinated three times over three weeks with vehicle only (PBS), or inactivated *S.* Tm^wt (PA-STm). On d21 post-infection, mice were pre-treated with 25mg streptomycin p.o. and 24h later, all animals were infected with 10^5 CFU of *S.* Tm^avir constitutively expressing GFP. Cecal content was collected at 24h and imaged directly after diluting 1 in 10 in PBS, or after bead beating for 2min at 25Hz with a large sterile steel bead. Scale bar: 10µm. Representative images.
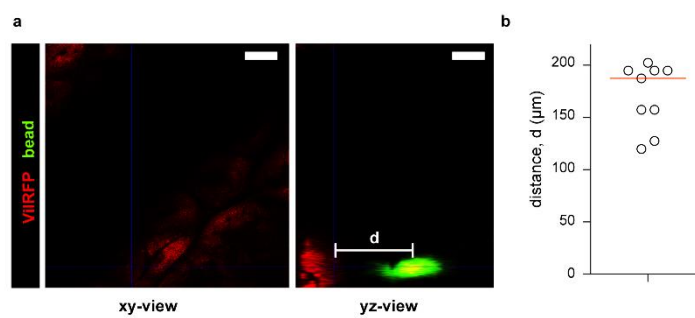

Extended Data Figure 5 | Location of ultrabright 25µm beads in the cecum of naive mice. VilRPF mice were streptomycin pre-treated and 24h later intubated and prepared for intravital confocal microscopy. 25µm YG-fluorescent latex beads (green) were injected directly into the cecum lumen. These beads were selected as having a similar diameter to an average *S.* Tm cluster in the gut lumen on vaccinated mice. **a.** Representative pictures of bead location relative to the surface of the intestinal epithelium Scale bar: 50µm. **b.** Quantification of data shown in (a). These data suggest that *S.* Tm is confined ≥ 100µm away from the gut epithelium in PA-STm vaccinated mice.

174

a

$$\frac{dC}{dt} = \frac{dC}{dt}\bigg|_{CA} + \frac{dC}{dt}\bigg|_{CG} = \left(\frac{dC}{dt}\bigg|_{mot} + \frac{dC}{dt}\bigg|_{mix}\right) + \left(\frac{dC}{dt}\bigg|_{grow}\right)$$

b

$$\frac{dC}{dt} = -16\pi a\sigma D C^2 - 10.4\sigma a^3 \left(\frac{\epsilon}{\nu}\right)^{0.5} C^2 + (2\delta - 1)\lambda C, \qquad C(0) = C_0$$
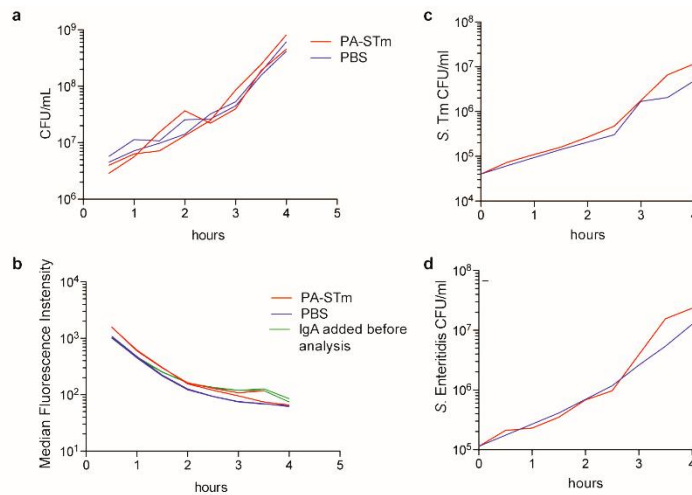
Extended Data Figure 6 | Simulating bacterial clustering dynamics during exponential growth (see Supplementary Manuscript). a. General equation stating the contributions of planktonic bacterial loss due to motility (mot) and mixing (mix) and generation by growth (grow) on overall dynamics of the planktonic population size C. **b.** Parameterized version of equation (a) based on Cell radius (a), Average run time (τ), Dimension of the system (n), Swimming reorientation cosine (α), Kinematic viscosity of fluid (ν), Cell growth rate (λ), Cross-linking strength coefficient (σ), Probability of escaping enchainment (δ), Cell swimming speed (v), Mixing dissipation rate (ε). **c.** Dynamics of the planktonic population during exponential growth for various values of δ (probability of escaping enchainment) with fixed σ (cross-linking strength coefficient)=0.6. **d.** Dynamics of the planktonic population during exponential growth for various values of σ with fixed δ=0.75. Other parameters are given by ε=10⁻² W/kg, λ=2hr⁻¹, a=0.5μm, v=2μm/s, C₀=10³ "CFU/g." **e.** Planktonic bacterial population dynamics with σ=1-δ. Other parameters are as in (c). **f.** Steady state planktonic bacterial concentration as a function of mixing dissipation rate ε and the bacterial swimming speed v. For these results we have used δ=0.9 and σ=0.1. All other parameters as in (c).

175
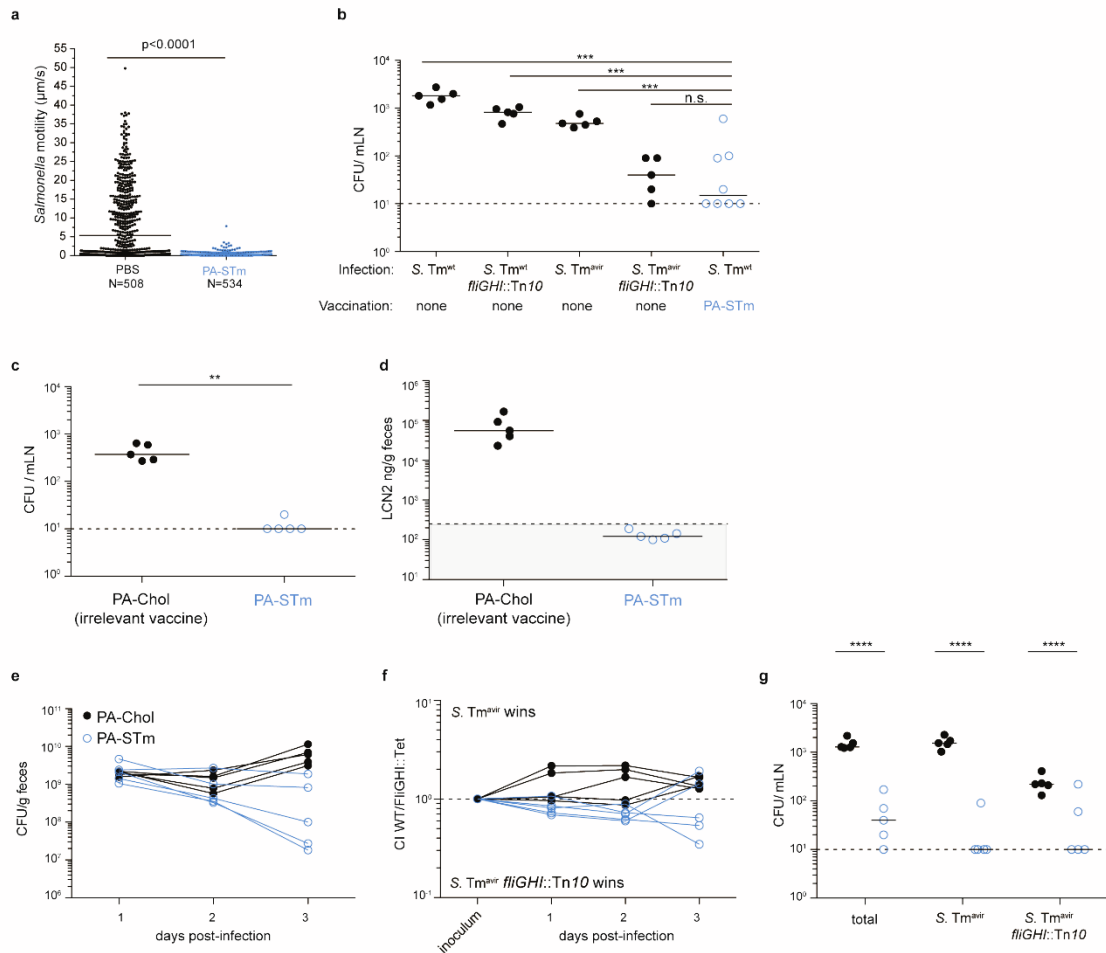
Extended Data Figure 7 | IgA-mediated loss of motility is a minor contributor to protection. **a**. Vaccinated (PA-STm) or mock-vaccinated (PBS) mice were streptomycin pre-treated and infected with 10^5 *S*. Tm^{avir} constitutively expressing GFP. At 18h post-infection, *S*. Tm motility was determined by measuring the length of individual bacterial trajectories by live microscopy of explanted cecal content taken with 1s exposure time. Mann-Whitney U, p<0.0001. **b**. PA-STm-vaccinated mice or naïve controls were streptomycin pre-treated and infected with 10^5 *S*. Tm^{wt}, *S*. Tm^{avir}, and their non-flagellated mutants (*fliGHI*::Tn*10*). Bacterial loads in the mesenteric lymph nodes 24h pi were determined by plating. Dashed line: lower detection limit. One-way ANOVA on log-normalized data with Dunnet's multiple comparison test: *** p<0.001, n.s. not-significant. **c and d**. Vaccinated (PA-STm) or control-vaccinated (peracetic acid-inactivated *S*. Choleraesuis, PA-Chol) mice were streptomycin pre-treated and infected with 10^5 flagella-deficient virulent *S*. Tm (*fliGHI*::Tn*10*). **c**. Bacteria in the mesenteric lymph nodes were enumerated at 24h p.i. by plating. Dashed line: detection limit. ** 2-tailed Mann-Whitney U test: p=0.0097. **d**. Intestinal inflammation as determined by fecal Lipocalin 2. Shaded area: normal non-inflamed values. ** 2-tailed Mann-Whitney U test: p=0.0079. Thus vaccination efficiently protects from non-motile *S*. Tm **e-g**. C57BL/6 mice, vaccinated and pre-treated as in (c) were infected with a 1:1 mixture of *ydgA::aphT S*. Tm^{avir} (neutral tag, avirulent) and *fliGHI*::Tn*10 S*. Tm^{avir} (non-motile, avirulent). **e**. Total *S*. Tm^{avir} CFU in feces determined by plating on streptomycin only. Repeat measures ANOVA on log-normalized data. Vaccination effect p<0.05. **f**. Competitive index (CI) of *ydgA::aphT S*. Tm^{avir} over *fliGHI*::Tn*10 S*. Tm^{avir}, as determined by selective plating of feces. Repeat measures ANOVA on log-normalized data. Vaccination effect p<0.01. **G**. Total, *ydgA::aphT S*. Tm^{avir} and *fliGHI*::Tn*10 S*. Tm^{avir} recoverable from the mesenteric lymph nodes at d3, as determined by selective plating. 2-way ANOVA on log-normalized data ****p<0.0001. Dashed line = lower detection limit. Vaccination therefore exerts a stronger effect on tissue invasion than combined loss of virulence and motility.

176
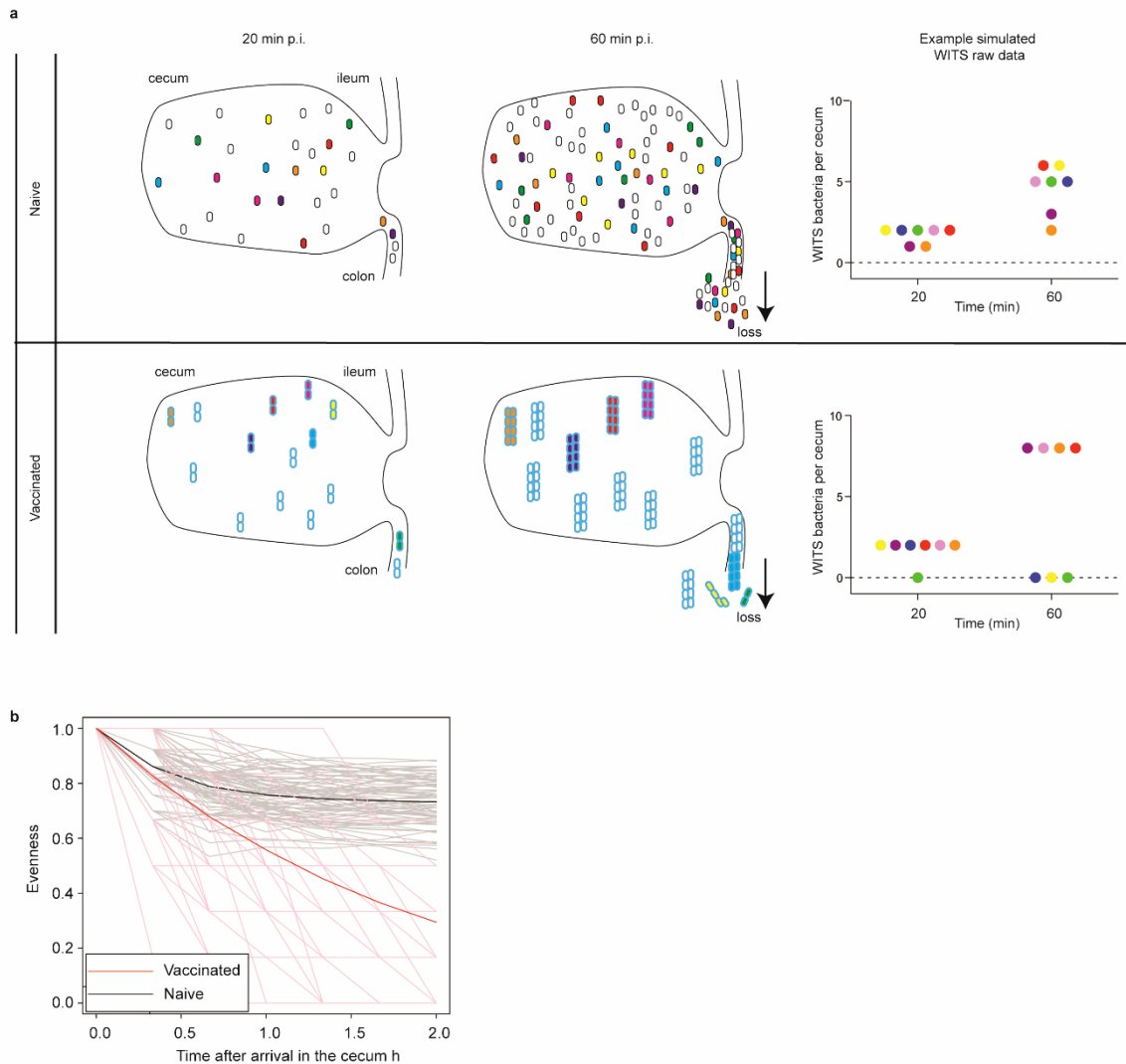
Extended Data Figure 8 | Simulating the effect of IgA-driven enchained growth on clonal extinction in the cecum lumen. A simple enchained growth scenario was envisaged where a single CFU of each of 7 neutrally-tagged clones arrives in the cecum (colored), together with 8 untagged CFU (white). After arrival, these strains become equally distributed in the cecal content by peristaltic mixing and enter a fast growth phase with a doubling time of 20mins. To maintain feces production, approximately 1/7 of the cecal content is cleared to the colon every 20min. **a**: A cartoon of an example clonal loss scenario showing the cecum population and the CFU lost to feces in the colon. The probability of IgA-driven enchained growth is taken as equal to 1, i.e. all dividing bacteria remain enchained in vaccinated mice, making this the extreme case. An example simulated distribution of WITS-tagged strains is shown as in the left-hand panels. Note that pure classical agglutination would be expected to behave as in the "naive" case, as aggregates lost would have no clonal structure. **b**. The "evenness" (Maier et al. 2015) of 3000 discrete simulations of this simplified model up to 2h post-infection (pale lines) and mean of these simulations (bold lines) in vaccinated and naive mice. Note that while in the unvaccinated case, the evenness stabilizes after 1h, evenness continues to drop in the vaccinated case.

Extended Data Figure 9 | No measurable effect of high-avidity IgA coating on bacterial growth/killing *in vitro.*
a. and b. An overnight culture of *S.* Tm^avir carrying an arabinose-inducible GFP (pBADGFPmut2) was diluted 1 in 100 into 1% arabinose(w/v)/LB with ampicillin selection for 3h to fully induce the reporter. Subsequently, the bacteria were thoroughly washed and diluted 1:100 into fresh LB containing secretory IgA purified from the small-intestinal lavages of mock-vaccinated mice ("PBS") or orally vaccinated animals ("PA-STm"), similarly to previously described fluorescence-dilution assays. Samples were removed and clusters disrupted by bead-beating for plating and flow cytometry every 30mins for 4h. **a**. CFU/ml. **b**. Median GFP fluorescence intensity. An additional control for the effect of agglutination on fluorescence intensity was carried out by adding purified IgA from PA-STm vaccinated mice to a sample with non-specific IgA just prior to flow cytometry staining "IgA added before analysis". p>0.05 by repeat-measures ANOVA on log-normalized data. One representative experiment of three. **c and d**. *S.* Tm carrying a neutral Kanamycin-resistance cassette (M2702 WITS KanR) and *S.* Enteritidis carrying a neutral Chloramphenicol-resistance cassette (M1513) were cultured separately overnight in LB. These cultures were mixed 1:1, then diluted 1:100 into LB without antibiotics, supplemented with IgA purified from PA-STm vaccinated (red) or PBS-treated mice (blue) as above. Every 30min a sample was removed and clusters disrupted by bead-beating. CFU densities of the IgA-bound strain (*S.* Typhimurium) and IgA-non-bound strain (*S.* Enteritidis) were determined by selective plating. p>0.05 by repeat-measures ANOVA on log-normalized data. One representative experiment of two. IgA coating of the samples incubated with IgA from vaccinated, but not PBS-treated mice was confirmed at the end of each experiment by bacterial flow cytometry (data not shown).
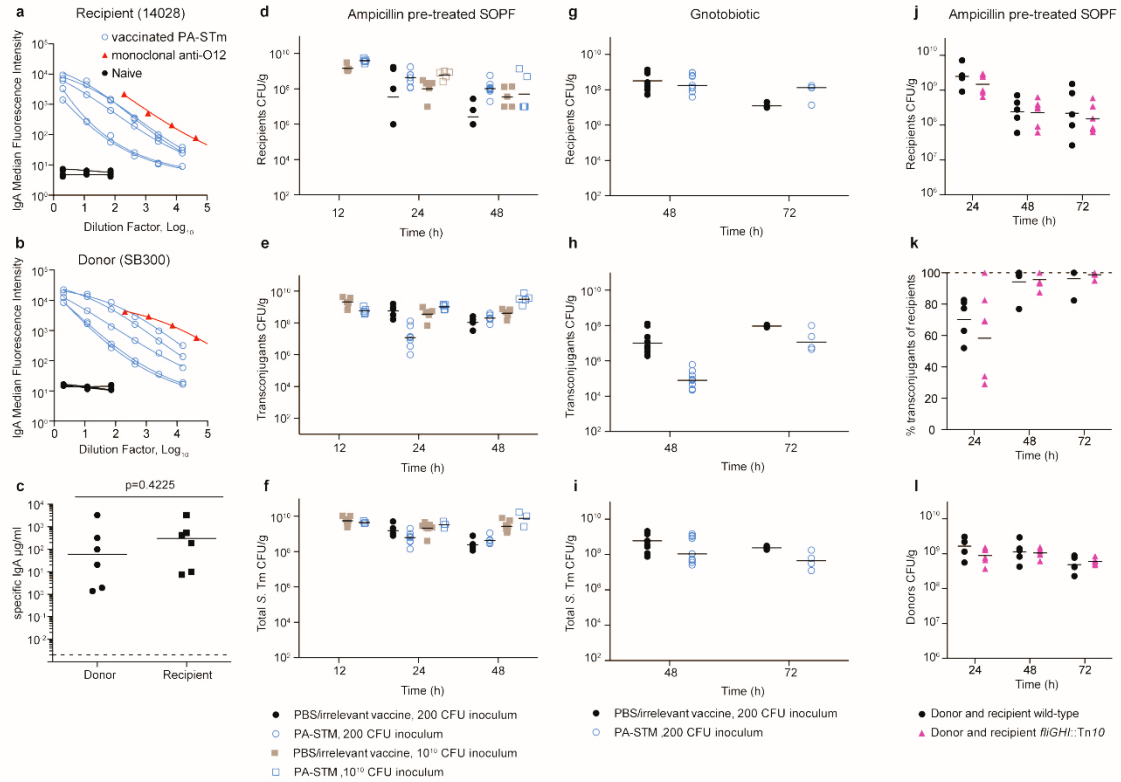
Extended Data Figure 10 | Raw data for conjugative plasmid transfer in vaccinated mice (Figure 4). a-c Small-intestinal lavages from PA-STm-vaccinated or naive mice were titered against the 14028 recipient *S.* Tm strain (**a**) and the SB300 donor *S.* Tm strain (**b**) and compared to a monoclonal dimeric murine IgA directed against the O12 antigen. **a and b**. Raw titration curves. **c**. Absolute titers defined relative to an O-12-specific monoclonal dimeric IgA. 2-tailed Mann-Whitney U test, not significant. **d-f:** C57BL/6 SOPF mice were orally vaccinated with PA-STm, PA-inactivated *S.* Choleraesuis (irrelevant vaccine) or PBS only, as indicated. On d21 after the first vaccination, all mice were ampicillin pre-treated and mice were sequentially infected with either 200 or 10^{10} CFU each of plasmid "donor" (SL1344 P2Cat) and "recipient" (14028) *S.* Tm. **d**. Number of Kanamycin-resistant recipients, **e**. Number of Kanamycin-Chloramphenicol double resistant transconjugants **f**. total number of Streptomycin-resistant *S.* Tm, determined from fecal samples by selective plating. (Corresponding to data in Fig. 4a and b). **g-i:** Low complexity microbiota (LCM) mice were orally vaccinated as in D. On d21 after the first vaccination, all mice were infected sequentially with 200 CFU each of plasmid "donor" (SL1344 P2Cat) and "recipient" (14028) *S.* Tm without antibiotic pre-treatment. **g**. Number of Kanamycin-resistant recipients, **h.** Number of Kanamycin-Chloramphenicol double resistant transconjugants **i**. total number of Streptomycin-resistant *S.* Tm, determined from fecal samples by selective plating **j-l.** .Naive C57BL/6 SOPF were ampicillin pre-treated. 24h later, mice were sequentially infected with either 200 CFU each of neutrally tagged or *fliGHI*::Tn*10* plasmid "donor" (SL1344 P2Cat) and "recipient" (14028) *S.* Tm. **j**. Number of Kanamycin-resistant plasmid-negative recipients **k**. % of transconjugants, of the total recipient population in feces. **l.** Number of Chloramphenicol-resistant donors. wt vs *fliGHI*::Tn*10* p>0.05 by repeat-measures two-way ANOVA on log-normalized data.

Supplementary Manuscript

In this section we present a mathematical model of the interactions between planktonic bacteria that lead to the formation of bacterial clumps. We will consider both the effects of small-scale turbulent mixing in the gut and motility-induced encounters on clump formation. Initially, we will ignore the effect of cell growth and focus on a fixed number of bacteria. In a second stage, we will include the effect of growth. For two particle types, indexed by i and j (for example, bacteria and tracer particles), with respective concentrations C_i and C_j, the encounter rate between them is given by (Kiørboe, T, 2008):

$$E = \beta C_i C_j \tag{1}$$

where E is the number of encounters between a particle of type i and a particle of type j per unit time and per unit volume. The encounter rate kernel β is determined by the process responsible for the encounter, and can include for example Brownian diffusion, sedimentation, motility and mixing. Each of these processes will have its own expression for β, but the encounter rate can still be predicted in the form of equation (1). In what follows, we calculate the relevant encounter rate kernels for the system at hand.

1. **Classical agglutination**

   a. **Motility-induced encounters**

We first consider encounters due to the swimming of bacteria in a quiescent fluid. For bacteria of different sizes/types, with radii a_i and a_j, diffusivities D_i and D_j, and concentrations C_i and C_j, the encounter rate kernel is $\beta = 4\pi(D_i + D_j)(a_i + a_j)$. The collision frequency between cells is therefore given by (Kiørboe, T, 2008):

$$E|_{\text{mot}} = 4\pi(D_i + D_j)(a_i + a_j)C_i C_j. \tag{2}$$

We are interested in the encounter dynamics within a single bacterial population, so can therefore set $i = j$ to find that $E|_{\text{mot}} = 16\pi DaC^2$. Upon collision, two bacteria will stick to one another with a probability σ. We call this parameter the particle cross-linking strength (sometimes also called the adsorption efficiency), a quantity whose value falls between 0 and 1 and which is related to the cross-linking strength of IgA. The diffusivity of a bacterium due to Brownian motion is of the order $D_B = 10^{-13}$ m^2/s, and for aggregates of bacteria it is even lower. In particular, Brownian motion is negligible as an encounter process when bacteria are motile. The diffusivity of bacteria due to swimming is much higher, and can be estimated using the relationship (Berg, 1993)

$$D = \frac{v^2 \tau}{3(1 - \alpha)}, \tag{3}$$

where v is the swimming speed, τ is the average run time (the time between reorientations in the bacterial trajectory), and α is the mean value of the cosine of the angle between successive runs.

Strictly speaking, the overall aggregation dynamics in the system are described by an infinite set of coupled ordinary differential equations (Jackson, 1990; Kiørboe, T. *et al.*, 1990) for the concentrations of different bacterial clump sizes. Single cells can either stick to one another, or join an existing clump of size $i \geq 2$. However, we ignore encounters with larger clumps due to the fact that their diffusivity is negligible (they are non-motile) and their concentration is very low at the beginning of the experiment. Motility-induced changes in the concentration of individual planktonic bacteria can be found simply by multiplying the cross-linking strength σ with the actual encounter rate due to motility $E|_{\text{mot}}$. That is,

$$\frac{dC}{dt}\bigg|_{\text{mot}} = -16\pi a\sigma D C^2 = -\frac{16\pi a\sigma v^2 \tau}{3(1-\alpha)} C^2. \tag{4}$$

b. Mixing-induced encounters

The fluid motion in the system will also contribute to the encounter between bacteria. In this calculation, we neglect the motility of the cells, and consider encounters only through turbulent mixing. As above, we will focus on the dynamics of individual bacteria, neglecting interactions with larger clumps. Under these circumstances, the encounter rate is known to be (Kiørboe, T, 2008)

$$E|_{\text{mix}} = 1.3\gamma \cdot 8a^3 C^2, \tag{5}$$

where the turbulent shear rate is estimated as $\gamma = (\epsilon/v)^{0.5}$, ϵ is the turbulent mixing dissipation rate (W/kg), and v is the kinematic viscosity of the fluid (m^2/s). Mixing-induced changes in the concentration of individual planktonic bacteria are therefore governed by the equation:

$$\frac{dC}{dt}\bigg|_{\text{mix}} = -10.4\sigma a^3 \left(\frac{\epsilon}{v}\right)^{0.5} C^2. \tag{6}$$

Note we have again included the cross-linking strength coefficient σ. Changes in the cell concentration C arising either through motility-induced encounters or mixing-induced encounters, together, fall under the umbrella of "classical agglutination". [2, 6-9]

2. Enchained growth

Thus far we have ignored in the model the influence of cell growth on the concentration of planktonic bacteria. We assume now that each cell grows at a constant rate λ (h^{-1}). In the

absence of IgA, cell growth almost always results in the production of distinct, planktonic daughter cells. However, high avidity IgA tends to enchain the progeny cells one another, inhibiting the production of planktonic daughter cells. This inhibition effect is called enchainment. We introduce the parameter δ (a number between 0 and 1) to quantify the probability that a dividing cell escapes enchainment and divides into two planktonic cells ($\delta = 0$ is complete enchainment). The contribution of enchained growth on the concentration of individual planktonic bacteria C is then given by

$$\left.\frac{dC}{dt}\right|_{\text{grow}} = (2\delta - 1)\lambda C. \tag{7}$$

In this model, we do not account for division of cells in clumps, nor for flow-induced fragmentation of clumps. In the context of this model, the only way in which single cells are produced is by division from other individuals. Therefore, if $\delta < 1/2$, then cell growth leads to a decline in the concentration of planktonic cells C, because a dividing cell will become a clump of size 2. However, if $\delta > 1/2$, growth leads to an increase in C.

3. Bacterial population dynamics

Changes in the concentration of planktonic cells occur through both classical agglutination, in the form of motility-induced and mixing-induced encounters (Eqs. (4) and (6)), and through enchained growth (Eq. (7)). The overall dynamics are then given by

$$\frac{dC}{dt} = \left.\frac{dC}{dt}\right|_{\text{mot}} + \left.\frac{dC}{dt}\right|_{\text{mix}} + \left.\frac{dC}{dt}\right|_{\text{grow}}, \tag{8}$$

or equivalently by

$$\frac{dC}{dt} = -16\pi a\sigma D C^2 - 10.4\sigma a^3 \left(\frac{\epsilon}{\nu}\right)^{0.5} C^2 + (2\delta - 1)\lambda C, \tag{9}$$

with initial condition $C(0) = C_0$. The motility-dependent diffusivity is $D = \frac{v^2\tau}{3(1-\alpha)}$. From Eq. (9) it is immediately obvious that if $\delta \leq 1/2$, the bacterial concentration will monotonically decrease towards zero ($dC/dt < 0$ for all t) if there is any form of classical agglutination ($\sigma \neq 0$ and at least one of $D, \epsilon \neq 0$). We therefore focus on the case in which $\delta > 1/2$.

Estimation of parameters. We now turn our attention to estimating the parameters of the model. The kinematic viscosity of pure water at 30°C is $8 \times 10^{-7} \text{m}^2/\text{s}$. However, for the intestinal contents of the common brushtail possum, which is expected to be similar to the present system, this value is at least three orders of magnitude larger (Lentle *et al.*, 2005). We therefore adopt the value $\nu = 8 \times 10^{-4} \text{ m}^2/\text{s}$. Larger values would further diminish the effect

of fluid mixing on classical agglutination. The cell growth rate is measured directly from experiments to be $\lambda = 2$ h^{-1}. The average run time τ and reorientation cosine α for the bacteria are taken as published values of *E. coli* [56]. The cell radius and swimming speeds are estimated for the present system (see Extended Data Fig. 7a). As a conservative upper bound on the turbulent mixing dissipation rate, we take $\epsilon = 10^{-2}$ W/kg. This is considerably higher than even typical values in ocean mixing, but is intended to provide a robust upper bound on the effect of fluid mixing in this system.

Parameter	Symbol	Value
Cell radius	a	0.5 μm
Average run time	τ	1 s
Kinematic viscosity of fluid	ν	8×10^{-4} m^2/s
Cell growth rate	λ	2 h^{-1}
Cross-linking strength coefficient	σ	$0 \leq \sigma \leq 1$
Probability of escaping enchainment	δ	$1/2 < \delta \leq 1$
Cell swimming speed	v	$0\ \mu$m/s $\leq v$ $\leq 10\ \mu$m/s
Turbulent mixing dissipation rate	ϵ	$\leq 10^{-2}$ W/kg

Solution curves. For $\delta > 1/2$, Eq. (9) has one stable equilibrium point at

$$C^* = \frac{(2\delta - 1)\lambda}{16\pi a\sigma D + 10.4\sigma a^3 \left(\frac{\epsilon}{\nu}\right)^{0.5}}. \tag{10}$$

Moreover, an analytical solution to Eq. (9) exists, and is given by

$$C(t) = \frac{A}{(A/C_0 - B)e^{-At} + B} \tag{11}$$

where $A = (2\delta - 1)\lambda$ and $B = 16\pi a\sigma D + 10.4\sigma a^3 (\epsilon/\nu)^{0.5}$. Extended Data Figure 6c and d show families of solution curves for $C(t)$ from Eq. (11) for different values of δ and σ, for a swimming speed $v = 2\ \mu$m/s and an initial concentration of cells $C_0 = 10^3$ CFU/g. The planktonic bacterial population grows exponentially for early times and then plateaus at an equilibrium concentration C^*. The main parameters that can be tuned by oral vaccination are δ and σ, as these characterize the physical interactions between the cells. Both of these parameters affect the predicted equilibrium concentration of planktonic bacteria C^* (Eq. (10)). This reflects the fact that the stable equilibrium is attained through a balance between

growth and clumping. Modifying the cross-linking strength parameter σ only influences the dynamics noticeably once the bacterial population grows to a point where significant encounters occur (i.e. it does not affect the initial increase in the concentration of planktonic bacteria). Increasing the value of σ results in a lower value of C^*. The effects of increasing δ are twofold, as evident in Extended Data Figure 6c,d. As δ is increased (*i.e.*, cells are more likely to divide successfully), both the initial growth in the concentration of planktonic bacteria (exponential part of Extended Data Figure 6c,d for $t \lesssim$ 5hr) and the equilibrium concentration C^* increase. It is worth noting that the swimming speed v also affects the value of C^* rather strongly, since the cell diffusivity is proportional to v^2. Halving the swimming speed to $v = 1\ \mu$m/s results in a four-fold increase in the value of C^*.

The two parameters δ and σ have been treated as independent so far. However, their values will both depend on the presence, concentration and avidity of specific IgA, and will therefore be correlated. A high concentration of specific IgA will give rise to a low value of δ (high probability of unsuccessful division) and a high value of σ (high probability of sticky collisions). We thus implement the interdependence between these two parameters through a simple assumption (by setting $\delta = 1 - \sigma$), since they represent related processes. While this assumed functional form is chosen for simplicity, it captures the intrinsic tradeoff between cross-linking strength at division, δ, and cross-linking strength in encounters, σ.

Since we require $\delta > 1/2$ in order to achieve a non-trivial steady state, this would require $\sigma < 1/2$ in our new model formulation. Introduction of IgA to the system will have a two-fold effect on the number of planktonic bacteria: it will reduce the rate of production of planktonic cells and increase the rate at which cells that are produced are lost through aggregation (Extended Data Fig. 6). Under the assumption $\sigma = 1 - \delta$, we find that C^*, given by

$$C^* = \frac{\lambda k}{16\pi a D + 10.4 a^3 (\epsilon/v)^{0.5}},\tag{12}$$

is proportional to $k = (2\delta - 1)/(1 - \delta)$, which then summarizes into a single parameter the influence of IgA. The parameter k is sensitive to changes in δ. For example, changing from $\delta = 0.95$ to $\delta = 0.80$ results in a six-fold decrease in C^*. Extended Data Fig. 6e shows four different solution curves for various values of σ (with $\delta = 1 - \sigma$). Each curve exhibits an initial exponential growth phase which saturates at a σ-dependent value of C^*. Small changes in either the cross-linking strength parameter σ or the successful division probability δ give rise to significant changes in the overall population dynamics.

Extended Data Fig. 6f shows the equilibrium bacterial concentration C^* as a function of the swimming speed and the turbulent mixing dissipation rate, i.e. in terms of the strength of the two mechanisms that drive classical agglutination. The value of the cross-linking strength parameter was been chosen to be $\sigma = 0.1$ in this case. It is evident that for a range of mixing

dissipation rates (10^{-6} W/kg $< \epsilon < 10^{-2}$ W/kg), the precise value of C^* is insensitive to the choice of ϵ. That is, classical agglutination is driven almost entirely by motility-induced encounters rather than fluid mixing.

We are now in a position to investigate the relative importance of classical agglutination and enchained bacterial growth. To do this, we consider the equilibrium bacterial concentration C^* as a function of the swimming speed v and the successful division probability δ (Fig. 2g). It is important to note that the IgA cross-linking strength σ contributes to both classical agglutination (through bacterial swimming), and enchained growth. The effect of the vaccine is to reduce the concentration of planktonic bacteria by 1.5 to 2 orders of magnitude, depending on the swimming speed. For a fixed value of δ, changes in the swimming speed have a relatively weak effect on C^* (Fig. 2g).

To assess the overall effect of the oral vaccine, it is necessary to consider simultaneous changes in σ (and therefore δ) and v due to the vaccine. The oral vaccine causes a decrease in δ, which in itself would decrease the value of C^*. However, this is partially offset by the fact that the oral vaccine also reduces the motility of the bacteria (see Extended Data Fig. 7a). Introducing IgA therefore corresponds to moving from the circle (black border) to the triangle (black border) (Fig 2g). The net effect is that the oral vaccine reduces the equilibrium concentration of planktonic bacteria by a factor of >30 (1.5 orders of magnitude).

Important points

While this model gives rise to an equilibrium concentration of planktonic bacteria, we emphasise that it is not due to a carrying capacity of the system in the traditional sense (i.e. nutrient limitation). Instead, the equilibrium concentration is a dynamic equilibrium in which the rate of production of individual planktonic cells from cell division is equal to the rate of loss of individual planktonic cells through encounter-driven aggregation.

In the context of this model, the only mechanisms by which a clump of two cells can form are (i) sticking together of two individual cells (by motility or mixing), or (ii) incomplete division of cells during growth. Both of these processes are irreversible in this framework. If equal proportions of the cells in the inoculum were labelled green and red, then clumps formed by the two above mechanisms would have very different colour signatures. Mechanism (i) would result in clumps that are red+green, red only, or green only, with the ratio 2:1:1 among these. Mechanism (ii) would give rise to clumps which were entirely clonal, i.e. only red or only green. The predictions of the model are that aggregation by growth is dominant at lower concentrations (i.e. early time), but aggregation by sticking becomes significant as the number of planktonic cells increases. This would suggest that, at early times, observed clumps would be mainly clonal [mechanism (ii)], while at later times the proportion of mixed clumps would

increase [mechanism (i)]. This prediction is qualitatively consistent with the experimental data (Fig. 1).

The planktonic bacterial population appears to be responsible for residual infection in the intestines of vaccinated mice. By considering the predominant processes leading to loss of planktonic bacteria, we can predict that IgA cross-linking strength is a critical determinant of the size of the population of planktonic bacteria. Of note, this parameter will be determined by the avidity of the IgA responses and the total IgA concentration, but also by the abundance of the recognized epitope on the bacterial surface, the anchoring of the epitope in the bacterial outer membrane and the ease with which the epitope can be modified. Thus, antibodies against weakly expressed surface proteins, or against weakly anchored epitopes will induce enchained growth to a much lesser extent. Further, phase-variation resulting in divergent structures, or highly variable epitope concentrations on progeny bacteria is expected to disrupt enchained growth. This consideration can inform the design of oral vaccines to induce IgA with optimal cross-linking ability.

References

Ackermann, M., Stecher, B., Freed, N. E., Songhet, P., Hardt, W. D., & Doebeli, M. (2008). Self-destructive cooperation mediated by phenotypic noise. *Nature, 454*(7207), 987-990.

Azegami, T., Yuki, Y., & Kiyono, H. (2014). Challenges in mucosal vaccines for the control of infectious diseases. *Int Immunol, 26*(9), 517-528.

Barthel, M., Hapfelmeier, S., Quintanilla-Martinez, L., Kremer, M., Rohde, M., Hogardt, M., Pfeffer, K., Russmann, H., & Hardt, W. D. (2003). Pretreatment of mice with streptomycin provides a Salmonella enterica serovar Typhimurium colitis model that allows analysis of both pathogen and host. *Infect Immun, 71*(5), 2839-2858.

Berg, H. C. (1993). *Random walks in biology*: Princeton University Press.

Bunker, J. J., Flynn, T. M., Koval, J. C., Shaw, D. G., Meisel, M., McDonald, B. D., Ishizuka, I. E., Dent, A. L., Wilson, P. C., Jabri, B., Antonopoulos, D. A., & Bendelac, A. (2015). Innate and Adaptive Humoral Responses Coat Distinct Commensal Bacteria with Immunoglobulin A. *Immunity, 43*(3), 541-553.

Chakraborty, S., Harro, C., DeNearing, B., Bream, J., Bauers, N., Dally, L., Flores, J., Van de Verg, L., Sack, D. A., & Walker, R. (2016). Evaluation of the Safety, Tolerability, and Immunogenicity of an Oral, Inactivated Whole-Cell Shigella flexneri 2a Vaccine in Healthy Adult Subjects. *Clin Vaccine Immunol, 23*(4), 315-325.

Chen, J., Trounstine, M., Alt, F. W., Young, F., Kurahara, C., Loring, J. F., & Huszar, D. (1993). Immunoglobulin gene rearrangement in B cell deficient mice generated by targeted deletion of the JH locus. *Int Immunol, 5*(6), 647-656.

Diard, M., Sellin, M. E., Dolowschiak, T., Arnoldini, M., Ackermann, M., & Hardt, W. D. (2014). Antibiotic treatment selects for cooperative virulence of Salmonella typhimurium. *Curr Biol, 24*(17), 2000-2005.

Drecktrah, D., Levine-Wilkinson, S., Dam, T., Winfree, S., Knodler, L. A., Schroer, T. A., & Steele-Mortimer, O. (2008). Dynamic behavior of Salmonella-induced membrane tubules in epithelial cells. *Traffic, 9*(12), 2117-2129.

Endt, K., Stecher, B., Chaffron, S., Slack, E., Tchitchek, N., Benecke, A., Van Maele, L., Sirard, J. C., Mueller, A. J., Heikenwalder, M., Macpherson, A. J., Strugnell, R., von Mering, C., & Hardt, W. D. (2010). The microbiota mediates pathogen clearance from the gut lumen after non-typhoidal Salmonella diarrhea. *PLoS Pathog, 6*(9), e1001097.

Gil, D, & Bouché, J P. (1991a). ColE1-type vectors with fully repressible replication. *Gene, 105*(1), 17-22.

Gil, D., & Bouche, J. P. (1991b). ColE1-type vectors with fully repressible replication. *Gene, 105*(1), 17-22.

Grant, A. J., Restif, O., McKinley, T. J., Sheppard, M., Maskell, D. J., & Mastroeni, P. (2008). Modelling within-host spatiotemporal dynamics of invasive bacterial disease. *PLoS Biol, 6*(4), e74.

Hapfelmeier, S., Stecher, B., Barthel, M., Kremer, M., Muller, A. J., Heikenwalder, M., Stallmach, T., Hensel, M., Pfeffer, K., Akira, S., & Hardt, W. D. (2005). The Salmonella pathogenicity island (SPI)-2 and SPI-1 type III secretion systems allow Salmonella serovar typhimurium to trigger colitis via MyD88-dependent and MyD88-independent mechanisms. *J Immunol, 174*(3), 1675-1685.

Harriman, G. R., Bogue, M., Rogers, P., Finegold, M., Pacheco, S., Bradley, A., Zhang, Y., & Mbawuike, I. N. (1999). Targeted deletion of the IgA constant region in mice leads to IgA deficiency with alterations in expression of other Ig isotypes. *J Immunol, 162*(5), 2521-2529.

Helaine, S., Thompson, J. A., Watson, K. G., Liu, M., Boyle, C., & Holden, D. W. (2010). Dynamics of intracellular bacterial replication at the single cell level. *Proc Natl Acad Sci U S A, 107*(8), 3746-3751.

Hendrickx, A. P., Top, J., Bayjanov, J. R., Kemperman, H., Rogers, M. R., Paganelli, F. L., Bonten, M. J., & Willems, R. J. (2015). Antibiotic-Driven Dysbiosis Mediates Intraluminal Agglutination and

Alternative Segregation of Enterococcus faecium from the Intestinal Epithelium. *MBio, 6*(6), e01346-01315.

Hoiseth, S. K., & Stocker, B. A. (1981). Aromatic-dependent Salmonella typhimurium are non-virulent and effective as live vaccines. *Nature, 291*(5812), 238-239.

Jackson, G. A. (1990). A model of the formation of marine algal flocs by physical coagulation processes. Deep Sea Research Part A. *Oceanographic Research Papers, 37*(8), 1197–1211.

Kabir, Shahjahan. (2014). Critical Analysis of Compositions and Protective Efficacies of Oral Killed Cholera Vaccines. *Clinical and Vaccine Immunology : CVI, 21*(9), 1195-1205.

Kaiser, P., Diard, M., Stecher, B., & Hardt, W. D. (2011). The streptomycin mouse model for Salmonella diarrhea: functional analysis of the microbiota, the pathogen's virulence factors, and the host's mucosal immune response. *Immunol Rev, 245*(1), 56-83.

Kaiser, P., Slack, E., Grant, A. J., Hardt, W. D., & Regoes, R. R. (2013). Lymph node colonization dynamics after oral Salmonella Typhimurium infection in mice. *PLoS Pathog, 9*(9), e1003532.

Kiørboe, T. (2008). *A mechanistic approach to plankton ecology*: Princeton University Press.

Kiørboe, T., Andersen, K. P., & Dam, H. G. (1990). Coagulation efficiency and aggregate formation in marine phytoplankton. . *Marine Biology, 107*(2), 235-245.

Lentle, R. G., Hemar, Y., Hall, C. E., & Stafford, K. J. (2005). Periodic fluid extrusion and models of digesta mixing in the intestine of a herbivore, the common brushtail possum (Trichosurus vulpecula). *Journal of Comparative Physiology B, 175*(5), 337-347.

Levinson, K. J., De Jesus, M., & Mantis, N. J. (2015). Rapid effects of a protective O-polysaccharide-specific monoclonal IgA on Vibrio cholerae agglutination, motility, and surface morphology. *Infect Immun, 83*(4), 1674-1683.

Lipsitch, M., & Siber, G. R. (2016). How Can Vaccines Contribute to Solving the Antimicrobial Resistance Problem? *MBio, 7*(3).

Lundgren, A., Jertborn, M., & Svennerholm, A. M. (2016). Induction of long term mucosal immunological memory in humans by an oral inactivated multivalent enterotoxigenic Escherichia coli vaccine. *Vaccine, 34*(27), 3132-3140.

Maier, L., Diard, M., Sellin, M. E., Chouffane, E. S., Trautwein-Weidner, K., Periaswamy, B., Slack, E., Dolowschiak, T., Stecher, B., Loverdo, C., Regoes, R. R., & Hardt, W. D. (2014). Granulocytes impose a tight bottleneck upon the gut luminal pathogen population during Salmonella typhimurium colitis. *PLoS Pathog, 10*(12), e1004557.

Maier, L., Vyas, R., Cordova, C. D., Lindsay, H., Schmidt, T. S., Brugiroux, S., Periaswamy, B., Bauer, R., Sturm, A., Schreiber, F., von Mering, C., Robinson, M. D., Stecher, B., & Hardt, W. D. (2013). Microbiota-derived hydrogen fuels Salmonella typhimurium invasion of the gut ecosystem. *Cell Host Microbe, 14*(6), 641-651.

McClelland, D. B., Samson, R. R., Parkin, D. M., & Shearman, D. J. (1972). Bacterial agglutination studies with secretory IgA prepared from human gastrointestinal secretions and colostrum. *Gut, 13*(6), 450-458.

Mirpuri, J., Raetz, M., Sturge, C. R., Wilhelm, C. L., Benson, A., Savani, R. C., Hooper, L. V., & Yarovinsky, F. (2014). Proteobacteria-specific IgA regulates maturation of the intestinal microbiota. *Gut Microbes, 5*(1), 28-39.

Mobley, H. L., Green, D. M., Trifillis, A. L., Johnson, D. E., Chippendale, G. R., Lockatell, C. V., Jones, B. D., & Warren, J. W. (1990). Pyelonephritogenic Escherichia coli and killing of cultured human renal proximal tubular epithelial cells: role of hemolysin in some strains. *Infect Immun, 58*(5), 1281-1289.

Moor, K., Wotzka, S. Y., Toska, A., Diard, M., Hapfelmeier, S., & Slack, E. (2016). Peracetic Acid Treatment Generates Potent Inactivated Oral Vaccines from a Broad Range of Culturable Bacterial Species. *Front Immunol, 7*, 34.

Müller, A. J., Kaiser, P., Dittmar, K. E. J., Weber, T. C., Haueter, S., Endt, K., Songhet, P., Zellweger, C., Kremer, M., Fehling, H. J., & Hardt, W. D. (2012). Salmonella Gut Invasion Involves TTSS-2-Dependent Epithelial Traversal, Basolateral Exit, and Uptake by Epithelium-Sampling Lamina Propria Phagocytes. *Cell Host Microbe, 11*(1), 19-32.

Muller, A. J., Kaiser, P., Dittmar, K. E., Weber, T. C., Haueter, S., Endt, K., Songhet, P., Zellweger, C., Kremer, M., Fehling, H. J., & Hardt, W. D. (2012). Salmonella gut invasion involves TTSS-2-dependent epithelial traversal, basolateral exit, and uptake by epithelium-sampling lamina propria phagocytes. *Cell Host Microbe, 11*(1), 19-32.

Nutter, R. L., Bullas, L. R., & Schultz, R. L. (1970). Some properties of five new Salmonella bacteriophages. *J Virol, 5*(6), 754-764.

Pabst, O. (2012). New concepts in the generation and functions of IgA. *Nat Rev Immunol, 12*(12), 821-832.

Palm, N. W., de Zoete, M. R., Cullen, T. W., Barry, N. A., Stefanowski, J., Hao, L., Degnan, P. H., Hu, J., Peter, I., Zhang, W., Ruggiero, E., Cho, J. H., Goodman, A. L., & Flavell, R. A. (2014). Immunoglobulin A coating identifies colitogenic bacteria in inflammatory bowel disease. *Cell, 158*(5), 1000-1010.

Planer, J. D., Peng, Y., Kau, A. L., Blanton, L. V., Ndao, I. M., Tarr, P. I., Warner, B. B., & Gordon, J. I. (2016). Development of the gut microbiota and mucosal IgA responses in twins and gnotobiotic mice. *Nature, 534*(7606), 263-266.

Qadri, F., Wierzba, T. F., Ali, M., Chowdhury, F., Khan, A. I., Saha, A., Khan, I. A., Asaduzzaman, M., Akter, A., Khan, A., Begum, Y. A., Bhuiyan, T. R., Khanam, F., Chowdhury, M. I., Islam, T., Chowdhury, A. I., Rahman, A., Siddique, S. A., You, Y. A., Kim, D. R., Siddik, A. U., Saha, N. C., Kabir, A., Cravioto, A., Desai, S. N., Singh, A. P., & Clemens, J. D. (2016). Efficacy of a Single-Dose, Inactivated Oral Cholera Vaccine in Bangladesh. *N Engl J Med, 374*(18), 1723-1732.

Roche, A. M., Richard, A. L., Rahkola, J. T., Janoff, E. N., & Weiser, J. N. (2015). Antibody blocks acquisition of bacterial colonization through agglutination. *Mucosal Immunol, 8*(1), 176-185.

Sellin, M. E., Muller, A. A., Felmy, B., Dolowschiak, T., Diard, M., Tardivel, A., Maslowski, K. M., & Hardt, W. D. (2014). Epithelium-intrinsic NAIP/NLRC4 inflammasome drives infected enterocyte expulsion to restrict Salmonella replication in the intestinal mucosa. *Cell Host Microbe, 16*(2), 237-248.

Shimada, S., Kawaguchi-Miyashita, M., Kushiro, A., Sato, T., Nanno, M., Sako, T., Matsuoka, Y., Sudo, K., Tagawa, Y., Iwakura, Y., & Ohwaki, M. (1999). Generation of polymeric immunoglobulin receptor-deficient mouse with marked reduction of secretory IgA. *J Immunol, 163*(10), 5367-5373.

Slack, E., Balmer, M. L., & Macpherson, A. J. (2014). B cells as a critical node in the microbiota-host immune system network. *Immunol Rev, 260*(1), 50-66.

Slack, E., Hapfelmeier, S., Stecher, B., Velykoredko, Y., Stoel, M., Lawson, M. A., Geuking, M. B., Beutler, B., Tedder, T. F., Hardt, W. D., Bercik, P., Verdu, E. F., McCoy, K. D., & Macpherson, A. J. (2009). Innate and adaptive immunity cooperate flexibly to maintain host-microbiota mutualism. *Science, 325*(5940), 617-620.

Stecher, B., Chaffron, S., Kappeli, R., Hapfelmeier, S., Freedrich, S., Weber, T. C., Kirundi, J., Suar, M., McCoy, K. D., von Mering, C., Macpherson, A. J., & Hardt, W. D. (2010). Like will to like: abundances of closely related species can predict susceptibility to intestinal colonization by pathogenic and commensal bacteria. *PLoS Pathog, 6*(1), e1000711.

Stecher, B., Denzler, R., Maier, L., Bernet, F., Sanders, M. J., Pickard, D. J., Barthel, M., Westendorf, A. M., Krogfelt, K. A., Walker, A. W., Ackermann, M., Dobrindt, U., Thomson, N. R., & Hardt, W. D. (2012). Gut inflammation can boost horizontal gene transfer between pathogenic and commensal Enterobacteriaceae. *Proc Natl Acad Sci U S A, 109*(4), 1269-1274.

Stecher, B., Hapfelmeier, S., Muller, C., Kremer, M., Stallmach, T., & Hardt, W. D. (2004). Flagella and chemotaxis are required for efficient induction of Salmonella enterica serovar Typhimurium colitis in streptomycin-pretreated mice. *Infect Immun, 72*(7), 4138-4150.

Stecher, B., Maier, L., & Hardt, W. D. (2013). 'Blooming' in the gut: how dysbiosis might contribute to pathogen evolution. *Nat Rev Microbiol, 11*(4), 277-284.

Traggiai, E., Becker, S., Subbarao, K., Kolesnikova, L., Uematsu, Y., Gismondo, M. R., Murphy, B. R., Rappuoli, R., & Lanzavecchia, A. (2004). An efficient method to make human monoclonal

antibodies from memory B cells: potent neutralization of SARS coronavirus. *Nat Med, 10*(8), 871-875.

Woof, J. M., & Russell, M. W. (2011). Structure and function relationships in IgA. *Mucosal Immunol, 4*(6), 590-597.

CHAPTER 6

-

THESIS CONCLUSIONS AND DISCUSSION

Need for a "clean" system to study the function of IgA

Gastro-intestinal infections are still a leading cause of morbidity and mortality in humans and a major economic problem in livestock populations. Oral vaccination against enteropathogens is therefore highly desirable - due to the requirement for local priming of mucosal immunity (Macpherson *et al.*, 2004; Martinoli *et al.*, 2007), as well as the ease of application of such vaccines. Nevertheless, only very few mucosal vaccines aimed at inducing intestinal IgA are in in regular clinical use, predominantly as trials have ended with excess adverse effects or poor protection (Lycke, 2012). This can most likely be attributed to our poor understanding of how exactly protective immunity at mucosal surfaces functions. In contrast to the blood antibody isotypes, IgA does not activate common bactericidal pathways (e.g. Complement, antibody-dependent cellular cytotoxicity) (Slack *et al.*, 2012). Although it is broadly accepted that IgA plays an important role in coordinating the establishment and the maintenance of the intestinal microbiota (Pabst *et al.*, 2016), very little is understood about the protective mechanisms attributed to this isotype.

Due to the constant presence of the intestinal microbiota, which is beneficial to its host, the induction of immune responses in the intestine are tightly regulated. The quantitative threshold for a non-invasive bacterium delivered orally to induce a high-avidity IgA response is therefore in excess of 10^9 CFU per gram luminal content (Hapfelmeier *et al.*, 2010). Correspondingly, the status quo in the field of mucosal vaccine research was, that inactivated oral vaccines without the addition of a mucosal adjuvant such as cholera toxin are inefficient in mice (Chapter1). However, our work clearly demonstrates that oral administration of high doses of inactivated bacteria is sufficient to induce high-avidity IgA responses without the need for mucosal adjuvants (Chapter 2, (Moor *et al.*, 2016)).

Of note, live attenuated vaccination strains that harbour a remaining level of pathogenicity, will induce mild inflammation. This is expected to deliver "danger" signals, on top of the high levels of PAMPs and antigen already present in these vaccines, amplifying germinal centre formation (Figure 1). Concomitantly, live-attenuated strains can often drive their own uptake into GALT (Kaiser *et al.*, 2011) and persistence within the GALT (Kaiser *et al.*, 2014) and/or can induce a change in the intestinal microenvironment that favours their growth ((Stecher *et al.*, 2013)), increasing antigen delivery to the GALT (Figure 1). Therefore the presence of pathogenicity will always generate a more efficient vaccine. However, this benefit is massively outweighed by the risk to induce severe pathology in a diverse human population, particularly in patients with increased susceptibility to bacterial infections (Burniat *et al.*, 1980; Felmy *et al.*, 2013). In research settings, the side-effects of pathogenicity as well as persistence can enormously complicate the interpretation of results. Our results clearly demonstrate that the requirement for pathogenicity in the induction of mucosal IgA responses can be overcome when sufficient doses of inactivated bacteria are administered orally (Figure1, (Moor *et al.*,

2016)). Importantly, peracetic acid inactivation was found to be broadly applicable for the production of oral vaccines from a range of bacterial strains, allowing immediate investigation of specific IgA in a broad range of research settings.
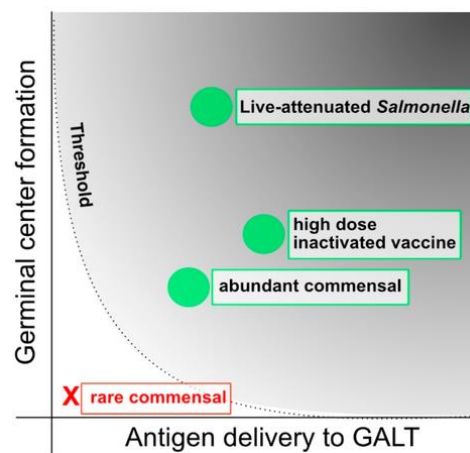

Figure 1. Induction of high-avidity IgA responses in the intestine. The potential of different vaccination methods and commensals for the induction of high-avidity IgA based on GALT entry and germinal centre formation. Grey shading indicates the areas where high-avidity IgA responses would be expected to be elicited. Entities known to elicit strong high-avidity IgA responses are shown with green circles. Entities eliciting poor or no antibody responses are shown with a red "X." Figure adapted from (Moor *et al.*, 2015).

New tools to induce and measure anti-bacterial IgA

We have shown that the oral administration of high doses of peracetic acid killed bacteria induces high levels of intestinal IgA specific for the strain used for vaccine preparation. This occurs in the complete absence of live bacteria, exogenous mucosal adjuvants, intestinal pathology and host colonization, and is safe even in the context of severe innate immune deficiency (Moor *et al.*, 2016). This technique delivers enormous amounts of antigen and PAMPs (e.g. bacterial LPS) into the small intestine. In a healthy individual, the proximal small intestine only harbours very low numbers of bacteria, therefore the local concertation of bacterial antigen and PAMPs is low (Donaldson *et al.*, 2016). One could therefore speculate that the unusual high amount of antigen/PAMPs that are delivered to the small intestine is the driver of the successful induction of high-avidity IgA responses by our newly developed vaccine. In agreement with this hypothesis, it was recently reported that anatomical location is the primary factor that determines whether a particular bacterium elicited an IgA response (Bunker *et al.*, 2015). Further, our weekly repeated vaccination procedure could have generated a positive feedback loop that drives the further induction of high-avidity IgA by IgA-mediated sampling into the GALT (Mantis *et al.*, 2002; Rochereau *et al.*, 2013). Such a mechanism was also proposed by Fransen et al., who show that IgA-bound microbes were

preferentially taken up into Peyer's patches independently of sampling by CX3CR1+ phagocytes and promoted further induction of specific IgA responses (Fransen *et al.*, 2015).

In order to measure the amount of high-avidity IgA induced by the PA.STm vaccine, we developed a flow cytometric approach (Chapter 3). This technique allows the quantification of bacterial surface-binding antibodies with a high-avidity cut-off. As bacterial surfaces tend to be biochemically diverse, when compared to cytosolic contents, this permits the definition of species specificity with much greater certainty than other techniques. Further, this technique can be used to study IgA coating of a specific species in complete intestinal content, due to the ability to gate on subpopulations.

When combined, these techniques allow us to induce a robust IgA in a minimally-perturbed host, as well as to accurately quantify the relevant surface-binding antibodies produced both *ex vivo* and *in situ.*

Unanswered questions in IgA induction

We could show that the induction of high-avidity IgA by our inactivated oral vaccines was T cell dependent (Moor *et al.*, 2016), indicating that follicular T helper responses are also induced. However we did not investigate if and to what extend we are also inducing effector T cell responses specific for the vaccine. In order to characterize the induction of effector and memory T cell responses one could determine the cytokine profiles and cytotoxic properties of isolated T cells after restimulation *in vitro* or perform T cell transfer experiments to study the proliferative capacity of the cells *in vivo*. Also we did not further characterize the host requirements for induction of the specific IgA response. Future work identifying the important PRRs and inductive sites may suggest improvements in the vaccine formulation or delivery. Of note, while we were successful at inducing high-avidity IgA against a number of different gammaproteobacteria species using this technique, some surface structures may be altered by peracetic acid treatment, and this will need to be empirically tested for each species and strain.

Despite these unknowns, due their simplicity, efficiency and safety, peracetic acid killed bacterial vaccines, combined with bacterial flow cytometry are extremely powerful tools to address the function of IgA *in vivo* and *in situ*.

Rethinking the role of IgA in the intestinal ecosystem

The establishment of the intestinal microbiota starts at birth and its complexity increases massively during early life (Funkhouser et al., 2013; Yatsunenko et al., 2012). Metagenomic

sequencing studies are now characterizing microbiota composition and its role in health and disease in ever more detail (Human Microbiome Project, 2012; Turnbaugh et al., 2007).

It is well known that the microbiota shapes an individual's IgA repertoire throughout its life (Granato *et al.*, 2015; Wesemann *et al.*, 2013). The number of IgA-secreting plasma cells in germ-free animals (with no detectable microbiota) is drastically reduced (Hapfelmeier et al., 2010; Moreau et al., 1978). Upon experimental colonization of a germ-free mouse, and also on initiation of colonization of the neonate after birth, expansion of the IgA plasma cell pool is initiated (Hapfelmeier *et al.*, 2010; Wesemann *et al.*, 2013). Each individual harbours an IgA repertoire that is unique, highly diverse, and polyclonal. With increasing age, this repertoire gains diversity and, in the murine model, the total intestinal IgA levels increase continuously with age (Lindner *et al.*, 2015; Lindner *et al.*, 2012). In agreement, IgA from adult mice was shown to have higher reactivity against intestinal microbes than IgA isolated from very young mice (Mirpuri *et al.*, 2014). It seems that a great proportion of the microbiota is bound by low-avidity IgA, whereas coating with high-avidity IgA is less frequent (Bunker *et al.*, 2015). Possibly related to the predominance of low-avidity interactions, there is relatively little evidence that the presence of IgA influences the healthy adult microbiota composition under homeostatic conditions. For example, it was shown the microbiota composition of Rag1-deficent mice and wildtype counterparts correlated more with the animal husbandry than with the animals' ability to produce IgA (Young *et al.*, 2012). Notably, high-avidity IgA is required to limit pathology induced by the colonization of some "pathobionts" such as segmented filamentous bacteria (Fagarasan *et al.*, 2002; Suzuki *et al.*, 2004).

Perturbations of the intestinal ecosystem open niches that render the microbiota prone to invasion and to blooms of enteropathogens (Stecher *et al.*, 2007). We found that after antibiotic-induced dysbiosis, high-avidity IgA enforces *Salmonella* to grow into clonally arrayed aggregates in the intestinal lumen (Chapter 5). In fact, caged growth is dramatically more efficient and aggregates fast-growing bacteria at lower bacterial densities than classical agglutination, which would require rare bacterial encounter events. It therefore seems that the IgA system is set up to specifically disadvantage rapidly growing bacteria. As turnover of the microbiota must equal turnover of the gut content to maintain homeostasis (max 1-2 times per day), net growth of microbiota species is slow in a healthy animal. However, during dysbiosis of the intestinal ecosystem rapid growth can occur (Stecher *et al.*, 2007), and IgA-mediated caged growth would specifically disadvantage out-growing species. Our observation is in agreement with a recent publication demonstrating the aggregation of *E. faecalis* only upon antibiotic-induced dysbiosis (Hendrickx *et al.*, 2015). Further, the colonization of the neonatal intestine after birth also represents a situation where rapid bacterial growth is expected. Correspondingly, IgA-deficient mouse pups show persistent high levels of Proteobacteria, whereas in IgA-sufficient littermates, these bacteria are only dominant until

shortly after waning (Mirpuri *et al.*, 2014). Further, a recent study could associate changes in bacterial growth rates of certain species to type II diabetes or inflammatory bowel disease (Korem *et al.*, 2015), highlighting the role of altered microbiota growth rates in a broad range of microbiota-associated diseases.

We therefore suggest that IgA-mediated caged growth is an important process targeting over-growing species that helps the microbiota to recover diversity after dysbiosis.

Modelling the effect of caged growth vs. classical agglutination on the infectious pool of *Salmonella*

Agglutination is a well-documented function of IgA *in vitro*. However, agglutination requires two or more bacteria to collide: a process governed by the bacterial density squared, as well as the speed of movement. An exception where the probability of interaction equals one is during cell division. Given that we observed IgA-bound aggregates immobilized and far from the cecal wall, we assume that the only bacteria capable of invading and causing disease in vaccinated animals is the small fraction that is not successfully aggregated. We therefore generated a model to predict how caged growth and agglutination affect the size of the non-aggregated bacterial population in the gut lumen based on the total population size (Chapter 5, Supplementary manuscript). In this model, the probability of two bacteria to stick together upon collision is dependent on the frequency of collision, which increases with cell density squared and the bacterial "diffusivity", and on the "stickiness" of IgA, which increases the probability that two interacting bacteria will remain stuck to one another. Caged growth was modelled simply as exponential growth with a probability that dividing cells successfully segregate, related to the IgA "stickiness". Clear from this model is, that the probability to from aggregates during growth is higher than with simple movement as the probability of encounter for non-growing bacteria is less than one. Further, this model predicted that for a given "stickiness of IgA", an equilibrium is reached where the number of free-swimming bacteria generated by successful segregation during cell division, is balanced by incorporation of these bacteria into aggregates by agglutination. Indeed, when we quantified the number of non-aggregated cells by microscopy, we found that in vaccinated mice, this number is 100-fold reduced at 24h post-infection, and the actual density of non-aggregated cells increases more slowly than the size of the total population (Chapter 5).

Of note, the model we generated does not require any special terms relating to viscosity or fluid movement and yet reasonably accurately describes what we see *in vivo,* i.e. that classical agglutination is only efficient at very high densities. In the nasal mucosa, bacterial agglutination is observed at much lower bacterial concentrations and in time-frames incompatible with growth (Roche *et al.*, 2015). This suggests that the fluid dynamics at other

mucosal surfaces may in fact be specialized to concentrate and agglutinate bacteria (e.g. via cilia movement) (Smith *et al.*, 2008).

So far we have only demonstrated IgA-mediated caged growth for *Salmonella* in the intestine. According to our model, caged growth is likely be a general mechanism, as long as sufficient high-avidity IgA is present and the bacteria are fast-growing. Importantly, the likelihood of undergoing caged growth may also depend on the nature of the bacterial surface. Mucosal bacterial pathogens that produce capsules, such as some *E. coli* strains (Corbett *et al.*, 2008), *Neisseria meningitidis* (Rouphael *et al.*, 2012), *Klebsiella pneumoniae* (Clegg *et al.*, 2016) or *Streptococcus pneumoniae (Hava et al., 2003)*, could be less affected. Capsules are only loosely bound to the bacteria surface and antibodies directed against the bacterial capsule would not be able to stably crosslink such bacteria, resulting in a rather low "IgA stickiness" as applied to our model. Also the rough laboratory strain *E.coli* K12, which was used in many previous studies, is not expected to undergo caged growth, as the enterobacterial common antigen (the main antigenic moiety on its surface) is non-covalently bound (Kuhn *et al.*, 1988). Further, bacteria undergoing extensive phase-shift variations are less likely to be affected by caged growth (Van Der Woude *et al.*, 2004). This and other mechanisms by which bacteria could escape IgA-mediated recognition are discussed below.

IgA-mediated aggregation results in a decreased "effective population size" without bacterial killing and affects the evolutionary dynamics of *Salmonella*

An aspect of IgA function that was initially very difficult to mechanistically dissect, was a loss of clonal diversity of an avirulent *Salmonella* population in the cecum lumen of vaccinated mice, despite identical colonization kinetics at the total population level. Extensive *in vitro* assays failed to reveal any bacteriotoxic or bacteriostatic effect of high-avidity IgA. However, closer examination of how caged growth affects the population structure revealed a killing-independent mechanism. The total cecal content is approximately 1g in a healthy SPF mouse. This content is ejected to the colon at a rate of 50-100mg every 15mins, such that as soon as an individual clone has 10-100 copies in a well-mixed planktonic bacterial population, it becomes highly unlikely that this clone reaches extinction. However, if upon growth, dividing bacteria remain tightly associated, this results in clonal aggregates. When material is ejected into the colon and disposed of in the faeces, this will tend to be one or two entire clones that are expelled, rather than a planktonic mixture of all clones present (Chapter 5).

Therefore, growth into aggregates could be regarded as a way to reduce the infectious bacterial population, but without actually reducing the total number of *Salmonella* in the intestine. This means, that the metabolic niche in the intestine stays occupied by *Salmonella* and cannot be invaded by another bacterial species, but nevertheless, the effective population

size is reduced. Increases clonal loss (Chapter 5) has several consequences: Beneficial mutations that are acquired during the growth in the intestine and would promote the bacterial virulence or persistence, are less likely to emerge. This of course does not hold true for the selection of mutations that allow the pathogen to escape IgA-binding and leave its cage (discussed below). Being aggregated in general (theoretically also through classical agglutination) was shown to be disadvantageous when closely related bacteria compete for the same niche (Stecher *et al.*, 2010). However, this decreased competitiveness can also be extended to competition with other members of the microbiota and could in the best case, accelerate the complete clearance of the pathogen.

A further consequence of the effective population size decreased due to IgA-mediated caged growth is a delay in plasmid transfer between *Salmonella* strains. As IgA-mediated caged growth leads to the confinement of potential plasmid donor and recipient clones in physically separated microcolonies, we observe a delay in the rate of plasmid transfer (Chapter 5). Therefore, clonal growth delays the density-dependent exchange of genetic material. Interestingly, we could also demonstrate a secondary effect of high-avidity IgA on induction of inflammation-mediated phage transfer between *Salmonella* spp. (Chapter 4). Therefore, vaccine induced high-avidity IgA has the potential to decrease horizontal gene transfer which can be observed during blooms of enteropathogens (Stecher *et al.*, 2012; Stecher *et al.*, 2013). This facet of IgA biology has been overlooked in vaccine trials to date, but suggests strongly that oral vaccination, particularly in live-stock presenting reservoirs of antibiotic-resistance pathogens, but also in at-risk patient groups, could be applied with the specific aim of reducing horizontal gene transfer (Sandoval-Motta *et al.*, 2016; Woolhouse *et al.*, 2015).

How does high-avidity IgA affect the systemic spread of *Salmonella*? What we learned by applying mathematical models

IgA-mediated agglutination results in the drastic reduction of the infectious *Salmonella* pool, whilst maintaining a large total population that occupies the metabolic niche. A recently developed mathematical model describes the first step of systemic spread of the pathogen as a stochastic birth-death process in the mLN, extended by an immigration term (Kaiser *et al.*, 2013). In this model, the success of an individual bacterium to spread to the mLN is dependent on its density in the cecum, an immigration rate into the mLN and a net bacterial replication rate in the mLN, which includes clearance from this anatomical compartment. In the absence of high-avidity IgA, the bacterial density in the intestine is 10^9 CFU/g (all expected to be non-aggregated) and approximately 300 bacteria migrate per day from the gut to the mLN (Kaiser *et al.*, 2013). Applying this model to analyse the protective effect of vaccine-induced IgA against systemic spread, we could show that in the presence of high-avidity IgA, the number

of bacteria reaching the mLN is roughly 100-fold reduced, whereas the replication rate of the bacteria reaching the mLN is not affected (Chapter 5). At first sight, this suggest that high-avidity IgA reduces the bacterial translocation rate. However, mathematically the translocation event across the intestinal epithelium is described as a product of the bacterial population density in the intestine and a very small migration rate. The observed reduction in bacterial tissue invasion can therefore be only a consequence of the reduced free and therefore potentially invasive *Salmonella* pool in the intestine.

Blindly using mathematical models that describe complex biological processes is potentially misleading. However, by taking care to understand the underlying biological functions represented by individual terms in the model, we could serially generate and test hypotheses that guided us towards a detailed investigation of the bacterial migration from the intestinal lumen to the mLN. Interestingly, if we now assume that IgA does not affect the migration rate per se, but only the size of the infectious gut luminal population, we can also estimate the size of the infectious gut lumen population from the model. This gives a luminal population size that is equal or larger to that observed by microscopy, suggesting that indeed aggregation alone could account for our observed protection. Of note, although we would require data where within-host population dynamics and microscopy quantification of luminal bacterial distribution were carried out on matched animals, the current data-set suggests that the invasion rate per bacterium is actually a little higher in vaccinated animals than in unvaccinated. This may relate to IgA-mediated sampling of intestinal content (Fransen *et al.*, 2015; Mantis *et al.*, 2002), or to a narrow time-window for mLN invasion early in the infection process when the ratio of free to aggregated bacteria is higher.

By using the mathematical models described above, we gained substantial understanding of a) how IgA-mediated caged growth leads to a reduction of the "infectious" bacterial population in the intestine of vaccinated mice and b) how this translates into a decreased bacterial migration rate into the mLN. In order to develop and test these models we were forced to investigate certain steps of the infection process in great detail. Thereby we were able to rapidly dissect a dynamic system with much greater efficiency than traditional endpoint analysis (simply determining the bacterial burden in the mLN).

A central postulate of biological mathematics is that "all models are wrong, some models are useful". It is generally impossible, and also undesirable, to generate a solvable mathematical model encompassing all of the chaotic complexity of a real biological system. By making clearly stated assumptions, we generate models that simplify this complexity, but nevertheless are informative about how the real system behaves in a limited set of conditions. For example, in the model describing bacterial encounters in the gut, we were forced to exclude bacteria from the calculations as soon as they form an aggregate. In reality, this is not the case, otherwise we would observe a decreased number of bacteria in the intestine of vaccinated mice.

Nevertheless, the generated model gives us an important quantitative insight into how bacterial aggregation takes place and the relative contributions of caged growth versus agglutination. In summary, models of within-host dynamical processes are an extremely useful tool that allows iterative hypothesis generation and testing of predicted parameters and thereby help to estimate if biological data can be explained by an infection theory.

Escape mechanisms

As caged-growth decreases the effective population size in terms of population genetics, we expect stochastically slower emergence of beneficial mutations. Despite this, the *Salmonella* population reaches an actual population size of more than 10^9 CFU, and given the error rate of bacterial DNA polymerases there is a high probability that mutations emerge over time (Traverse *et al.*, 2016). Notably, typical mutations increasing the growth rate may not confer a benefit in a caged-growth situation, as this would simply generate larger aggregates. However, mutations that lead to decreased IgA binding could be highly beneficial. Previous publications have observed induction of phase-variation in *Bacteroides thetaiotamicron* in animals supplemented with high amounts of a monoclonal IgA-specific for one phase-type (Peterson *et al.*, 2007). Further, a number of mucosal pathogens produce loosely attached capsules, which would increase the ability of bacteria to escape "IgA stickiness"(Clegg *et al.*, 2016; Corbett *et al.*, 2008; Hava *et al.*, 2003; Rouphael *et al.*, 2012).

As we typically monitor the faecal *Salmonella* population for IgA coating during the course of infection, we were able to observe the complete or partial loss of IgA binding at d2-3 post-infection in a small fraction of infected animals (Supplementary Figure, page 204). Interestingly, all bacterial clones showing a decreased IgA binding had lost expression of the O5 epitope of the O antigen. This is biochemically defined as an acetylation of an phospho-abequose residue in the O antigen structure, and is carried out by a single acetyl transferase *OafA (Hauser et al., 2011).* Targeted deletion of *OafA* resulted in the same phenotype as the evolved clones, and sequencing of the *OafA* gene revealed a microsatellite slippage at the start of the open reading frame in all clones. It therefore appears that *Salmonella* Typhimurium has at least one mechanism by which it can efficiently alter surface carbohydrate structures to evade recognition of PA.STm induced IgA. Such an escape mechanism could also explain the loss of vaccination-protection we occasionally observe at later stages of infection (Supplementary Figure, page 200). This immediately suggests the possibility to generate mucosal vaccines against both the common O-antigen type and the evolved "escape mutant" types, to generate tighter IgA-mediated protection.

The selection of mutants with decreased IgA binding may also explain an apparent non sequitur in IgA function. The presence of high-avidity IgA against a fraction of endogenous

microbiota strains would actually be expected to disadvantage them in competition against invasive species. In fact, the opposite is often observed: i.e. that the resident strains will outcompete an intruder (Seedorf *et al.*, 2014). In these cases, within-host evolution will lead to the generation of resident strains with an advantage over the parental strain in the presence of IgA. Thus the potential destabilizing effect of IgA is reduced.

Implications for vaccine development

I would like to highlight at this point that "caged growth" is not the only potential function of IgA. We in fact observe a direct effect of high-avidity IgA on bacterial motility in *Salmonella* although control experiments determined that this is only a minor contributor to the protective effect. However, IgA is clearly also able to neutralize toxins (Apter *et al.*, 1993; Mantis *et al.*, 2006; Stubbe *et al.*, 2000), and in some cases can mediate direct toxic effects on bacteria (Forbes *et al.*, 2012). However, bacterial surface-specific IgA that is easy to induce by oral vaccination seems to act predominantly via "caged growth" as long as the luminal bacterial density remains below 10^9 CFU/g (when classical agglutination can occur). This raises several issues in vaccine design:

Is O-antigen-binding IgA alone ever going to be completely protective? The answer clearly depends on the disease course. In the model of non-typhoidal Salmonellosis*,* the population size in the gut lumen is effectively reduced by caged growth, but takes quite some time to be eliminated. Therefore there remains a statistical chance of infection which increases with time. In human non-typhoidal Salmonellosis, similarly large intestinal population sizes can be reached if microbiota disruption is present, and in these cases O-antigen-specific IgA may only completely protect in a small percentage of cases. Clearly combining oral inactivated vaccines with a parenteral vaccination aimed at inducing a tissue-protective responses (for example engineered virus-like particles) would be far more robust.

In contrast, *Vibrio cholera* is a small intestinal pathogen that grows rapidly to a final density of 10^7 CFU/g (Nelson *et al.*, 2009). Here, O-antigen-specific IgA would be expected to mediate caged growth. Importantly, where very high *Vibrio cholera* exposure occurs, up to 10^7 CFU can be directly ingested, little local growth occurs and we therefore expect caged-growth to fail. This may explain the less than 100% protection offered by these vaccines (Kabir, 2014). *Campylobacter* strains (Fitzgerald, 2015) *Shigella (Niyogi,* 2005*)*, enteropathogenic and enterohaemorrhagic *E.coli* (Lai *et al.*, 2013) may also be good targets for this type of vaccination.

Salmonella Typhi actually does not grow in the human intestinal lumen, but rather directly invades into GALT and spreads systemically to finally re-seed the intestine via the gall bladder

(Dougan *et al.*, 2014). As the infectious dose is below the density required to see efficient aggregation, and caged growth cannot occur, it appears that either other functions of IgA, or other immune mechanisms must be the main protective effects induced by the Ty21a oral Typhoid vaccine.

Antibiotic resistance is a rapidly emerging medical problem, related to overuse of antibiotics in live-stock husbandry and patients (Sandoval-Motta *et al.*, 2016; Woolhouse *et al.*, 2015). Of note, in *Salmonella,* high-avidity IgA inhibits plasmid transfer directly by clonal isolation and inhibits phage transfer indirectly, by preventing the inflammation driven reactivation of temperate phages (Chapter 4 and 5). There is therefore clearly an untapped potential for oral vaccines to eliminate antibiotic-resistant donor strains and to inhibit spread of resistance to other gut-resident bacteria. Examples are vancomycin-resistant *Enterococci* (VRE) that are not pathogenic in healthy individuals but can cause septicaemia in the immunocompromised, e.g. during transplantation (Gold, 2001). As inactivated oral vaccines are simple to produce, as well as safe to apply, it could reasonably be envisaged that personalized vaccines could be developed for a patient's own VRE strain. This is clearly an important future research direction.

Supplementary Figure for Chapter 6
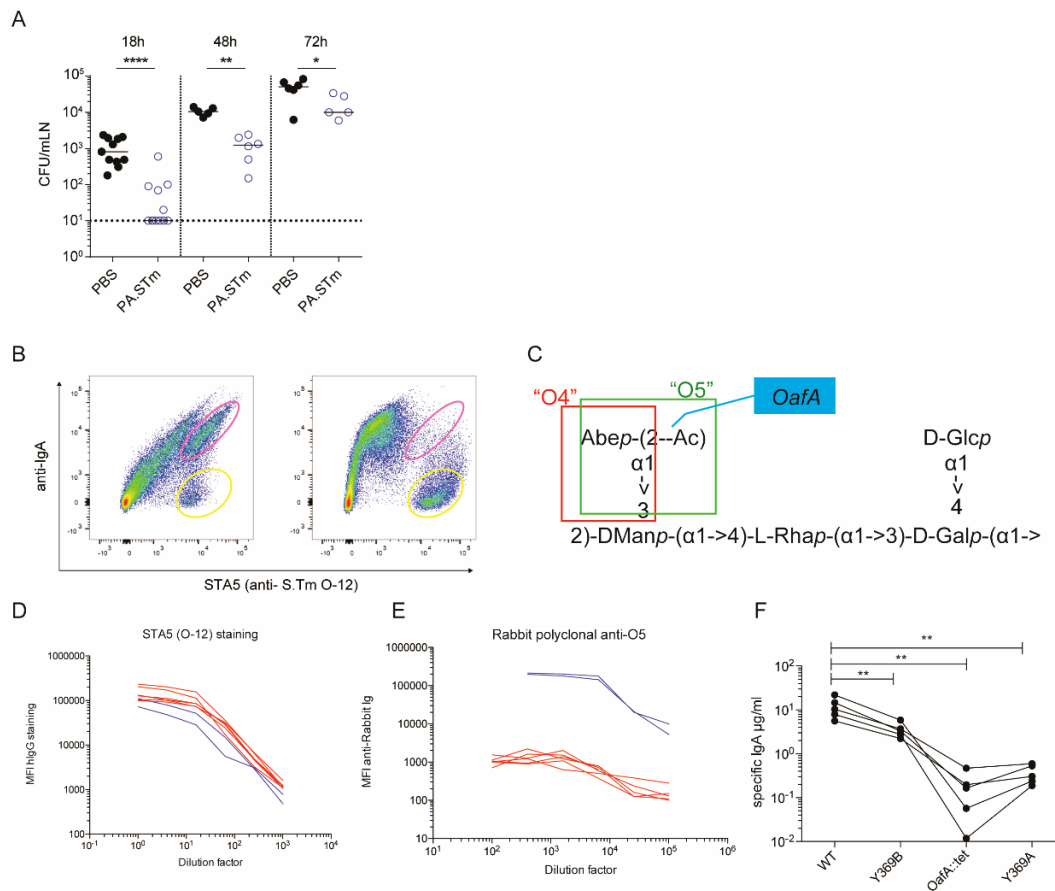
Loss of PA.STm-mediated protection over time. A and B. C57BL/6 SOPF mice were orally vaccinated with PA.STm, or PBS-only as indicated. On d21 after the first vaccination, all mice were streptomycin pre-treated and 24h later, mice were infected with 10^5 CFU virulent *S.* Typhimurium (A), or sequentially infected with 10^2 CFU of each S.Tm phage donor (SL1344 [SopEΦ^{aphT}]; kan^R; amp^R) and S.Tm phage recipient (14028S; *marT*::*cat*; cm^R, amp^R) (B, for details see Material and Methods Chapter 4). A. Bacterial counts in the mesenteric lymph node at the indicated timepoints. Note that the approximately 24h delay of bacterial spread to the mLN in the PA.STm vaccinated mice compared to the PBS treated controls. B. FACS plots of fecal samples from the same mouse taken at d1 (left) and d3 pi (right). Pre-gated for bacterial-sized particles and stained for IgA-binding (x-axis) and with STA5 recognizing the O12 epitope in the *Salmonella* O-antigen structure (y-axis). Note the predominance of the IgA-stained *Salmonella*-population on d1 (pink circle), which is lost on d3 (only non-IgA-coated *Salmonella* are detected, yellow circle). C. Representation of the Salmonella O antigen structure. The acetylation of an phospho-abequose residue in the O antigen structure differentiates between the O4 epitope (red box) and the O5 epitope and is carried out by a single acetyl transferase *OafA* (blue box) (Hauser et al., 2011). D and E: Bacterial flow cytometry titration curves of *Salmonella* clones isolated from feces of the mouse shown in (B) on d1 (blue) or d3 (red) pi and stained with an anti-O-12 monoclonal antibody, or an anti-O5 rabbit polyclonal antiserum. d3 clones have lost binding to the O5 antiserum, and were found to carry frame-shift mutations in the *OafA* gene by sanger sequencing. F. Bacterial flow cytometry was carried out with intestinal lavages from n=5 orally vaccinated mice and a murine dimeric IgA specific for the O-12 antigen with known concentration. These IgA preparations were serially diluted and used to stain two evolved clones isolated on d4 pi from vaccinated mice infected with an avirulent *S.* Typhimurium (Y369B - O5 positive, Y369A - O5-negative), as well as a constructed OafA deletion mutant and the parental wild-type strain. IgA binding was detected with a FITC-conjugated anti-mouse IgA antibody and absolute concentrations of specific IgA against each strain were calculated by comparison to the monoclonal control. Whilst loss of O5 is associated with a 10-100-fold reduction in specific IgA, even the evolved strain that retains O5 production shows a 1-2-fold drop in specific IgA binding, suggesting a rapid selection for *Salmonella* strains with lower IgA binding *in vivo*.

References

Apter, F. M., Michetti, P., Winner, L. S., 3rd, Mack, J. A., Mekalanos, J. J., & Neutra, M. R. (1993). Analysis of the roles of antilipopolysaccharide and anti-cholera toxin immunoglobulin A (IgA) antibodies in protection against Vibrio cholerae and cholera toxin by use of monoclonal IgA antibodies in vivo. *Infect Immun, 61*(12), 5279-5285.

Bunker, J. J., Flynn, T. M., Koval, J. C., Shaw, D. G., Meisel, M., McDonald, B. D., Ishizuka, I. E., Dent, A. L., Wilson, P. C., Jabri, B., Antonopoulos, D. A., & Bendelac, A. (2015). Innate and Adaptive Humoral Responses Coat Distinct Commensal Bacteria with Immunoglobulin A. *Immunity, 43*(3), 541-553.

Burniat, W., Toppet, M., & De Mol, P. (1980). Acute and recurrent salmonella infections in three children with chronic granulomatous disease. *J Infect, 2*(3), 263-268.

Clegg, S., & Murphy, C. N. (2016). Epidemiology and Virulence of Klebsiella pneumoniae. *Microbiol Spectr, 4*(1).

Corbett, D., & Roberts, I. S. (2008). Capsular polysaccharides in Escherichia coli. *Adv Appl Microbiol, 65*, 1-26.

Donaldson, G. P., Lee, S. M., & Mazmanian, S. K. (2016). Gut biogeography of the bacterial microbiota. *Nat Rev Microbiol, 14*(1), 20-32.

Dougan, G., & Baker, S. (2014). Salmonella enterica serovar Typhi and the pathogenesis of typhoid fever. *Annu Rev Microbiol, 68*, 317-336.

Fagarasan, S., Muramatsu, M., Suzuki, K., Nagaoka, H., Hiai, H., & Honjo, T. (2002). Critical roles of activation-induced cytidine deaminase in the homeostasis of gut flora. *Science, 298*(5597), 1424-1427.

Felmy, B., Songhet, P., Slack, E. M., Muller, A. J., Kremer, M., Van Maele, L., Cayet, D., Heikenwalder, M., Sirard, J. C., & Hardt, W. D. (2013). NADPH oxidase deficient mice develop colitis and bacteremia upon infection with normally avirulent, TTSS-1- and TTSS-2-deficient Salmonella Typhimurium. *PLoS One, 8*(10), e77204.

Fitzgerald, C. (2015). Campylobacter. *Clin Lab Med, 35*(2), 289-298.

Forbes, S. J., Martinelli, D., Hsieh, C., Ault, J. G., Marko, M., Mannella, C. A., & Mantis, N. J. (2012). Association of a protective monoclonal IgA with the O antigen of Salmonella enterica serovar Typhimurium impacts type 3 secretion and outer membrane integrity. *Infect Immun, 80*(7), 2454-2463.

Fransen, F., Zagato, E., Mazzini, E., Fosso, B., Manzari, C., El Aidy, S., Chiavelli, A., D'Erchia, A. M., Sethi, M. K., Pabst, O., Marzano, M., Moretti, S., Romani, L., Penna, G., Pesole, G., & Rescigno, M. (2015). BALB/c and C57BL/6 Mice Differ in Polyreactive IgA Abundance, which Impacts the Generation of Antigen-Specific IgA and Microbiota Diversity. *Immunity, 43*(3), 527-540.

Funkhouser, L. J., & Bordenstein, S. R. (2013). Mom knows best: the universality of maternal microbial transmission. *PLoS Biol, 11*(8), e1001631.

Gold, H. S. (2001). Vancomycin-resistant enterococci: mechanisms and clinical observations. *Clin Infect Dis, 33*(2), 210-219.

Granato, A., Chen, Y., & Wesemann, D. R. (2015). Primary immunoglobulin repertoire development: time and space matter. *Curr Opin Immunol, 33*, 126-131.

Hapfelmeier, S., Lawson, M. A., Slack, E., Kirundi, J. K., Stoel, M., Heikenwalder, M., Cahenzli, J., Velykoredko, Y., Balmer, M. L., Endt, K., Geuking, M. B., Curtiss, R., 3rd, McCoy, K. D., & Macpherson, A. J. (2010). Reversible microbial colonization of germ-free mice reveals the dynamics of IgA immune responses. *Science, 328*(5986), 1705-1709.

Hauser, E., Junker, E., Helmuth, R., & Malorny, B. (2011). Different mutations in the oafA gene lead to loss of O5-antigen expression in Salmonella enterica serovar Typhimurium. *J Appl Microbiol, 110*(1), 248-253.

Hava, D. L., LeMieux, J., & Camilli, A. (2003). From nose to lung: the regulation behind Streptococcus pneumoniae virulence factors. *Mol Microbiol, 50*(4), 1103-1110.

Hendrickx, A. P., Top, J., Bayjanov, J. R., Kemperman, H., Rogers, M. R., Paganelli, F. L., Bonten, M. J., & Willems, R. J. (2015). Antibiotic-Driven Dysbiosis Mediates Intraluminal Agglutination and Alternative Segregation of Enterococcus faecium from the Intestinal Epithelium. *MBio, 6*(6), e01346-01315.

Human Microbiome Project, Consortium. (2012). Structure, function and diversity of the healthy human microbiome. *Nature, 486*(7402), 207-214.

Kabir, S. (2014). Critical analysis of compositions and protective efficacies of oral killed cholera vaccines. *Clin Vaccine Immunol, 21*(9), 1195-1205.

Kaiser, P., & Hardt, W. D. (2011). Salmonella typhimurium diarrhea: switching the mucosal epithelium from homeostasis to defense. *Curr Opin Immunol, 23*(4), 456-463.

Kaiser, P., Regoes, R. R., Dolowschiak, T., Wotzka, S. Y., Lengefeld, J., Slack, E., Grant, A. J., Ackermann, M., & Hardt, W. D. (2014). Cecum lymph node dendritic cells harbor slow-growing bacteria phenotypically tolerant to antibiotic treatment. *PLoS Biol, 12*(2), e1001793.

Kaiser, P., Slack, E., Grant, A. J., Hardt, W. D., & Regoes, R. R. (2013). Lymph node colonization dynamics after oral Salmonella Typhimurium infection in mice. *PLoS Pathog, 9*(9), e1003532.

Korem, T., Zeevi, D., Suez, J., Weinberger, A., Avnit-Sagi, T., Pompan-Lotan, M., Matot, E., Jona, G., Harmelin, A., Cohen, N., Sirota-Madi, A., Thaiss, C. A., Pevsner-Fischer, M., Sorek, R., Xavier, R. J., Elinav, E., & Segal, E. (2015). Growth dynamics of gut microbiota in health and disease inferred from single metagenomic samples. *Science, 349*(6252), 1101-1106.

Kuhn, H. M., Meier-Dieter, U., & Mayer, H. (1988). ECA, the enterobacterial common antigen. *FEMS Microbiol Rev, 4*(3), 195-222.

Lai, Y., Rosenshine, I., Leong, J. M., & Frankel, G. (2013). Intimate host attachment: enteropathogenic and enterohaemorrhagic Escherichia coli. *Cell Microbiol, 15*(11), 1796-1808.

Lindner, C., Thomsen, I., Wahl, B., Ugur, M., Sethi, M. K., Friedrichsen, M., Smoczek, A., Ott, S., Baumann, U., Suerbaum, S., Schreiber, S., Bleich, A., Gaboriau-Routhiau, V., Cerf-Bensussan, N., Hazanov, H., Mehr, R., Boysen, P., Rosenstiel, P., & Pabst, O. (2015). Diversification of memory B cells drives the continuous adaptation of secretory antibodies to gut microbiota. *Nat Immunol*.

Lindner, C., Wahl, B., Fohse, L., Suerbaum, S., Macpherson, A. J., Prinz, I., & Pabst, O. (2012). Age, microbiota, and T cells shape diverse individual IgA repertoires in the intestine. *J Exp Med, 209*(2), 365-377.

Lycke, N. (2012). Recent progress in mucosal vaccine development: potential and limitations. *Nat Rev Immunol, 12*(8), 592-605.

Macpherson, A. J., & Uhr, T. (2004). Compartmentalization of the mucosal immune responses to commensal intestinal bacteria. *Ann N Y Acad Sci, 1029*, 36-43.

Mantis, N. J., Cheung, M. C., Chintalacharuvu, K. R., Rey, J., Corthesy, B., & Neutra, M. R. (2002). Selective adherence of IgA to murine Peyer's patch M cells: evidence for a novel IgA receptor. *J Immunol, 169*(4), 1844-1851.

Mantis, N. J., McGuinness, C. R., Sonuyi, O., Edwards, G., & Farrant, S. A. (2006). Immunoglobulin A antibodies against ricin A and B subunits protect epithelial cells from ricin intoxication. *Infect Immun, 74*(6), 3455-3462.

Martinoli, C., Chiavelli, A., & Rescigno, M. (2007). Entry route of Salmonella typhimurium directs the type of induced immune response. *Immunity, 27*(6), 975-984.

Mirpuri, J., Raetz, M., Sturge, C. R., Wilhelm, C. L., Benson, A., Savani, R. C., Hooper, L. V., & Yarovinsky, F. (2014). Proteobacteria-specific IgA regulates maturation of the intestinal microbiota. *Gut Microbes, 5*(1), 28-39.

Moor, K., & Slack, E. (2015). What Makes A Bacterial Oral Vaccine a Strong Inducer of High-Affinity IgA Responses? *Antibodies (Basel), 4*(4), 295.

Moor, K., Wotzka, S. Y., Toska, A., Diard, M., Hapfelmeier, S., & Slack, E. (2016). Peracetic Acid Treatment Generates Potent Inactivated Oral Vaccines from a Broad Range of Culturable Bacterial Species. *Front Immunol, 7*, 34.

Moreau, M. C., Ducluzeau, R., Guy-Grand, D., & Muller, M. C. (1978). Increase in the population of duodenal immunoglobulin A plasmocytes in axenic mice associated with different living or dead bacterial strains of intestinal origin. *Infect Immun, 21*(2), 532-539.

Nelson, E. J., Harris, J. B., Morris, J. G., Jr., Calderwood, S. B., & Camilli, A. (2009). Cholera transmission: the host, pathogen and bacteriophage dynamic. *Nat Rev Microbiol, 7*(10), 693-702.

Niyogi, S. K. (2005). Shigellosis. *J Microbiol, 43*(2), 133-143.

Pabst, O., Cerovic, V., & Hornef, M. (2016). Secretory IgA in the Coordination of Establishment and Maintenance of the Microbiota. *Trends Immunol, 37*(5), 287-296.

Peterson, D. A., McNulty, N. P., Guruge, J. L., & Gordon, J. I. (2007). IgA response to symbiotic bacteria as a mediator of gut homeostasis. *Cell Host Microbe, 2*(5), 328-339.

Roche, A. M., Richard, A. L., Rahkola, J. T., Janoff, E. N., & Weiser, J. N. (2015). Antibody blocks acquisition of bacterial colonization through agglutination. *Mucosal Immunol, 8*(1), 176-185.

Rochereau, N., Drocourt, D., Perouzel, E., Pavot, V., Redelinghuys, P., Brown, G. D., Tiraby, G., Roblin, X., Verrier, B., Genin, C., Corthesy, B., & Paul, S. (2013). Dectin-1 is essential for reverse transcytosis of glycosylated SIgA-antigen complexes by intestinal M cells. *PLoS Biol, 11*(9), e1001658.

Rouphael, N. G., & Stephens, D. S. (2012). Neisseria meningitidis: biology, microbiology, and epidemiology. *Methods Mol Biol, 799*, 1-20.

Sandoval-Motta, S., & Aldana, M. (2016). Adaptive resistance to antibiotics in bacteria: a systems biology perspective. *Wiley Interdiscip Rev Syst Biol Med, 8*(3), 253-267.

Seedorf, H., Griffin, N. W., Ridaura, V. K., Reyes, A., Cheng, J., Rey, F. E., Smith, M. I., Simon, G. M., Scheffrahn, R. H., Woebken, D., Spormann, A. M., Van Treuren, W., Ursell, L. K., Pirrung, M., Robbins-Pianka, A., Cantarel, B. L., Lombard, V., Henrissat, B., Knight, R., & Gordon, J. I. (2014). Bacteria from diverse habitats colonize and compete in the mouse gut. *Cell, 159*(2), 253-266.

Slack, E., Balmer, M. L., Fritz, J. H., & Hapfelmeier, S. (2012). Functional flexibility of intestinal IgA - broadening the fine line. *Front Immunol, 3*, 100.

Smith, D. J., Gaffney, E. A., & Blake, J. R. (2008). Modelling mucociliary clearance. *Respir Physiol Neurobiol, 163*(1-3), 178-188.

Stecher, B., Chaffron, S., Kappeli, R., Hapfelmeier, S., Freedrich, S., Weber, T. C., Kirundi, J., Suar, M., McCoy, K. D., von Mering, C., Macpherson, A. J., & Hardt, W. D. (2010). Like will to like: abundances of closely related species can predict susceptibility to intestinal colonization by pathogenic and commensal bacteria. *PLoS Pathog, 6*(1), e1000711.

Stecher, B., Denzler, R., Maier, L., Bernet, F., Sanders, M. J., Pickard, D. J., Barthel, M., Westendorf, A. M., Krogfelt, K. A., Walker, A. W., Ackermann, M., Dobrindt, U., Thomson, N. R., & Hardt, W. D. (2012). Gut inflammation can boost horizontal gene transfer between pathogenic and commensal Enterobacteriaceae. *Proc Natl Acad Sci U S A, 109*(4), 1269-1274.

Stecher, B., Maier, L., & Hardt, W. D. (2013). 'Blooming' in the gut: how dysbiosis might contribute to pathogen evolution. *Nat Rev Microbiol, 11*(4), 277-284.

Stecher, B., Robbiani, R., Walker, A. W., Westendorf, A. M., Barthel, M., Kremer, M., Chaffron, S., Macpherson, A. J., Buer, J., Parkhill, J., Dougan, G., von Mering, C., & Hardt, W. D. (2007). Salmonella enterica serovar typhimurium exploits inflammation to compete with the intestinal microbiota. *PLoS Biol, 5*(10), 2177-2189.

Stubbe, H., Berdoz, J., Kraehenbuhl, J. P., & Corthesy, B. (2000). Polymeric IgA is superior to monomeric IgA and IgG carrying the same variable domain in preventing Clostridium difficile toxin A damaging of T84 monolayers. *J Immunol, 164*(4), 1952-1960.

Suzuki, K., Meek, B., Doi, Y., Muramatsu, M., Chiba, T., Honjo, T., & Fagarasan, S. (2004). Aberrant expansion of segmented filamentous bacteria in IgA-deficient gut. *Proc Natl Acad Sci U S A, 101*(7), 1981-1986.

Traverse, C. C., & Ochman, H. (2016). Conserved rates and patterns of transcription errors across bacterial growth states and lifestyles. *Proc Natl Acad Sci U S A, 113*(12), 3311-3316.

Turnbaugh, P. J., Ley, R. E., Hamady, M., Fraser-Liggett, C. M., Knight, R., & Gordon, J. I. (2007). The human microbiome project. *Nature, 449*(7164), 804-810.

van der Woude, M. W., & Baumler, A. J. (2004). Phase and antigenic variation in bacteria. *Clin Microbiol Rev, 17*(3), 581-611, table of contents.

Wesemann, D. R., Portuguese, A. J., Meyers, R. M., Gallagher, M. P., Cluff-Jones, K., Magee, J. M., Panchakshari, R. A., Rodig, S. J., Kepler, T. B., & Alt, F. W. (2013). Microbial colonization influences early B-lineage development in the gut lamina propria. *Nature, 501*(7465), 112-115.

Woolhouse, M., Ward, M., van Bunnik, B., & Farrar, J. (2015). Antimicrobial resistance in humans, livestock and the wider environment. *Philos Trans R Soc Lond B Biol Sci, 370*(1670), 20140083.

Yatsunenko, T., Rey, F. E., Manary, M. J., Trehan, I., Dominguez-Bello, M. G., Contreras, M., Magris, M., Hidalgo, G., Baldassano, R. N., Anokhin, A. P., Heath, A. C., Warner, B., Reeder, J., Kuczynski, J., Caporaso, J. G., Lozupone, C. A., Lauber, C., Clemente, J. C., Knights, D., Knight, R., & Gordon, J. I. (2012). Human gut microbiome viewed across age and geography. *Nature, 486*(7402), 222-227.

Young, G. R., Eksmond, U., Salcedo, R., Alexopoulou, L., Stoye, J. P., & Kassiotis, G. (2012). Resurrection of endogenous retroviruses in antibody-deficient mice. *Nature, 491*(7426), 774-778.

ACKNOWLEDGEMENTS

CURRICULUM VITAE

PERSONAL DATA

Name   Kathrin Moor
Address   Seefeldstrasse 204, 8008 Zürich
Telephone   079 471 98 51
E-Mail   kathrin.moor@micro.biol.ethz.ch

Date of Birth   14.05.1985
Place of Birth   Zofingen AG
Citizenship: Swiss

WORK EXPERIENCE

05/2012-09/2016   ETH Zurich, Institute of Microbiology
                    Research Assistant
                    - Planning and execution of a multi-year research project with the focus on developing and testing a new oral vaccine in a preclinical mouse model
                    - Techniques: vaccine production, *in vivo* mouse experiments, flow cytometric analysis of antibody responses, histopathological evaluations, immunofluorescence microscopy, assistance with intravital microscopy
                    - Fitting experimental data to mathematical models
                    - Project presentation at seminars and national conferences
                    - Writing scientific publications
                    - Data base research
                    - Supervising Master students
                    - Organizing and leading the practical course for undergraduate students

2010-2012   ETH Zürich, Institute of Microbiology
                    Master Student
                    - Development of an *in vitro* fungal killing assay
                    - Characterization of immune cell activation and apoptosis
                    - Techniques: cell isolation and cell culture, flow cytometry, cytometric bead array, RNA and DNA isolation, real-time qPCR, ELISA, Western Blot

2008-2012   Candrian Catering AG
                    Assistant (part time)
                    - First point of contact for restaurant and seminar guests
                    - Handling reservations via phone and e-mail

2006   Unipress AG
                    Assistant for sales and logistics (8 months internship)
                    - Administrative duties in the accountants section
                    - Optimization of packing instructions

EDUCATION

2012-2016	PhD Thesis in Infection Immunology at ETH Zurich Title: *"IgA enforces "caged growth" of Salmonella Typhimurium - a story of being trapped."*
2010-2012	Postgraduate studies at ETH Zurich Master of Sciences ETH in Biology (Microbiology and Immunology) Title: *"The protective role of innate Interleukin-17 during systemic Candida albicans infections."*
2006-2010:	Undergraduate studies at University of Zürich Bachelor of Sciences in Biology
2005-2006	Undergraduate studies at University of Basel Pharmaceutical Sciences
2001-2005	High school Kantonsschule Zofingen Matura/A-Levels (Main subjects: Biology, Chemistry and Sports)

COURSES

09/2016	Good Clinical Practice, Module 2 (Clinical Trial Centre, USZ)
08/2016	Good Clinical Practice, Module 1 (Clinical Trial Centre, USZ)
10/2014	Scientific writing for Science and Medicine (University of Zurich)
02/2014	Mathematical Models for Infectious Disease Dynamics (Wellcome Trust Advanced Courses, Hinxton, United Kingdom)
02/2013	Introductory course to R (ETH Zurich)
10/2012	Presentation skill course for scientists (ETH Zurich)
10/2012	Project management for researchers (Life Science Zurich Graduate School)
06/2012	Introductory course in laboratory animal science (University of Zurich)

COMPUTER SKILLS

MS Office, EndNote, GraphPad Prism, FloJo, R Studio, Adobe Illustrator, ImageJ

LANGUAGE COMPETENCES

German	native language
English	professional working proficiency
French	working proficiency

OTHER INTERESTS

Scuba diving, running, skiing

PUBLICATIONS

K. Moor, M. Diard, M. Sellin, B. Felmy, S. Wotzka, A. Toska, A. Dal Co, F. Bansept, L. Piccoli, C. Casiraghi, D. Corti, A. Lanzavecchia, M. Ackermann, R. Regoes, C. Loverdo, D. Brumley, R. Stocker, WD. Hardt, E. Slack. *IgA protects the intestine by enchaining rapidly dividing bacteria.* Manuscript in preparation

M. Diard, K. Moor, M. Sellin, A. Aertsen, M. Ackermann, E. Slack, WD Hardt. *Vaccination prevents inflammation-mediated bacteriophage-transfer between Salmonella spp.* Manuscript in revision.

K. Moor, J. Fadlallah, A. Toska, D. Sterlin, ML. Balmer, AJ. Macpherson, G. Gorochov, M. Larsen, E. Slack. *Analysis of bacterial surface-specific antibodies in body fluids using bacterial flow cytometry.* Nature Protocols. 2016

K. Moor, S. Wotzka, A. Toska, M. Diard, S. Hapfelmeier, E. Slack. *Peracetic acid treatment generates potent inactivated oral vaccines from a broad range of culturable bacterial species.* Frontiers in Immunology. 2016

K. Moor, E. Slack. *What makes a bacterial oral vaccine a strong inducer of high-affinity IgA responses?* Antibodies. 2015

Bär E, Whitney PG, Moor K, Reis e Sousa C, LeibundGut-Landmann S. *IL-17 regulates systemic fungal immunity by controlling the functional competence of NK cells.* Immunity. 2014

CONFERENCES AND SEMINARS

08/2016	ASM Conference on Salmonella, Potsdam, Germany Poster: *"Inactivated oral vaccines and within-host dynamics reveal the protective mechanism of bacterial surface-specific IgA"*
11/2015	Seminars in Microbiology, ETH Zürich, Switzerland. PhD-Talk: *"Mechanism of IgA-mediated protection from Salmonella Typhimurium"*
04/2015	Joint Immunology Meeting, Zürich, Switzerland. Talk: *"Within-host dynamics reveal mechanism of IgA-mediated protection from Salmonella Typhimurium."*
03/2015	SAAI Basel, Switzerland. Poster Presentation: *"Within-host population dynamics reveal mechanism of IgA-mediated protection from Salmonella Typhimurium"*
02/2015	Meeting of Swiss Immunology PhD students, Ermatingen, Switzerland. Talk: *"Influences of Salmonella-specific antibodies on within-host population dynamics."*
09/2014	Salmonella-Meeting 2014, Schmitten, Germany. Talk: *"How IgA responses affect Salmonella Typhimurium gut infection"*

06/2014	Department of Biology ETH Symposium, Davos, Switzerland.
	Poster Presentation: *"Within-host population dynamics of Salmonella Typhimurium."*
04/2014	Meeting of Swiss Immunology PhD students, Ermatingen, Switzerland.
	Talk: *"Vaccination-mediated protection from Salmonella Typhimurium."*
09/2013	Salmonella-Meeting 2013, Wiesbaden, Germany.
	Talk: *"Vaccination-mediated protection from Salmonella Typhimurium."*
09/2012	Salmonella-Meeting 2012, Bad Homburg, Germany.
	Talk: *"The ability of adaptive immunity to protect animals with bacterial killing deficiencies from Salmonella infection"*